ROLE OF MEMBRANE TRANSPORTERS IN DRUG DELIVERY, DRUG DISPOSITION AND DRUG-DRUG INTERACTIONS

A DISSERTATION IN
Pharmaceutical Sciences
and
Chemistry

Presented to the Faculty of University
of Missouri-Kansas City in partial fulfillment
of the requirements for the degree

DOCTOR OF PHILOSOPHY

By

VARUN KHURANA

B. Pharmacy, Guru Gobind Singh Indraprastha University, India, 2008

Kansas City, Missouri

2014

ROLE OF MEMBRANE TRANSPORTERS IN DRUG DELIVERY, DRUG DISPOSITION AND DRUG-DRUG INTERACTIONS

Varun Khurana, Candidate for the Doctor of Philosophy Degree

University of Missouri-Kansas City, 2014

ABSTRACT

Tissues such as liver, kidney, brain and intestine expresses membrane transporters which play a vital role in drug absorption, distribution, metabolism and excretion. Understanding of functionality and molecular expression of drug transporters can prove to be of utmost importance in drug delivery or drug design by targeting specific transporter proteins. It's a well-known fact that drug transporters play an important role in governing drug disposition which act as potential piece of information during the drug discovery and development process. By exploring the transporter functionality chances of delivering a therapeutic agent to the target organ enhances. Transporter targeted drug delivery helps in improving the bioavailability, controlling the elimination process and also avoid distribution to non-specific organs, hence diminishes the odds of toxic adverse effects. It is always suitable to choose a potential molecule which may or may not interact with the membrane transporters, depending on whether such an interaction is of any use or not. Activity of individual transport process can be examined by exploring the expression system of transporters. Therapeutic efficacy many important drugs, directly or indirectly, get affected due to genetic polymorphisms and drug-drug interactions involving membrane transporters which ultimately effects the pharmacokinetics of a drug molecule. During the drug discovery and development process, knowledge about the contribution of these transporters

towards interindividual differences by regulating drug absorption, distribution, metabolism and excretion will act as an important tool. The objective of this dissertation project was to understand the role of hepatic uptake transporters (OATP-1B1 and -1B3) in governing the disposition of tyrosine kinase inhibitors (TKIs). Since selected TKIs are the substrates and/or inhibitors of OATP-1B1 and -1B3 expressed in hepatic tissue, these compounds can be regarded as molecular targets for transporter mediated drug-drug interactions (DDIs). Any alteration in the function of these hepatic OATPs might account for the pharmacokinetic variability of TKIs. These finding also provide the basis of further pre-clinical and clinical studies investigating the transporter based DDI potential of TKIs.

As a secondary aim of this investigation we developed novel pentablock (PB) copolymer nanoparticles of pazopanib for treatment of ocular neovascularization. Our results indicated that PB copolymer based drug delivery systems can serve as a platform technology for the development of sustained release therapy along with evasion of drug efflux for the treatment of ocular neovascularization. This drug delivery system can also be utilized for other chronic diseases as well.

We also investigated the presence of ascorbic acid-specific transport system and delineate the functional and molecular aspects of vitamin C transporter (SVCT2) in ocular and breast cancer cells. SVCT2 system can be targeted for the design of ascorbic acid prodrugs or for NPs surface modified with ascorbic acid to achieve enhanced permeability for highly potent but poorly bioavailable drugs by evading drug efflux in the treatment of cancer and ocular diseases.

Interaction of TKIs with hepatic OATP-1B1 and -1B3 delineates the role of hepatic uptake transporters in drug disposition and drug-drug interactions. These OATP transporters in conjunction with the efflux proteins (P-gp, MRP and BCRP) may eventually decide on the overall

flux/loss of the therapeutic agents within the hepatic tissue. Similary, functionality of membrane tranporters have been exploited and examined in terms of drug delivery. Pazopanib encapsulated nanoparticles of novel pentablock polymers were successful in bypass drug efflux mediated via efflux proteins. Also, influx transporters (vitamin C transporter, SVCT2) on ocular cell lines can be further utilized as a potential target for enhancing absorption and permeability of AA-conjugated drugs or drug delivery systems by evading drug efflux.

APPROVAL PAGE

The faculty listed below, appointed by the Dean of the School of Graduate Studies have examined a dissertation titled 'Role of Membrane Transporters in Drug Delivery, Drug Disposition And Drug-Drug Interactions', presented by Varun Khurana, candidate for the Doctor of Philosophy degree, and certify that in their opinion it is worthy of acceptance.

Supervisory Committee

Ashim K. Mitra, Ph.D., Committee Chair
Department of Pharmaceutical Sciences

Kun Cheng, Ph.D.

Department of Pharmaceutical Sciences

Betty Herndon, Ph.D.

Department of Basic Medical Science

Karen B. Williams, Ph.D.

Department of Medical Bioinformatics

James R. Durig, Ph.D.

Department of Chemistry

TABLE OF CONTENTS

LIST OF ILLUSTRATIONS

LIST OF TABLES

ACKNOWLEDGEMENTS

I would like to express my deepest gratitude to my advisor Dr. Ashim K Mitra, for his guidance, kindness, patience and providing me with an outstanding atmosphere for doing research. Also, Dr. Mitra always provided his valuable recommendation involved in practical issues beyond the textbooks, patiently corrected my writing and financially supported my research. With his wisdom, understanding and commitment to the highest standards, he always encouraged and motivated me. I am also thankful to the members of my supervisory committee Drs. Kun Cheng, Karen Williams, Betty Herndon and James Durig for both serving on my committee as well as all their help and guidance throughout my graduate work. I sincerely thank Dr. Russell Melchert, Dean, UMKC School of Pharmacy for his support and motivation at various stages of graduate studies.

I am very thankful to Dr. Dhananjay Pal for sharing his insightful knowledge in the area of *in vitro* techniques and drug-drug interactions, and giving me emotional support in the time of need. A special thanks to Mrs. Ranjana Mitra for her cheerful encouragement and in particular for her moral support throughout my graduate studies at UMKC. I am particularly grateful for the assistance given by Dr. Ravinder Earla with respect to analytical method development and troubleshooting. I would also like to recognize Joyce Johnson and Sharon Self for always being there to help me with all my administrative needs. I appreciate support from Nancy Hoover and Connie Mahone from School of Graduate Studies. I am thankful to National Institute of Health and School of Graduate Studies for constant financial support. I would also express my sincere thanks to Dr. James B. Murowchick (School of Geological Sciences) for his help in XRD analysis. I would (particularly) like to thank Dr. Bruno Stieger (Department of Clinical Pharmacology and Toxicology, University Hospital Zürich, Switzerland) for their generous gift of OATP transfected

cell lines, and, Dr. Walter Jäger University of Vienna, Austria) and Dr. A.J. van Agthoven (Josephine Nefkens Institute, Netherlands) for gifting breast cancer cell lines.

I am greatly thankful to Ravi Vaishya, Sujay Shah, Drs. Mukul Minocha, Sulabh Patel, Ripal Gaudana and Mitan Gokulgandhi for their valuable suggestion and inputs for the betterment of my career. We've laughed, cried and among other things, cursed together. I owe my deepest gratitude to Dr. Deep Kwatra for not only helping me in professional matters but also for being persistent and encouraging, for believing in me, and for the many priceless memories along the way.

I thank my colleagues Mitesh Patel, Dr. Megha Barot, Asha Patel, Animikh Ray, Dr. Aswani Dutt Vadlapudi, Ramya Krishna Vadlapatla, Kishore Cholkar, Vibhuti Agrahari, Chandramouli Natrajan, Maria Joseph, Akshay Jain, Abhirup Mandal, Ashutosh Barve and Anwesha Ray for their timely help and creating such a cheerful environment all through my graduate career. My special thanks to Drs. Shuanghui Luo, Zhiying Wang, Durga Kalyani Paturi, Sagar Boddu, Sriram Gunda and Nanda Kishore Mandava for providing their valuable inputs for successful completion of my PhD.

My heartfelt appreciation goes to all my close friends Nilesh Gupta, Piyush Jain, Ashish Kala, Sharad Sharma, Neel Fofaria, Anand Choubey, Priyanka Agarwal, Gurpreet Gill, Sohail Anwar, Gulshan Mehta, Unnati Patel, Rutva Trivedi, Rajneet Oberoi, Nisha Kwatra, Mrinalini Das, Nitika Anand and Kanika Malik for their contribution to the various domains in my convoluted life.

Of course no acknowledgments would be complete without giving thanks to my parents (Sh. Ashok Khurana and Shmt. Paramjit Khurana). Both have inculcated many worthy qualities in me and set me with a good foundation to meet life. They have always taught me about hard work

and self-respect, about how to be persistent and independent. Also, I would like to express the deepest appreciation to my brother Tarun Khurana and sister-in-law Shikha Khurana for sharing my joys and sorrows and giving me continuous support, inspiration, assistance and guidance. Last but not the least, I would like to thank my niece Aashita Khurana (Gugli/Gapla). Her innocent and sweet smile always keeps me motivated and acts as a stress buster in this last phase of my Ph.D completion.

Dedicated to My Family

CHAPTER 1

THE CONVOLUTIONS INVOLVED IN HEPATIC DRUG TRANSPORT: FOCUS ON MEMBRANE TRANSPORTERS

Rationale

Impact of hepatic transport systems in drug disposition [1]

Liver is mainly responsible for the metabolism and/or excretion of many endogenous and exogenous compounds from the body. Research on the metabolic aspects of hepatic clearance has been a prime area of interest since many decades, although, currently the focus has also been also shifted to examine and evaluate the role of hepatic transport systems in the hepatobiliary disposition of drugs and metabolites. It's a known fact that translocation of lipophilic molecules from plasma to hepatic cytosol is mediated via simple or facilitated diffusion. However, basolateral transport proteins consist of several membrane transporters were involved in uptake of amphipathic and polar organic compounds, in addition to some lipophilic molecules, from sinusoidal plasma to hepatic cytosol. Hepatobiliary disposition of some compounds is also influenced by hepatocellular protein binding and sequestration. As mentioned above that excretion of drugs and metabolites from the hepatocyte is mediated via hepatic transport proteins. Translocation of polar molecules from hepatic cytosol into blood is mediated via uni- or bi-directional basolateral transport systems, however, biliary excretion of drugs and metabolites is mediated via active canalicular transport systems. Recently, there has been a surge of interest in the field of drug transport, and knowledge regarding hepatic transport systems has grown substantially. There is widespread interest in the hepatic transport of drugs and metabolites among pharmaceutical scientists, including medicinal chemists, pharmacologists, and clinicians, for several reasons:

Drug Design (Drug Delivery)

Understanding of structure-transport relationships for hepatic transport proteins would provide an extra edge in designing of compounds with finest transport properties. For a potential drug candidate, extensive hepatic uptake or enhanced biliary excretion may be considered as appropriate characteristic, whereas in others, reduce systemic exposure and limit pharmacological activity due to extensive hepatic uptake and biliary excretion can be regarded as an unattractive property of the potential molecule.

Bioavailability

The liver is an important organ of first-pass elimination. Dietary, disease, or drug-induced alterations in hepatic transport systems may lead to reduced or erratic systemic availability of drugs after oral administration. In some cases, diminished systemic availability of a drug after oral administration has been attributed as an outcome of induction of a hepatic transport protein responsible for the hepatic uptake or biliary excretion of that drug. Besides liver, membrane transporters expressed on the basolateral and apical membranes of the gastrointestinal epithelial cells also play an important role in altering the bioavailability of several drug molecules.

Biliary Excretion

ATP-dependent canalicular transport proteins are responsible for biliary excretion of compounds. In humans, the degree to which most drugs and metabolites go through biliary excretion is not freely valued due to the innate difficulties in directly accessing bile drainage in healthy individuals. Extensive biliary secretion of therapeutic agents limits their systemic exposure which leads to the exclusion of possibly beneficial therapeutic agents in the early stages of drug development. Biliary excretion of drugs or metabolites can exert dose-limit toxicities on exposure of intestinal epithelia to pharmacologically active or toxic species. Compounds that experience

biliary excretion undergoes systemic reabsorption followed by metabolism or elimination in feces. Hepatic transport systems are considered as one of the critical factor of the enterohepatic recycling of compounds.

***Interindividual Variability In Drug Pharmacokinetics And Pharmacodynamics*.**

Disposition of many endogenous and exogenous compounds, including drugs and metabolites may alter significantly on any disease-associated or genetic alterations in the expression and/or function of hepatic transport proteins. Hepatic transporters are known to be responsible for causing important variations in the disposition, pharmacological activity, and toxicity of many therapeutic agents. A major prerequisite in order to achieve therapeutic outcomes in varied patient population is the extensive knowledge about mechanism responsible causing interpatient variability via hepatic drug transport systems.

Drug/Nutrient-Transport Interactions

Activity of hepatic transport protein may be enhanced or impaired on interacting with drug and nutrients. These interactions may alter the expression and function of hepatic transporters and can be direct or indirect in nature. In future, revelation of clinically important interaction with hepatic transporters and the approaches to foresee these interactions may offer several exciting prospects for membrane transporter related research.

Nomenclature [1]

Nomenclature of hepatic transport system is a challenging discipline. New proteins were promptly recognized and termed with the introduction of molecular biology methods. Early nomenclature of hepatic transporters is recognized as descriptive, cumbersome and duplicative. In order to avoid this timeworn convoluted nomenclature, guidelines approved by HUGO Gene Nomenclature Committee were employed. Hepatic transporters belongs two major families: (i)

solute carriers superfamily (SLC/SLCO) and (ii) ATP-binding cassette superfamily (ABC). As per guidelines, upper case refers to the human and lower case refers to the rodent genes and gene products.

Drug or Membrane Transporters of the Hepatic Basolateral Membrane

Elimination via hepatic route is usually an order of events which involves uptake of xenobiotics from the sinusoidal blood followed by intracellular metabolism, and finally excretion. In humans, molecules excreted from hepatocytes into the bile were stored in the gallbladder and released intermittently into the upper small intestine or the basolateral membrane into sinusoidal blood followed by elimination by other excretory organs. Hepatocytes having dissimilar basolateral (sinusoidal and lateral) and apical (canalicular) membrane domains that be at variance in lipid and protein composition facilitates the flux of drug molecules/substrates through the hepatobiliary system. Gene superfamily of solute carriers (SLC) represents the basolateral hepatic transport proteins which helps in translocation of substrates to and from the sinusoidal blood **(Fig.1.1)**. Selected substrates and inhibitors of the human transport proteins expressed on the hepatic basolateral and apical (canalicular) membranes are mentioned in **Tables 1.1 and 1.2**, respectively.

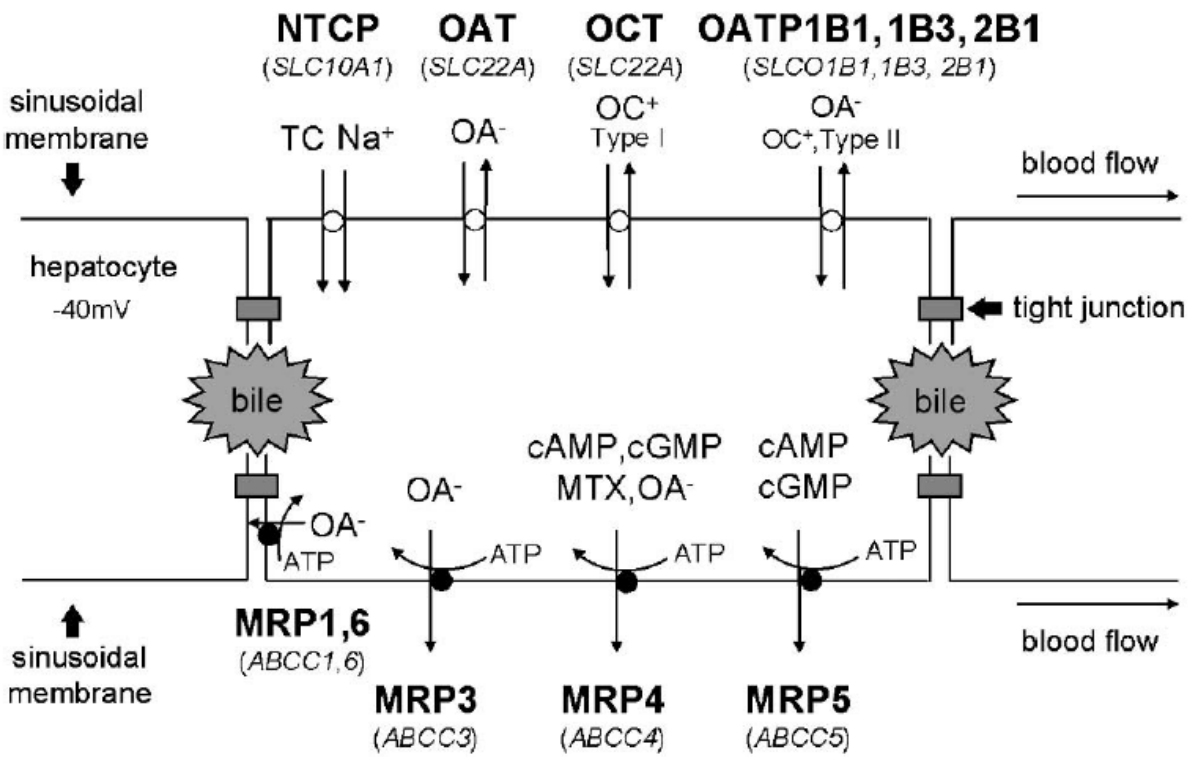

Fig.1.1: Human hepatic basolateral transport proteins. Schematic representation of three adjacent hepatocytes with interconnecting canalicular spaces sealed by tight junctions. Sinuosoidal blood flowing through the liver bathes hepatocytes and delivers solutes to the basolateral hepatic membrane for uptake. Important basolateral transport proteins (protein name is in bold type with gene symbol listed below) are depicted with arrows denoting the direction of transport and ATP-dependent transporters designated by ●. For the OAT and OCT families, only mRNA have been detected in human liver. Typical substrates are listed (OA-, organic anions; OC+, organic cations; MTX, methotrexate; cAMP, adenosine 3',5'-cyclic monophosphate; cGMP, guanosine 3',5'cyclic monophosphate). (Reproduced with permission, Brouwer K.M. *et al* [1])

Table 1.1: Human Hepatic Basolateral Transport Proteins

(Reproduced and modified with permission, Brouwer K.M. *et al* [1])

Basolateral Protein	Gene Symbol	Substrates	Inhibitors
NTCP	*SLC10A1*	Bromosulphophthalein, cholate, estrone-3-sulfate, glycocholate taurochenodeoxycholate, tauroursodeoxycholate,	Cyclosporine, irbesartan, ritonavir, bendroflumethiazide, doxazosin, rifampicin
OATP1A2	*SLCO1A2*	Bile acids, methotrexate, estrone-3-sulfate, n-methyl quinine; ouabain, dehydroepiandrosterone sulphate, fexofenadine, bromosulphophthalein, digoxin, levofloxacin,statin	Naringin, ritonavir, lopinavir, saquinavir, rifampicin
OATP1B1	*SLCO1B1*	Bile acids, ouabain, estrone-3-sulfate, bromosulphophthalein, estradiol-17β-glucuronide, statins, repaglinide, valsartan, olmesartan,	Saquinavir, ritonavir, lopinavir, rifampicin, cyclosporine

		bilirubin glucuronide, bilirubin,	
OATP1B3	*SLCO1B3*	Bile acids, ouabain, estrone-3-sulfate, bromosulphophthalein, estradiol-17β-glucuronide, cholecystokinin 8, statins, digoxin, fexofenadine, telmisartan glucuronide, telmisartan, valsartan, olmesartan,	Rifampicin, cyclosporine, ritonavir, lopinavir
OATP2B1	*SLCO2B1*	Benzylpenicillin, estrone-3-sulfate, bromosulphophthalein, taurocholate, statins, fexofenadine, glyburide, taurocholate	Rifampicin, cyclosporine
OAT2	*SLC22A7*	Prostaglandin E_2, prostaglandin $F_{2\alpha}$, salicylate, tetracycline, zidovudine, paclitaxel, theophylline	Diclofenac, mefenamic acid, bumetanide, cyclothiazide
OAT4	*SLC22A11*	Bumetanide, estrone-3-sulfate ketoprofen, salicylate,	Telmisartan, losartan, valsartan,

		methotrexate, ochratoxin A prostaglandin E_2, prostaglandin $F_{2\alpha}$, tetracycline, zidovudine, uric acid	olmesartan, indomethacin, furosemide
OCT1	*SLC22A1*	Azidoprocainamide methoiodide, n-methyl-quinidine, n-methyl-quinine, tributylmethylammonium, tetraethylammonium, 1-methyl-4-phenylpyridinium	Imatinib, nilotinib, gefitinib, erlotinib, atropine, prazosin
OCT3	*SLC22A3*	Adrenaline, noradrenaline, tyramine, agmatine, 1-methyl-4-phenylpyridinium, metformin, pindolol, procainamide, ranitidine, varenicline	Quinidine, cimetidine, testosterone
MRP1	*ABCC1*	Daunorubicin, doxorubicin, etoposide, vincristine	MK-571, probenecid, reversan, JS-2190
MRP3	*ABCC3*	Estradiol-17β-glucuronide, methotrexate, fexofenadine, glucuronate conjugates, acetaminophen, monovalent and sulfated bile salts	Delaviridine, efavirenz, emtricitabine

MRP4	*ABCC4*	Adefovir, tenofovir, dehydroepiandrosterone sulphate, methotrexate, topotecan, furosemide, adenosine 3', 5'-cyclic monophosphate, guanosine 3',5'-cyclic monophosphate, bile acids plus glutathione, azidothymidine, 9-(2-phosphonomethoxyethyl) adenine	Celecoxib, diclofenac
MRP5	*ABCC5*	adenosine 3', 5'-cyclic monophosphate, guanosine 3',5'-cyclic monophosphate, pemetrexed	Methotrexate, sildenafil, 5-fluorodeoxyuridine monophosphate, dipyridamole, methotrexate
MRP6	*ABCC6*	9-(2-phosphonomethoxyethyl) adenine, cisplatin, daunorubicin, Leukotriene C4, [cyclo(D-Trp-D-Asp-L-Pro-D-Val-L-Leu)]	Benzbromarone, indomethacin, probenecid

MRP7	*ABCC10*	Leukotriene C4, Estradiol-17β-glucuronide	Lapatinib, erlotinib, ponatinib, tariquidar
MRP8	*ABCC11*	Adenosine and guanosine 3', 5'-cyclic monophosphate	

Table 1.2: Human Hepatic Apical (Canalicular) Transport Proteins

(Reproduced and modified with permission, Brouwer K.M. et al [1])

Apical (Canalicular) Protein	**Gene Symbol**	**Substrates**	**Inhibitors**
BSEP	*ABCB11*	Conjugated and unconjugated bile salts, taurocholate, pravastatin	Cyclosporin A, rifampicin, glibenclamide
MRP2	*ABCC2*	Acetaminophen glucuronide, carboxydichlorofluorescein, camptothecin, doxorubicin cisplatin, vincristine, etoposide, glibenclamide; indomethacin, rifampin, glucuronide, glutathione, and sulfate conjugates, leukotriene C4, methotrexate, pravastatin, valsartan, olmesartan,	Cyclosporine, delaviridine, efavirenz, emtricitabine

		glucuronidated SN-38	
MDR1 or P-gp	*ABCB1*	Amprenavir, indinavir, nelfinavir, ritonavir, saquinavir Aldosterone, corticosterone, dexamethasone, digoxin, cyclosporin A, mitoxantrone, debrisosoquine, erythromycin, lovastatin, terfenadine, digoxin, quinidine, doxorubicin, paclitaxel, rhodamine 123, etoposide, fexofenadine, losartan, vinblastine, tacrolimus, talinolol, loperamide, berberine, irinotecan,	Cyclosporine, quinidine, tariquidar, verapamil
MDR3	*ABCB4*	Phosphatidylcholine, paclitaxel, digoxin, vinblastine, phospholipids	Verapamil, cyclosporine
BCRP	*ABCG2*	Mitoxantrone, methotrexate, topotecan, imatinib, irinotecan, statins, sulphate conjugates, porphyrins, daunorubicin, doxorubicin	Estrone, 17β-estradiol, fumitre - morgin C

Na^+-taurocholate co-transporting polypeptide (NTCP)

NTCP is a membrane transporter responsible for uptake of sodium-dependent bile salt [2]. This membrane transporters requires two sodium for translocation of each taurocholate (TC) molecule and is also responsible for uptake of bile salt in rodents [3]. NTCP shows higher affinity towards conjugated bile salts (TC, tauroursodeoxycholate, taurochenodeoxycholate) than unconjugated bile salts (cholate). Non-bile salt substrate for this transporter protein are dehydroepiandrosterone sulfate (DHEAS), thyroxine (T4), bromosulfophthalein (BSP), 3,3',5-triiodo-L-thyronine (T3) and estrone-3-sulfate [3] [4, 5].

Organic Anion Transporting Polypeptides (OATPs)

OATP family of transporter proteins play a vital role clearance of many drugs via hepatic route. Substrates of OATPs are unrestrained rather than specific, which includes variety of organic anions, few type II cations (bulky molecules with cationic groups located near the ring; e.g., quinidine) and neutral steroids. OATP transporter proteins may act in a bi-directional manner and are sodium independent. High concentration of reduced glutathione within the hepatocyte may act as the driving force for the translocation of substrates of hepatic OATPs [3, 6]. Eleven members of the OATP transporter proteins have been identified in humans **Table 1.3**. Expression of OATPs has been reported in various tissues including intestine, liver, kidney and brain, and are recognized to play an important role in drug absorption, distribution and the elimination of endogenous and exogenous compounds including drugs in clinical use [7].

Table 1.3: Characteristics of human OATP family members

(Reproduced and modified with permission, Jorg Konig [8])

Protein Name	Gene Symbol	Amino Acids	Tissue Distribution
OATP1A2	*SLCO1A2*	670	Brain, Kidney
OATP1B1	*SLCO1B1*	691	Liver
OATP1B3	*SLCO1B3*	702	Liver
OATP1C1	*SLCO1C1*	712	Brain, Testis
OATP2A1	*SLCO2A1*	643	Ubiquitous
OATP2B1	*SLCO2B1*	709	Ubiquitous
OATP3A1	*SLCO3A1*	710	Ubiquitous
OATP4A1	*SLCO4A1*	722	Ubiquitous
OATP4C1	*SLCO4C1*	724	Kidney
OATP5A1	*SLCO5A1*	848	Kidney, Ovary
OATP6A1	*SLCO6A1*	719	Testis

Expression of OATP1A2, OATP1B1 and OATP1B3 has been predominantly found in human liver. In comparison to OATP1A2 and OATP1B3, OATP1B1 plays a critical role in Na^+-independent bile salt uptake system in human liver, whereas OATP2B1 does not play any role in translocation of bile salts. All four human OATP proteins transports bromosulphophthalein (BSP), estrone-3-sulfate and dehydroepiandrosterone (DHEAS), however extent of uptake differs due to varied affinity [9]. Affinity of OATP isoforms of rodent and human species cannot be predicted on the basis of amino acid sequence, since the Slco gene products corresponding to rodents are not orthologs of human OATP proteins [10]. This poses a major challenge in the process of drug development as OATPs are involved in the hepatic uptake of many therapeutic agents. These variability in the affinity of substrates towards OATPs of different species will make it difficult to predict hepatic clearance or drug interactions in hepatic transport (if hepatic uptake is the rate-limiting step in hepatic clearance of a compound) considering that distinct proteins exhibiting different substrate specificities may be involved. Deltorphin II is a specific substrate for rat Oatp1a1 whereas its other substrates include monovalent and sulfated bile salts, glucuronide, and glutathione conjugates [11, 12]. Rat Oatp1a1 shares this substrate specificity except sulfate conjugates with Oatp1a4. However, digoxin is a specific substrate of Oatp1b4 [3]. Oatp1b2 is expressed on the basolateral membrane of liver and expresses high affinity towards DHEAS, BSP, leukotriene C4 (LTC4), and anionic peptides [12]. mRNA expression of OATP3A1 and OATP4A1 has been reported in hepatic tissue, also translocation of estrone-3-sulfate is mediated via OATP1B1, 2B1, 3A1, and 4A1 whereas OATP4A1 also was helps in transport of 3,3’,5-triiodo-L-thyronine, thyroxine and taurocholate [10, 13]. Little information has been available so far regarding the transport and biochemical properties of OATP5A1 [14].

Organic Anion Transporters (OATs)

OATs gene family (Slc22) was first cloned in kidney. Expression of Oat2 and Oat3 was found to be predominant in rat hepatic tissue and helps in translocation of prototypic anionic substrate paraaminohippurate. Also Oat 2 play a vital role in uptake of dicarboxylates, indomethacin, methotrexate, salicylate, prostaglandinE2 (PGE2), and nucleoside derivatives, whereas uptake of cimetidine, estrone-3-sulfate, and ochratoxin A is mediated via Oat3 [15] [16]. It has been postulated that Oat proteins expressed on basolateral membrane of hepatic tissue physiologically function as excretion system. mRNA expression of Oat3 has been reported in human liver [17, 18]. OAT2 and OAT4 exhibits overlapping substrate specificities including prostaglandin F2α (PGF2α), tetracycline, salicylate, zidovudine, and PGE2 [19-23], also OAT4 shows its substrate specificity towards methotrexate and ochratoxin A [24, 25].

Organic Cation Transporters (OCTs and OCTNs)

OCTs are responsible for hepatic uptake of smaller type I organic cations (e.g., tetraethylammonium, azidoprocainamide methoiodide) [26, 27]. Expression of Oct1 has been reported on basolateral membrane of rat hepatocytes [28]. Little information is available on the expression and function of OCT3, however it has been reported that OCT3 helps in transport of -methyl-4-phenylpuridinium iodide in the HepG2 hepatoma cell line [29]. Novel organic cation transporters were classified as OCTN1 and OCTN2 of SLC22 gene family containing a nucleotide binding site sequence motif [30, 31]. Information is still missing on exact membrane localization and substrate specificity of these novel OCTs in rat and human liver.

Multidrug Resistance Associated Protein1 (MRP1)

MRP subfamily may play a major role in excretion of drugs or metabolites from the human hepatocyte to sinusoidal blood. MRP family is classified into nine members, out of which, 7

members are responsible for hepatic elimination of organic anions. Expression of MRP1 is lower in lateral levels and is primarily expressed in intracellular vesicles in human hepatocytes [32-34]. It has been reported that intracellular GSH has one of the requirement for transport of drugs mediated via MRP1, however it's not the case with the transport of conjugated drugs [35].

Multidrug Resistance Associated Protein3 (MRP3)

Mrp3 expressed on basolateral membrane of hepatic tissues mediates the hepatic elimination of monovalent (e.g., taurocholate and glycocholate) and sulfated bile salts, as well as other organic anions such as E217G, methotrexate and acetaminophen glucuronide [36-38]. Mrp3 shows higher affinity towards glucuronide conjugates than glutathione conjugates [37]. Phenobarbital and cholestatic conditions induces the expression level of Mrp3 in rats [39]. Humans exhibiting naturally occurring hereditary defects in biliary excretion of organic anions shows induced levels of MRP3/Mrp3 [40]. Induced expression of MRP3/Mrp3 acts as a compensatory mechanism for the reduced ability to excrete organic anions into bile. Mrp3 is hypothesized to play a vital role in enterohepatic circulation of bile salts [37].

Multidrug Resistance Associated Protein4 and 5 (MRP4 and MRP 5)

Translocation of cyclic nucleotides adenosine 3', 5'-cyclic monophosphate (cAMP) and guanosine 3', 5'-cyclic monophosphate (cGMP) is mediated via MRP4 and MRP5 expressed on the basolateral membrane of hepatic tissue [41]. Due to utilization of different *in vitro* systems, various discrepancies has been reported in the K_m values for MRP4 and MRP5 [42, 43]. These transporter proteins also translocates methotrexate (42), the antiviral agent 9-(2-phosphonomethoxyethyl) adenine and the reverse transcriptase inhibitor azidothymidine [44, 45]. Sulfated bile acids and steroids competitively inhibit transport of MRP4 substrates. Induced level of expression of Mrp4 was reported with chronic elevation of bile acid levels [46, 47].

Multidrug Resistance Associated Protein6 (MRP6)

Expression of Mrp6 has been reported on both apical and basolateral in rat hepatocytes. Mrp6 transporter protein does not play any vital role in governing hepatic excretion of phase II biotransformation products (e.g., glucuronide, sulfate, and glutathione conjugates), since it is not involved in the translocation of typical anionic substrates except cyclopentapeptide BQ-123. Mrp6 transporter exhibit high levels of expression in human liver and kidney, although information is still lacking examining the role of this transporter in drug transport [48, 49].

Multidrug Resistance Associated Protein7 and 8 (MRP7 and MRP 8)

mRNA expression of MRP7 has been reported in various tissues including liver. Also, E217G and LTC4 exhibited their substrate specificity towards MRP7 [50, 51]**.** Liver shows higher mRNA expression of MRP8 in comparison to breast and testis. MRP8 shares overlapping substrate specificity with MRP5 including transport of cyclic nucleotides [52, 53].

Drug or Membrane Transporters of the Hepatic Apical (Canalicular) Membrane

Bile Salt Export Pump (BSEP)

These export pumps transports xenobiotics and metabolites across the canalicular membrane into bile via unidirectional ATP-dependent process **(Fig.1.2)**. These canalicular membrane transporters belong to the ABC superfamily of transporters **[54]**. This transporter is also referred as sister gene of P-glycoprotein and eliminates conjugated and unconjugated bile salts into the canalicular space **[55]**. Absence of BSEP from the apical membrane and mutation in *ABCB11* gene in patients with progressive familial intrahepatic cholestasis type 2 (PFIC2) leads to diminished biliary bile salt concentrations relative to normal patient **[56, 57]**. BSEP does not play any important role in hepatic excretion of therapeutic agents, however it may act as an important site for transporter mediated drug interactions.

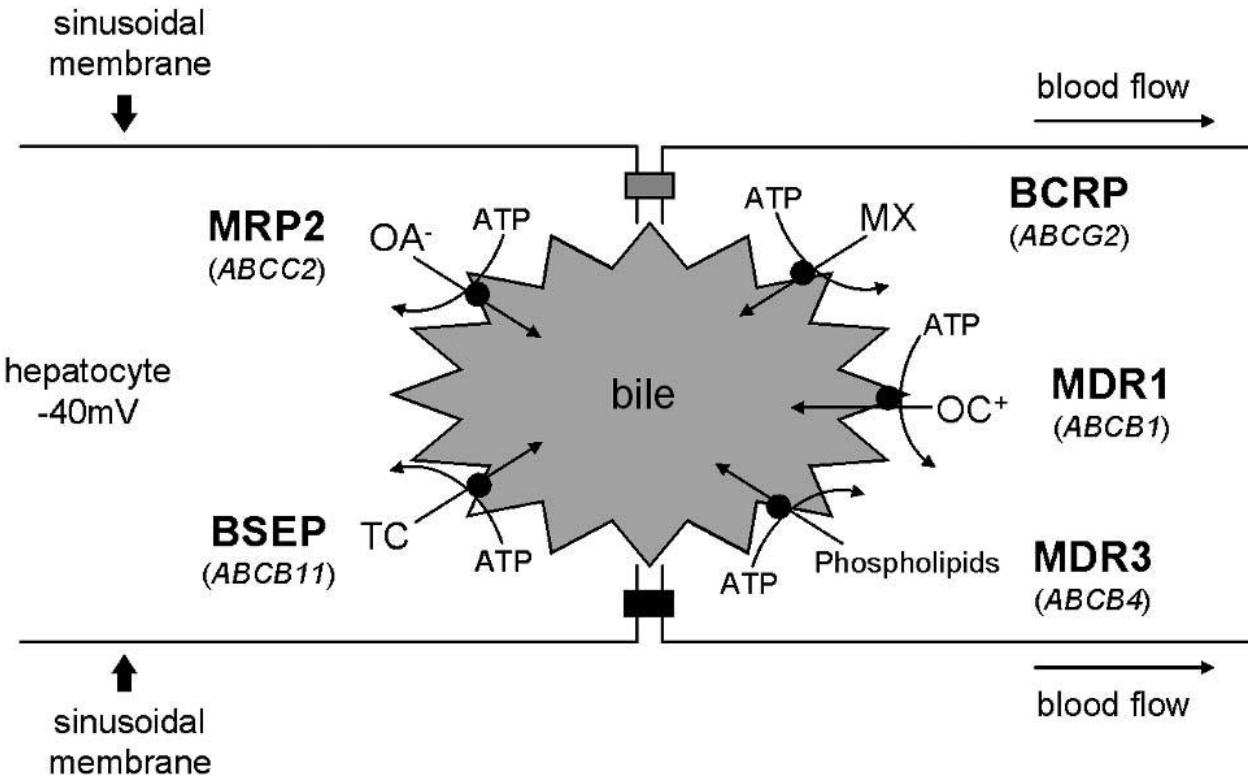

Fig.1.2: Human hepatic canalicular transport proteins. Schematic representation of two adjacent hepatocytes as described in Fig.1.1. Important canalicular transport proteins (protein name is in bold type with gene symbol listed below) are depicted with arrows denoting the direction of transport and ATP-dependent transporters designated by ●. Typical substrates are listed (OA-, organic anions; OC+, organic cations; TC, taurocholate; MX, mitoxantrone). (Reproduced with permission, Brouwer K.M. *et al* [1])

Multidrug Resistance Associated Protein2 (MRP2)

This membrane transporter was earlier referred as the canalicular multispecific organic anion transporter (cMOAT) and is the most extensively evaluated canalicular member of the MRP/Mrp family. It is responsible for biliary excretion of organic anions including LTC4, divalent bile salts, and glutathione, glucuronide, and sulfate conjugates [58]. In patients with Dubin-Johnson syndrome, Groningen Yellow/Transport-deficient Wistar rats (GY/TR^-) and Eisai hyperbilirubinemic Sprague-Dawley rats (EHBR), absence of these apical hepatic transporter forms the basis for the defect in biliary excretion of organic anions [40, 59-61]. In rats and patients with downregulated expression of Mrp2, biliary excretion of organic anions, including conjugated bile acids is compensated by upregulated expression of MRP3/Mrp3 which help in elimination of organic anions, including conjugated bile acids [62]. Elimination profile of compound, whether the compound gets eliminated in bile or urine, will determine its affinity towards canalicular and basolateral excretory transporters, as well as the activity of the respective transporters. Hepatic elimination of compounds get significantly influenced by altered transporter activity due to drug or nutrient interactions or patient-specific factors such as disease, genetics.

Multidrug Resistance Protein1 or P-glycoprotein (MDR1 or P-gp)

It is the most widely studied and examined hepatic canalicular transporter. Interactio of anti-cancer agents with P-gp has been postulated as one of the major reason for the development of chemo resistance to an array of chemotherapeutic agents that exhibit a wide range of structures and mechanisms of action [63]. Translocation of hydrophobic cations is mediated via MDR1 transporter protein. Characteristics of typical substrate of MDR1 are presence of planar aromatic rings which interacts with a hypothesized “flat” hydrophobic region of the MDR1 drug-binding domain, a cationic charge at physiological pH, a bulky structure having molecular weight >400

and a log partition coefficient >2 [64, 65]. Importance of MDR1 in the distribution and elimination of relatively small, aliphatic and aromatic, permanently charged cationic molecules has been demonstrated in several studies carried out on Mdr1 gene knockout mice [66, 67]. Various MDR1 substrates include

daunorubicin, doxorubicin, etoposide, paclitaxel, vinblastine, vincristine, pazopanib, vandetanib, sorafenib, digoxin, methadone, morphine, rhodamine 123, cyclosporin A, etc [68]. In order to narrow down the substrate affinities, specificities, structural requirement, binding sites of modulators towards MDR1, a three-dimensional quantitative structure- activity relationship (QSAR) models for MDR1 have been developed [69-71]. Evidently, in the hepatic excretion of a xenobiotics including many drugs and metabolites, MDR1 plays an important role.

Protein-calorie malnutrition downregulates levels of expression and activity of Mdr1 in rat canalicular plasma membrane vesicles by ∼22% and ∼35%, respectively [72]. Overexpression of COX-2 has been directly related to overexpression Mdr1 protein levels in renal rat mesangial cells, leading to increased Mdr1 activity as measured by rhodamine 123 efflux [73]. Also, upregulated levels of Mdr1 expression has been reported on exposure to ultraviolet irradiation and heat shock, however downregulation of Mdr1 expression has resulted in rodents from lipopolysaccharide induced endotoxemia [74, 75]. Release of cytokines such as interleukin-1β and -6 also modulates expression of Mdr1 [75]. In addition, Mdr1 may be regulated by a variety of factors.

Multidrug Resistance Protein3 (MDR3)

Uptake of phosphatidylcholine translocase is primarily mediated via MDR3 and its rodent ortholog Mdr2. Biliary phospholipid secretion is regulated via MDR3 and Mdr2 in humans and rodents, respectively. Mutation in ABCB4 gene has been reported in patients classified with PFIC

type 3 cholestasis. Still more information is needed in order to establish the physiologic role of MDR3 as a drug transporter [76].

Breast Cancer Resistance Protein (BCRP)

Breast cancer resistance protein, a 72-kDa transporter protein also referred as half ABC transporter [77]. It confers resistance to mitoxantrone, doxorubicin, daunorubicin and sulfated conjugates by causing protein dimerization in the plasma membrane [78]. BCRP is reported to express in several tissues placenta, small intestine, blood-brain barrier, colon, hepatic canalicular membrane, breast, and venous and capillary endothelium [79]. Apart from other apical hepatic transporters, biliary excretion of the sulfated conjugates of steroids and xenobiotics is also mediated via BCRP.

Hepatobiliary Drug Transport Model Systems

Absence of suitable model systems that replicate hepatic anatomy, hepatocyte function and bile formation is a major restriction in the field of hepatobiliary transport. The advantages of *in vivo* and isolated perfused liver techniques, in terms of reflecting the true physiologic state of the liver, are offset by difference in hepatic transport proteins and varied affinity of compounds may exist between rodents and humans. Also, it is very difficult to examine individual hepatic uptake and excretion mechanisms due to the complications associated with whole organ. It is very difficult to assess the role of individual hepatic transporter on drug disposition due to the non-existence of specific and potent inhibitors for the hepatic transport proteins. Relative to other *in vitro* systems, hepatocytes are more advantageous in terms of providing liver-specific cellular functions (plasma membrane vesicles; transport proteins transfected in non-mammalian cells) and can be utilized to study function of specific transport proteins. Also, hepatocytes of free of any concerns related to species differences in hepatobiliary disposition [80, 81]. For studying hepatic excretion, isolated

hepatocytes poses some challenges like loss of cell polarity and redistribution of canalicular membrane proteins, however, these cells have been extensively employed to evaluate hepatic transport mechanism [82]. In various transport trafficking and regulation studies, hepatocyte-derived cell lines (WIF-B and HepG2) showing strong correlation to bile canaliculi has been utilized [83-86]. Sandwich culture hepatocytes that demonstrates strong and intact canalicular networks and also maintains hepatic transport protein expression and function are employed as an important *in vitro* model system to study hepatobiliary disposition of therapeutic agent and metabolites [87-89].

For uptake transporter analysis, human embryonic kidneys (HEK) and Chinese hamster ovary (CHO) cells transfected with the respective transport protein were utilized. These cell systems are employed to standardize uptake assays and also for comparing, for example, regarding drug-drug interactions (DDIs). These analyzing of DDIs involves comparing the uptake of the single drug with the uptake of the single drug in the presence of a drug which can modulate the function of respective transporter protein. These cell systems provides great advantages regarding the standardization of the uptake assay, by using the same cell density, different uptake assays can be compared from different days. These *in vitro* model based systems are frequently employed for the analysis of DDIs and also for the functional consequences of polymorphisms [90, 91]. Although, these transfected cell lines play a major role in demonstrating the uptake of a compound via specific transporter but still may poses a challenge in predicting the role of specific transport protein in overall hepatobiliary disposition of a compound when multiple transport systems are present.

Sandwich cultured can be employed to evaluate analogs of specific transport properties (limited or enhanced hepatobiliary uptake or efflux) at the early stages of lead optimization and

candidate selection in the process of drug development. At later stages of drug development, tranfected cell lines or *in vivo* models systems may act beneficial in order to study the significance of transport inhibition and/or identify contrivances responsible for hepatotoxicity [1].

Advancements In Hepatobiliary Drug Transport

In order to enhance understanding hepatic transport biology and how drugs and/or disease affecting intracellular regulatory mechanisms may modify hepatic transport of endogenous and exogenous compounds, one should have knowledge about the basic regulation hepatic transport. Alteration in the membrane transporter function or deviations in the number of molecules translocate across membrane defines the mechanism governing membrane transport. Modulation of transporter protein expression can occur at any level protein synthesis including transcription, translation, and post-translation. Modulation of transporter gene expression in hepatocytes is governed by transcription factors [92]. Developmental as well as physiological responses to both endogenous and exogenous compounds is mediated via nuclear hormone receptors comprising of superfamily of ligand-activated transcription factors. Interaction of xenobiotics with these receptors results in formation of complex with regulatory region of the gene leading modification in expression these receptors. On binding of ligand to receptor, already formed complex binds with heterodimeric partner retinoic acid X receptor (RXR) leading to initiation of transcription. Various nuclear hormone receptor types were reported to be involved in the transcriptional regulation of hepatic transport proteins: pregnane X receptor (PXR), peroxisome proliferator-activated receptor α (PPARα), farnesoid X receptor (FXR), liver X receptor (LXR), and the constitutive androstane receptor (CAR). Till now, research is still ongoing in order to decode the ligands essential or required for these nuclear hormone receptors and the role they play in transcriptional control of

transporter gene expression. **Table 1.4** summarizes the information on regulation of hepatic transport proteins.

Table 1.4: Regulation of Hepatic Transport Proteins

(Reproduced with permission, Brouwer K.M. *et al* [1])

Transport protein	Suppression (↓) activation (↑)	Nuclear receptor*	Ligand
NTCP	↑	RARα	Retinoids
	↓	SHP	Activation by FXR
OATP1B1	↓	SHP	Activation by FXR
OATP1B3	↑	FXR	Bile Acids
MRP3	↑	CAR	Phenobarbital
BSEP	↑	FXR	Bile Acids
MRP2	↑	PXR, CAR, FXR	Xenobiotics
MDR1	↑	PXR	Xenobiotics
MDR3/Mdr2	↑	PPARα	Fatty acids, fibrates, DHEAS

***Abbreviations used: CAR, constitutive androstane receptor; FXR, farnesoid X receptor; PPAR, peroxisome proliferator-activated receptor; PXR, pregnane X receptor; RAR, retinoic acid receptor; SHP, small heterodimer partner**

Downregulation of Slc10a1 via an Fxr-mediated induction of shp (small heterodimeric protein) has been reported in primary rat hepatocytes and transfected HepG2 cells on bile acid treatment [93]. Transcriptional down regulation of Slc10a1 and Abcc2 gene expression by the retinoic acid receptor and RXR leads to cytokine-mediated inflammatory cholestasis [94]. On treating HepG2 cells with chenodeoxycholic acid, enhanced expression SLCO1B3 mRNA was reported, which was attributed to FXR mediated regulation of SLCO1B3 [95]. Also, studies reported on PXR negative mice showed that regulation of Slco1a4 is mediated via PXR dependent pathway. Enhanced expression of Abcc3 mRNA was observed on administering wild type mice

with pregnenolone-16α-carbonitrile (PXR ligand), however PXR knockout mice did not show any effect [96]. On the basis of studies carried out using Wistar Kyoto rats revealed that induction of Mrp3 by phenobarbital does not involve any active involvement of CAR [97]. FXR/RXRα heterodimer plays a vital role on transcriptional regulation of ABCB11 gene on exposure to bile acid chenodeoxycholic acid [98]. Induction of ABCC1 and ABCC2 gene expression on exposure to redox-active compounds has been reported by Kauffman *et al* [99]. On incubating rat hepatocytes and Abcc2 promotor-transfected HepG2 cells with agonists of these nuclear hormone receptors, induction in Abcc2 mRNA was observed in a PXR, CAR, and FXR-dependent manner [100]. Transcription regulation of CYP3A4 and MDR1 is mediated via PXR [101-103]. Studies using wild-type and PPARα-knockout mice demonstrated fibrates induced stimulation of the phospholipid flippase MDR3 is mediated by PPARα [104].

Short-term regulation and trafficking of hepatic transporters has been examined and reported in some of the recent work [105-107]. Recruitment and storage of transporters occurs from a compartment referred as intracellular vesicles in which membrane protein resides [108, 109]. In response to several different cellular stimuli insertion or recruitment of transporter takes place. Internalization of Mrp2 occurs on disruption of cell-cell contacts in hepatocytes [110]. Internalization of Mrp2 molecules in hepatic intracellular vesicles occurs in hyperosmotic conditions, however increased Mrp2 content in the canalicular membrane was observed in hypoosmolarity [111]. Various signaling pathways governs the transporter translocation to and from the canalicular membrane. Protein content of Mdr1, Mdr2, Bsep, and Mrp2 increased 1.5-fold by TC and 3-fold by 2'-O-dibutyryl adenosine 3', 5'-cyclic monophosphate (DBcAMP), a cell-permeable cAMP analog in canalicular membrane vesicles [112]. On treating Mdr1, Mdr2, Bsep, and Mrp2 with colchicine (a microtubule inhibitor), the effect of TC was completed blocked

whereas the effect of DBcAMP was partially blocked, proposing that trafficking of these transporters to the apical (canalicular) membrane occurs moderately through microtubules. The short-term regulation of hepatic basolateral transporters also has been investigated. On treatment with cAMP, trafficking of Ntcp from endosomes to the basolateral membrane was revealed by employing cellular fractionation studies [106]. This mechanism involves several pathways including phosphoinositide 3-kinase and protein kinase B and was sensitive to cytochalasin D (actin filament formation inhibitor). cAMP directly affects protein activity via direct phosphorylation of the transporter, apart from stimulating trafficking of proteins from endosomal compartments to their respective membrane. Increased phosphorylation without internalization of the protein has been recognized as a major reason for the loss of transport activity of Oatp1a1 [113]. The examples mentioned before demonstrates that intracellular cAMP levels can be modulated in a therapeutic manner to regulate hepatocyte function in liver disease (i.e., cholestasis). Hepatic transport including the hepatobililary disposition and systemic exposure to drugs and metabolites is a highly governed process and can be influenced translocation of proteins.

Drug Interactions Involved In Hepatic Transport

Several drug interaction in regards to hepatic transport have been reported in last decade **(Table 1.5)**. Partial inhibition of uptake of cerivastatin in human hepatocytes was observed on treatment with cyclosporin A (CsA). CsA is an inhibitor of OATP1B1 transporter protein whereas cerivastatin is a substrate of same transporter. Inhibition of OATP1B1 transporter results in 3 to 4 fold increase in the in the plasma AUC and C_{max} of cerivastatin on coadministration of CsA in kidney transplant patients [114, 115]. Quinidine is an inhibitor of MDR1 transporter. Co-administration quinidine with digoxin (MDR1 substrate) resulted in diminished biliary excretion of digoxin by 42% [116, 117]. Decrease in cumulative biliary excretion of doxorubicin and its

major metabolite, doxorubicinol, by 84% and 72%, respectively, was observed in comparison to control, when doxorubicin, a Mdr1 substrate, was coadministered with GF120918 (MDR1/Mdr1 inhibitor) [118]. This transporter mediated drug interaction leading to diminished biliary excretion of doxorubicin and doxorubicinol by 82% and 62%, respectively, in comparison to wild-type mice was confirmed *in vivo* with bile-duct cannulated Abcb1a(−/−) mice [119]. Besides inhibition interactions, increase biliary clearance of substrates of the hepatic transporters has been observed when the expression of these transporters get induced. Example, long term treatment of rats with tamoxifen (an Mdr1 substrate and inducer) leads to not only ∼12-fold increase in hepatic Abcb1b mRNA but also enhanced biliary excretion of tamoxifen and metabolites from 8–51% [120]. Transporter mediated drug interaction has also been held responsible for drug-induced hepatotoxicity. Inhibition of Bsep by bosentan leads to enhanced intracellular accumulation of cytotoxic bile salts which may cause bile salt-induced liver damage which ultimately causes cholestatic liver injury. Research is still going on in many laboratories in order to reveal the exact mechanism accountable for hepatic transporter mediated drug interactions [121].

Table 1.5: Transporter based clinical drug–drug interactions

(Modified from Giacomini KM *et al* [122] and Brouwer K.M. *et al* [1])

Drug Transporter	Interacting Drug	Affected Drug	Clinical Pharmacokinetic Impact On Affected Drug
Organic Anion Transporting Polypeptides	Cyclosporine	Pravastatin	AUC ↑890% and C_{max} ↑678%
	Cyclosporine	Rosuvastatin	AUC ↑610%
	Cyclosporine	Pitavastatin	AUC ↑360% and C_{max} ↑560%
	Cyclosporine	Cerivastatin	3- to 4- fold ↑ in AUC and C_{max}
	Rifampicin (single dose)	Glyburide	AUC ↑125%
	Rifampicin (single dose)	Bosentan	C_{trough} ↑500%
	Lopinavir/ritonavir	Bosentan	Day4: C_{trough} ↑4,700% and day10: C_{trough} ↑400%
	Lopinavir/ritonavir	Rosuvastatin	AUC ↑107% and C_{max} ↑365%
Organic Anion Transporters	Probenecid	Cidofovir	CL_r ↓32%
	Probenecid	Furosemide	CLr ↓66%
	Probenecid	Acyclovir	CL_r ↓32% and AUC ↑40%

	Probenecid	Cidofovir	CL_r ↓32%
	Probenecid	Furosemide	CL_r ↓66%
	Probenecid	Acyclovir	CL_r ↓32% and AUC ↑40%
Organic Cation Transporters	Cimetidine	Metformin	AUC ↑50% and CL_r ↓ 27%
	Cimetidine	Pindolol	CL_r ↓~34%
	Cimetidine	Varenicline	AUC ↑29%
	Cimetidine	Pilsicainide	AUC ↑33%, CL_r ↓28%
	Cetirizine	Pilsicainide	CL_r ↓41%
	Cimetidine	Dofetilide	CL_r ↓33%
	Cimetidine	Metformin	AUC ↑50% and CL_r ↓ 27%
	Cimetidine	Pindolol	CL_r ↓~34%
P-glycoprotein	Quinidine	Digoxin	CL_r ↓34–48%
	Ritonavir	Digoxin	AUC ↑86%
	Dronedarone	Digoxin	AUC ↑157% and C_{max} ↑75%
	Ranolazine	Digoxin	AUC ↑60% and C_{max} ↑46%
	Quinidine	Digoxin	CL_r ↓34–48%
	GF120918	Doxorubicin	CL_r ↓ 84%

Breast Cancer Resistance Protein	GF120918	Topotecan	AUC ↑143%

Hepatic Drug Transport And Metabolic Systems Correlation

It has been reported that many drugs or metabolites exhibits significant overlap in substrate specificities among MDR1 and CYP3A4 [123]. Induced levels of both intestinal Mdr1 and hepatic CYP3A levels have been reported on exposure to protease inhibitors such as amprenavir and nelfinavir [124]. Treatment with rifampin, reserpine, phenobarbital, and clotrimazole in a human colon carcinoma cell line leads to induced expression of MDR1 and CYP3A4 proteins [125]. These two proteins functions together in order to detoxify and eliminate xenobiotics from the body. Any alteration in the levels of expression of these proteins will modify the concentration-time profile and therapeutic effects of many drugs. Also, by changing the intracellular concentrations of substrates that induce CYP enzymes, MDR1 plays an important role in altering the expression of CYP3A4 [126]. This interaction may arise grave concerns for effective drug therapy. Combination of vincristine- doxorubicin-dexamethasone (VAD) is used in treatment multiple myeloma. Dexamethasone (inducer of both CYP3A4 and MDR1) induces MDR1 activity which will ultimately leads to diminished intracellular concentrations of vincristine and doxorubicin, and further lower intracellular concentrations of vincristine due to enhanced activity of CYP3A4 [123]. Also, dexamethasone long term treatment leads to induced levels both Mdr1 and CYP3A4 in male and female rat livers [127]. MDR1 and CYP3A4 not only shares similar substrate specificities but also have similar inhibitors too. Azole antifungals, ergot alkaloids, and macrolide antibiotics, not only inhibits CYP3A4 but also leads to varied degree of inhibition of MDR1 function [128]. Inhibition of Mdr1 by GF120918 in isolated perfused rat livers leads to enhanced metabolism of

tacrolimus because of the increased availability of tacrolimus to metabolizing enzymes backing up the idea of an relationship between CYP3A and Mdr1 [129]. Also, several reports were published demonstrating the elevated levels of hepatic CYP3A4 in Abcb1b(−/−) mice suggesting some level of coordinated regulation of both these proteins [130]. In Abcb1b(−/−) and Abcb1a(−/−) mice, AUC of erythromycin (substrate of MDR1 and CYP3A4) metabolites was observed to be 1.9- and 1.5-fold higher in comparison to wild-type mice. This interaction or results supports the elevated expression of CYP3A4 in Abcb1b(−/−) and Abcb1a(−/−) mice resulting in higher AUC of erythromycin metabolites [131].

Several PXR ligands are known substrate of MDR1 and also PXR is a well-known key modulator of CYP3A4 gene. Rifampicin induced MDR1 induction was identified because of presence of a distinct PXR binding site (DR4 nuclear response element) in the 5'-upstream region [102]. Similar to MDR1 knockout mice, diminished levels of Bsep and hence increased level of hepatic bile acid due to enhanced activity of CYP3A and CYP2B drug-metabolizing enzymes was observed in FXR nullizygous mice [47]. In order to have more advance knowledge about the coordinate regulation of hepatic drug metabolizing enzymes and transporters by PXR or other nuclear hormone receptors, *in vitro* models with hepatic transport and metabolic systems will be required to reveal the contrivances of these multifaceted interactions.

Genetic Variations in Hepatic Transport

Alteration in disposition and pharmacokinetic parameters of several therapeutic agents which arise due to deviations in levels of expression and activity of hepatic transporter may significantly impact therapeutic efficacy of the drug molecule. Currently, many research based studies have focused their area on elucidating the mechanism involved in governing these hepatic transporters at protein level. In *in vitro* studies, polymorphisms in transport proteins resulted in

alteration of transport capacity of these proteins, whereas single nucleotide polymorphisms (SNPs) associated with hepatic transporters have shown its effect *in vivo* also. No functional evidence has been produced on various SNPs observed in the SLCO1A2 and SLCO1B3 genes in Japanese subjects [132]. Decreased transport capacity of OATP2B1 to 42.5% in comparison to control Japanese subjects has been attributed to the genetic polymorphism associated with SLCO2B1 gene [133]. Genetic polymorphisms associated with hepatic OATP1B1 (SLCO1B1) has been examined and evaluated comprehensively. In a study involving 81 human livers, genetic polymorphisms associated with SLCO1B1 leads to diminished transport function of OATP1B1 [134]. Reduced transport and diminished expression of OATP1B1 in European- and African- Americans has been associated with the several SNPs identified in SLCO1B1 [135]. Population with genetic variants of SLCO1B1 gene exhibited altered pravastatin (OATP1B1 substrate) kinetics [136]. Naturally occurring mutation in MRP1 resulted due to amino acid substitution affected the transporter capacity of MRP1 and resulted in 2-fold decreased transport of LTC4 via MRP1 [136]. It is not necessary that all the genetic polymorphisms associated with transporter gene will yield beneficial or harmful effects. Example, genetic polymorphism associated with MRP6 demonstrated no effects on transport activity of MRP6 [137, 138]. Dubin-Johnson syndrome has been associated with polymorphisms leading to non-functional activity of MRP2 which ultimately results in hyperbilirubinemic condition [139]. Liver biopsies of patients suffering Dubin-Johnson syndrome confirms the absence of MRP2 protein [140]. Impaired maturation and/or trafficking/localization of the protein or compromised ATP-hydrolysis has been attributed to different mutations in the MRP2 gene [141-143]. In recent years, revelation of genetic polymorphisms in hepatic transport genes, evaluation and examination of their functional significance, and development of assays to

identify patients exhibiting clinically significant polymorphisms have gained significant interest in the field of transporter based research [1].

Future Of Hepatobiliary Drug Transport Research

This chapter highlights the highlights the major hepatic transport systems identified so far that mediate hepatic uptake, excretion, and/or interactions with xenobiotics, including therapeutic agents and their metabolites. Although our understanding of hepatic transport from a physiologic, pharmacological, and clinical perspective has amplified extensively during the past decade, we clearly lack complete knowledge about the complex processes involved in hepatobiliary drug disposition. Many vital questions still needs to be answered. Example, uptake/transport of xenobiotics through hepatocyte from the basolateral domain to metabolic sites, and from sites of metabolism to the basolateral or canalicular domains? Excretion of some drug molecules into bile whereas translocation of other molecules across the basolateral membrane into sinusoidal blood? Important concerns which governs the hepatic transport processes in normal and diseased liver still needs proper understanding. Current research focused on the transporter mediated hepatic uptake of substrates will enhance our current understanding of hepatobiliary drug transport by identifying the transporter proteins responsible for uptake of drugs into hepatocytes prior to metabolism and biliary excretion. This knowledge will provided an extra edge in the process of drug development by representing a new and exciting aspect of the discipline. Also, research area is focused towards identifying new chemical entities that are substrates for specific hepatic transport systems by a moderate/high-throughput screening methods. These methods will help in generating data which in turn will provide systematic characterization of structure-transport relationships for both animal and human hepatic transport proteins. Various *in vitro* assays to evaluate and examine hepatic drug transport will provide more in depth knowledge regarding

hepatobiliary drug disposition in humans. By elucidating the transporters responsible for uptake of compounds into the hepatic tissue prior to metabolism and biliary excretion will not only provided information about pharmacokinetics of the substrate molecule but will also provide information about potential transporter based drug interactions. This information or knowledge will act as a prerequisite in drug development process in order to achieve desirable clinical outcomes [1].

CHAPTER 2

ROLE OF OATP-1B1 AND/OR OATP-1B3 IN HEPATIC DISPOSITION OF TYROSINE KINASE INHIBITORS

Rationale

Hepatic uptake of drugs is mediated via various members of membrane transporter families. Membrane transporters localized on the basolateral side of hepatic tissue are known to play an important role in the uptake of therapeutic agents/metabolites from blood into the hepatocytes. This uptake process is recognized as the first step in hepatocellular elimination and plays a vital role in hepatic drug disposition. Organic anion transporting polypeptides (OATPs) appear to play a critical role in bioavailability, distribution and excretion of numerous exogenous amphipathic organic anionic compounds including anionic oligopeptides, steroid conjugates, organic dyes, bile salts, thyroid hormones and many drugs such as pravastatin, rifampicin etc.[144-147].

Tyrosine kinase inhibitors (TKIs) target intracellular tyrosine kinase domain of various tyrosine kinase receptors which are often over expressed in cancer tissues. Human genome sequence data have indicated that deregulation of protein kinase pathway is one of the main mechanisms underlying tumor growth. Over the past few years, attention has been focused towards the discovery of a targeted therapy which will act against defining characteristics of cancer resulting from abnormal function of protein kinases [148, 149]. In the past decade, U.S. Food and Drug Administration (FDA) has approved several TKIs. Many of these compounds have been associated with low patient response along with unwanted effects of toxicity, which is unexpected and largely unexplained. Comprehensive data from Phase I studies of these TKIs establishes the optimized dose for Phase II. Even though TKIs offer theoretical advantages (selectively target/kill

the cancer precursor cells and protect normal tissues) over traditional anti-cancer agents, these agents are still associated with unpredictable clinical effects because of inter-individual pharmacokinetic variability and narrow therapeutic window [148, 150]. Substantial inter-individual differences in the concentration-time profiles of TKIs range from 32-118% and is mostly unexplained. Many TKIs exhibit limited efficacy with significant degree of unexpected and unexplained toxicity [151]. Inter-individual pharmacokinetic variation in TKIs can have both genetic and non-genetic origins. This pharmacokinetic variation can be due to many plausible sources, including inter-individual differences in absorption, distribution, metabolism and excretion (ADME). TKIs are primarily metabolized in liver by CYP enzymes (mainly CYP3A4) and are eliminated via biliary excretion route into feces as unchanged drug or metabolites [151]. Hepatic uptake of TKIs can be attributed as a major source of pharmacokinetic variability, which is also recognized as one of the most crucial and complex steps in drug disposition [148]. Currently, various OATP family transporters such as OATP-1B1, -1B3 and -2B1 have been identified and characterized on sinusoidal membrane of hepatic tissue [144]. However the mechanisms responsible for hepatocellular accumulation of TKIs prior to metabolism and biliary secretion are still largely unexplained. Previous investigations have reported that organic anion transporting polypeptide transporters (OATPs) namely OATP-1B1 and -1B3 are responsible for uptake of TKIs into human liver cells [148]. Uptake of TKIs such as axitinib, lapatinib and sorafenib into human hepatocytes is regulated by OATP-1B1 and/or -1B3. Also, some of the TKIs, namely, pazopanib and lapatinib are known to inhibit the functional capacity of OATP-1B1 and/or -1B3 transporter proteins [148]. However, there is still a need for systematic approach to delineate the mechanism involved in hepatic uptake of these TKIs. Since, hepatic system possesses many transporters (both influx and efflux), it is difficult to delineate the affinity of individual transporters

towards these TKIs. Hence, it is of utmost importance to estimate the relative contribution of OATP-1B1 and -1B3 in hepatic uptake of TKIs [144]. In the present study, we evaluated the interaction of the TKIs (pazopanib, erlotinib, canertinib, nilotinib and vandetanib) with the human OATPs expressed on sinusoidal membrane of liver by employing *in vitro* model system with wild type and transfected Chinese hamster ovary (CHO) cells.

Materials And Methods

Chemicals

Pazopanib, erlotinib, canertinib, nilotinib and vandetanib were purchased from LC Laboratories (Woburn, MA). All other chemicals used were of high performance liquid chromatography grade and were obtained from either Sigma Aldrich or Fisher Scientific.

In Vitro Studies

Cell Lines

Chinese hamster ovary (CHO) cells (passage number 17-50) were selected for all *in vitro* experiments. Wild-type (WT), OATP-1B1 and -1B3 CHO transfected cells were a gift from Dr. Bruno Stieger (Department of Clinical Pharmacology and Toxicology, University Hospital Zürich, Switzerland). Cells were cultured in Dulbecco's modified Eagle's medium (DMEM), supplemented with 10% heat inactivated fetal bovine serum (FBS), L-proline (50µg/mL), HEPES, penicillin (100µg/ml), streptomycin (100µg/ml), and maintained at 37°C with 5% CO_2 under humidifying conditions. For OATP-1B1 and -1B3 expressing CHO cells, the medium was also supplemented with geneticin (100µg/mL).

In Vitro Cellular Accumulation Studies

Cellular accumulation studies were conducted in 24 well polystyrene plates (Costar Corning, NY). CHO cells (WT and transfected) were plated at a seeding density of 3×10^5

cells/well. The medium was changed every alternate day. Cells formed confluent monolayers in 3–4 days. Twenty-four hours before any experiment, the cells were exposed to 10mM sodium butyrate to induce higher expression of the transfected transporter. On the day of experiment, medium was aspirated and cells were rinsed three times with cell assay buffer (116.4 mM NaCl, 5.3 mM KCl, 1 mM NaH_2PO_4, 0.8 mM $MgSO_4$, 5.5 mM D-glucose and 20 mM Hepes/Tris; pH 7.4) pre-warmed at 37ºC. The uptake experiment was initiated by adding 0.5 mL of fresh serum free medium containing 0.25 and 0.5μM of TKIs (pazopanib, erlotinib, canertinib, nilotinib and vandetanib) in WT as well as OATP-1B type transfected cells. After incubating cells for 10 minutes with TKIs, uptake solution was aspirated and the cells were washed twice with 2 mL of ice-cold uptake buffer. This resulted in removal of the non-specifically bound substrate from the membrane as well as arrested further cellular accumulation. Finally, 0.5 mL of fresh DMEM was added to each well and cell lysis was carried out by storing the culture plates overnight at −80°C. On the following day, intracellular drug concentration was quantified using liquid chromatography tandem mass spectrometry (LC/MS–MS) as described in previous publications from our group as well as others [152-156]. Based on the time points for uptake the minimum concentration observed were well beyond the detection limit. The amount of TKIs accumulated was normalized to the protein content in each well with Bradford's reagent (Bio-Rad, California). All stock solutions were prepared in dimethyl sulfoxide (DMSO) and diluted using medium such that the final DMSO concentration did not exceed 0.5% (v/v).

Estimation Of Michaelis-Menten Kinetics

To determine the kinetic basis for the differential uptake of OATP-1B1 and -1B3 transporter proteins, concentration dependent uptake of TKIs were carried out. Using a concentrated stock solution of the TKIs, several working concentrations were prepared ranging

from (0.01µM - 50µM) in serum free fresh medium. Uptake was carried out at different concentration of TKIs in WT, OATP-1B1 and -1B3 transfected CHO cells.

Data Analysis

Kinetic parameters of TKIs uptake via hepatic OATP-1B1 and -1B3 were calculated with a nonlinear least squares regression analysis program KaleidaGraph version 3.5. The data was plotted and fitted to Michaelis-Menten equation (1) and the maximum transport rate (V_{max}) and Michaelis-Menten constant (K_m) were calculated.

$$v = \frac{Vmax[C]}{Km + [C]} \qquad \textbf{Eq. 1}$$

v is the initial uptake rate, V_{max} is the maximal velocity, K_m is Michaelis–Menten constant, and C is the total concentration of TKIs.

Cytotoxicity Studies

Cell Titer 96® Aqueous Non-Radioactive Cell Proliferation Assay Kit (Promega, Madison, WI) was employed to carry out cytotoxicity assay. WT, OATP-1B1 and -1B3 transfected CHO cells were cultured in 96-well plate. Sterile drug solutions of highest concentration (50µM) of TKIs are prepared in the culture medium using 0.22µm nylon sterile membrane filters. Aliquots of TKIs having a volume of 100µL (previously made in culture medium) were added to each well and incubated for 24h. Cell proliferation of the cells in the presence of TKIs was compared with a negative control (medium without TKIs) and a positive control (Triton X). Twenty microliters of dye solution was added to each well after 24h of incubation with TKIs. Cells were then incubated for 4h in order to complete the reaction of cells with dye. UV absorbance of purple formazan formed was quantified at a wavelength of 590nm with a 96-well micro titer plate reader (SpectraFluor Plus, Tecan, Maennedorf, Switzerland). Toxicity of TKIs in WT and OATP-1B type

transfected CHO cells was estimated by the amount of formazan formed, which is directly proportional to the viable cells.

Statistical Analysis

All the experiments were conducted at least in quadruplicate (n=4) and the outcomes were expressed as mean±standard deviation (SD). To calculate statistical significance, student's t test was performed. Any difference between mean values is considered statistically significant for P value ≤ 0.05.

Results

In Vitro Cellular Accumulation Of Tyrosine Kinase Inhibitors

Initial *in vitro* uptake experiments were carried out to determine cellular accumulation of TKIs in WT, OATP-1B1 and -1B3 transfected CHO cells. Cellular accumulation was measured by exposing the WT and OATP-1B1 transfected CHO cells to two different concentrations (0.25 and 0.5μM) of TKIs. In previously reported results, concentration ranges from 0.1 to 10μM has been shown to be non-saturating for OATP-1B1 and -1B3 mediated transport **[157]**. We performed our studies within these linear non-saturable ranges and also at concentration which were well within our detection limit. Also, while studying transporter mediated uptakes, we always aim to use as low a concentration as possible so as to limit any toxicity. Hence, based on these considerations we chose 0.25 and 0.5 μM as our concentration ranges. Out of the selected TKIs, nilotinib and vandetanib showed significantly enhanced cellular accumulation in OATP-1B1 transfected cells relative to WT cells. The remaining 3 TKIs (canertinib, pazopanib and erlotinib) did not show any significant enhanced cellular accumulation in OATP-1B1 transfected cells compared to WT cells. Vandetanib (0.25 and 0.5μM) showed the highest uptake, about 1.3 fold ($p<0.01$) in OATP-1B1 transfected cells compared to WT cells. Nilotinib (0.25 and 0.5μM) also

showed higher uptake about ~1.3 ($p<0.01$) and 1.2 ($p<0.05$) fold respectively in transfected cells relative to WT cells **(Fig 2.1)**. It has been reported previously that OATP-1B3 shares 80% amino acid identity with OATP-1B1. Also, both the OATP isoforms share multiple overlapping substrates, such as rifampicin pravastatin, pitvastatin and docetaxel [158, 159].

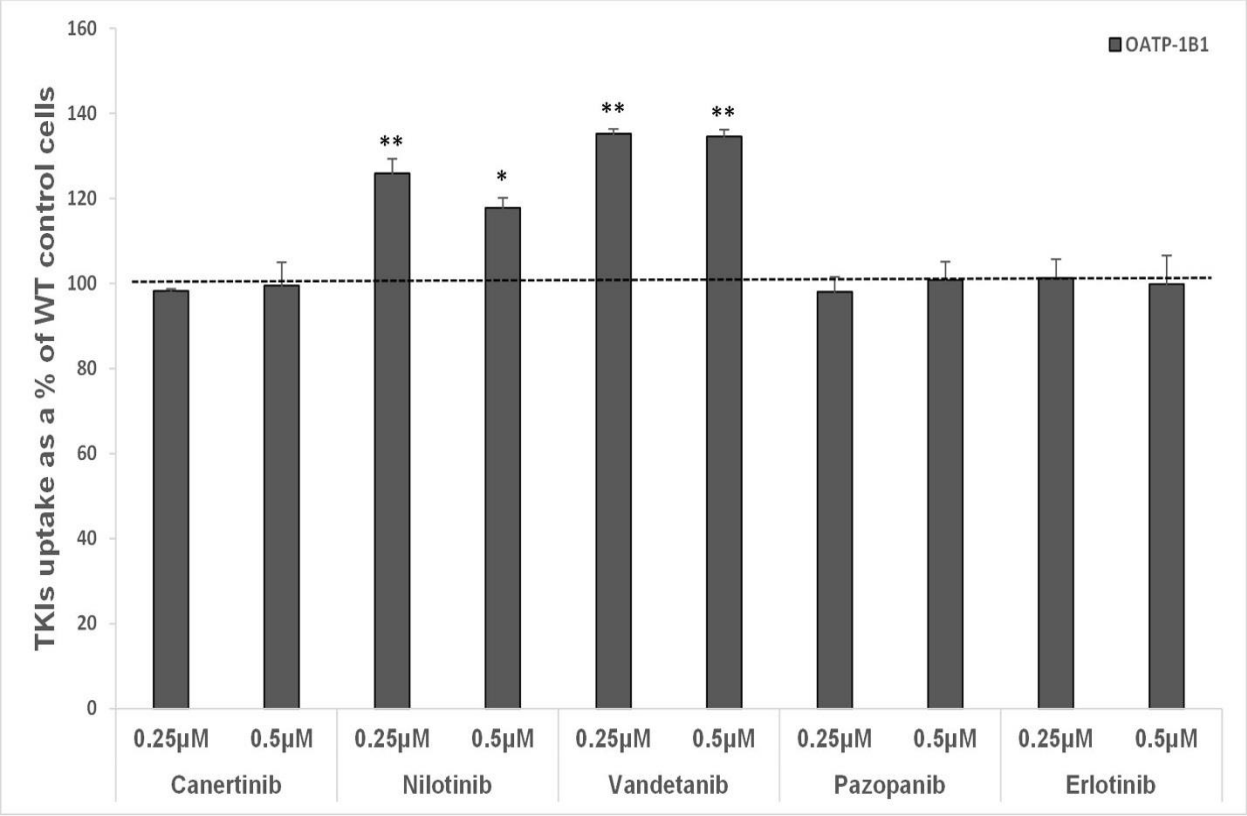

Fig.2.1: Cellular accumulation of TKIs at two concentrations (0.25 and 0.5µM) by OATP-1B1 transporter. TKIs were incubated with WT and CHO-OATP-1B1 transfected CHO cells for 10 minutes. Intracellular drug concentration was quantified using liquid chromatography tandem mass spectrometry (LC/MS–MS). Data represent the mean±SD, n=4 (*$p<0.05$, **$p<0.01$).

In this study, we have also determined the cellular uptake of TKIs at two different concentrations (0.25 and 0.5µM) in WT and OATP-1B3 transfected cells. Canertinib, nilotinib and vandetanib at both concentrations showed significantly enhanced cellular accumulation in OATP-1B3 transfected cells compared to WT cells ($p<0.01$). No difference was observed in cellular accumulation of pazopanib and erlotinib in OATP-1B3 transfected cells compared to WT cells (Fig 2.2). Highest uptake of canertinib (0.25 and 0.5µM) was observed, about 2 ($p<0.01$) and ~5 ($p<0.01$) times respectively, in OATP-1B3 transfected cells than the WT cells. A significantly higher uptake of vandetanib and nilotinib was also evident in OATP-1B3 cells than WT (Fig 2.2). No statistically significant changes in cellular accumulation of pazopanib and erlotinib were found between WT and OATP-1B3 transfected cells (Fig.2.2). Nilotinib and vandetanib showed overlapping substrate specificity towards OATP-1B1 and -1B3 while canertinib only showed affinity towards OATP-1B3.

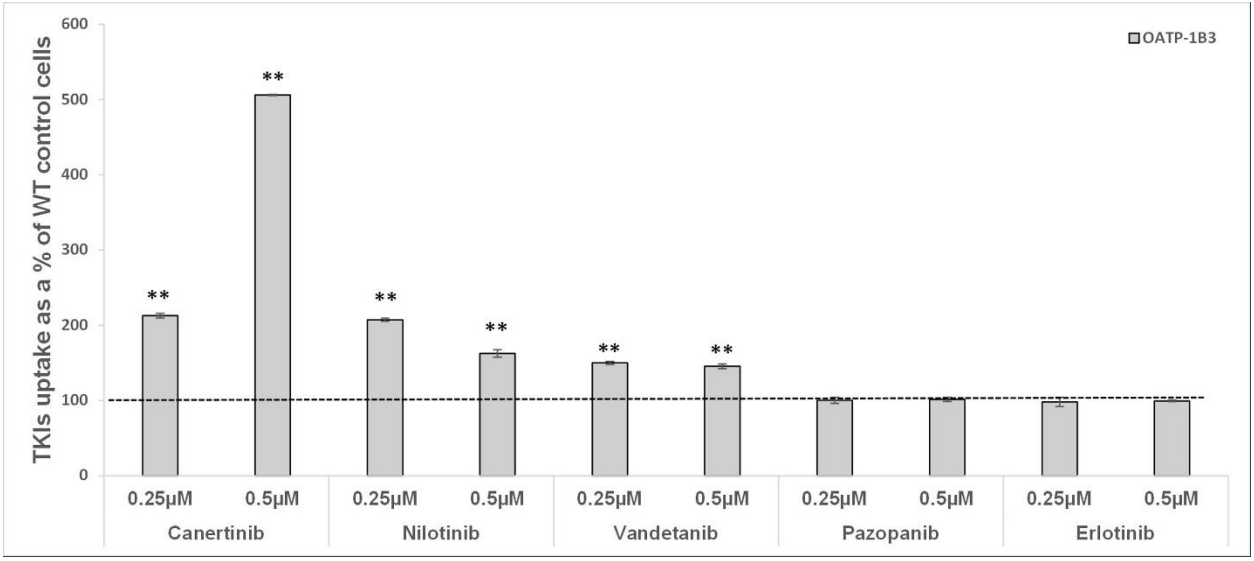

Fig 2.2: Cellular accumulation of TKIs at two concentrations (0.25 and 0.5µM) by OATP-1B3 transporter. TKIs were incubated with WT and OATP-1B3 transfected CHO cells for 10 minutes.

Intracellular drug concentration was quantified using liquid chromatography tandem mass spectrometry (LC/MS–MS). Data represent the mean±SD, n=4 (*p<0.05, **p<0.01).

Estimation Of Michaelis-Menten (MM) Kinetics

For estimation of MM kinetics, WT, OATP-1B1 and -1B3 transfected CHO cells were incubated with various concentration (0.01μM - 50μM) of TKIs. Previous studies have shown time-dependent uptake on similar cell lines to be linear up to 15 minutes [160-162]. We incubated our cells for 10 minutes as it falls within the linear range of uptake as well as gives us concentrations that lie well within the detectable range. **Figs 2.3 and 2.4** clearly demonstrate that carrier mediated uptake of TKIs via OATP-1B1 and OATP-1B3 is concentration-dependent and saturable at higher concentrations. This is the first study where Michaelis-Menten kinetic parameters of OATP-1B1 and OATP-1B3 have been evaluated for selected TKIs (canertinib, pazopanib, nilotinib, vandetanib and erlotinib). The values obtained for kinetic parameters have been summarized in **Table 2.1**. Despite no significant changes in cellular accumulation of canertinib and nilotinib at lower concentration (0.01-0.075μM), these drugs showed greater accumulation at higher concentrations (0.1-50 μM) in OATP-1B1 and/or -1B3 cells in comparison to CHO-WT cells. For vandetanib, kinetic parameter were evaluated in the concentration range of 0.01μM - 50μM. Intracellular accumulation of nilotinib and vandetanib was mediated via OATP-1B1 transporter protein. K_m value of 2.72 ± 0.25μM for vandetanib showed higher affinity towards OATP-1B1 transporter than nilotinib (K_m = 10.14 ± 1.91μM).

Three TKIs (vandetanib, nilotinib and canertinib) appeared to have affinity towards OATP-1B3. Affinity of these TKIs towards OATP-1B3 transporter was in following order: vandetanib>nilotinib>canertinib (K_m = 4.37 ± 0.79, 7.84 ± 1.43 and 19.87 ± 2.20μM, respectively). Also, vandetanib showed greater affinity towards OATP-1B1 than OATP-1B3 transporter protein

whereas nilotinib showed higher affinity for OATP-1B3 than OATP-1B1. Canertinib exhibited its affinity only towards OATP-1B3. V_{max} values of both the hepatic uptake transporters for TKIs were calculated and summarized in **Table 2.1**.

No statistically significant cellular accumulation was observed for pazopanib and erlotinib in OATP-1B1 and -1B3 transfected cells in comparison to WT cells.

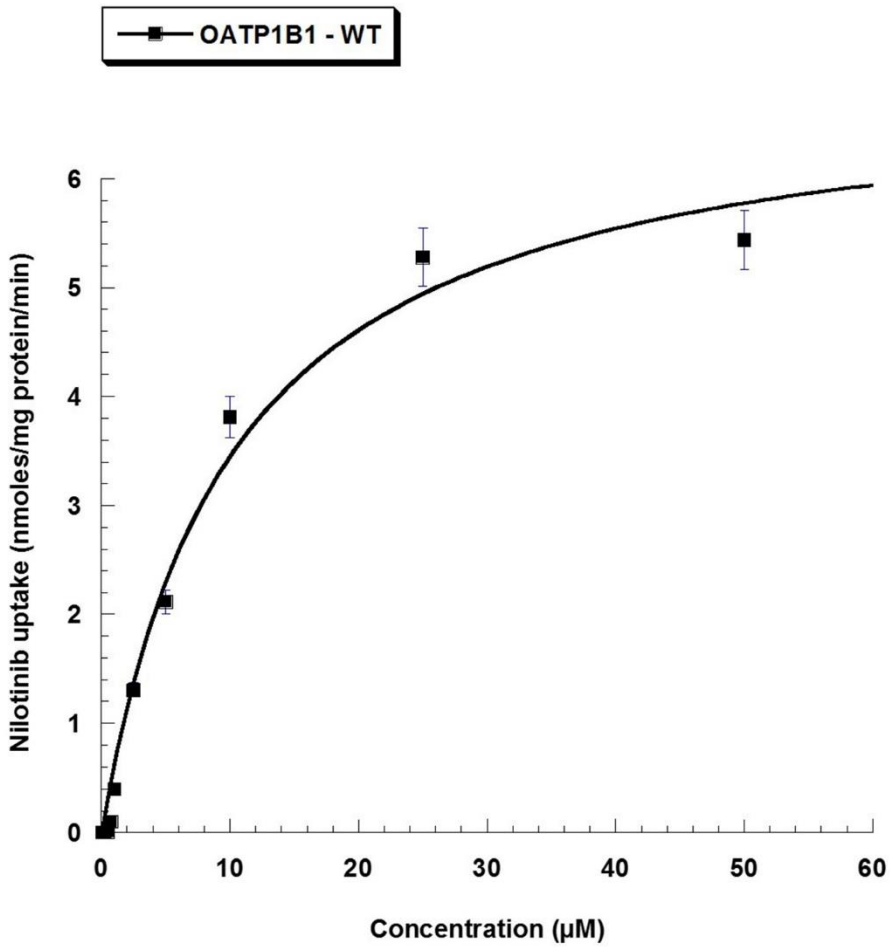

Fig 2.3.1: Concentration dependent uptake of nilotinib in OATP-1B1 transfected CHO cells. OATP-1B1 mediated nilotinib transport determined as the difference in uptake in OATP-1B1 and WT CHO cells at each substrate concentration. Each data point is expressed as mean±SD, n=4.

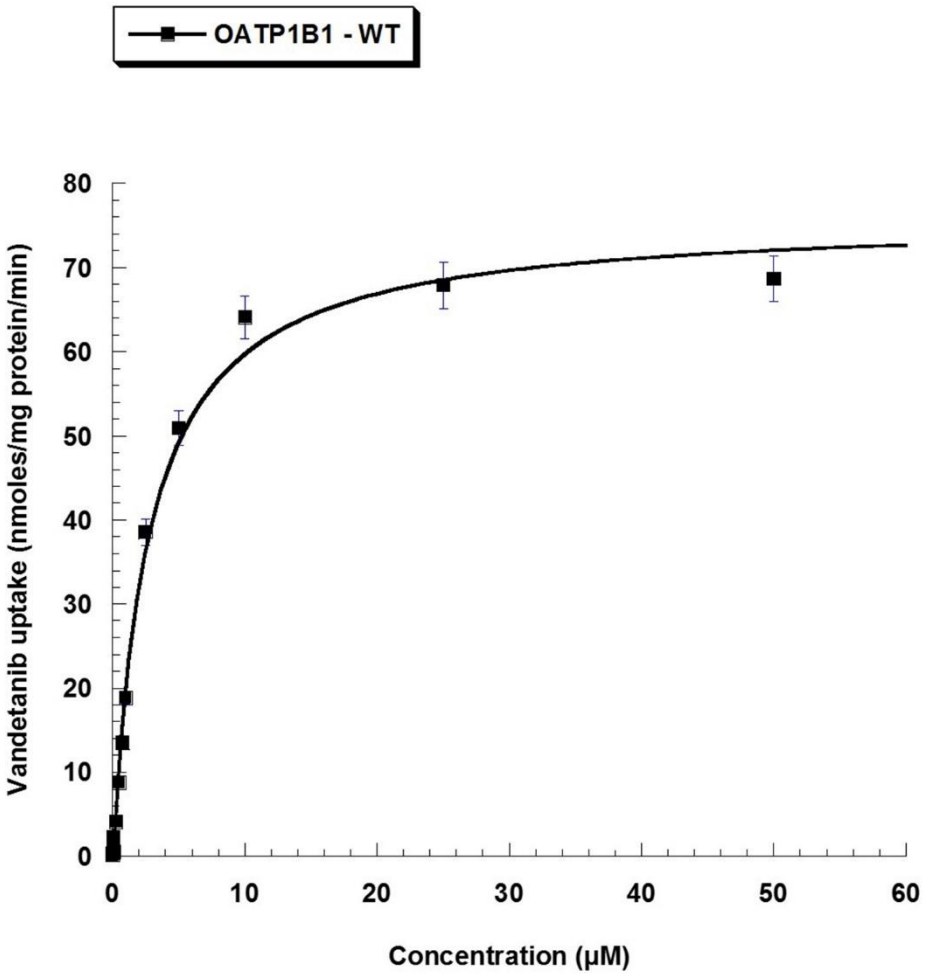

Fig 2.3.2: Concentration dependent uptake of vandetanib in OATP-1B1 transfected CHO cells. OATP-1B1 mediated vandetanib transport determined as the difference in uptake in OATP-1B1 and WT CHO cells at each substrate concentration. Each data point is expressed as mean±SD, n=4.

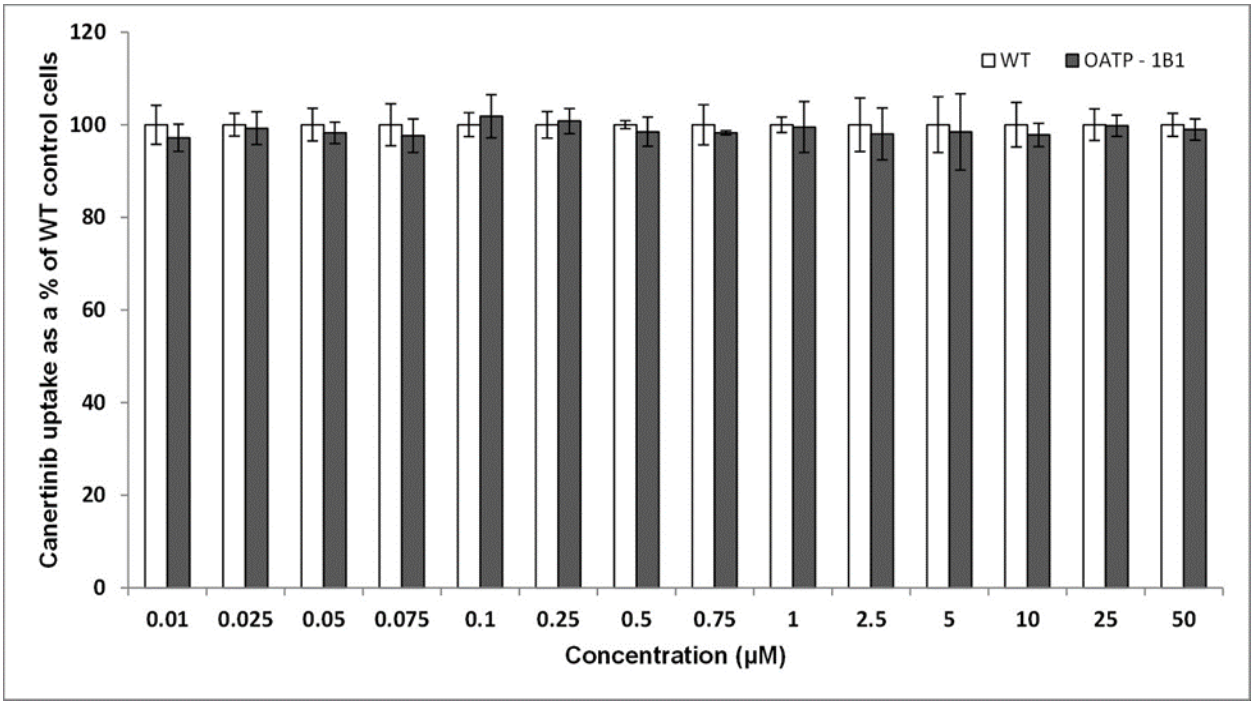

Fig 2.3.3: Concentration dependent uptake of canertinib in WT and OATP-1B1 transfected CHO cells. Each data point is expressed as mean±SD, n=4.

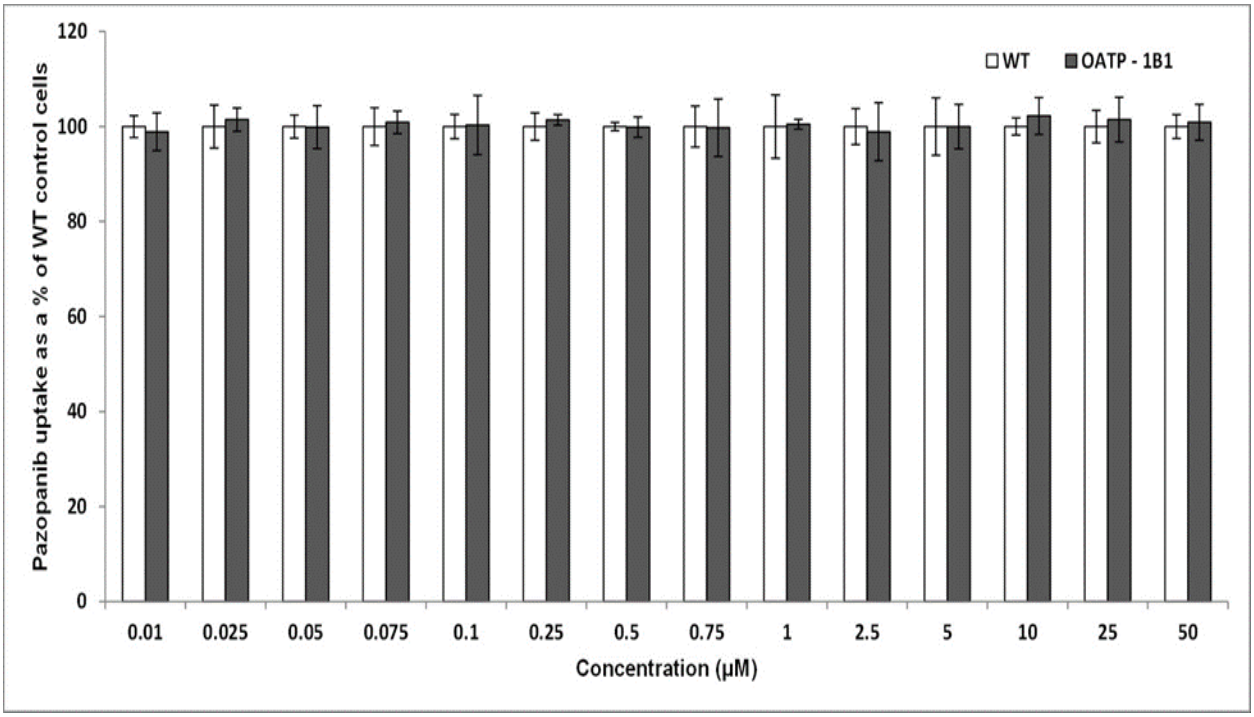

Fig 2.3.4: Concentration dependent uptake of pazopanib in WT and OATP-1B1 transfected CHO cells. Each data point is expressed as mean±SD, n=4.

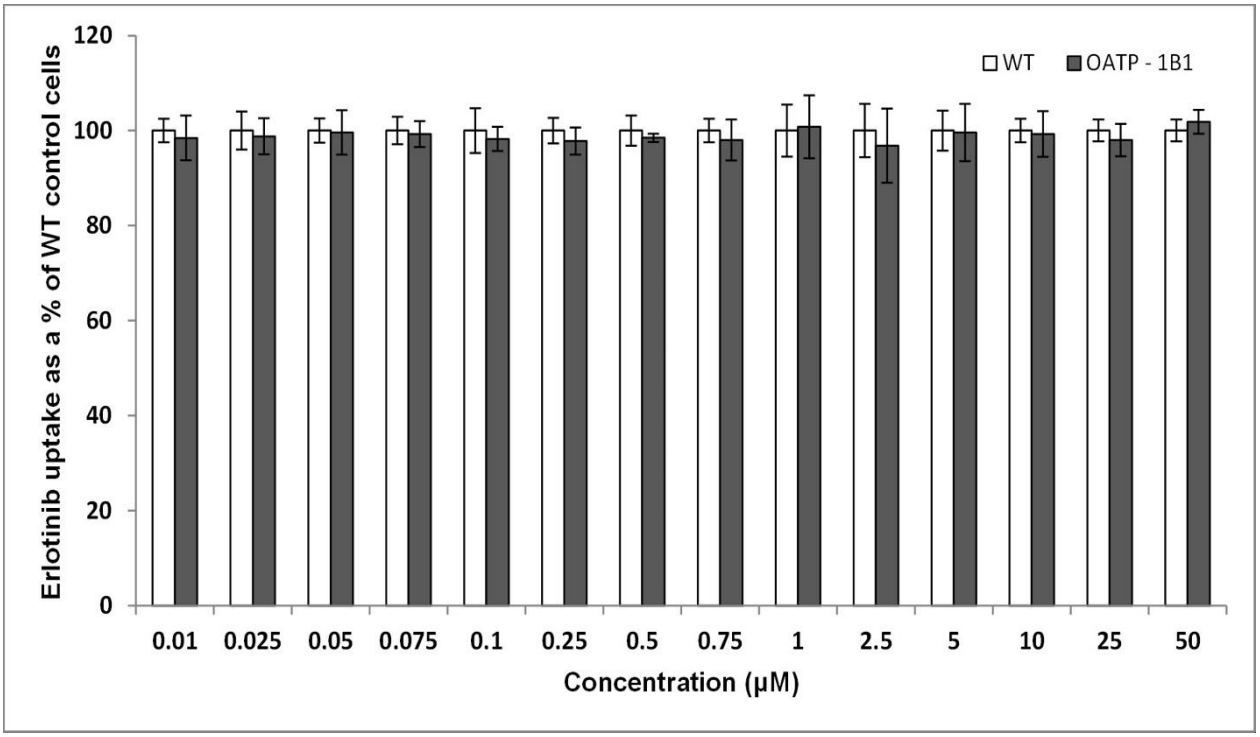

Fig 2.3.5. Concentration dependent uptake of erlotinib in WT and OATP-1B1 transfected CHO cells. Each data point is expressed as mean±SD, n=4.

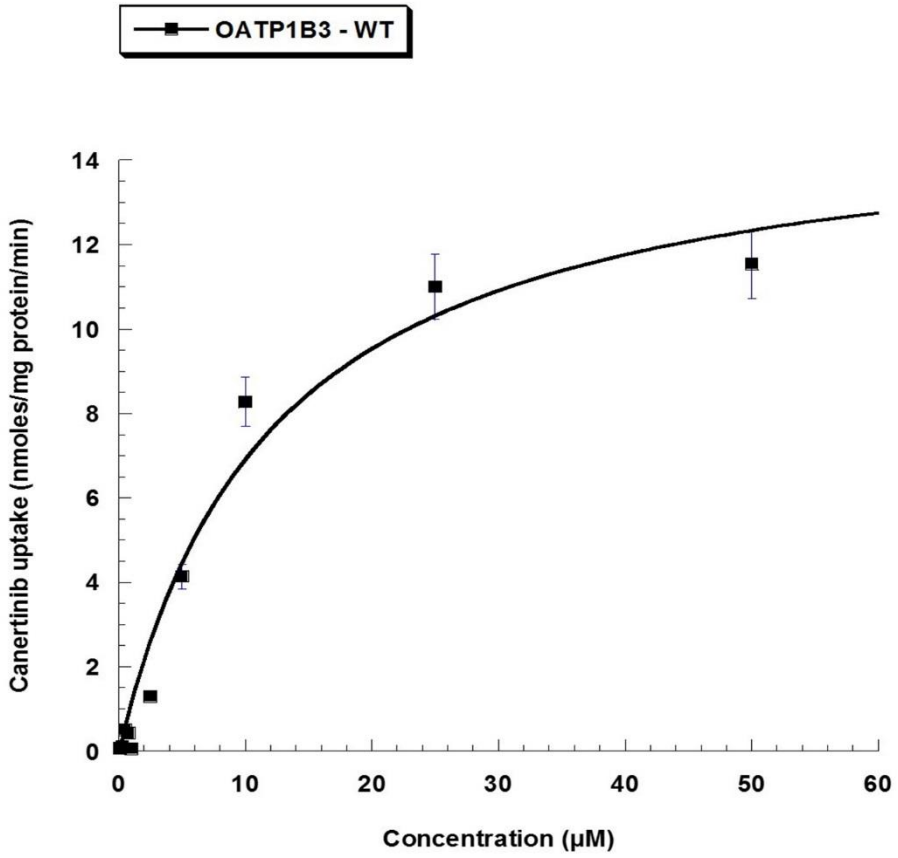

Fig 2.4.1: Concentration dependent uptake of canertinib in OATP-1B3 transfected CHO cells. OATP-1B3 mediated canertinib transport determined as the difference in uptake in OATP-1B3 and WT CHO cells at each substrate concentration. Each data point is expressed as mean±SD, n=4.

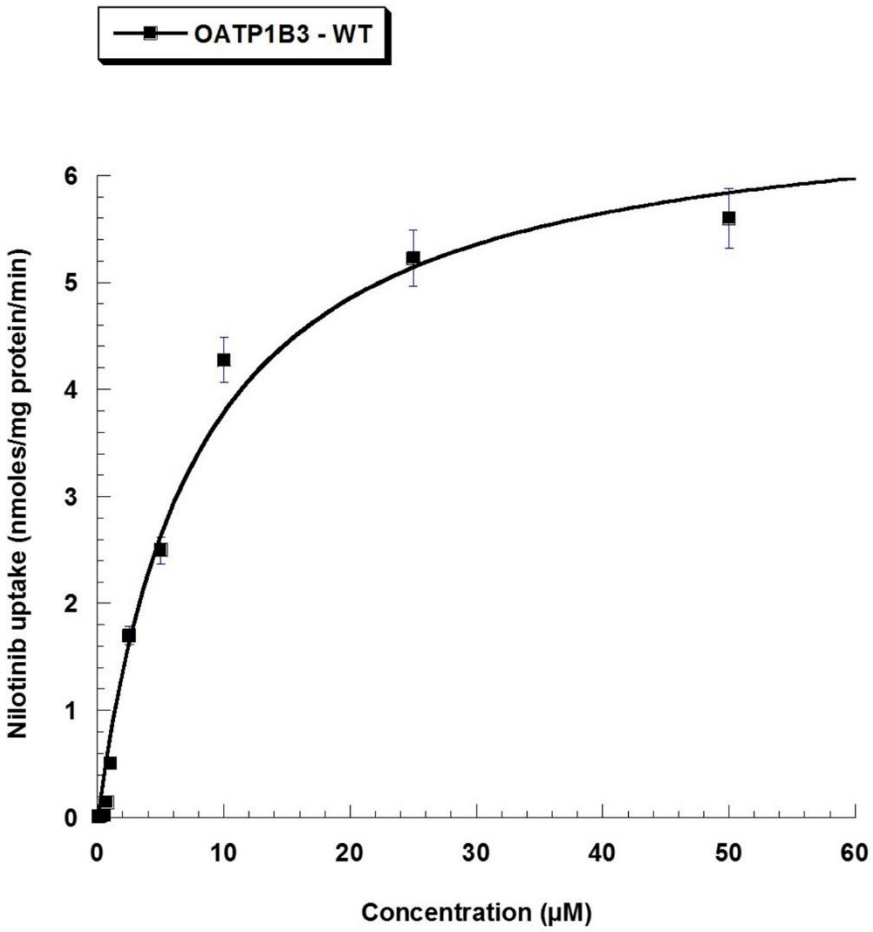

Fig 2.4.2: Concentration dependent uptake of nilotinib in OATP-1B3 transfected CHO cells. OATP-1B3 mediated nilotinib transport determined as the difference in uptake in OATP-1B3 and WT CHO cells at each substrate concentration. Each data point is expressed as mean±SD, n=4.

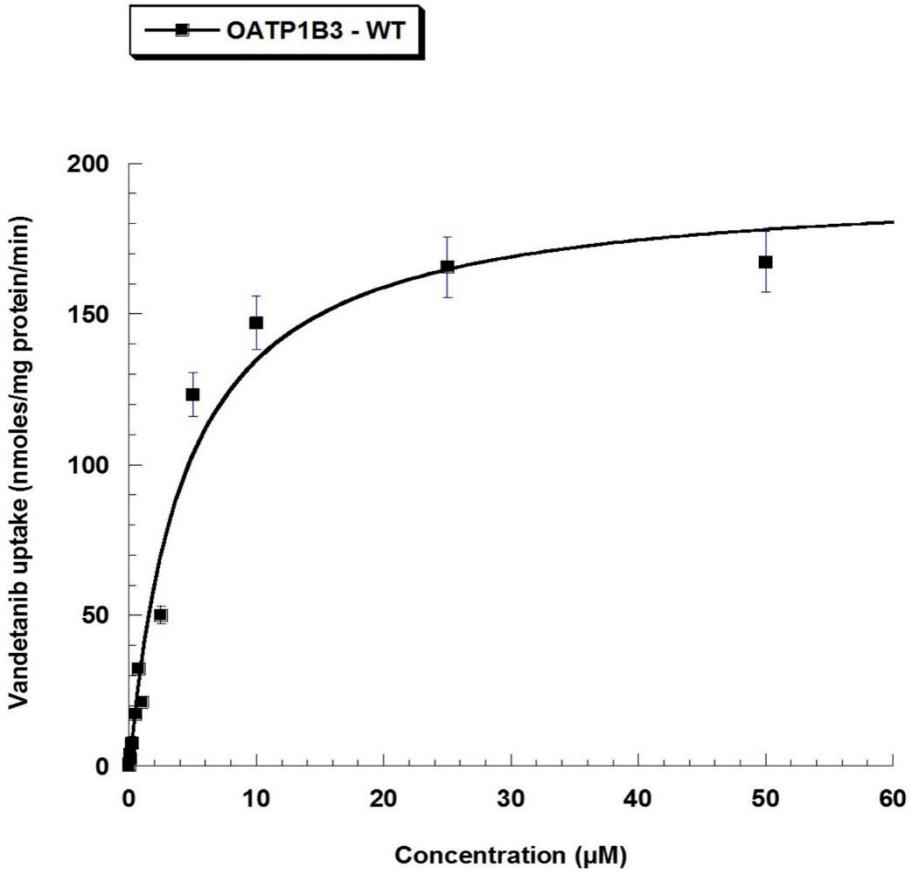

Fig 2.4.3: Concentration dependent uptake of vandetanib in OATP-1B3 transfected CHO cells. OATP-1B3 mediated vandetanib transport determined as the difference in uptake in OATP-1B3 and WT CHO cells at each substrate concentration. Each data point is expressed as mean±SD, n=4.

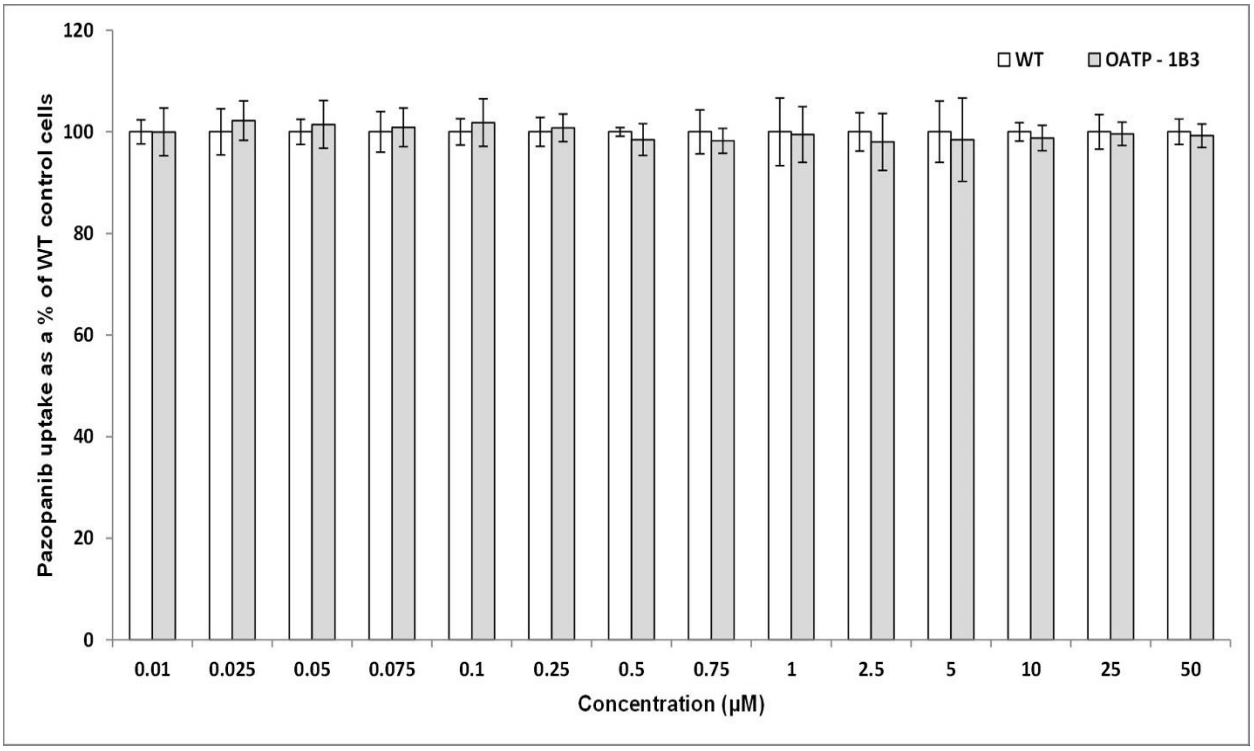

Fig 2.4.4: Concentration dependent uptake of pazopanib in WT and OATP-1B3 transfected CHO cells. Each data point is expressed as mean±SD, n=4.

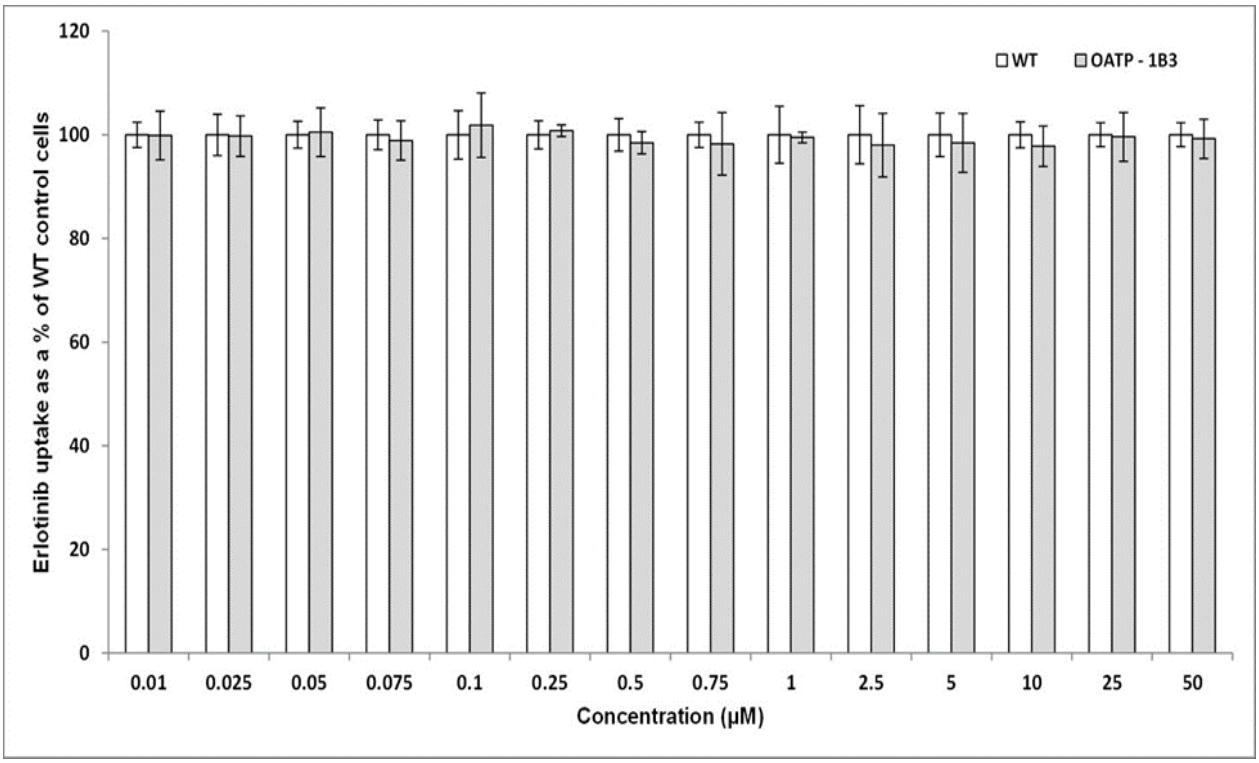

Fig 2.4.5: Concentration dependent uptake of erlotinib in WT and OATP-1B3 transfected CHO cells. Each data point is expressed as mean±SD, n=4.

Table 2.1: Michaelis–Menten kinetic parameters (V_{max} and K_m) and catalytic efficiency (V_{max}/K_m) estimated for tested TKIs for OATP-1B1 and/or OATP-1B3 transporter proteins. Units of K_m: micromolar (μM), V_{max}: nmoles/mg protein/min and V_{max}/K_m: ml/mg protein/min

TKIs	**OATP-1B1**			**OATP-1B3**		
	K_m	**V_{max}**	**V_{max}/K_m**	**K_m**	**V_{max}**	**V_{max}/K_m**
Canertinib	-	-	-	12.18 ± 3.32	15.34 ± 1.59	1.25
Nilotinib	10.14 ± 1.91	6.95 ± 0.47	0.68	7.84 ± 1.43	6.75 ± 0.42	0.86
Vandetanib	2.72 ± 0.25	75.95 ± 1.99	27.92	4.37 ± 0.79	193.64 ± 10.58	44.31
Erlotinib	-	-	-	-	-	-
Pazopanib	-	-	-	-	-	-

Cytotoxicity Studies

To evaluate the cytotoxic effect of the selected TKIs, a cell proliferation assay was performed on cell monolayers of WT and transfected CHO cells for a period of 24h. No cytotoxic effects of pazopanib, erlotinib, canertinib, vandetanib and nilotinib at a concentration of 50µM were observed with WT and transfected cells in comparison to positive control (Triton X). The findings from this study clearly demonstrate that the selected TKIs are non-cytotoxic at a concentration of 50µM **(Fig 2.5)**.

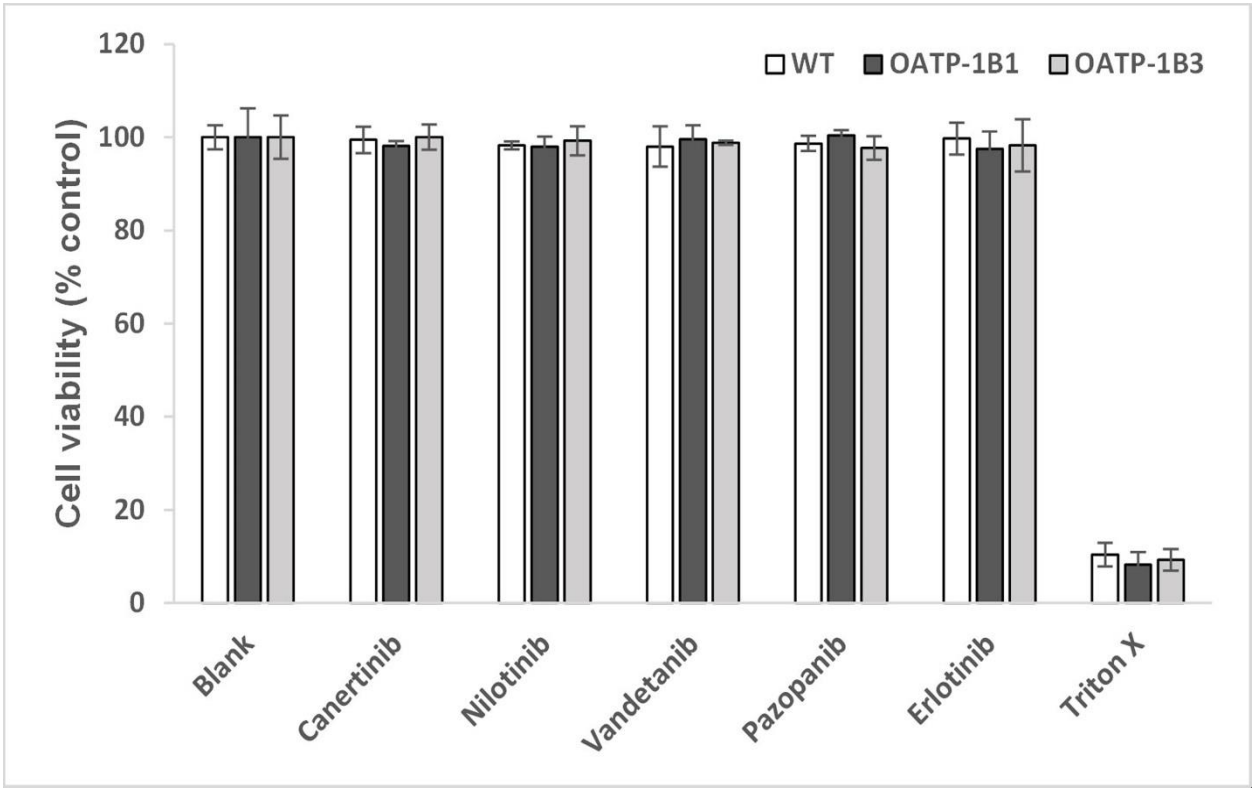

Fig 2.5: Cytotoxicity in the presence of TKIs at highest studied concentration (50µM) on CHO-WT, OATP-1B1 and -1B3 transfected cells. Data represent the mean±SD, n=4.

Discussion

In the present study, we investigated the role of OATP family transporters in the hepatic uptake process of TKIs. This work also estimated the contribution of OATP-1B1 and -1B3 in hepatocellular accumulation of TKIs with *in vitro* model based systems. For uptake transporter analysis, we utilized CHO cells, WT as well as transfected with specifically expressing OATP transport protein. CHO cells were originally selected for the transfection because of the lack of expression of these family of proteins in the parent cell line resulting in minimal background activity. Also, these cells can be maintained in culture for sustained periods and can be ready for use in a specific experiment within few days. Our findings are in partial agreement with the study done by Zimmerman *et al.*[148], where the authors reported the uptake of nilotinib (only at 0.1µM) in HEK293 cells expressing OATP-1B1 and -1B3 and uptake of vandetanib (only at 0.1µM) via OATP-1B3 transporter. Similar results were observed in the *in vitro* cellular accumulation studies performed, demonstrating the uptake of nilotinib and vandetanib via OATP-1B1 and -1B3 transporter proteins. Zimmermann *et al*. [148] also reported the uptake of pazopanib in cells expressing OATP-1B1 and -1B3 at a concentration of 0.1µM and no statistically significant uptake of vandetanib (0.1µM) in cells expressing OATP-1B1 transporter protein. Conversely, our findings demonstrate that there is no active involvement of OATP-1B1 and -1B3 in intracellular accumulation of pazopanib while uptake of vandetanib in hepatic tissue is mediated via OATP-1B1 and -1B3. These contrasting results suggests that utilization of different concentration of TKIs and *in vitro* model based systems may affect the cellular accumulation of TKIs via OATP and can lead to misinterpretation of the role of OATPs in cellular accumulation of TKIs. The current concentrations used in this manuscript (0.25 and 0.5 µM) were selected based on previously published results for *in vitro* uptake studies of TKIs and their toxicity for CHO cells. The

concentration ranges used were close to clinically observed C_{max} values but may not exactly mimic tissue concentration in clinic. These studies act as a proof of concept but further studies may be needed to make the data more clinically relevant.

It has been already reported that the tyrosine kinase inhibitors are substrate of efflux transporter proteins such as P-gp, MRPs and BCRP [152, 153, 163-166]. These efflux transporters are also expressed in the bile canalicular membrane and are responsible for excretion of drug and their metabolites from blood into bile. The membrane transporters (OATPs) along with efflux transporters and metabolizing enzymes play a vital role in hepatic disposition of drugs. Seithel *et al.* reported that coadministration of pravastatin together with macrolides (clarithromycin and roxithromycin) results in increased plasma concentration of pravastatin. It is a substrate for OATP-1B1, -1B3 and CYP3A4 whereas clarithromycin and roxithromycin are inhibitors of OATP-1B1, -1B3 and CYP3A4. Since pravastatin is not extensively metabolized and is excreted almost unchanged into bile and urine, this DDI studies suggests the major involvement of hepatic uptake transporters than metabolizing enzymes for macrolide-induced altered plasma concentration of pravastatin [167]. Similarly, Backman *et al.* demonstrated that co-administration of cerivastatin and simvastatin (OATP-1B1 and CYP2C8 substrate) together with gemifibrozil resulted in a 6-fold rise in the cerivastatin and simvastatin exposure. Such increase in plasma concentration of cerivastatin and simvastatin was due to the inhibitory potency of gemifibrozil on OATP-1B1 [168, 169]. Uptake of drugs mediated via OATP can be considered as an important additional mechanism essential for DDIs [170]. Unlike statins, information on the role of hepatic uptake transporters (OATP-1B1 and -1B3) for TKIs is very sparse. Thus, it is of utmost importance to understand the role of OATPs in hepatocellular accumulation of TKIs. The results obtained from *in vitro* cellular accumulation studies, suggests for the very first time the involvement of OATP-

1B1 and/or OATP-1B3 in hepatocellular accumulation of TKIs (canertinib, nilotinib and vandetanib). This article is the first to report the affinity of selected TKIs for OATP-1B1 and/or -1B3 by estimating the MM kinetic parameters. These findings suggest that OATP-1B1 exhibits greater affinity towards vandetanib than nilotinib. The ratio of these kinetic parameters (V_{max}/K_m) provides an estimate of the catalytic efficiency of OATP-1B1 transporter. The transport efficiency (V_{max}/K_m) of OATP-1B1 transporter was observed for nilotinib and vandetanib as 0.68 and 27.92 ml/mg protein/min, respectively. While comparing the efficiency values, OATP-1B1 transport efficiency was found to be higher for vandetanib than nilotinib. No significant changes in uptake of canertinib, pazopanib and erlotinib were observed in WT and OATP-1B1 transfected cells. Similarly, for OATP-1B3 transporter protein, the ratio of V_{max}/K_m provides an estimate of the catalytic efficiency of OATP-1B3 transporter. Such transport efficiency (V_{max}/K_m) of OATP-1B3 transporter observed for canertinib, nilotinib and vandetanib was 1.25, 0.86 and 44.31 ml/mg protein/min, respectively. OATP-1B3 transporter exhibits highest transport rate for vandetanib than nilotinib and canertinib. In pazopanib and erlotinib, no significant difference was observed in uptake values of WT and OATP-1B3 suggesting that OATP-1B3 transporter does not play in major role in their hepatic accumulation. On comparing the K_m values of OATP-1B1 and -1B3 transporter for nilotinib, it is apparent that nilotinib exerts higher affinity towards OATP-1B3 relative to OATP-1B1, whereas, V_{max} values of OATP-1B1 and -1B3 are comparable to nilotinib. These MM kinetic parameters play an important role in determining differential transport efficiency of OATP-1B1 and -1B3 in hepatic uptake of nilotinib. A distinction in K_m values of OATP-1B1 and -1B3 for nilotinib can be attributed as the primary driving force in determining its transport efficiency, since no difference was observed in V_{max} values of both the OATP-1B type transporters. The difference in the transport efficiencies (V_{max}/K_m) of OATP-1B1 and -1B3 was not very large

suggesting equal involvement of both the OATPs in the hepatic uptake of nilotinib. On comparing K_m values, vandetanib exhibits higher affinity towards OATP-1B1 than -1B3. Higher V_{max} values were observed for OATP-1B3 (~2.6 fold) than -1B1. Large differences in V_{max} has a significant contribution in determining the substrate specificity of vandetanib for OATP-1B1 and -1B3. Transport efficiency (V_{max}/K_m) of OATP-1B3 for vandetanib showed ~2 fold difference than -1B1, showing greater contribution of OATP-1B3 than -1B1 in hepatic uptake of vandetanib. Therefore, hepatic uptake of vandetanib and nilotinib is tightly regulated by OATP-1B1 and -1B3 which act as two gatekeepers localized on liver. Hence, OATP-1B1 and -1B3 can be considered as important factors in determining pharmacokinetics or DDIs of vandetanib and nilotinib. For canertinib, only OATP-1B3 was observed to be responsible for its hepatic uptake and it can act as key determinants in bioavailability of canertinib. These results though act mainly as a proof of concept and the actual rate constants in humans may vary based on various physiological and pathological conditions resulting in altered expression of these transporters within the liver.

Inter-individual pharmacokinetic variability can arise at many stages of ADME. For individual therapy, dosing strategies can be based on pharmacokinetic properties. Decisive tailoring of individual dosing to a patient necessitates minimizing these inter-individual pharmacokinetic differences and reducing the risks of both toxicity and subtherapeutic dosing [150]. Till now most of the studies performed with TKIs have not considered affinity of hepatic uptake transporters as a determinant of pharmacokinetic profiles of TKIs. Inter-individual pharmacokinetic variability has been associated with OATP1B1 and -1B3 genetic polymorphisms in patients taking statins and irinotecan [162, 171]. Expression and involvement of these OATP-1B type isoforms in liver has important implications for better understanding of the factors governing ADME of TKIs. Any compromise in the activity of OATP-1B type transporter proteins

will result in suboptimal treatment or high toxicity considering the wide inter-individual pharmacokinetic variability of the tested TKIs. Since vandetanib and nilotinib exhibit substrate specificity towards OATP-1B1 and -1B3, these results led us to the hypothesis that an inactive phenotypic variant of OATP-1B type transporter may determine the clinical pharmacokinetics of these TKIs.

Previously published reports have only considered the role of efflux transporters and metabolizing enzymes in determining the pharmacokinetic profile of TKIs [152, 153, 158, 172-175]. In this study we have observed that a carrier mediated uptake process via OATP-1B1 transporter is involved in cellular accumulation of nilotinib and vandetanib in hepatic tissue. Also, OATP-1B3 is responsible for hepatocellular accumulation of canertinib, vandetanib and nilotinib. OATP-1B1 and/or -1B3 regulate the initial step of hepatic elimination of TKIs by carrying out the uptake of selected TKIs into the hepatic tissue exposing the molecules to CYP enzyme mediated metabolism and elimination via biliary secretion. These OATPs expressed on basolateral membrane of hepatocytes will induce uptake of TKIs and can be regarded as one of the determinants of overall metabolic rate of TKIs in liver [176]. An efficient directional movement of therapeutic agents across hepatic tissues requires the manifestation and synchronized activity of hepatic uptake, metabolizing enzymes and efflux transporters [177]. Duckett D.R. *et al.* [178] reported that coadministration of ketoconazole (CYP3A4 and P-gp inhibitor) with nilotinib resulted in 3-fold increase in the plasma concentration of nilotinib. Ketoconazole is also a well-known inhibitor of OATP-1B type transporters [179] and we have shown that OATP-1B1 and -1B3 transporters are responsible for hepatic uptake of nilotinib. Therefore, the 3-fold increase in the plasma concentration of nilotinib may not be just due to the inhibition of efflux transporter and metabolizing enzyme but also could be due to inhibition of OATP-1B type transporter. OATP-

1B1 and -1B3 transporters also play a vital role in hepatic uptake of nilotinib making it vulnerable to metabolism by CYP3A4 and ultimately causing its elimination by biliary secretion via P-gp. Since a major fraction of nilotinib is eliminated into feces in unchanged form suggesting that the transmembrane localization of nilotinib by OATPs in liver has a major impact on its pharmacokinetics than metabolization. Similarly, Minocha *et al.* reported that the coadministration vandetanib and everolimus resulted in increased plasma concentration of vandetanib. Everolimus increases plasma concentration of vandetanib by inhibiting efflux transporters (P-gp and BCRP) which are also localized on the bile canalicular membrane. Everolimus is also a well-known inhibitor for OATP-1B1 and -1B3 transporters which are responsible for hepatocellular accumulation of therapeutic agents. In this article we have reported the involvement of OATP-1B1 and -1B3 in hepatic uptake of vandetanib. Taken together, it is reasonable to assume that elevation in plasma concentration of vandetanib is not only due to the inhibition of P-gp and BCRP but also due to inhibition of OATP-1B1 and -1B3 by everolimus. Complex interplay of OATPs (localized on basloateral membrane of hepatic tissues) and efflux transporters (expressed on bile canalicular membrane) may be responsible for the hepatobiliary excretion of TKIs. Inhibition of TKIs uptake via hepatic OATPs by coadministration of drugs that are also substrate or inhibitor of these hepatic uptake transporters is a plausible explanation of several *in vivo* observed DDIs. Inhibition of metabolizing enzymes and/or efflux transporter could not be the only cause of the experimental effects. Drug induced alteration of OATP-1B1 and -1B3 transporter function is, therefore, an essential auxiliary mechanism underlying DDIs [170].

OATPs mediated DDIs have the potential to completely influence drug efficacy and toxicity. Therefore, coadministration of canertinib, vandetanib and nilotinib (OATP-1B1 and/or -1B3 substrates) along with other hepatic OATP substrates/inhibitors (paclitaxel, cyclosporine,

protease inhibitors, rifampicin, statins, telmisartan, valsartan, mTOR inhibitors, antibiotics etc.) may result in altered pharmacokinetics and pharmacodynamics of TKIs. On the other hand, induction of the expression of hepatic OATPs can also result in increased detoxification and elimination of numerous OATP-1B1 and -1B3 substrates from the body [158, 180-182]. Pharmacokinetic profile of TKIs is likely to be modified in subjects with hepatic impairment, since TKIs are primarily eliminated via hepatic metabolism and biliary excretion. Down-regulation of OATP-1B type transporter protein in liver disease has been reported by Oswald M *et al.* and Kietel V *et al.* [183, 184]. Also, reduced expression of OATP-1B1 and -1B3 in liver cancer compared to non-cancerous liver tissues has been reported by various investigators [185-187]. For hepatically impaired population, dose reduction of nilotinib has been proposed along with recommendation of lower starting dose and monitoring of any liver function abnormalities [188, 189]. Also, dose of vandetanib in patients with moderate and severe hepatic impairment has not been recommended as its safety and efficacy has not been established [188, 189]. *In vitro* accumulation studies along with estimation of MM kinetic profiles confirms the role of OATP-1B1 and -1B3 in hepatic uptake of nilotinib and vandetanib. On the basis of our findings along with already published reports mentioned above, we can hypothesize that higher plasma concentration of nilotinib or other TKIs in patients with hepatic impairment can be attributed to compromised/downregulated expression of OATP-1B1 and -1B3 transporter which can be responsible for any alteration in the pharmacokinetic profile of nilotinib or other TKIs. Similar findings have been reported by Baker SD *et al.*, showing the involvement of OATP-1B1 and-1B3 in hepatic elimination of sorafenib and longer systemic accumulation due to compromised activity of OATP-1B type transporter protein [148].

Conclusion

In conclusion, we have shown OATP-1B1 and OATP-1B3 are responsible for hepatocellular accumulation of nilotinib and vandetanib whereas only OATP-1B3 is responsible for the carrier mediated uptake of canertinib in hepatic tissue. These findings delineate the involvement of OATP-1B1 and/or -1B3 in hepatic uptake of tested TKIs and confirms the affinity of these hepatic uptake transporters as a determinant of the pharmacokinetic profile of TKIs. Since co-administration of TKIs with other therapeutic agents is becoming common in multi-drug therapy, hepatic uptake transporters OATP-1B1 and -1B3 can be regarded as important molecular targets for potential DDIs. Thus, hepatic uptake mediated by OATP-1B1 and -1B3 for selected TKIs should be dynamically scrutinized in order to circumvent DDIs. These transporters in conjunction with the efflux proteins may eventually decide on the overall flux of the TKIs within the hepatic tissue. These studies act as a proof of concept substantiating the need for further clinical studies investigating the OATP based DDI potential of TKIs. Further *in vivo* studies are required for better understanding of the contribution of OATP-1B1 and/or -1B3 transporter proteins in the hepatic disposition of TKIs and for predicting any adverse drug reactions associated with DDIs [190].

Acknowledgement

This work was supported by National Institutes of Health grant 1R01 AI071199. The authors highly appreciate Dr. Bruno Stieger for their generous gift of CHO-WT and OATP-1B type transporter protein transfected cell lines.

CHAPTER 3

INHIBITION OF OATP-1B1 AND OATP-1B3 BY TYROSINE KINASE INHIBITORS

Rationale

Role of membrane transporters in drug disposition, safety and efficacy i.e., particularly concerning drug-drug interactions (DDIs) has been extensively investigated [191]. Giacomini KM *et al* recently emphasized drug development information on *in vitro* studies of drug-transporter interactions can be extrapolated to clinical studies of transporter based DDIs. Such transporter mediated DDIs can occur by (i) inhibition of membrane transporter resulting in potential DDI, and/or (ii) interacting drug may be a substrate for the transporter. Attention has been drawn towards various approaches and algorithms for predicting transporter mediated DDIs. I*n vitro* and preclinical transport studies are pre-requisites for drug development. Recent progress in clinical translation of these results may impact on regulatory matters for delineation of transport mediated DDIs [122]. In order to predict whether a potential DDI may occur, *in vitro* studies were performed to compare concentration of an inhibitor (I, the maximum unbound plasma concentration) and it's half maximal inhibitory concentration (IC_{50}) for a transporter. Lower IC_{50} of the drug relative to it unbound plasma concentration is a strong indicator of a potential clinical DDIs. An I/IC_{50} value $\geq$ 0.1 has been advocated as a measure to evaluate clinical transporter-based DDIs [122].

Tyrosine kinase inhibitors (TKIs) are the new class of anticancer drugs that specifically targets tyrosine kinases which are fused, mutated and over expressed in cancer [191, 192]. Many of these compounds have been associated with low patient response along with unwanted toxicity, which is unexpected and also largely unexplained. Even though TKIs offer theoretical advantages (selectively target/kill the cancer precursor cells and protect normal tissues) over traditional anti-

cancer agents, these agents are still associated with unpredictable toxicity [150, 157]. Many TKIs exhibit limited efficacy with a high degree of unexpected and unexplained toxicity [151]. Most common side effects associated with TKIs are diarrhea, hypertension, nausea, anorexia and vomiting. The most common treatment-emergent laboratory abnormalities noticed were elevation of total bilirubin, liver transaminases and alanine aminotransferases. Hepatotoxicity is the most frequently reported toxicity among the TKIs with mandatory black box warnings [193]. There is a possibility that treatment associated elevation in liver enzymes with TKIs reveal over-lapping on-target and off-target class effects, however, exact mechanism needs to be clarified [191, 194, 195]. These hepatic abnormalities associated with TKIs may lead to treatment interruption, compromising the potential treatment benefit to the patient. A clear understanding of the exact mechanism responsible for hepatic abnormalities, will give a better chance to interpret and manage these adverse effects which will ultimately benefit patients from continued chemotherapeutic treatment [194].

Despite their frequent use as a chemotherapeutic agent, limited studies have been performed to examine the interactions of these TKIs with hepatic uptake transporters such as organic anion transporting polypeptide (OATP) transporters. Most studies examining interaction of TKIs with these transporters have focused on substrate specificity instead of inhibition interactions [153, 157, 172, 191, 196, 197]. Also, several TKIs have higher molecular weight, polar surface area and lipophilicity, which are essential for OATP inhibition and therefore have potential to inhibit OATPs including OATP-1B1 and OATP-1B3 [198]. Several *in vitro* and *in vivo* studies have indicated that drugs inhibiting these OATPs are responsible for clinically relevant drug-drug interactions. In such cases, inhibition of OATPs can lead to unexpected toxicity, causing marked increase in plasma concentration and area under the plasma concentration time curve

(AUC) for compounds which are substrates of these hepatic transporters. DDIs caused by the inhibition of these transporters represent a large number of drugs which act as substrate or inhibitor of OATP-1B1 and/or -1B3 [199]. Hence, it is of utmost importance to estimate the inhibitory potential of TKIs on OATP-1B1 and -1B3. In the present study, we have evaluated the interaction of TKIs (pazopanib, erlotinib, canertinib, nilotinib and vandetanib) with human OATPs expressed on sinusoidal membrane of liver by employing *in vitro* model system with transfected Chinese hamster ovary (CHO) cells. I*n vitro* studies were designed to compare the inhibitory potential of TKIs on the transport of [^{3}H] estrone sulfate (substrate for OATP-1B1) and cholecystokinin octapeptide (CCK-8, substrate for OATP-1B3) in OATP-1B1 and -1B3 transfected CHO cells.

Materials And Methods

Chemicals

Pazopanib, erlotinib, canertinib, nilotinib and vandetanib were purchased from LC Laboratories (Woburn, MA). Rifampicin was purchased from TCI America, PA. [^{3}H] Estrone sulfate ([^{3}H] ES, specific activity 40-60 Ci/mmol) and [^{3}H] cholecystokinin octapeptide ([^{3}H] CCK-8, specific activity 60-100 Ci/mmol) was procured from Perkin Elmer (Boston, MA, USA). All other chemicals used were of high performance liquid chromatography grade and were obtained from either Sigma Aldrich or Fisher Scientific. Cell culture medium and other ingredients were purchased from Life Sciences. Fetal bovine serum was received from Atlanta Biologicals.

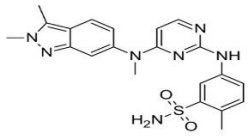

Pazopanib (437.517 g/mol)

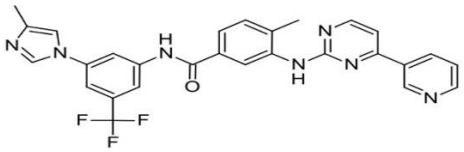

Nilotinib (529.5245 g/mol)

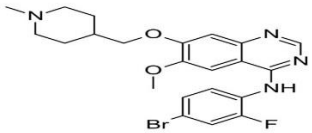

Vandetainib (475.354 g/mol)

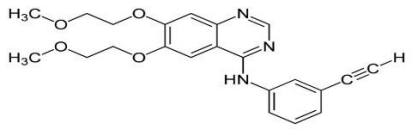

Erlotinib (393.436 g/mol)

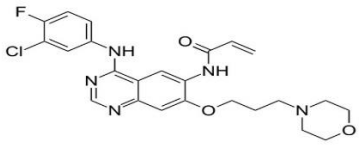

Canertinib (485.94 g/mol)

In Vitro Studies

Cell Lines

Chinese hamster ovary (CHO) cells (passage number 17-50) were selected for all *in vitro* experiments. OATP-1B1 and -1B3 CHO transfected cells were obtained as a gift from Dr. Bruno Stieger (Department of Clinical Pharmacology and Toxicology, University Hospital Zürich, Switzerland). Cells were cultured in Dulbecco's modified Eagle's medium (DMEM), supplemented with 10% heat inactivated fetal bovine serum (FBS), L-proline (50µg/mL), HEPES, penicillin (100µg/ml), streptomycin (100µg/ml), geneticin (100µg/mL). Cell cultures were maintained at 37°C with 5% CO_2 under humidifying conditions.

In Vitro Cellular Accumulation Studies

Confluent CHO OATP-1B1 and -1B3 cells were utilized for uptake experiments. Following medium removal, cells were rinsed thrice for 5 min each with 1–2 ml of Dulbecco's phosphate-buffered saline (DPBS) containing 130 mM NaCl, 0.03 mM KCl, 7.5 mM Na_2HPO_4, 1.5 mM KH_2PO_4, 1 mM $CaCl_2$, 0.5 mM $MgSO_4$, 20 mM HEPES, and 5 mM glucose maintained at pH 7.4. Uptake studies were initiated by adding 250µl of solution containing 0.25 µCi/ml of [^{3}H] ES (for OATP-1B1) or [^{3}H] CCK-8 (for OATP-1B3) in the presence of two different concentrations of (25 and 50µM) of TKIs and rifampicin (positive control). Following incubation,

the solution was removed and uptake was terminated with 2 ml of ice-cold stop solution containing 200 mM KCl and 2 mM HEPES. The cell monolayer was washed thrice, 5 min each and 1ml of lysis buffer (0.1% Triton-X solution in 0.3% NaOH) was added to each well and plates were stored overnight at room temperature. Subsequently, cell lysate (400µl) from each well was transferred to scintillation vials containing 3 ml of scintillation cocktail (Universal ES from MP Biomedicals). Samples were analyzed by measuring the radioactivity in a liquid scintillation counter (Beckman Instruments Inc., Fullerton, CA, USA, model LS-6500). Protein content of each sample was estimated by BioRad Protein Estimation Kit (BioRad Protein Estimation Kit, Hercules, CA, USA).

Estimation Of Half Maximal Inhibitory Concentration (IC_{50})

To determine the half maximal inhibitory concentration (IC_{50}) of TKIs for the differential uptake of OATP-1B1 and -1B3 transporter proteins, intracellular accumulation of the probe substrates (ES and CCK-8) in the presence of increasing concentrations (0.1-100µm) of TKIs was measured. Using a concentrated stock solution of the TKIs, several working concentrations were prepared ranging from (0.1µM - 100µM) in fresh DPBS buffer spiked with [^{3}H] ES (0.25µCi/ml) or [^{3}H] CCK-8 (0.25µCi/ml). Uptake was carried out at different concentration of TKIs in OATP-1B1 and -1B3 transfected CHO cells. The data was fitted to equation as shown in section 2.3 and the IC_{50} values were calculated according to nonlinear least squares regression analysis program; GraphPad Prism version 5.

Data Analysis

IC_{50} values of TKIs on intracellular accumulation of the probe substrates uptake via hepatic OATP-1B1 and -1B3 were calculated with a nonlinear least squares regression analysis program GraphPad Prism version 5. The data was plotted and fitted to (Eq.1) and the half maximal inhibitory concentration (IC_{50}) were calculated.

$$Y = min + \frac{max - min}{1 + 10^{(LogIC50 - x) * H}} \qquad \textbf{Eq. 1}$$

x denotes the log conc. of the inhibitors, Y is the cellular accumulation of the probe substrate (ES or CCK-8), IC_{50} represents the TKIs conc. where the influx of the substrate is inhibited by 50% and H is the Hill constant. Y starts at a min value and then plateaus at a max value resulting in a sigmoidal plot.

Cytotoxicity Studies

Cell Titer 96® Aqueous Non-Radioactive Cell Proliferation Assay Kit (Promega, Madison, WI) was employed to carry out cytotoxicity assay. OATP-1B1 and -1B3 transfected CHO cells were cultured in 96-well plate. Sterile drug solutions of highest concentration (100µM) of TKIs are prepared in the culture medium using 0.22µm nylon sterile membrane filters. Aliquots of TKIs having a volume of 100µL (previously made in culture medium) were added to each well and incubated for 24h. Cell proliferation in the presence of TKIs was measured and compared with a negative control (medium without TKIs) and a positive control (Triton X). Twenty microliters of dye solution was added to each well after 24h of incubation with TKIs. Cells were then incubated for 4h in order to complete the reaction with dye. UV absorbance of purple formazan product was measured at a wavelength of 590nm with a 96-well micro titer plate reader (SpectraFluor Plus, Tecan, Maennedorf, Switzerland). Toxicity of TKIs in OATP-1B type transfected CHO cells was estimated by the amount of formazan formed, which is directly proportional to viable cells.

Statistical Analysis

All the experiments were conducted at least in quadruplicate (n=4) and the outcomes were expressed as mean±standard deviation (SD). To calculate statistical significance, student's t-test was performed. Any difference between mean values is considered statistically significant for P value ≤ 0.05.

Results

In Vitro Inhibitory Activity Of Tyrosine Kinase Inhibitors

Initial *in vitro* uptake experiments were carried out to determine inhibitory activity of TKIs for OATP-1B1 and -1B3 transfected CHO cells utilizing radiolabelled substrates. [^{3}H] ES (5nM) and [^{3}H] CCK-8 (3.1 nM) were employed as radiolabelled probe substrate for OATP-1B1 and -1B3 transporter proteins, respectively. Cellular accumulation of [^{3}H] ES was measured by exposing OATP-1B1 transfected CHO cells to two different concentrations (25 and 50µM) of TKIs and rifampicin (positive control). Out of the selected TKIs, pazopanib and nilotinib showed significant inhibition on cellular accumulation of [^{3}H] ES in OATP-1B1 transfected cells. The remaining 3 TKIs (canertinib, vandetanib and erlotinib) did not show any significant inhibitory activity on cellular accumulation of [^{3}H] ES in OATP-1B1 transfected cells. Pazopanib and nilotinib (25 and 50µM) diminish the uptake of [^{3}H] ES by ~90% ($p<0.05$) in OATP-1B1 transfected cells. Rifampicin reduced uptake of [^{3}H] ES by ~50% and 70% at 25 and 50µM, respectively **(Fig.3.1)**.

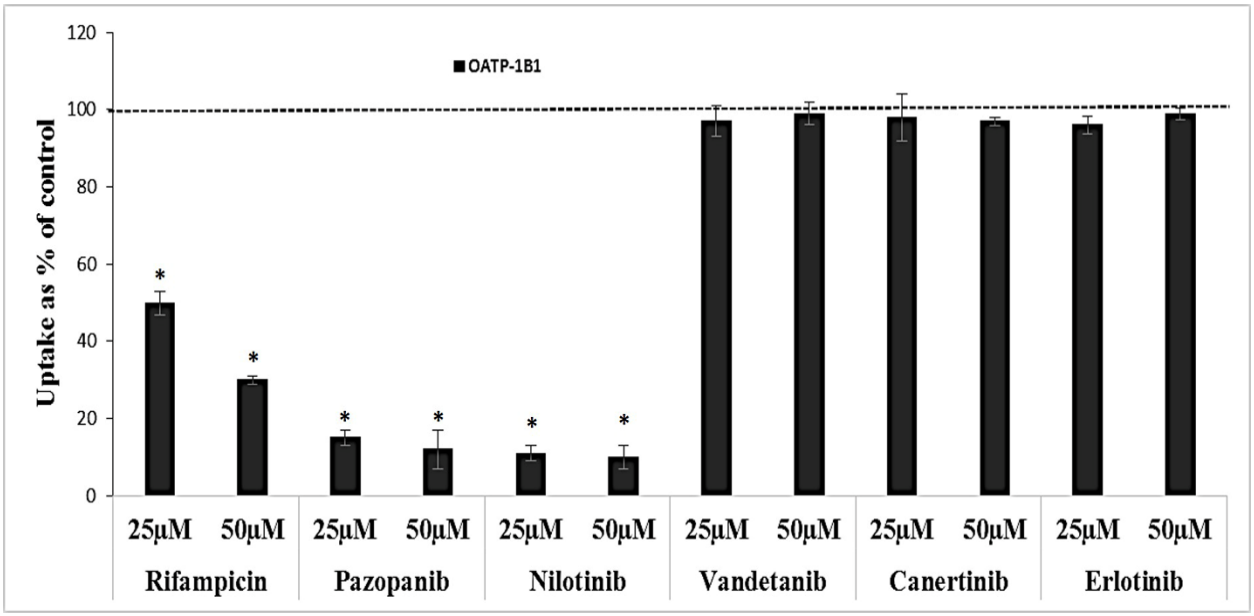

Fig.3.1: Influence of 5 different TKIs and rifampicin at two different concentrations (25 and

50μM) on the activity of OATP-1B1, expressed in CHO cells, as determined by the intracellular accumulation of [^{3}H] estrone sulfate ([^{3}H] ES, 10 min incubation). Data are shown as mean±S.D. n=4. S.D. means standard derivation. (*$p<0.05$)

It has been reported previously that OATP-1B3 shares 80% amino acid homolog with OATP-1B1. Also, both the OATP isoforms share multiple overlapping substrates, such as rifampicin pravastatin, pitvastatin and docetaxel [158, 159]. In this study, we have also determined the inhibitory activity of TKIs and rifampicin (positive control) at two different concentrations (25 and 50μM) on cellular accumulation of [^{3}H] CCK-8 in OATP-1B3 transfected cells. Only vandetanib showed significant inhibition on cellular accumulation of [^{3}H] CCK-8 in OATP-1B3 transfected cells. Pazopanib, nilotinib, canertinib and erlotinib at both concentrations did not showed any significant effect on the cellular accumulation of [^{3}H] CCK-8 in OATP-1B3 transfected cells. Reduced uptake of [^{3}H] CCK-8 was aslo observed in the presence of rifampicin in OATP-1B3 transfected cells. Uptake of [^{3}H] CCK-8 in OATP-1B3 transfected cells was reduced to ~10% to 20% and ~5% to 10% in the presence of vandetanib and rifampicin (25 and 50μM), respectively **(Fig.3.2).** Pazopanib and nilotinib showed inhibitory activity towards OATP-1B1 while vandetanib only indicated inhibitory potential towards OATP-1B3.

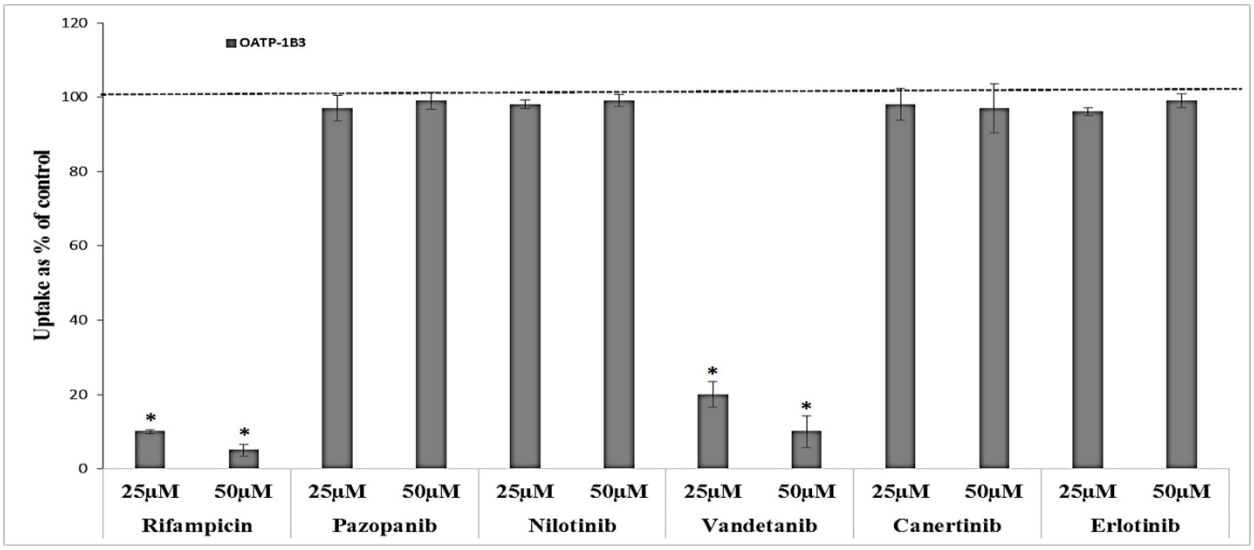

Fig.3.2: Influence of 5 different TKIs and rifampicin at two different concentrations (25 and 50µM) on the activity of OATP-1B3, expressed in CHO cells, as determined by the intracellular accumulation of [^{3}H] cholecystokinin octapeptide ([^{3}H] CCK-8, 10 min incubation). Data are shown as mean±S.D. n=4. (*$p<0.05$)

Estimation Of Half Maximal Inhibitory Concentration (IC_{50})

To determine the half maximal inhibitory concentration (IC_{50}) concentrations of TKIs to inhibit OATP-1B1 and -1B3 functional activity, cellular accumulation experiments were conducted using probe substrates, ([^{3}H] ES for OATP-1B1 and [^{3}H] CCK-8 for OATP-1B3) in the presence of increasing concentrations (0.1-100µM) of TKIs and rifampicin. Previous studies have shown time-dependent uptake on similar cell lines to be linear up to 15 minutes [160-162, 200]. We incubated cells for 10 minutes as it remains within the linear range of uptake as well as gives us concentrations well within the detectable range. A modified log [dose]-response curve was applied to fit the data (Eq. 1) in order to obtain IC_{50} values. Diminished net uptake rate of probe substrate ([^{3}H] ES) in the presence of increasing concentrations of the TKIs was observed in

OATP-1B1 cells. IC_{50} values for rifampicin, pazopanib and nilotinib towards OATP-1B1 transporter inhibition were 10.46±1.15, 3.89±1.21 and 2.78±1.13 µM respectively **(Figs.3.3, 3.4, 3.5 and Table 3.1)**. Nilotinib appeared to be more potent inhibitor of OATP-1B1 than pazopanib. Vandetanib, canertinib and erlotinib did not cause any concentration dependent inhibition on cellular accumulation of probe substrate ([^{3}H] ES) via OATP-1B1 transporter (**Figs.3.6, 3.7 and 3.8)**. Also, reduced intracellular accumulation of [^{3}H] CCK-8 was observed in OATP-1B3 transfected cells in a concentration dependent manner in the presence of vandetanib. IC_{50} values for rifampicin and vandetanib for OATP-1B3 transporter inhibition were 3.67±1.20 and 18.13±1.21 µM respectively **(Figs.3.9, 3.10 and Table 3.1).** Likewise, no significant inhibition in net uptake rate of probe substrate ([^{3}H] CCK-8) was observed in OATP-1B3 cells in presence of pazopanib, nilotinib, canertinib and erlotinib **(Figs.3.11, 3.12, 3.13 and 3.14).**

Cytotoxicity Studies

To evaluate the cytotoxic effect of the selected TKIs, a cell proliferation assay was performed on cell monolayers of transfected CHO cells for a period of 24h. No cytotoxic effects of pazopanib, erlotinib, canertinib, vandetanib and nilotinib at a concentration of 100µM were observed in OATP-1B1 and -1B3 transfected cells in relative to positive control (Triton X). The findings from this study clearly demonstrate that the selected TKIs are non-cytotoxic even at a concentration of 100µM **(Fig.3.15)**.

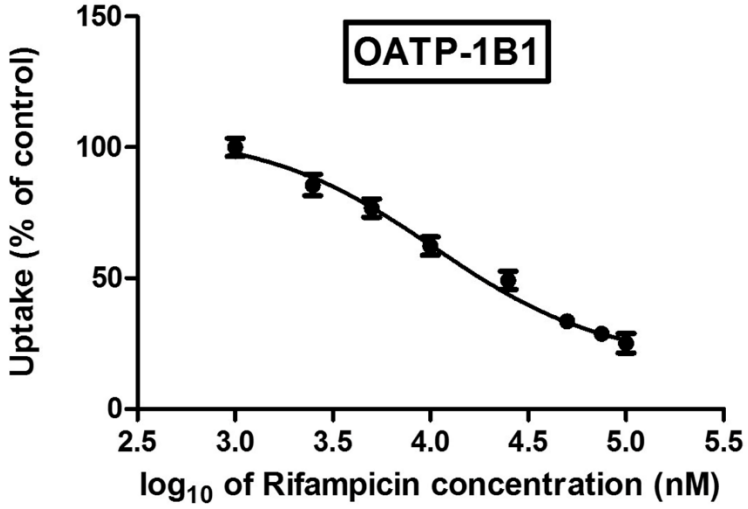

Fig.3.3: Inhibitory potency of rifampicin towards OATP-1B1. Intracellular accumulation of OATP-1B1 substrate [^{3}H] ES in the presence of increasing concentrations of rifampicin (0.1-100µM). Data is shown as mean±S.D. n=4.

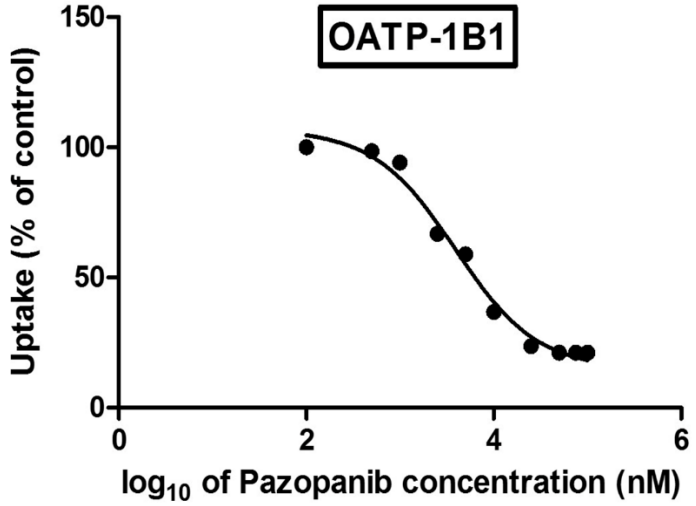

Fig.3.4: Inhibitory potency of pazopanib towards OATP-1B1. Intracellular accumulation of OATP-1B1 substrate [^{3}H] ES in the presence of increasing concentrations of pazopanib (0.1-100µM). Data is shown as mean±S.D. n=4.

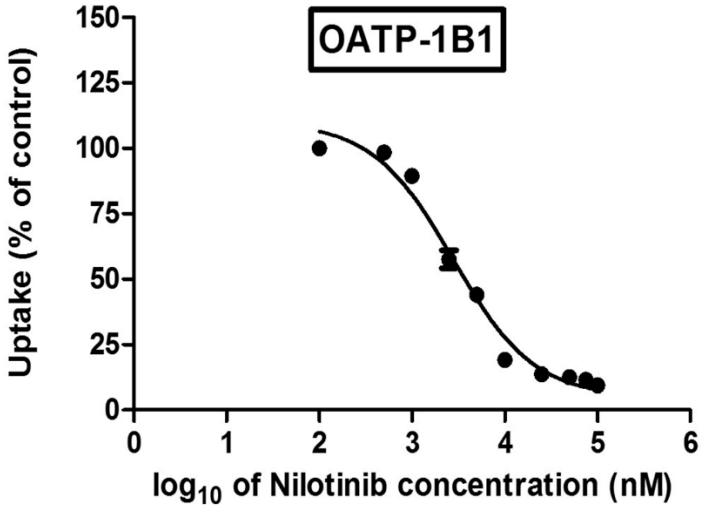

Fig.3.5: Inhibitory potency of nilotinib towards OATP-1B1. Intracellular accumulation of OATP-1B1 substrate [^{3}H] ES in the presence of increasing concentrations of nilotinib (0.1-100µM). Data is shown as mean±S.D. n=4.

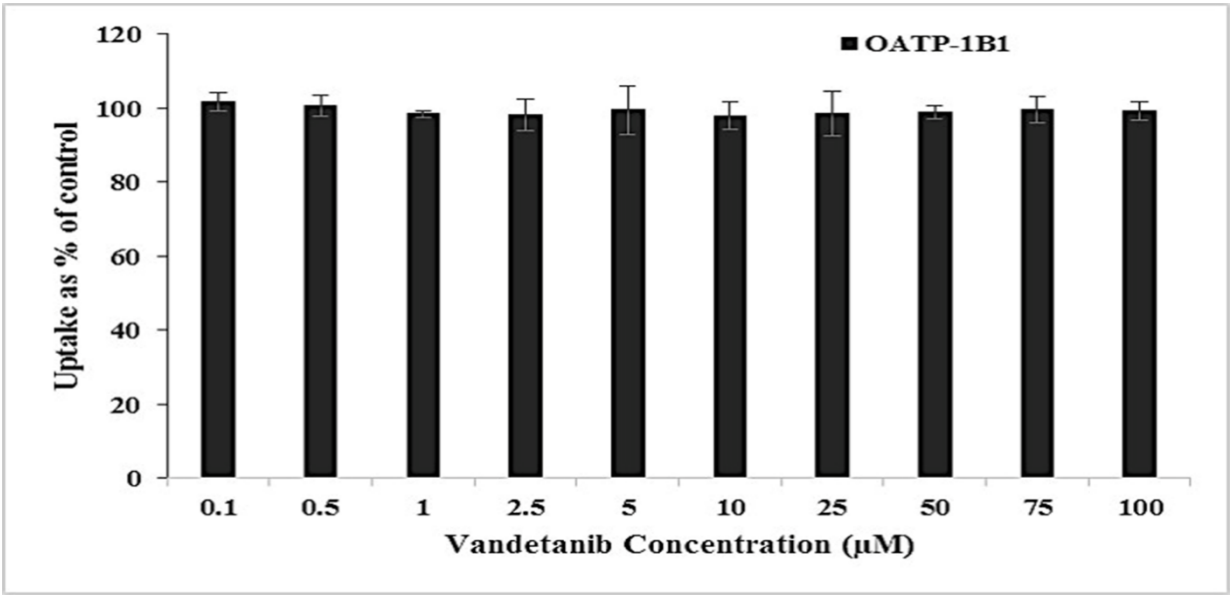

Fig.3.6: Inhibitory potency of vandetanib towards OATP-1B1. Intracellular accumulation of OATP-1B1 substrate [^{3}H] ES in the presence of increasing concentrations of vandetanib (0.1-100µM). Data is shown as mean±S.D. n=4.

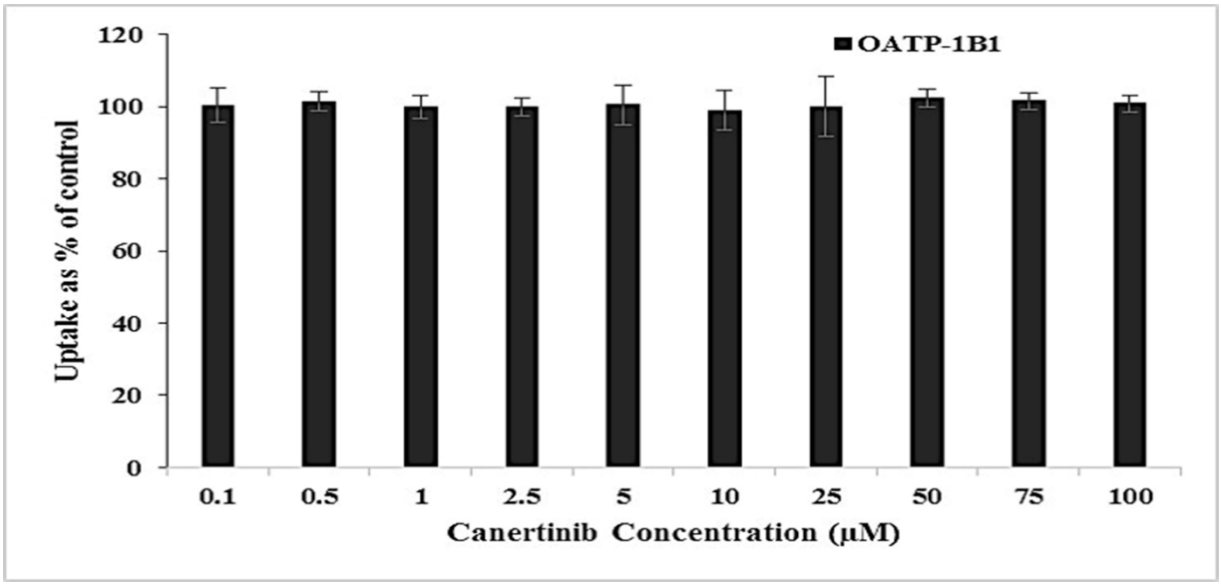

Fig.3.7: Inhibitory potency of canertinib towards OATP-1B1. Intracellular accumulation of OATP-1B1 substrate [^{3}H] ES in the presence of increasing concentrations of canertinib (0.1-100µM). Data is shown as mean±S.D. n=4.

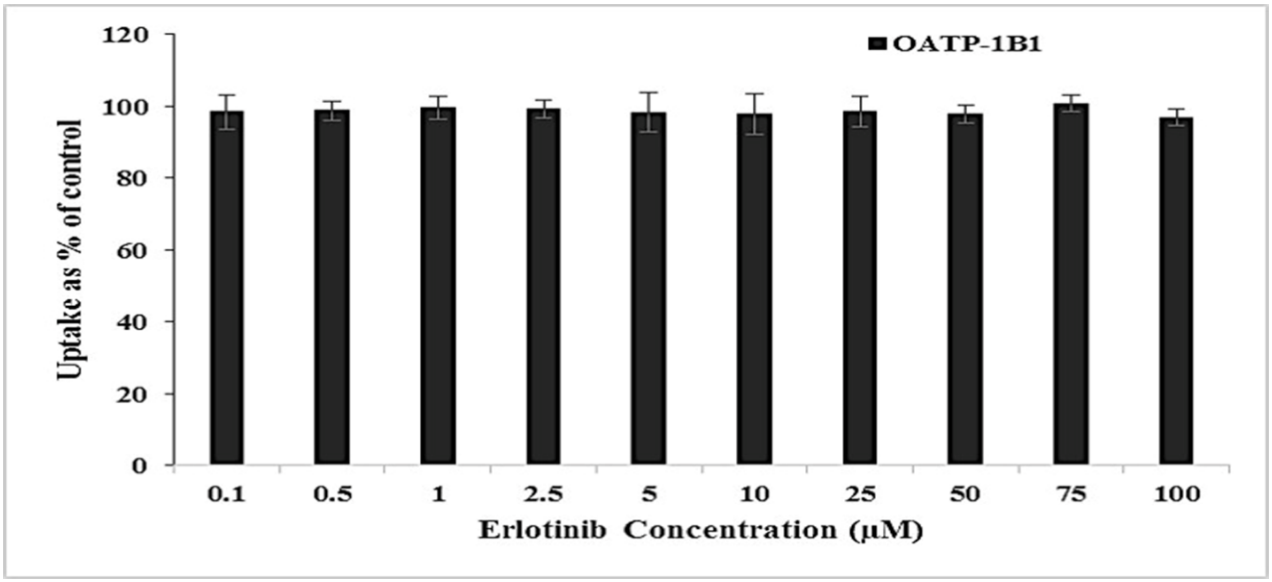

Fig.3.8: Inhibitory potency of erlotinib towards OATP-1B1. Intracellular accumulation of OATP-1B1 substrate [^{3}H] ES in the presence of increasing concentrations of erlotinib (0.1-100µM). Data is shown as mean±S.D. n=4.

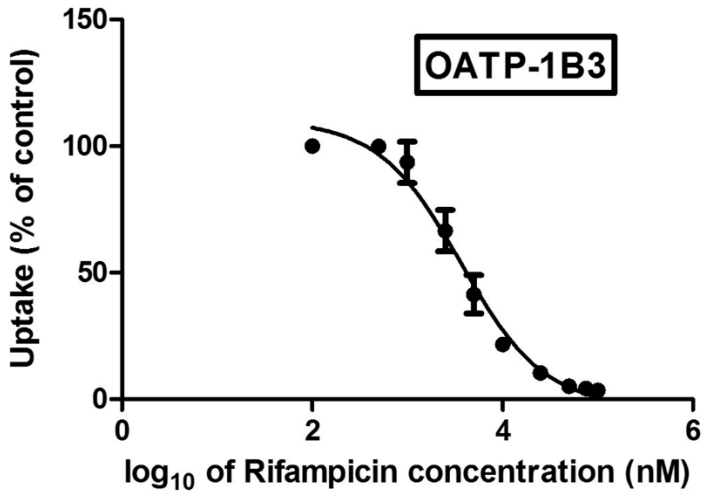

Fig.3.9: Inhibitory potency of rifampicin towards OATP-1B3. Intracellular accumulation of OATP-1B3 substrate [^{3}H] CCK-8 in the presence of increasing concentrations of rifampicin (0.1-100µM). Data is shown as mean±S.D. n=4.

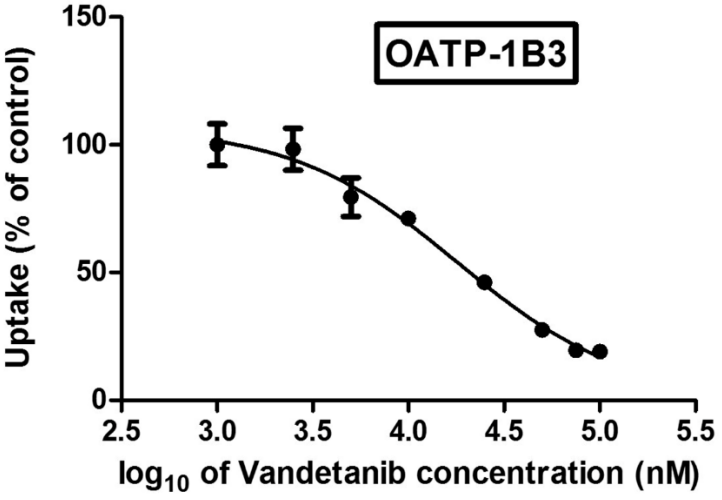

Fig.3.10: Inhibitory potency of vandetanib towards OATP-1B3. Intracellular accumulation of OATP-1B3 substrate [^{3}H] CCK-8 in the presence of increasing concentrations of vandetanib (0.1-100µM). Data is shown as mean±S.D. n=4.

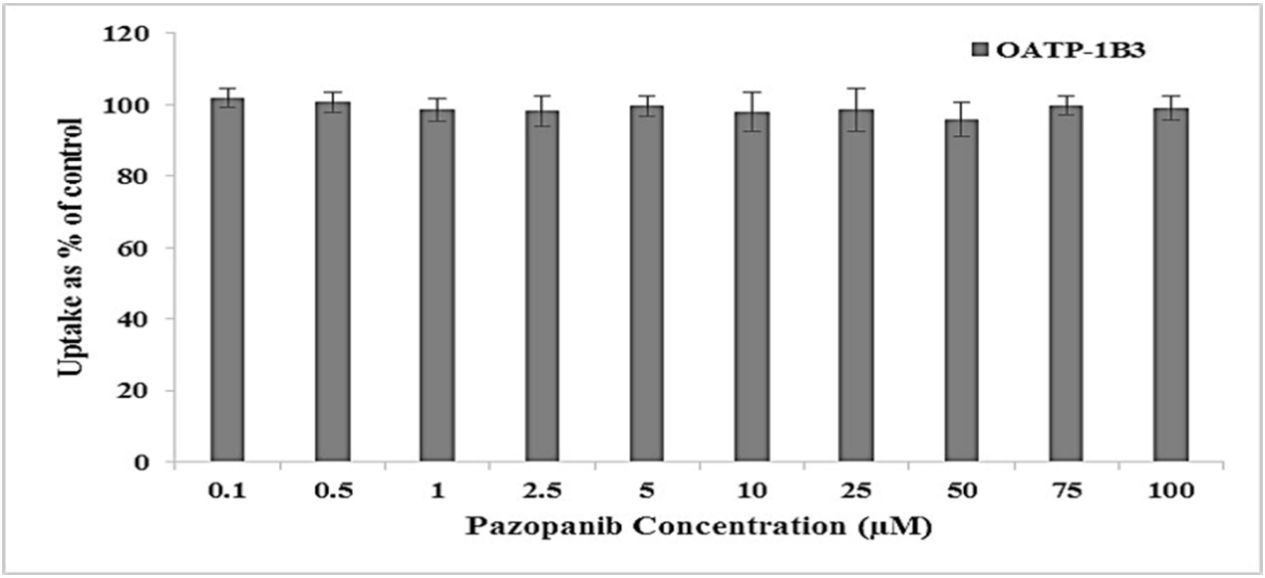

Fig.3.11: Inhibitory potency of pazopanib towards OATP-1B3. Intracellular accumulation of OATP-1B3 substrate [^{3}H] CCK-8 in the presence of increasing concentrations of pazopanib (0.1-100µM). Data is shown as mean±S.D. n=4.

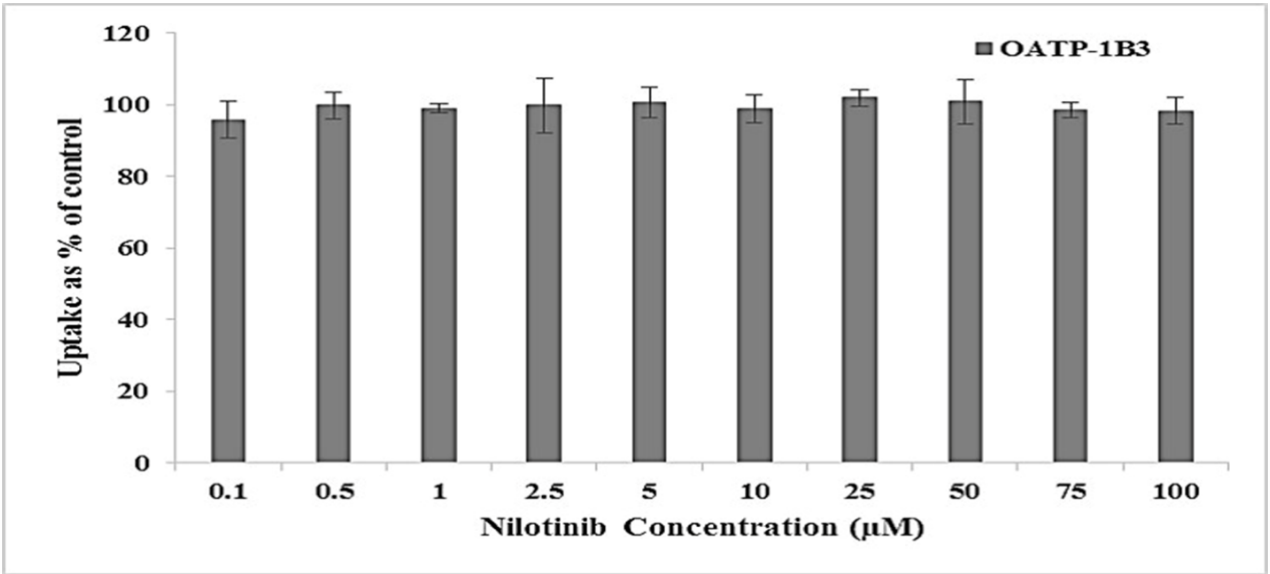

Fig.3.12: Inhibitory potency of nilotinib towards OATP-1B3. Intracellular accumulation of OATP-1B3 substrate [^{3}H] CCK-8 in the presence of increasing concentrations of nilotinib (0.1-100µM). Data is shown as mean±S.D. n=4.

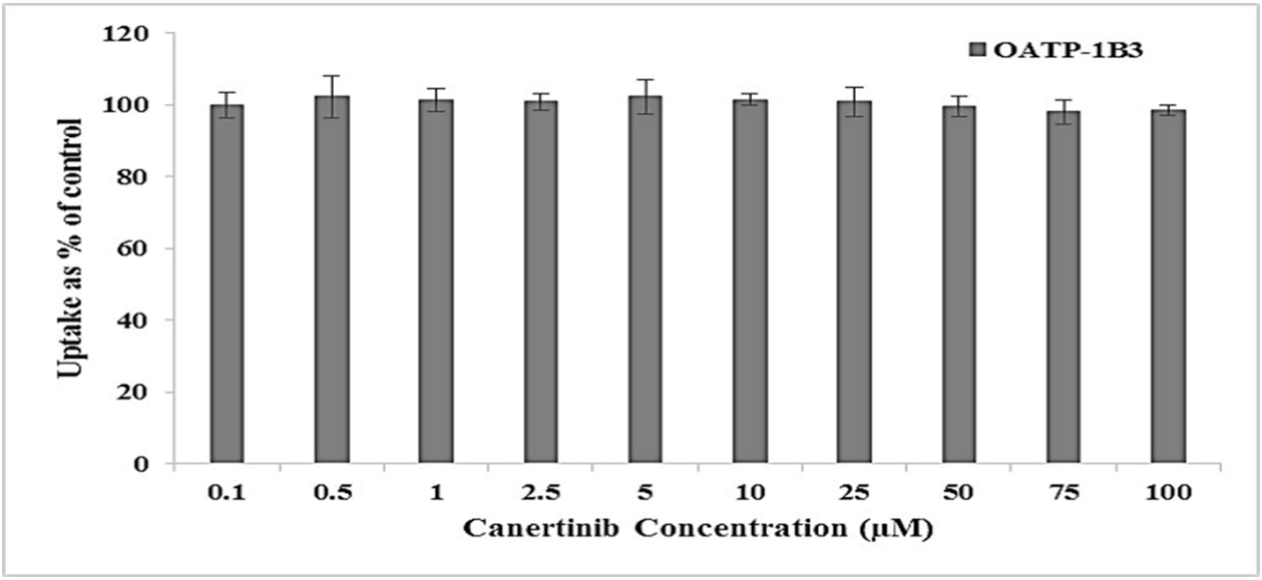

Fig.3.13: Inhibitory potency of canertinib towards OATP-1B3. Intracellular accumulation of OATP-1B3 substrate [^{3}H] CCK-8 in the presence of increasing concentrations of canertinib (0.1-100µM). Data is shown as mean±S.D. n=4.

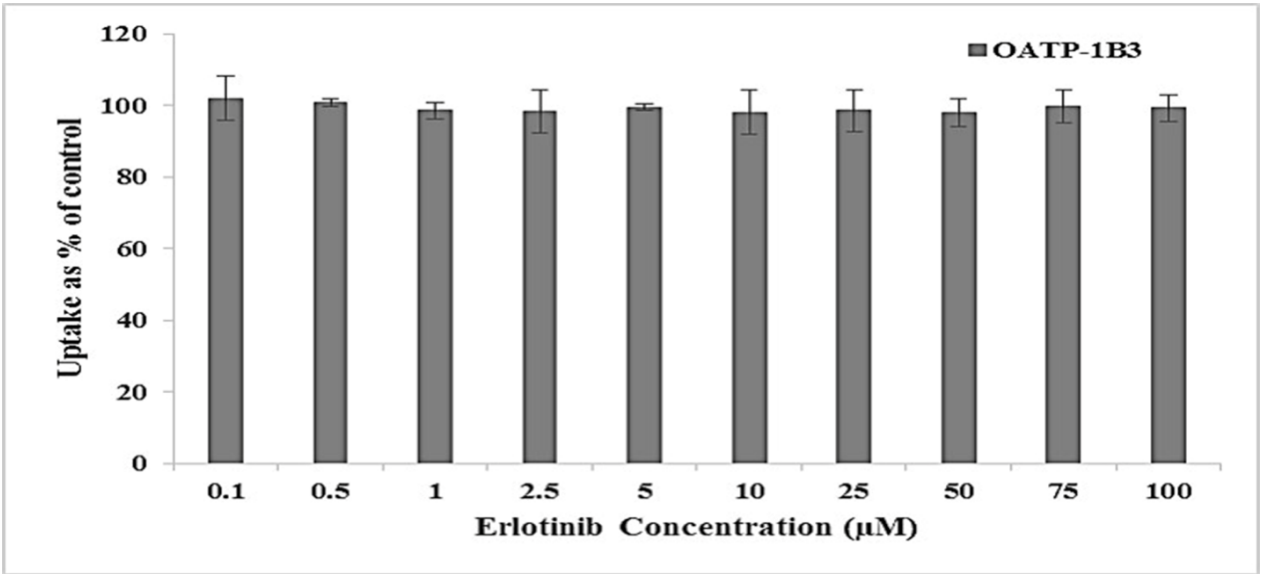

Fig.3.14: Inhibitory potency of erlotinib towards OATP-1B3. Intracellular accumulation of OATP-1B3 substrate [^{3}H] CCK-8 in the presence of increasing concentrations of erlotinib (0.1-100µM). Data is shown as mean±S.D. n=4.

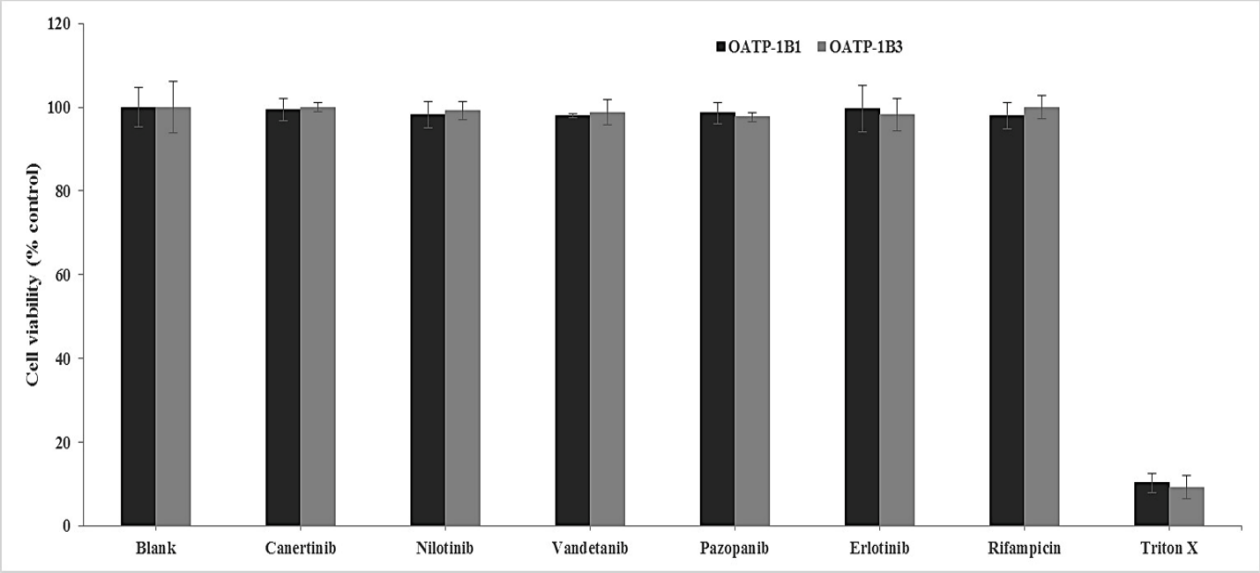

Fig.3.15: Cytotoxicity in the presence of TKIs at highest studied concentration (100µM) on OATP-1B1 and -1B3 transfected cells. Data represent the mean±SD, n=4.

Discussion

In the present study, we investigated the inhibitory potential of several TKIs on OATP family transporters. This study also estimated the half maximal inhibitory concentration (IC_{50}) of TKIs for OATP-1B1 and -1B3. CHO cells were originally selected for the transfection because of the lack of expression of these family of proteins in the parent cell line resulting in minimal background activity. Also, these cells can be maintained in culture for sustained periods and can be ready for use in a specific experiment within a few days. Our findings are in partial agreement with the study done by Hu S *et al* [200], where the authors reported the inhibitory potency of nilotinib and pazopanib (only at 10µM) in Flp-In T-Rex293 cells expressing OATP-1B1. Similar results were observed in studies evaluating *in vitro* inhibitory activity of TKIs, demonstrating inhibition of OATP-1B1 transporter protein by nilotinib and pazopanib. S Hu *et al*. [148, 200][1] also reported the inhibitory activity of erlotinib and vandetanib in Flp-In T-Rex293 cells expressing OATP-1B1 at a concentration of 10µM. Conversely, our findings demonstrate that

there is no active involvement of erlotinib and vandetanib in the inhibition of OATP-1B1 transporter proteins. These contrasting results suggest that utilization of different radiolabelled probe substrate and *in vitro* model based systems may affect the inhibitory action of TKIs on cellular accumulation of probe substrate via OATP and can lead to misinterpretation of the role of TKIs causing inhibition of OATPs.

Expression of OATP-1B1 and -1B3 have been exclusively reported on liver, suggesting their vital role in hepatic uptake of many drugs. Moreover expression of OATP-1B3 has also been reported on cancer tissues [90, 145, 199, 201-203]. Several substrates of OATP like statins, paclitaxel, and docetaxel are taken and metabolized by liver. Rate of hepatic transporter mediated uptake is considered as one of the important parameter of total metabolic rate [199, 204-207]. Hence, plasma concentration of drugs which undergo hepatic metabolism may be altered by inhibition of hepatic uptake transporters (OATPs). Cyclosporin A (CsA) is a well-known inhibitor of OATP-1B1, CYP3A4 and MDR1. It is a more potent inhibitor of OATP-1B1 (IC_{50}: 0.2µM) than CYP3A4 (IC_{50}: >0.3µM). Coadministration of pravastatin, rosuvastatin and atorvastatin together with CsA resulted in increased AUC by 9.93, 7.08 and 8.69 fold, espectively [199, 208, 209]. Considering this result, concentration of CsA in systemic circulation was not high enough from oral administration to inhibit hepatic CYP3A4 function. Thus, increase in AUC of statins on coadministring CsA was due to inhibition of OATP-1B1. Similarly, gemfibrozil is also a more potent inhibitor of OATP-1B1 than metabolic enzymes, i.e., CYP1A2, 2C8, 2C9 and 2C19. Coadministration of pravastatin, rosuvastatin and atorvastatin together with CsA results in higher AUC by 2.01, 1.88 and 1.35 fold, respectively [199, 210-212]. Since, these statins are primarily excreted from the liver in an unchanged form, magnitude of increase can be attributed as a result of inhibition of OATP-1B1. Hence inhibition of hepatic uptake transporters (OATPs) can result in

many clinically relevant DDIs. Unlike statins, information on the inhibitory potency of TKIs on hepatic uptake transporters (OATP-1B1 and -1B3) is very sparse. Thus, it is of utmost importance to understand clinically relevant DDIs which may arise due to inhibitory action of TKIs on OATP-1B1 and -1B3.

The results obtained from our studies evaluating *in vitro* inhibitory activity of TKIs reveals inhibition of OATP-1B1 and/or-1B3 by selected TKIs. In this article, we have reported inhibitory potential of TKIs for OATP-1B1 and/or -1B3 by estimating half maximal inhibitory concentration (IC_{50}). Our findings suggest that nilotinib is a more potent inhibitor of OATP-1B1 than pazopanib. No significant inhibition in uptake of radiolabelled probe substrates were observed in OATP-1B1 transfected cells with vandetanib, canertinib and erlotinib indicating that all tested TKIs do not act as inhibitor for OATP-1B1. Similarly for OATP-1B3 transporter protein, while vandetanib showed its inhibitory action on the probe radiolabelled substrate intracellular accumulation, pazopanib, nilotinib, canertinib and erlotinib did not produce any inhibitory effect on OATP-1B3. Hence, OATP-1B1 and/or -1B3 can be considered as important factors in determining pharmacokinetics or DDIs of pazopanib, nilotinib and vandetanib. These results though act mainly as a proof of concept and the actual inhibitory potency/activity in humans may vary based on various physiological and pathological conditions resulting in altered expression of these transporters in liver.

Although TKIs share similar structural backbone but minor changes in the structure can lead to drastic changes in binding affinities to OATP-1B1 and-1B3 transporter and hence, it might be a reason for the large disparity in the inhibition potential among the various drugs for the hepatic uptake transporters. Additionally, a single radioactive substrate was used to determine the inhibition efficiency of the drugs for respective transporters. Since there can be multiple binding

sites on a single transporter for various substrates as previously reported [213, 214] the positive inhibitors might only inhibit the specific substrate-transporter site interaction. It might happen that if a different substrate that binds to a different binding site is used, then we might see the other non-positive inhibitors to become active for OATP-1B1 and-1B3.

Currently, OATP-1B1 and -1B3 related DDIs involving clinical as well as pre-clinical interactions has been published in many reports. These DDIs are considered as vital components in discovery and development of drugs with safer profiles since these DDIs may lead to elevated risk of drug induced adverse effects, even resulting in withdrawal from the market. Many therapeutic agents are substrates or inhibitors of OATP-1B1 and/or -1B3. Alteration in the hepatic uptake of these compounds via OATPs may result in clinically relevant DDIs. Expression and involvement of these OATP-1B type isoforms in liver needs to be delineated for better understanding of the factors governing absorption, distribution, metabolism and elimination (ADME) of therapeutic agents. Any change in the activity of OATP-1B type transporter proteins will result in suboptimal treatment or high toxicity. Thus it is necessary to investigate the role of these transporters in order to avoid DDIs [199].

Previously published articles have focused on TKIs as substrates and not on the inhibition potential of these agents with OATPs [153, 157, 172, 191, 196, 197]. In this study we have observed concentration dependent inhibition of OATP-1B1 transporter by pazopanib and nilotinib in *in vitro* model system. Also, concentration dependent inhibition of OATP-1B3 in presence of vandetanib.

OATP-1B1 and/or -1B3 are responsible for regulating the initial step of hepatic elimination of therapeutic agents (substrates of OATPs) by carrying out the uptake of selected agents into the hepatic tissue exposing the molecules to CYP enzyme mediated metabolism followed by

elimination via biliary secretion. These OATPs expressed on basolateral membrane of hepatocytes may induce drug uptake and can be regarded as one of the determinants of overall metabolic rate in liver [147]. An efficient directional movement of therapeutic agents across hepatic tissues requires synchronized activity of hepatic uptake, metabolizing enzymes and efflux transporters [177]. Tan AR *et al*, reported that coadministration of pazopanib (weak CYP3A4 and CYP2C8 inhibitor) with paclitaxel resulted in 14% lower paclitaxel clearance and a 31% higher concentration [215]. We have shown that pazopanib inhibits OATP-1B1 transporter which is responsible for hepatic uptake of paclitaxel. Therefore, 31% higher plasma concentration of paclitaxel may not be just due to the inhibition of metabolizing enzymes but also may be due to inhibition of OATP-1B1 transporter. This hypothesis of OATP inhibition by TKIs resulting in increased plasma taxol concentration (docetaxel) has also been reported by Hu S *et al* [200]. OATP-1B1 plays a vital role in hepatic uptake of paclitaxel making it vulnerable to metabolism by CYP3A4 and ultimately accelerating elimination by biliary secretion via P-gp [216, 217].

Coadministration of vandetanib has been warranted with digoxin. Vandetanib is a weak inhibitor of the efflux pump P-glycoprotein (P-gp). Coadministration of vandetanib and digoxin (substrate of P-glycoprotein, P-gp) may result in increased plasma concentrations of digoxin (caprelsa, product monograph). Also, digoxin is a well know substrate of OATP-1B3 as well [122]. We have shown that vandetanib inhibits OATP-1B3 transporter which is responsible for hepatic uptake of digoxin. Hence, enhanced plasma concentration of digoxin will not be just because of the inhibition of P-gp but also may be due to inhibition of OATP-1B3 transporter by vandetanib. Inhibition of OATPs (localized on basloateral membrane of hepatic tissues), metabolizing enzymes and efflux transporters (expressed on bile canalicular membrane) may be responsible for enhance plasma concentration of OATP substrates.

OATPs mediated DDIs have the potential to influence drug efficacy and toxicity. Therefore, coadministration of pazopanib, nilotinib and vandetanib (OATP-1B1 and/or -1B3 inhibitors) along with other hepatic OATP substrates (paclitaxel, docetaxel, cyclosporine, protease inhibitors, rifampicin, statins, telmisartan, valsartan, mTOR inhibitors, antibiotics etc.) may result in altered pharmacokinetics and pharmacodynamics of OATP substrates. Inhibition of hepatic uptake of OATP substrates by coadministration of OATPs inhibitor is a plausible explanation of several clinically observed DDIs. Inhibition of metabolizing enzymes and/or efflux transporter may not be the only cause of DDI induced effects. Drug induced alteration of OATP-1B1 and -1B3 transporter function is an essential auxiliary mechanism underlying DDIs [170].

Several TKIs are associated with drug induced hepatotoxicity. Rise in serum transaminase levels and bilirubin were the common adverse effects associated with TKIs therapeutic regimen. Xu CF *et al* [194], reported that higher bilirubin levels in plasma or hyperbilirubinemia is associated with the inhibition of both OATP-1B1 and enzyme uridine diphosphate glucuronosyltransferase 1A1 (UGT1A1). OATP-1B1 is responsible for hepatic uptake of bilirubin whereas UGT1A1 is responsible for bilirubin metabolism prior to its elimination. Hence, pazopanib induced hyperbilirubinemia may result due to inhibition of both OATP-1B1 and UGT1A1. We have also here reported the inhibitory potency of pazopanib for OATP-1B1. This result is consistent with the observation that pazopanib induced inhibition of OATP-1B1 may cause diminished hepatic uptake of bilirubin resulting in hyperbilirubinemia. Similarly, we have reported inhibitory activity of nilotinib towards OATP-1B1 transporter proteins. Singer JB *et al* [218], reported that inhibition of UGT1A1 activity by nilotinib and genetic polymorphism can be attributed as the cause of increased rate of hyperbilirubinemia. On the basis of our findings along

with published reports, we postulate that nilotinib induced hyperbilirubinemia may be the result of inhibition of both OATP-1B1 and UGT1A1.

Conclusion

In conclusion, we have shown that selected TKIs may cause inhibition of OATP-1B1 and OATP-1B3. Pazopanib and nilotinib exhibit concentration dependent inhibitory activity against OATP-1B1 whereas vandetanib generates inhibitory action with OATP-1B3. These findings delineate the involvement of TKIs in inhibiting hepatic uptake of OATP-1B1 and -1B3 substrate. These findings also confirm that inhibitory activity of TKIs towards hepatic uptake transporters and can be utilized as a vital determinant of the pharmacokinetic profile of coadministered therapeutic agents. Since co-administration of TKIs with other drugs is fairly common in multi-drug therapy, hepatic uptake transporters OATP-1B1 and -1B3 can be regarded as important molecular targets for potential DDIs. Thus, hepatic uptake mediated by OATP-1B1 and -1B3 for selected TKIs should be dynamically scrutinized in order to circumvent DDIs. These transporters in conjunction with the metabolizing enzymes and efflux proteins may eventually decide on the overall flux/loss of the therapeutic agents within the hepatic tissue. These studies act as a proof of concept substantiating the need for further clinical studies investigating the OATP based DDI potential of TKIs. Further *in vivo* studies are required for better understanding of the contribution of OATP-1B1 and/or -1B3 transporter proteins in the hepatic disposition of drugs coadministered with TKIs and for predicting any adverse drug reactions associated with these hepatic transporter mediated DDIs [219].

Acknowledgement

This work was supported by National Institutes of Health grant 1R01 AI071199. The authors highly appreciate Dr. Bruno Stieger for their generous gift of OATP-1B type transporter protein transfected cell lines.

CHAPTER 4

THE ROLE OF TRANSPORTERS AND EFFLUX SYSTEM IN DRUG DELIVERY

Rationale

The transporters are membrane proteins and integral part of cell membrane. These proteins are broadly involved in selective absorption of endogenous substances (substances such as anions and cations, vitamins, sugars, nucleosides, amino acids, peptides, etc) and elimination of toxic substances. In fact, transporters direct the influx of essential nutrients and ions and the efflux of cellular metabolites and xenobiotics. These proteins also play a pivotal role in drug absorption, distribution, elimination, and drug-drug interactions. Although the occurrence of multidrug resistance of bacteria was noticed more than fifty years ago, the discovery of P-glycoprotein (P-gp), a major factor for efflux of xenobiotics out of cell took twenty years, It is clear now that apart

from intestinal absorption barrier and blood brain barrier, different tumor cells express P-gp which contributes a major role to the drug resistance in chemotherapy. In fact, these transporters take part a considerable role in the process of drug absorption, distribution, metabolism and elimination (ADME) of drugs. Almost 2000 genes have been identified for transporters or transporter-related proteins [220]. Approximately 400 membrane transporters, in two superfamilies, have been identified and characterized for specific tissue localization, and a number of these transporters have been cloned [122]. From pharmacological point of view two major superfamilies, ABC (ATP binding cassette) and SLC (solute carrier) transporters, are focused. The ABC, as active transporters, operates by ATP hydrolysis to expel their substrate out of cells across lipid bilayer. The ABC proteins are encoded by 49 genes and are categorized into seven subclasses [221] P-glycoprotein (P-gp) is the most well documented transporter in the ABC superfamily and encoded by the MDR1 (ABCB1) gene. The SLC superfamily consists of forty three families [221] which participate in drug absorption. There are many well-known SLC transporters include serotonin (*SLC6A4*) and dopamine (*SLC6A3)* transporters. Besides carrying nutrients or extruding cellular waste or, toxins, the wide-ranging role of membrane transporters is drug absorption, distribution and elimination. These transporters also participate in drug-drug interactions. The role of these transporters in multidrug resistance has been well recognized. In addition to drug delivery service, some of these transporter proteins also provide as a protective barrier to particular organ such as the brain. For example, P-gp in the blood-brain-barrier (BBB) or blood-retinal barrier protects the brain and eyes respectively from toxic influx of a variety of structurally diverse molecules through efflux pump. The ABC transporters also work in concert with drug metabolizing enzymes by eliminating drugs and their metabolites. Molecular cloning of transporter genes reveals the association of multiple genes encoding subtypes with similar function with different tissue

distribution and specificity towards drugs. Studying these subtypes (eg. glucose transporters, GLUT 1-4) can unravel the structure-activity correlation for drug transport which may allow modulation of its activity when considered necessary. Sometimes transporters can be present in the form of multiple alleles with functional defects resulting in defective drug binding or transport. Although the importance of drug transporters in the process of ADME and drug-drug interactions is well documented, our knowledge in this area is still emerging. The US Food and Drug Administration (FDA) and International Transporter Consortium (ITC) recently selected few transporters: organic anion transporter (OAT), organic anion transporting polypeptide (OATP), organic cation transporter (OCT), peptide transporter (PEPT), P-gp, multidrug resistance associated protein (MRP) and breast cancer resistance protein (BCRP) which are decisive to xenobiotics absorption, and drug-drug interactions. From pharmacokinetic point of view, localization and function of these transporters in the intestine, liver and kidney receives major attention. However, current evidence suggests that some of these transporters, particularly ABC transporters in the BBB also have drawn interest for delivering drugs to the brain. In this chapter, we will discuss mainly those transporters as well as vitamin transporters which appear to be significant for drug delivery.

ABC Transporters

ABC Proteins

ATP binding cassette (ABC) family is a superfamily of membrane proteins responsible for translocation of various substances comprising sugars, amino acids, sterols, peptides, proteins, antibiotics, toxins and xenobiotics. These proteins utilize the energy derived from hydrolysis of ATP for translocations various substances across a concentration gradient. Forty eight different ABC transporters have been in human genome. The ABC transporter genes stand for the largest

family of transmembrane proteins. Based on sequence homology and domain structure, they are categorized into seven different classes (ABCA-ABCG). So far, thirteen different transporters have been identified from classes A, B, C and G. These transporters play a significant role in the development of multidrug resistance (MDR) [222, 223]. First, Biedler and Riehm (1970) reported that Chinese hamster ovary (CHO) cells identified for resistance to Actinomycin D also demonstrated cross-resistance to many other drugs such as duramycin, democoline, mithramycin, mytomycin C, puromycin, vinblastin and vincristine [224-227]. It is also accountable for the efflux of HIV-protease inhibitors, anti-cancer agents and many others drugs. It appeared that after selection of a single cytotoxic drug, mammalian cells simultaneously developed cross-resistant to a variety of therapeutic agents with different chemical structures and functions. This phenomenon was referred to multidrug resistance. While it was believed that this drug resistance was due to permeation alteration of cell membrane, Juliano and Ling (1976) revealed that drug resistance in CHO cells was due to the presence of P-glycoprotein [225]. Why so many efflux transporters present in life forms? Many toxins are present in the nature, and clinicians administer many toxins to treat life threatening diseases (cancer, HIV, diabetes, etc). The amphiphilic drug molecules are hydrophobic enough to diffuse through lipid bilayer, but hydrophilic enough to reach the target. Once inside cells, these drugs can be inactivated by oxidation or conjugation to become more hydrophilic and get trapped inside the cells. These efflux transporters help them get out. While P-gp become warrior in effluxing wide range of therapeutic agents, MRP family deserves credit in extruding drugs conjugated to GSH, glucuronate, or sulfate and many other organic anions such as methotrexate.

These ABC transporters always function unidirectional as opposed to several others transporters which function bidirectional [228]. All these ABC proteins show a minimal

requirement of two transmembrane domains (TMDs) and two nucleotide binding domains (NBDs). This structural requirement can be assured by a single polypeptide chain or gathered from two homo-dimeric (equal) to hetero-dimeric (unequal) chains [229, 230]. All ABC transporters include a conserved sequence in NBD for binding ATP. The hydrolysis of ATP is required as a standard power for translocation by these transporters [231]. All the ABC transporters demonstrate 25 % homology. The conserved regions of sequence motifs consist of (i) Walker A region, (ii) Walker B region, (iii) signature C motif (90-120 amino acids linker between Walker A and B regions) (iv) glutamine loop (Q-loop) (v) histidine loop (H-loop) and (vi) D-loop [232-234]. The Walker A and B regions play a vital role in nucleotide binding. The signature motif is considered as a hallmark of ABC transporters which aids in communicating TMDs and also ATP hydrolysis [235]. The glutamate and histidine loops assist in ATP hydrolysis [236, 237]. The other trademark of ABC transporters is the D-loop which contributes a vital function in communicating the catalytic sites [238]. Three important ABC transporters: P-gp, MRP and BCRP will be discussed further from drug delivery point of view.

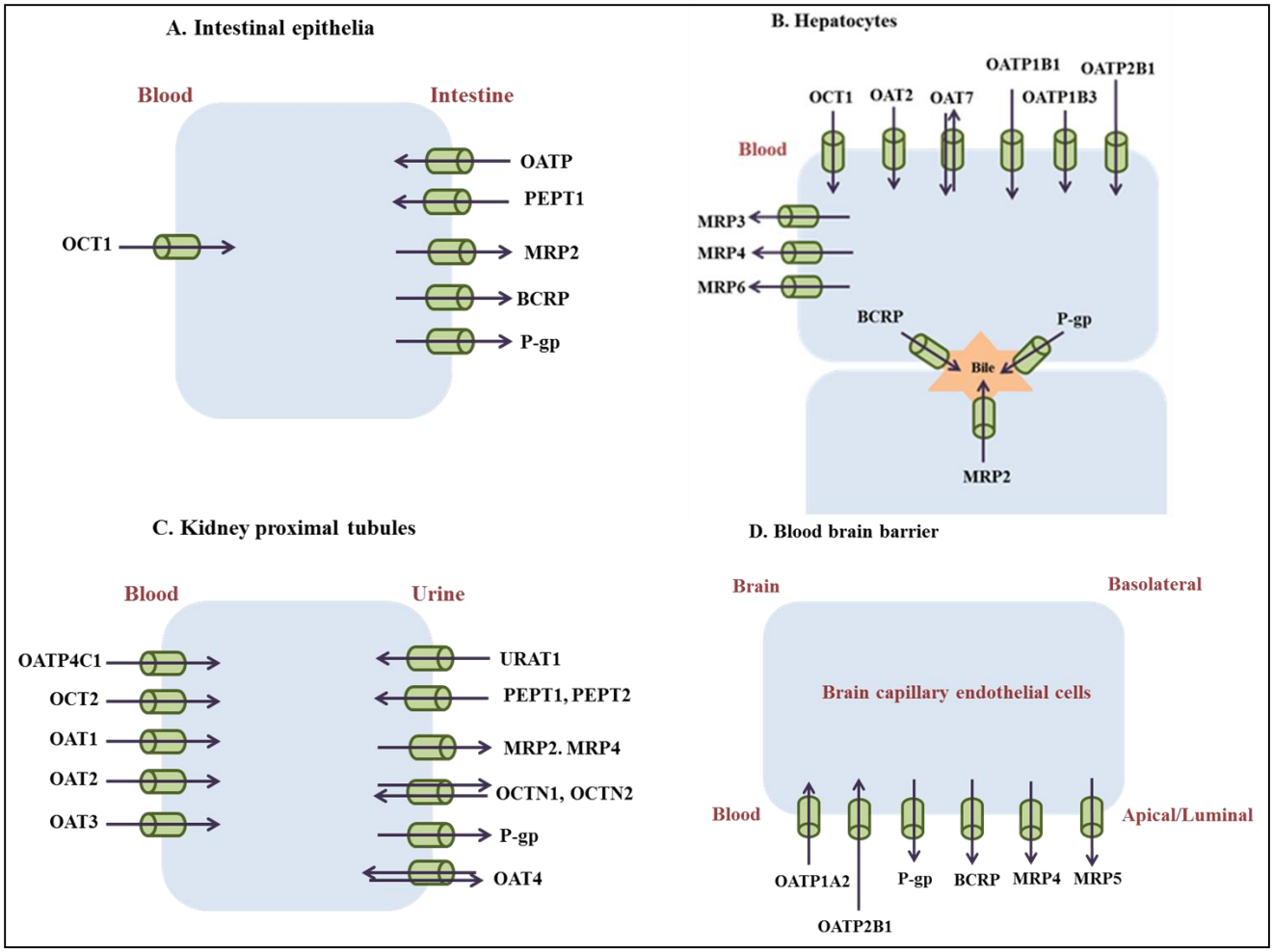

Fig.4.1: Localization of selected transporters in 4 tissues involved in ADME of drugs. Adapted from Giacomini *et al*., 2010 [122]

Efflux transporters

The efflux transporter proteins belong to ATP-binding cassette family. In particular, we are interested in the efflux transporters that are expressed at physiological barriers (e.g. intestinal absorption barrier, BBB, placental barrier, corneal and retinal barriers), in the liver, cancer cells, and other tissues responsible for drug clearance or excretion of xenobiotics. In this chapter, we will focus on three efflux transporters: P-gp, MRP and BCRP. These transporters significantly influence ADME of a number of drugs and their metabolites and cause drug resistance for many therapeutic agents. The tissue distribution of these transporters (**Table 4.1**) and their localizations

in various tissues are illustrated in **Fig. 4.1**. These proteins along with primary metabolizing enzyme–cytochrome P450 (CYP) together constitute a highly efficient barrier for oral drug absorption. P-gp is the most extensively studied efflux transporter which functions as a biological barrier by extruding toxins and xenobiotics into extracellular fluid. MRP belongs to the same ABC super family. Human MRP-1, MRP-2 and MRP-3 are known to be involved in efflux of anti-HIV agents and their conjugated metabolites [239-243]. Substrate specificity and tissue localization of MDR protein differs from MRP. As a consequence of efflux, drug absorption is reduced and bioavailability of xenobiotics diminishes at the target organs [244, 245]. In recent reviews we have elaborately discussed the role of these efflux transporters in drug-drug and drug-herbal interactions [246, 247].

Table 4.1: Tissue Distribution of P-gp, MRP and BCRP [221, 246, 247]

Tissue	P-gp	MRP-1	MRP-2	BCRP
Small intestine	Epithelium, apical side of lumen	Basolateral membrane of lumen	Epical membrane of the lumen	Apical side of lumen
Colon	Epithelium, apical side of lumen	Not present	Apical membrane of the lumen	Apical side of lumen
Liver	Bile canalicular face of hepatocytes	Basolateral membrane of hepatocytes	Apical bile canalicular	Bile canalicular

Kidney	Brush border surface of proximal tubules (apical)	Basolateral membrane of tubules	Apical proximal tubules	Not present
Placenta	Trophoblasts	Trophoblasts	Trophoblasts	Trophoblasts (facing maternal blood)
BBB	Luminal side of brain endothelium	Luminal side of brain endothelial cells	Luminal side of brain endothelial cells	Brain endothelial cells
Ocular	Rabbit corneal epithelium, rabbit PCEC, human cornea, Human RPE, porcine RPE, D407, h1RPE, rat retinal vessels, TR-iBRB	Human corneal epithelium, Primary human RPE cells, ARPE-19, porcine RPE	Rabbit corneal epithelium, ARPE-19, D407, primary human RPE cells	Human limbal epithelial cells, primary human limbal epithelial culture, human corneal

				epithelium, Mouse retinal vessels, TR-iBRB
Other major organs	Abundant on adrenal cortex.	Basolateral membrane of sertoli cells	None	Breast lobules, apical; stem cells

P-glycoprotein

P-gp, a product of MDR gene, was first characterized as the ATP-dependent transporter, responsible for the efflux of therapeutic agents from resistant cancer cells. In early seventies, Juliano and Ling demonstrated a 170 kDa protein in Chinese hamster ovary cells resistant to colchicines [225] and that protein was absent in drug-sensitive cells. The word 'P' stands for permeability because this transporter caused marked alteration in the permeation of several drugs across cell membranes. P-gp is an integral membrane protein having two homologous halves, each consisting of one hydrophobic domain with six transmembrane segments and one hydrophilic nucleotide-binding domain. Two halves are connected by a short flexible polypeptide linker to form the functionally active 1280 amino acid protein. P-gp encoding genes have been identified in hamster, mice, human and other species. It is a transporter protein, encoded by a small multi gene family, described by MDR I, II, III. P-gp from all three classes are present in rodents, while human cells express P-gp belonging to class I and III. It is the first ATP-dependent transporter found in

the liver and it represents the most studied member of the ATP binding cassette family of transporters. MDR proteins in humans and other species play a central role in protecting the cells against cytotoxic agents [248]. These efflux proteins exhibit a broad range of substrate specificity, such as digoxin, loperamide, doxorubicin, vinblastine, paclitaxel, fexofenadine cyclosporine-A, taxol, dexamethasone, lidocaine, erythromycin, ketoconazole, rifampicin, protease inhibitors and many anti-cancer agents [249-255]. Several P-gp substrates (including anticancer drugs, protease inhibitors and a variety of other therapeutic agents from different classes) and its inhibitors are given in the **Table 4.2**.

Table 4.2: P-gp Substrates and Inhibitors [256]

Substrates	**Inhibitors**
Acebutolol, Acetaminophen, Actinomycin D, h-Acetyldigoxin, Amitriptyline, Amprenavir, Apafant, Asimadoline, Atenolol, Atorvastatin, Azidopine, Azidoprocainamide methoiodide, Azithromycin, Benzo(a)pyrene, Betamethasone, Bisantrene, Bromocriptine, Bunitrolol, Calcein-AM, Camptothecin, Carbamazepine, Carvedilol, Celiprolol, Cepharanthin, Cerivastatin, Chloroquine, Chlorpromazine, Chlorothiazide, Clarithromycin, Colchicine, Corticosterone, Cortisol, Cyclosporin A, Daunorubicin (Daunomycin), Debrisoquine,	Amiodarone, Amitriptyline, Amlodipine, Astemizole, Atemoyacin-B, Atorvastatin, Aureobasidin A, Azelastine, Barnidipine, Benidipine, Bepridil, Bergamottin, Bergapten, Bergaptol, Biochanin A, Biricodar (VX-710), Bromocriptine, Buspirone, Caffeine, Carvedilol, Celiprolol, Cepharanthin, Chlorpyrifos, Cholesterol, Cimetidine, Clarithromycin, Clofazimine, Clomipramine, Clotrimazole, Colchicine, Cortisol, Cremophor EL, Cyclosporin, Cytochalasin E, Daunorubicin (Daunomycin), Desethylamiodarone, Desipramine, Desloratadine, Desmethylazelastine, Dexamethasone,

Desoxycorticosterone, Dexamethasone, Digitoxin, Digoxin, Diltiazem, Dipyridamole, Docetaxel, Dolastatin 10, Domperidone, Doxorubicin (Adriamycin), Eletriptan, Emetine, Endosulfan, Erythromycin, h-Estradiol, Estradiol-17h-d-glucuronide, Etoposide (VP-16), Fexofenadine, GF120918, Grepafloxacin, Hoechst 33342, Hydroxyrubicin, Imatinib, Indinavir, Ivermectin, Levofloxacin, Loperamide, Losartan, Lovastatin, Methadone, Methotrexate, Methylprednisolone, Metoprolol, Mitoxantrone, Monensin, Morphine, 99mTc-sestamibi, N-desmethyltamoxifen, Nadolol, Nelfinavir, Nicardipine, Nifedipine, Nitrendipine, Norverapamil, Olanzapine, Omeprazole, PSC-833 (Valspodar), Perphenazine, Prazosin, Prednisone, Pristinamycin IA, Puromycin, Quetiapine, Quinidine, Quinine, Ranitidine, Reserpine, Rhodamine 123, Risperidone, Ritonavir, Roxithromycin, Saquinavir, Sirolimus, Sparfloxacin, Sumatriptan,	Dexniguldipine, Digoxin, 6V,7V-Dihydroxybergamottin, Dihydrocytochalasin B, Diltiazem, Dipyridamole, Doxepin, Doxorubicin (Adriamycin), [d-Pen2, d-Pen5]-enkephalin, Efonidipine, Eletriptan, Emetine, Endosulfan, Epiabeodendroidin F, Ergometrine, Ergotamine, Erythromycin, Estramustine, Etoposide (VP-16), Fangchinoline, Felodipine, Fentanyl, Fluconazole, Fluoxetine, Fluphenazine, Fluvoxamine, Forskolin, Gallopamil, Genistein, GF120918, Haloperidol, Hydrocortisone, 1V-Hydroxymidazolam, Indinavir, Itraconazole, Ivermectin, Ketoconazole, Lansoprazole, Loperamide, Loratadine, Lovastatin, Manidipine, Methadone, Metoprolol, Mibefradil, Miconazole, Midazolam, Morin, Morphine, Naringenin, Nefazodone, Nelfinavir, Nicardipine, Nifedipine, Nilvadipine, Nisoldipine, Nitrendipine, Nobiletin, Norverapamil, Omeprazole, Pafenolol, Pantoprazole, Phenylhexyl isothiocyanate, Pimozide, Piperine, Pluronic block copolymer, Pristinamycin IA, Progesterone, Promethazine, PSC-833 (Valspodar), Quercetin, Quinacrine,

Tacrolimus, Talinolol, Tamoxifen, Taxol(Paclitaxel), Telithromycin, Terfenadine, Timolol, Toremifene, Tributylmethylammonium, Trimethoprim, Valinomycin, Vecuronium, Verapamil, Vinblastine,Vincristine, Vindoline, Vinorelbine.	Quinidine, Quinine, Ranitidine, Rapamycin, Reserpine, Ritonavir, Saquinavir, Silymarin, Simvastatin, Sirolimus, Mephenytoin, Spironolactone, Staurosporine, Sufentanil, Talinolol, Tamoxifen, Tangeretin, Taxol (Paclitaxel), Terfenadine, Tetrandine, Tetraphenylphosphonium, Trans-flupenthixol, Trifluoperazine, Triflupromazine, Trimethoxybenzoylyohimbine, Troleandomycin, Tween 80, Valinomycin, Verapamil, Vinblastine, Vincristine

Multidrug Resistance Associated Proteins (MRPs)

MRP family consists of at least nine members: MRP-1 and its eight isoforms, known as MRP2-9. MRP-2has been recognized in the apical (luminal) membrane of rat brain capillary endothelium [257]. The transmembrane domains in this family vary among the members. MRP-4 (ABCC4), MRP-5 (ABCC5), and MRP-7 (ABCC7) have 12 transmembrane domains and two NBD-binding sites. Other members of MRP family such as MRP-1 (ABCC1), MRP-2 (ABCC2), MRP-3 (ABCC3), and MRP-6 (ABCC6) have 17 transmembrane domains and two cytoplasmic NBD-binding sites. These membrane proteins (190kD) mediate ATP-dependent unidirectional efflux of glutathione, glucuronate, or sulfate conjugates of lipophilic drugs. In addition to many anionic conjugates, a number of unconjugated amphiphilic anions can serve as substrates for MRPs. There are numerous overlapping substrates between MRP, MATE (multidrug and toxin

extrusion transporters) and MOAT (multi-specific organic anion transporter) [122]. Gene symbol and other names used for human MRP family have been shown in **Fig.4.2.**

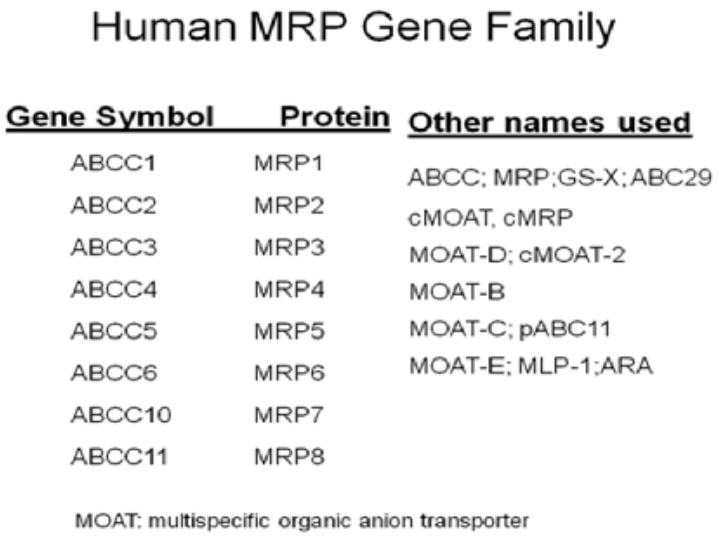

Fig.4.2: Human MRP gene family

Recent reports have identified MRP in the brain capillary endothelium. A recent report revealed that MRPs play a significant role in-vivo in the absorption of saquinavir across BBB [258]. Since MRP family is capable of exporting GHS complexes such as cisplatin, their importance in drug resistance are gaining attention. MRP4 and MRP5 can develop resistance to nucleotide analogues (PMEA) and purine base analogues (thioguanine and 6-mercaptopurine). Therefore, role of MRPs in drug resistance cannot be ignored. A wide range of MRP substrates and inhibitors is provided in the **Table 4.3.**

Table 4.3: Substrates and Inhibitors for MRP2 [256]

Substrates	**Inhibitors**

N-Acetyl leukotriene E4, p-Aminohippurate, Arsenic, Azithromycin, Benzbromarone, Bilirubin bisglucuronide, Bilirubin monoglucuronide, Cadmium, Calcein, 5-Carboxyfluorescein, Cefodizime, Cisplatin, Copper, S-Decyl-glutathione, Dibromosulfophtalein, 2,4-Dinitrophenyl-S-glutathione (DNP-SG), Epicatechin-3-gallate, Epigallocatechin-3-gallate, Estradiol-17h-d-glucuronide, Etoposide (VP-16), N-Ethylmaleimide-glutathione, Ethinylestradiol-3-O-glucuronide, Ethinylestradiol-3-O-sulfate, Fluo-3, Glutathione, Glutathione-bimane, Glutathion-methylfluorescein, Glycyrrhizin, Grepafloxacin, Grepafloxacin glucuronide, Indinavir, Irinotecan, Leucovorin, Leukotriene C4, Leukotriene D4, Leukotriene E4, Methotrexate, 4_-OMethyl-epigallocatechin gallate, Ochratoxin A, Oxidized glutathione, Pravastatin, Probenecid, Ritonavir, Saquinavir, SN-38 carboxylate, SN-38 glucuronide	Benzbromarone, Bergamottin, Bilirubin bisglucuronide, Bilirubin monoglucuronide, Cyclosporin, Daunorubicin, Etoposide (VP-16), 6V,7V-Dihydroxybergamottin, Furosemide, GF120918, Glibenclamide, Glutathione, LY335979, Leukotriene C4, MK571, Ochratoxin A, Oxidized glutathione, Pravastatin, Probenecid, Sulfinpyrazone, Tangeretin, Vincristine.

Breast Cancer Resistant Protein (BCRP)

BCRP belongs to a novel branch, subfamily G, of the large ABC transporter super family. The founding member of ABCG subfamily, ABCG1 has been implicated in the regulation of cellular lipid homeostasis in macrophages through facilitating efflux of cellular lipids including cholesterol and phospholipids. It is also known as mitoxantrone-resistance protein. BCRP is a 72 kD protein, described as a half transporter which contains only six transmembrane domains and one NBD-binding site. Predicted secondary structures of these drug efflux transporters of the ATP-binding cassette family are illustrated in the **Fig.4.3.**

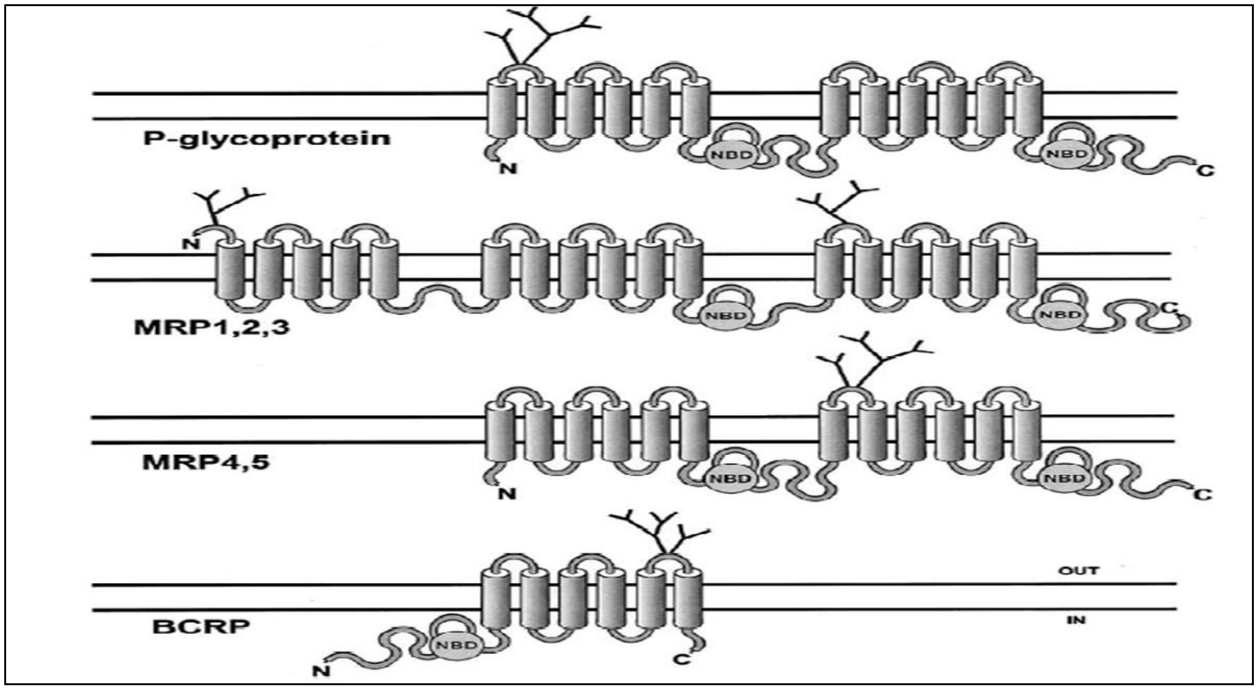

Fig.4.3. Predicted secondary structures of drug efflux transporters of the ATP-binding cassette family: four classes are distinguished here, based on predicted structure and amino acid sequence homology. (1) P-glycoprotein consists of two transmembrane domains, each containing 6 transmembrane segments, and two nucleotide binding domains (NBDs). It is N-glycosylated (branches) at the first extracellular loop; (2) MRP1, 2 and 3 have an additional amino terminal extension containing 5 transmembrane segments and they are N-glycosylated near the N-terminus and at the sixth extracellular loop; (3) MRP4 and 5 lack the amino terminal extension of MRP1–3, and are N-glycosylated at the fourth extracellular loop; (4) BCRP is a 'half transporter' consisting of one NBD and 6 transmembrane segments, and it is most likely N-glycosylated at the third extracellular loop. Note that, in contrast to the other transporters, the NBD of BCRP is at the amino terminal end of the polypeptide. BCRP almost certainly functions as a homodimer. N and C denote amino- and carboxy-terminal ends of the proteins, respectively. Cytoplasmic (IN) and extracellular (OUT) orientation indicated for BCRP applies to all transporters drawn here. (Reproduce with permission from Schinkel, A.H. and Jonker, J.W., (2003) [259])

Two features that distinguish the subfamily G members from other ABC transporters are their unique domain organization. Functional characterization has demonstrated that BCRP can transport a wide range of substrates ranging from chemotherapeutic agents to organic anion conjugates. P-gp substrates have a tendency to overlap BCRP but the later includes acids or drug conjugates (mitoxantrone, methotrexate, topotecan, imatinib, irinotecan, statins, sulphate conjugates, porphyrins, etc). More evidence is emerging to suggest that BCRP plays a significant role in drug disposition. Hence, it is important to examine its effect on pharmacokinetics and drug-drug interactions of therapeutic agents [260-266]. Information regarding various substrates and inhibitors of BCRP has been depicted in the **Table 4.4**.

Table 4.4: Substrates and Inhibitors for BCRP [256]

Substrates	Inhibitors
Actinomycin D, 9-Aminocamptothecin, 2-Amino-1-methyl-6-phenylimidazole [4,5-b]pyridine (PhIP), Azidodeoxythymidine, Bodipy-FLPrazosin, C6-NBD-phosphatidylcholine, C6-NBD-phosphatidylserine, Cholesterol, Cimetidine, Daunorubicin, Dehydroepiandrosterone sulfate, Doxorubicin, Epirubicin, 17h-Estradiol, 17h-Estradiol-glucuronide, 17h-Estradiol-3-sulfate, Estrone, Estrone-3-sulfate	Acacetin, Apigenin, Beclomethasone, Biochanin A, Chrysin, Corticosterone, Cyclosporin A, Daidzein, Dehydroepiandrostrone sulfate, Diethylstilbestrol, Digoxin, Dexamethasone, Doxorubicin

Genetic Factors In Drug Response

Growing evidence suggests that genetic factors influence inter-individual variation in drug response. Polymorphism has been indicated to vary with ethnicity. Mutations in genes may lead to genetic polymorphism. Several reports suggest that inter-individual variability in drug response

is linked to single nucleotide polymorphisms (SNP). Polymorphism in a number of genes encoding for drug metabolizing enzymes and transporters has been reported. So far 28 SNPs have been detected at 27 positions on MDR1 gene [267]. Mutations at exon 26 (C3435T) and 21(G2677T/A) of MDR are responsible for duodenal expression of P-gp. A significantly reduced duodenal P-gp expression in homozygous (3435TT) individuals has been linked to higher plasma digoxin level [241]. Also C3435T has been reported to be a risk factor for HIV infection [268]. Chowbay et al., have described ethnic variability among Chinese, Malays and Indians [269]. Pharmacogenetics of MDR1 in Asian populations is different from those in Caucasian and African populations. MDR1 is a well conserved gene. But current evidence indicates that its polymorphism affects substrate specificity. Three SNPs frequently arise at positions 1236C>T, 2677G>T and 3435C>T. In a recent review Fung and Gottesman have indicated that the frequency of synonymous 3435C>T polymorphism appears to vary significantly with ethnicity [270]. *ABCB1* 3435C>T genotype was also found to alter serum levels of cortisol and aldosterone during postmenstrual phase of a normal cycle [271]. Common haplotype plays a significant role in drug response and efficacy. An evidence of high CYP3A4 expression in MDR1 2677T carriers was found in human intestine [272]. The influence of MDR1 genotype on CYP3A4 expression adds additional complexity in drug-drug interaction.

Substrate Recognition By P-Glycoprotein

P-gp actively exports wide range chemically diverse compounds out of cells. TMDs 5-6 and 11-12 play a critical role in recognizing and binding its substrates. Seelig has reported a general pattern for substrate recognition by P-gp by analyzing more than a hundred diverse compounds [273]. A well-defined two or three electron donor groups (recognition elements) are required for a substrate to bind P-gp. These recognition elements are classified into two groups: Type I and Type

II. Type I units compose of two electron donor groups with a spatial separation of 2.5 ± 0.3 Å whereas type II units either consist of two or three electron donor groups with a spatial separation of 4.6 ± 0.6 Å. Accordingly, if a compound contains at least type I or type II unit is expected to be recognized by P-gp. On the basis of the type and number of recognition elements, various compounds can be classified as non-substrate, weak substrate or strong substrate. The structural elements responsible for a substrate-P-gp interaction reside in specific hydrogen bonding acceptor units. P-gp-substrate binding and its over-expression enhance with the number and strength of hydrogen bonding acceptor units [273].

Substrate And Inhibitor Selectivity

P-gp mediated efflux of substrates or therapeutic agents plays a major role in drug disposition across biological barrier. Apart from cancer cells, P-gp is expressed in many organs such as the intestine, liver, kidney, eye and brain [274]. It has been proven that the oral absorption and brain penetration of P-gp substrates are significantly enhanced in mdr1 knockout mice compared to normal mice [275]. The oral bioavailability and brain permeability of P-gp substrates can be significantly enhanced by co-administration of P-gp modulators [276, 277]. Both biliary excretion and renal clearance are significantly reduced in the presence of P-gp inhibitors [278, 279]. Now it is well accepted that appropriate P-gp inhibitors should be co-administrated with P-gp substrates for therapeutic effectiveness. The activity of P-gp mediated efflux is a saturable process. This is a complex area of drug-drug or drug-inhibitor interactions. Such interactions can give rise to competitive inhibition, noncompetitive inhibition, and cooperative simulation [224]. These interactions can take place either at the P-gp binding site or at ATP binding domains. There is more than one P-gp binding locations. The exact numbers of P-gp binding locations are yet to be confirmed. However, P-gp substrates and inhibitors can bind at different locations. In general,

the substrate binding site and the two ATP-binding domains act together to operate efflux pump. Therefore, inhibition of P-gp mediated drug efflux could potentially take place either due to the contest of P-gp-binding site and ATP-binding domains or due to blockage of ATP hydrolysis.

Strategies To Overcome Active Efflux

As we mentioned that MDR mediated efflux poses a major impediment for successful drug delivery. Hence strategies to overcome efflux proteins are warranted. We have briefly discussed the recent developments and research strategies to circumvent MDR mediated efflux.

Pharmacological Inhibition Of Efflux Proteins

Co-administration of chemical agents that can inhibit the activity of efflux proteins by either competitive or non-competitive binding appears to be an attractive strategy to avoid drug efflux. An ideal efflux modulator can inhibit the activity of efflux pumps at the apical membrane and subsequently enhance permeability of drug molecule in desired tissues. A schematic of this mechanism is depicted in **Fig.4.4**

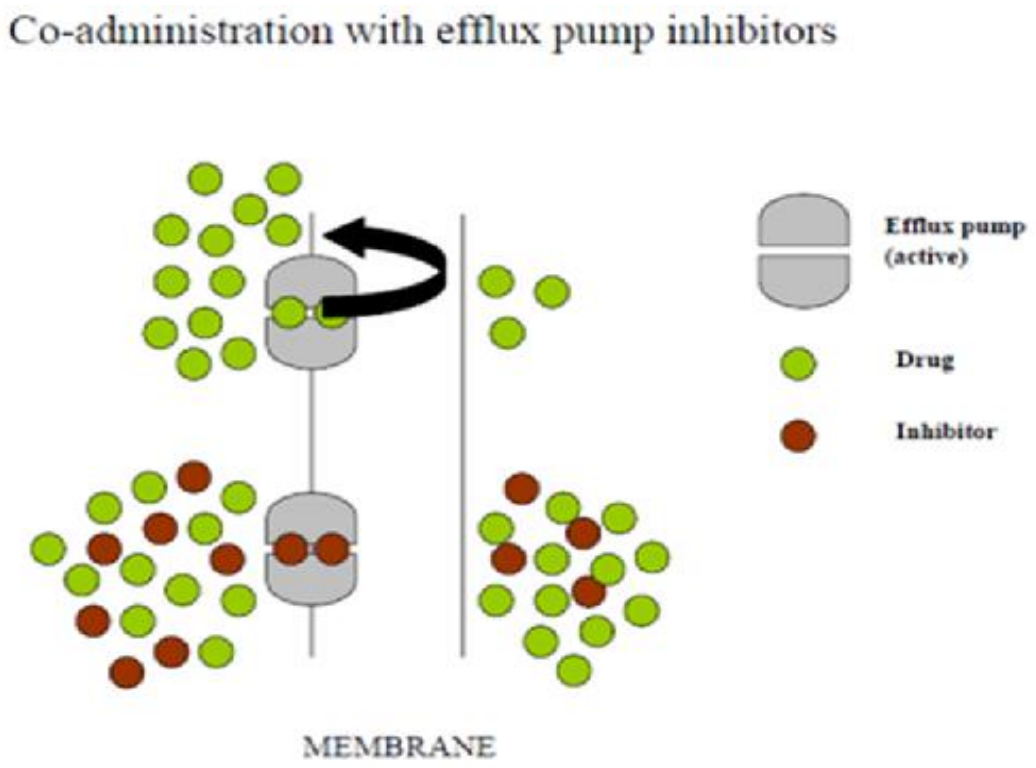

Fig.4.4: Combination Therapy Approach

First -Generation MDR Modulators

Clinically approved Ca^{2+} channel blocker Verapamil restored the cellular accumulation of vincristine in P-gp overexpressing cell lines. This finding stimulated to develop several P-gp inhibitors [280, 281]. Antimalarial drugs quinine, quinidine and immunosuppressant cyclosporine A emerged as other first-generation inhibitors and approved for the therapeutic use in clinic [282-284]. Although these first-generation inhibitors were potent *in vitro*, but very high doses required to block MDR mediated efflux in humans, leading to potential life threatening toxicity [285].

Second-Generation MDR Modulators

Due to high toxicity with the first-generation modulators, the development of new MDR modulators with lower inherent toxicities was essential. Structural analogues of verapamil, including dexverapamil and an analogue of Cyclosporin A, PSC-833 (Valspodar) were thus

developed as second-generation modulators [286, 287]. However, these compounds appeared to alter the pharmacokinetic properties of co-administered anticancer drugs, such as paclitaxel, and doxorubicin, producing dose dependent haematological side effects [288, 289]. This altered pharmacokinetic profile of co-administered drugs, and caused nonspecific interactions with CYP enzymes [290]. As a consequence, the dose adjustment of anticancer drugs appeared imminent to prevent adverse outcome of the therapy.

Third Generation MDR Modulators

These agents were designed to overcome the limitations of these previous modulators. These new set of efflux modulators are highly specific for MDR efflux pumps sparing any interaction with drug metabolizing (CYP-450) enzymes and do not alter pharmacokinetic interaction with other therapeutic agents. For example, zosuquidar [291], tariquidar [292]and elacridar [293]are the MDR inhibitors that have shown promise in pre-clinical mouse model and more recently in the clinic. Zosuquidar and tariquidar are specific inhibitors of P-gp. A non-competitive inhibitory mechanism has been suggested since these are neither substrates for P-gp and nor be transported by the ABC transporter [294]. Preclinical studies using such inhibitors with anticancer drugs showed significantly prolonged survival and reduction of MDR-bearing human tumours engrafted in mice [294]. No alterations in pharmacokinetic parameters of anticancer drugs such as doxorubicin, etoposide, daunorubicin, vincristine and paclitaxel have been demonstrated upon such co-administrations. Various Phase1 and phase II studies have been conducted upon co-administration of zosuquidar with docetaxel and Daunorubicin and doxorubicin for the treatment of breast cancer, leukaemia and non-Hodgkin's lymphoma [295-298]. Elacridar is a dual inhibitor of P-gp and BCRP. Co-administration of elacridar has been reported to increase the oral

bioavailability of topotecan in patients [299]. Pre-clinical studies suggest effective reversal of chemo-resistance upon co-administration of elacridar [300].

Herbal Modulation Of MDR Efflux Proteins

Flavonoids such as chalcones, flavonols, flavones, procyanidins, flavan-3-ols (catechins), flavanones, and isoflavones are the major constituents among numerous other constituents of many naturally occurring herbal products in the market. There have been well documented reports in the literature suggesting their interactions with efflux transporters particularly P-gp [247]. To name a few, St.john's wort, garlic, ginseng and grapefruit juice are well known as over the counter herbal products as dietary supplements, and medications. Both in preclinical and clinical settings these products have been shown to interact with drugs that are substrates for P-gp. These herbal ingredients can either inhibit the ATPase activity of efflux pumps or act as competitive inhibitors for other drug molecules. Patel et al demonstrated that P-gp mediated efflux of ritonavir was greatly reduced by quercetin in Caco-2 cells and MDCKII-MDR1 cells [301]. Similarly, intracellular accumulation of daunomycin was greatly enhanced in P-gp over-expressing K562 cells, with co-administration of various flavonoids [302]. Similar interactions of herbal products with other efflux transporters such as MRP2 and BCRP have also been reported in the literature. Flavonols such as myricetin and robinetin were shown to inhibit MRP2 mediated efflux of calcein in MRP2-over expressing MDCKII cells [303]. Zhang et al. showed that chrysin, biochanin A and 7,8-benzoflavone, were the most potent flavonoids for inhibiting the efflux of mitoxantrone among 25 naturally occurring flavonoids tested in MCF-7 cells overexpressing BCRP [304, 305]. Likewise, genistein and naringenin were shown to reverse BCRP-mediated resistance [306].

Although exact mechanism of P-gp-mediated drug-drug interaction during co-administration of modulators and substrates yet to be comprehended, it appears that substrate

bioavailability does not follow simple kinetics. The competitive inhibition indicates two substrates operate at the same binding site of P-gp where only one can bind on any one occasion, whereas non-competitive inhibition suggests that two substrates are competent to translocate simultaneously at two distinct P-gp binding sites and may function independently. The situation may change when allosteric effects are engaged during interaction between substrate and modulator.

When single drug is substrate for more than one efflux transporters, one specific inhibitor may not alter pharmacokinetics profile. For example vincristine is substrate for both P-gp and MRP2. In that case coadministration of vincristine with either quinidine (inhibitor of P-gp) or MK571 (inhibitor of MRP) may not significantly change its brain absorption of vincristine. Because when one transporter is inhibited, other transporter overworks for pumping that drug out of the brain. In that case selection of a duel inhibitor is critical. Recently we have shown that brain uptake of vandetanib (trade name Caprelsa), an anti-cancer drug was significantly enhanced in the presence of either GF120918 (elacridar) or everolimus (m-TOR inhibitor) compared to either Ko143 or, LY335979. Vandetanib is a substrate for both P-gp and BCRP. While Ko143 and LY335979 are inhibitors of P-gp and BCRP respectively, GF120918 (elacridar) or everolimus can inhibit both P-gp and BCRP mediated efflux of vandetanib in mouse brain [197].

Pharmaceutical Excipients As Inhibitors Of MDR Efflux Proteins

Drug delivery system using novel Pluronic block copolymers becomes popular to overcome efflux pump to overcome multidrug-resistant cancers. Improved oral drug absorption of topotecan, a model BCRP substrate was observed after pre-tretament of wild type mice with Pluronic 85 (P85) and tween 20 [307]. In a separate study, the cellular accumulation of digoxin was increased by 3-fold in LLC-PK1 cells and by 5-fold in the LLC-PK1-MDR1- transfected cells

following addition of P85. Similar effects were observed for rhodamine-123 [308]. The co-administration of 1% P85 with radiolabeled digoxin in wild-type mice increased its brain permeation by 3-fold [308]. These data indicate that excipients such as P85 and tween 20 can enhance the delivery of drug substrates through the inhibition of the P-gp and BCRP mediated efflux mechanism.

Prodrug Strategy

Besides efflux transporters, such as P-gp, MRP2 and BCRP, a number of nutrient (influx) transporters are also expressed on the cellular membranes. These nutrient transporters are responsible for the influx of various nutrients and drugs into various epithelial (enterocytes) and endothelial cells (e.g. blood–brain barrier). Recently, transporter targeted prodrug derivatization has received great attention amongst drug delivery scientists. Prodrugs have been designed such that the modified compounds become substrates of nutrient transporters leading to enhanced absorption of these compounds across various physiological barriers, which upon crossing the membrane get bio-transformed to parent drug and the pro-moiety **(Fig 4.5)**. This strategy not only circumvents efflux pumps but can also reduce the toxic effects of the P-gp modulators. Jain et.al reported evasion of P-gp mediated cellular efflux and enhanced permeability of HIV protease inhibitor saquinavir upon prodrug modification. Di-peptide prodrugs namely valine-valine-saquinavir and glycine-valine-saquinavir showed enhanced absorption with reduced efflux relative to unmodified saquinavir across MDCKII-MDR1 cells [309]. In a similar study, parallel results were reported for evasion of P-gp mediated efflux of lopinavir [310] and quinidine [311] upon peptide prodrug modifications.

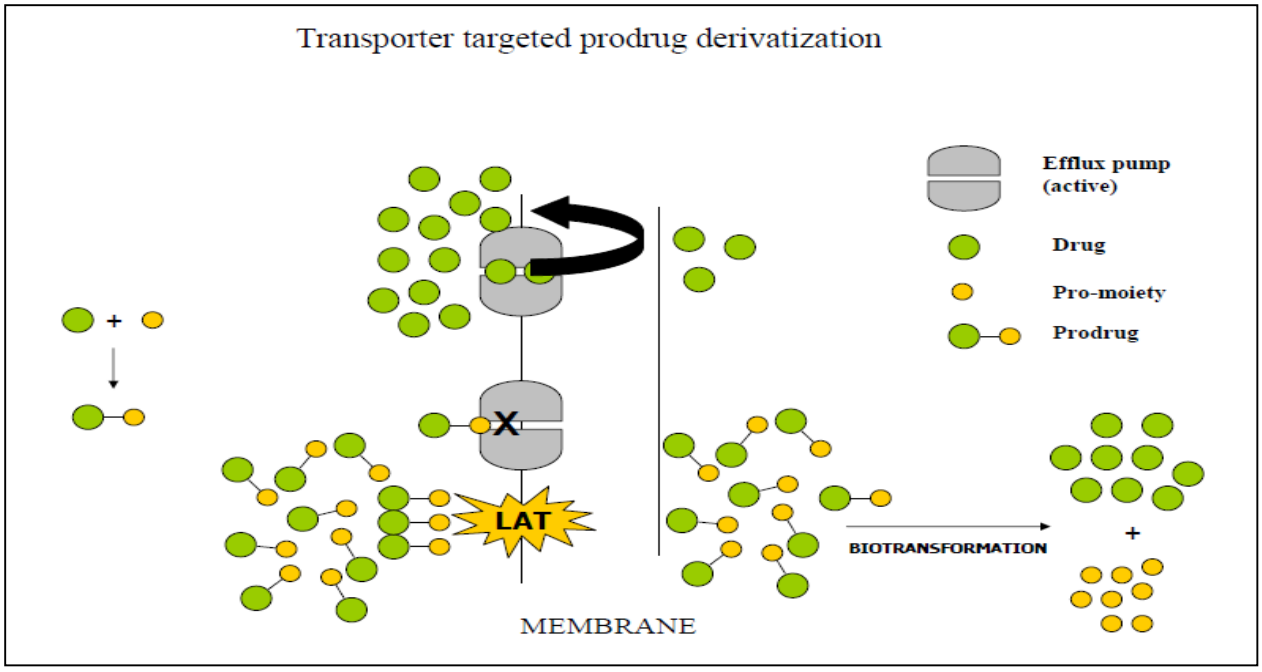

Fig 4.5: Transporter targeted prodrug strategy: improved permeability could be achieved by overcoming MDR efflux transporters upon chemical modification of parent drug molecule.

Nanotechnology

Nanotechnology provides an alternative strategy to circumvent MDR by offering a means to encapsulate drugs to lipids, gelatine and polymers producing nanoparticles which are resistant to drug efflux. These nanoparticles take advantage of the endocytosis process simultaneously evading MDR proteins on cell membranes. Moreover, these nanoparticles can be surface-decorated with folic acid, biotin etc for receptor mediated targeted delivery. **Fig 4.6** demonstrates the mechanism of efflux evasion via endocytosis following encapsulation of the drug molecules in nanoparticles. Inclusion of targeting ligands on the surface of nanoparticles has the potential of tumor-specific drug delivery and retention, thus minimizing systemic toxicity [312].

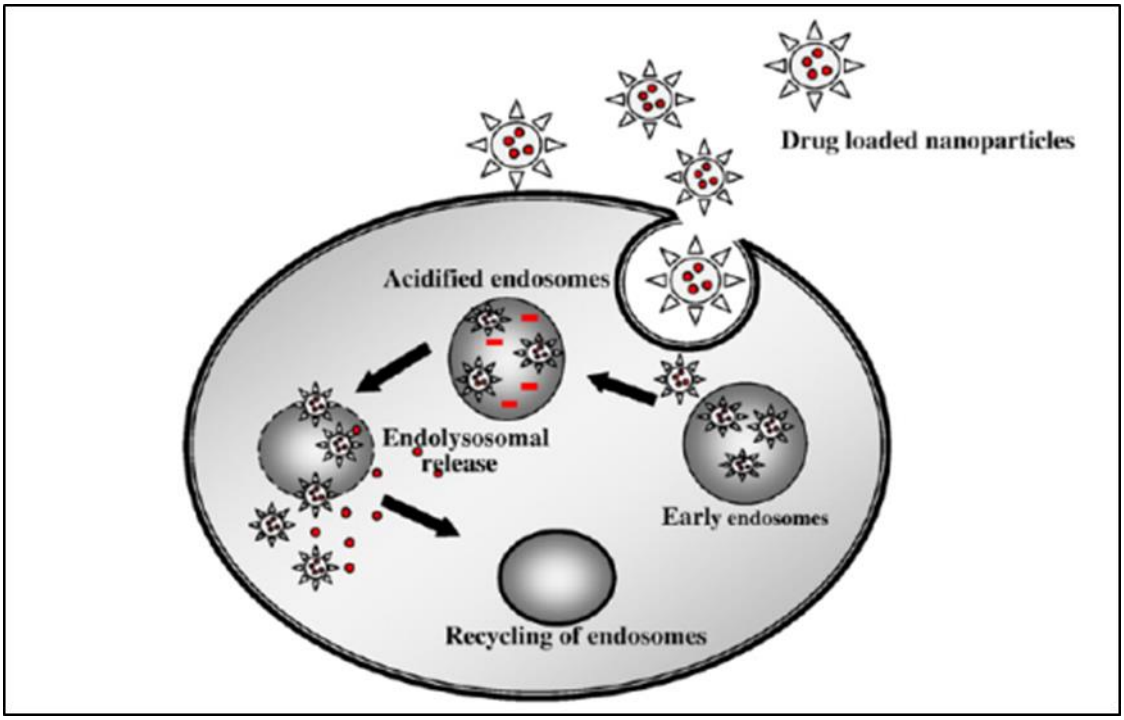

Fig 4.6: Evasion of MDR efflux proteins by surface-decorated nanoparticles: substrate drug molecules encapsulated in the nanoparticles can evade MDR proteins upon endocytosis Acharya, S. and Sahoo, S.K., 2011[313].

Recently, numerous reports have been published showing encapsulation of chemotherapeutic agents such as doxorubicin and paclitaxel in liposomes or micelles. These encapsulated drugs exhibited high intracellular accumulations and 5-10 fold lower IC_{50} values in P-gp overexpressing cell lines in comparison to the free drugs [314] . Furthermore, accumulation DOX in the xenograft was approximately 20 fold higher when doxorubicin loaded micelles with folate in their surface was administered in mice [269].

Antibodies Specific To MDR1 Protein

To avoid the clinical side effects associated with pharmacological chemosensitizer, monoclonal antibodies recognizing P-gp have been explored as potential inhibitors of P-gp.. The studies using MRK-16, one of the P-gp monoclonal antibodies, suggested that their use, together

with MDR-related cytotoxic drugs with or without chemosensitizer, may have a potential effect as an anti-MDR therapy [315, 316]. Besides MRK-16, another monoclonal antibody UIC2 that targets extracellular domain of P-gp has been characterized [252]. However, an effective delivery of these large molecular weight monoclonal antibodies is a challenging task. To overcome this issue recombinant DNA technology can be exercised to isolate new recombinant scFv antibodies which have much smaller molecular weight with desired specificity and affinity directed toward a large array of antigens such as MDR1 protein. Haus-Cohen et al. isolated and characterized such recombinant scFv fragment capable of disrupting P-gp efflux activity thereby reversing the MDR phenotype of drug-resistant human tumor cell lines [317].

Influx Transporters

Influx transporters are integral plasma membrane proteins that control the influx of essential nutrients and ions. The presence of these transporters has been reported on various tissues and cell lines. These proteins play an important role in drug delivery. These influx transporters belong to SLC (solute carrier) transporter family. These include carriers for peptides, vitamins, organic anions, organic cations, glucose and other nutrients. These transporters are involved in pharmacokinetic and pharmacodynamic pathways of drug molecule. A number of drug molecules are modified chemically in order to achieve desired lipophilicity and solubility which will ultimately improve drug bioavailability. Designing a transporter targeted drug can be considered as a rational approach for improving drug bioavailability. These modified drugs are often called ‘prodrugs’ that are designed to target influx transporters. In this part, we will be discussing about the influx transporters that can be exploited as molecular targets for tissue-selective drug delivery which may reduce systemic toxicity [318, 319]

Peptide Transporters

The cellular intake of dipeptides and tripeptides along with other peptidomimetics is mediated by peptide transporters. In mammals two peptide transporters have been identified, peptide transporter 1 (PEPT1, SLC15A1) and peptide transporter 2 (PEPT2, SLC15A2). PEPT1 and PEPT2 share similar topology and consist of 708 and 709 amino acid residues, respectively. Apart from the intestine PEPT is present in many tissues such colon, kidney, liver, lung, mammary gland, pancreas, eye and CNS **(Table 4.5)**. Various drugs and prodrugs are substrates for peptide transporters like β – lactam antibiotics (cefadroxil, cefime, cefadrine, cycleacilin and ceftibuten), angiotensin converting enzyme (ACE) inhibitors (captopril, enalapril and fosinopril), aminopeptidase inhibitors (bestatin), and prodrugs & non – peptidic compounds (L- DOPA and valacyclovir) **(Table 4.6)** [320]. Drug molecules can be chemically modified by introducing structural fragments (valyl, leucyl, isoleucyl or glycine residues) for the recognition by peptide transporters. Such strategy has been successfully employed to nucleoside drugs such as acyclovir [321-323], ganciclovir [321, 324], azidothymidine [321, 325], floxuridine [321, 326], HIV protease inhibitors [310, 321] and L-DOPA [321, 327, 328] resulting in a significant improvement of oral absorption of these drugs by making use of the peptide transporter pathways [321]. In order to exert their pharmacological activity, these peptide prodrugs are metabolized by peptidase to release the free active drugs required for desired therapeutic effects.

Table 4.5: Distribution of peptide transporters in tissues, cells and sub-cellular compartments. Modified from Rubio-Aliaga, I. and Daniel, H., (2002) [320]

Transporters	Tissue	Localization	References
PEPT1	Small Intestine	Brush border membrane of enterocytes	[320, 329]
	Kidney	Brush border membrane of epithelial cells of the proximal tubule S1 segment	[320, 330]
	Bile Duct	Apical membrane of cholangiocytes	[320, 331]
	Pancreas	Lysosomes of acinar cells	[320, 332]
	Cornea	Apical membrane	[333]
PEPT2	Kidney	Brush border membrane of epithelial cells of the proximal tubule (S2 and S3 segment)	[320, 330]
	Central Nervous System	Epithelial cells of the choroid plexus, ependymal cells and astrocytes	[320, 334]
	Peripheral Nervous System	Membrane and cytoplasm of glial cells	[320, 335]
	Lung	Apical membrane of bronchial and tracheal epithelial cells, membrane and cytoplasm pneumocytes type II	[320, 336]

PEPT2	Mammary gland	Epithelial cells of the glands and ducts	[320, 337]
	Cornea	Apical membrane	[333]
	Iris ciliary body	-	[333]
	Retina/Choroid	Basolateral Membrane	[333]

Dipeptides, tripeptides, β-lactams, angiotensin-converting enzyme (ACE) inhibitors and several prodrugs are taken up into cells by peptide transporter 1 (PEPT1) and PEPT2, against a concentration gradient. The acidic pH of the intestine generated by the brush-border Na^+/H^+ exchanger serves as driving force for intestinal absorption of dipeptides and tripeptides and peptidomimetic drugs. The velocity of transport is determined by membrane voltage. By and large, the proton gradient is generated and maintained by NHE-3, the apical Na^+ -H^+ antiporter with intracellular Na^+ removed by Na^+-K^+ ATPase in the basolateral membrane. Whereas dipeptides and tripeptides undergo rapid intracellular hydrolysis and free amino acids leave cells via basolateral transporters. Hydrolysis-resistant substrates, such as most peptidomimetics, are released into the circulation by a basolateral peptide transporter that is yet to be identified and/or by other drug transporting systems. A list of clinically relevant drugs or inhibitors of peptide transporter is presented in the **Table 4.6**.

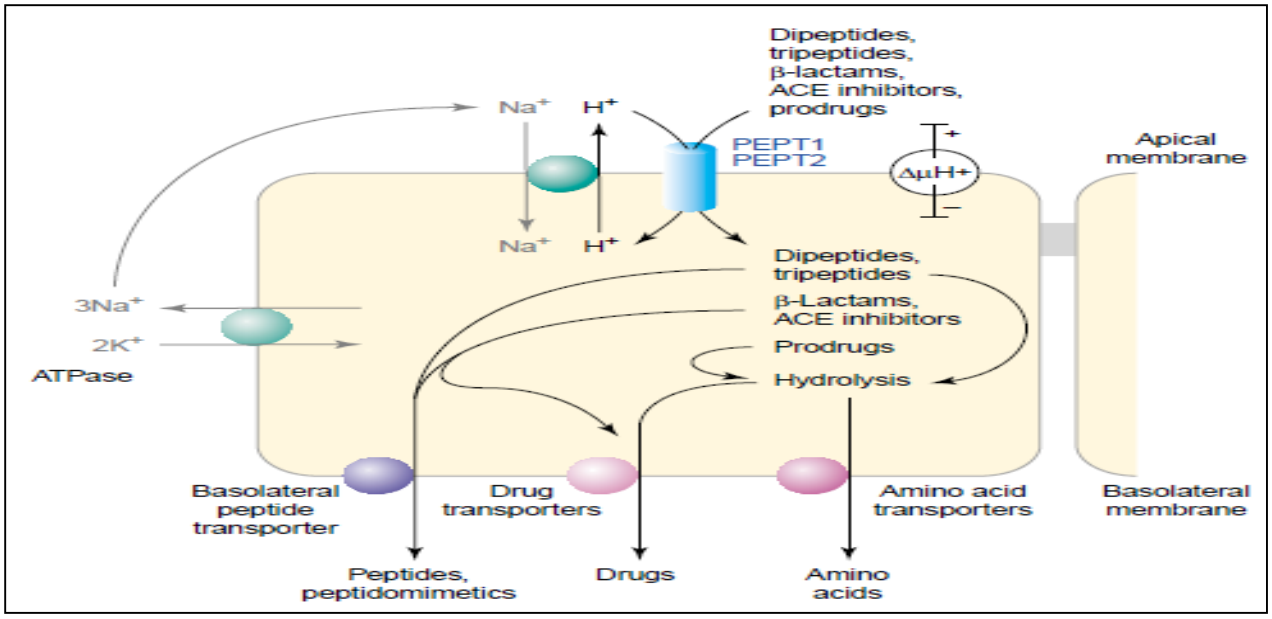

Fig. 4.7: Model of peptide transport in epithelial cells from intestine and kidney. (Reproduced with permission from Rubio-Aliaga, I. and Daniel, H., (2002) [320])

Table 4.6: Example of various drugs/prodrugs acting as substrates/ competitive inhibitors of peptide transporters

Drug	Substrates/Competitive inhibitors of		Reference
	PEPT1	PEPT2	
β-lactam antibiotics			
Cephalexin	+	+	[327, 338, 339]
Ceftibuten	+	+	[327, 340]
Cefadroxil	+	+	[327, 341, 342]
Ciclacillin	+	+	[327, 343, 344]
Cefixime	+	+	[327, 340, 345]
Photosensitizing agents			
5-Aminolevulinic acid	+	+	[327, 346]
Antitumour agents			
Bestatin	+	+	[327, 347]

Floxuridine (prolyl- and lysil-prodrugs)	+	n.d.	[327, 348]
Hypotensives			
Midodrine	+	n.d.	[327, 349]
Antivirals			
Acyclovir	+	+	[324, 327, 350]
Zidovudine	+	n.d.	[327, 350]
Dopamine receptor interactors			
Sulpiride	+	n.d.	[327, 351]
Amino ester derivatives of L-DOPA	+	n.d.	[327, 328]
Angiotensin-converting enzymes (ACE) inhibitors			
Fosinopril	+	+	[327, 352]
Captopril	+	+	[327, 353]
Enalapril	+	+	[327, 353]

+: Confirmed; n.d.: Not determined

Organic Anion Transporting Polypeptide (OATP)

OATP are the members of the solute carrier organic anion transporter family (SLCO) classified within the solute carrier class (SLC) superfamily. OATP protein encodes for 643-722 amino acids and has 9-12 transmembrane domains with intracellular amino and carboxy termini [7]. So far, 11 human isoforms **(Table 4.7)** and 14 rat isoforms have been identified in the OATP family. The OATP superfamily has been divided according to amino acid sequence identity i.e. families (≥ 40% amino acid sequence identity) and subfamilies (≥ 60% amino acid sequence identity). OATP1B1, -1B3 and -2B1 are involved in the hepatic uptake of bulky and relatively hydrophobic organic anions. Several other OATPs are expressed in many tissues, such as the choroids plexus, brain, placenta, heart, intestine, lungs, kidneys and testes [354]. Substrates for OATP include bile acids, eicosanoids, steroids, thyroid hormones, and their conjugates as well as

xenobiotics such as anionic oligopeptides, organic dyes, several toxins and numerous drugs (**Table 7)** [7, 355]. OATPs are ubiquitously expressed in human body and mediate the Na^+-independent uptake of wide range of amphipathic molecules (molecular weight >300kDa). The substrates of OATP are not limited to anions; they also transport cationic and neutral compounds. Altered expression levels of OATPs have been reported in different types of cancers **(Table 4.8)** [356].

Table 4.7: Characteristics and selective substrates of human OATP family members

Protein name	**Amino acids**	**Tissue distribution**	**Substrates**	**Kinetic Parameter (K_m)**	**Reference**
OATP1A2	670	Brain, kidney, Rat RPE, retinal vessels	Bromosulfophthalein Estrone-3-sulfate Rosuvastatin Saquinavir Fexofenadine	20µM 16µM 3µM 36µM 6µM	[357-361]
OATP1B1	691	Liver	Atorvastatin Bilirubin Estrone-3-sulfate Valsartan Enalapril	10µM 0.01µM 0.5µM 1.4µM 262µM	[362-366]
OATP1B3	702	Liver	Amanitin Estradiol-17β-glucuronide Methotrexate Paciltaxel Rifampicin	4µM 5-25µM 25-39µM 7µM 2µM	[202, 204, 366-370]
OATP1C1	712	Brain, testis, retinal vessels	Reverse triiodothyronine Thyroxine	0.12µM 0.09µM	[371]
OATP2A1	643	Ubiquitous	Latanoprost	5.4µM	[372]

OATP2B1	709	Ubiquitous	Fluvastatin Bosentan Taurocholate	0.7µM 202µM 72µM	[373-375]
OATP3A1	710	Ubiquitous	Prostaglandin E1 Prostagalndin E2	0.05-0.1µM 0.06-0.2µM	[376, 377]
OATP4A1	722	Ubiquitous, rat corneal epithelium, RPE cells	Taurocholate Triiodothyronine	15µM 1µM	[13]
OATP4C1	724	Kidney	Digoxin Oubain	8µM 0.4µM	[378]
OATP5A1	848	-	-	-	-
OATP6A1	719	Testis	-	-	-

Table 4.8: Expression of OATP in various cancer tissues

OATP	**Cancer tissue expression**		**Reference**
	Increased	**Reduced**	
OATP1A2	In breast carcinoma cells and malignant breast tissue	In colon polyps and cancer	[379-381]
OATP1B1	-	In hepatocellular carcinoma	[187, 382]
OATP1B3	-	In hepatocellular carcinoma	[186]
OATP2A1	In malignant breast tissue and liver cancer	In tumors of bowel, stomach, ovary, lung and kidney	[383-385]
OATP2B1	In bone cysts	-	[386]

Organic Anion Transporter (OAT)

OATs are another family of multispecific transporters, the major facilitator superfamily (MFS) and are encoded by the SLC22/Slc22 gene superfamily. OATs differ in their composition of amino acids. Human OAT1 and OAT3 consist of 563 and 542 amino acids, respectively. They

have 12 α-helical transmembrane domains (TMDs) with intracellular amino and carboxy-termini [387, 388]. Main function of these transporters is to act as transmembrane uniporters, symporters, and antiporters, and translocate a diverse range of xenobiotics (drugs and toxins), endogenous metabolites (amino acids, sugars, neurotransmitters, etc.) and hydrophilic and amphiphilic substrates including inorganic ions (Na^+, Cl^-, HCO_3^-, etc.). They are responsible for the uptake of a wide range of low molecular weight substrates including steroid hormone conjugates, biogenic amines, various drugs and toxins **(Table 4.9)** [387-391]. Due to their expression on liver and kidneys, they might play a substantial role in maintaining endogenous homeostasis. They are capable of translocating a number of prescribed pharmaceuticals, such as loop and thiazide diuretics, methotrexate, angiotensin-converting enzyme (ACE) inhibitors, nonsteroidal anti-inflammatory drugs and β-lactam antibiotics [392]. The presence of OATs on olfactory mucosa, choroid plexus, and retina corroborates their involvement in secretory processes [393]. OAT family majorly represents the classic renal organic anion transport system. So far, eight isoforms (OAT 1-7 and URAT 1) of OAT have been identified **(Table 4.9)**. Members of OAT belong to SLC22A gene family and are structurally similar to organic cation transporters (OCTs) [354]. It is of clinical importance to understand the transport mechanism of OATs for critical elucidation related to drug handling and nephrotoxicity.

Table 4.9: Tissue expression and prototypical substrates of OAT family members

OAT	Tissue expression		Substrates	Inhibitors	Reference
	Apical	**Basolateral**			
OAT1	Mouse and rat choroid plexus	Renal proximal tubules and plasma membrane of skeletal muscles	p-Aminohippurate	Probenecid, novobiocin	[122, 387, 394-400]
OAT2	-	Renal proximal tubules and hepatocytes (rodents)	p-Aminohippurate	Bumetanide, Chlorothiazide, Cyclothiazide	[387, 401, 402]
OAT3	-	Renal proximal tubules	Estrone 3-sulfate	Probenecid, novobiocin	[122, 387, 403]
OAT4	Renal proximal tubules	Syncytiotrophoblasts in placenta	Estrone 3-sulfate	Olmesartan, telmisartan	[25, 387, 401, 404, 405]
OAT5	-	-	Ochratoxin A	Bumetanide, furosemide	[387, 401, 406]
OAT6	-	-	Estrone 3-sulfate	Benzylpenicillin, Carbenicillin	[18, 387, 401]
OAT7	-	Hepatocytes	Estrone 3-sulfate	-	[387, 407]
URAT1	Renal proximal tubules	-	Urate	Losartan, telmisartan, furosemide	[387, 401, 408]

Organic Cation Transporter (OCT)

OCTs are also members of SLC22A family of solute carrier (SLC) transporters including novel organic cation transporters OCTN1 and OCTN2 (encoded by genes SLC22A4 and SLC22A5 respectively). They are responsible for the uptake of a wide range of low-molecular-weight, relatively hydrophilic organic cations such as prototypical cation TEA, neurotoxin MPP+, and endogenous compound N-methylnicotinamide (NMN) **(Table 4.10)** [409-411]. OCT consists of 543-557 amino acids. They have 12 transmembrane domains (TMDs) with intracellular amino and carboxy-termini. Facilitated diffusion driven by the inside-negative membrane potential is the

mechanism of uptake of organic cations via OCT [387, 409, 412-417]. The substrates of the OCTs are mostly cations with rare exception for anionic or neutral compounds at physiological pH. Three isoforms of OCTs (OCT 1-3) has been cloned from human, rabbits, rats and mice. The paralogs of OCT1 and OCT2 share about 68–69% sequence homology for humans, rats, and mice, and 71% for rabbits [418]. Substrate specificity for orthologous OCT may vary due to difference in species. For example, the transport of tetrapropylammonium (TPA) or tetrabutylammonium (TBA) is mediated by human and rabbit OCT1 but not by rat and mouse Oct1. This example acts as a supporting statement for differences in recognition of OCT substrates across species [419]. Both the tissue expression and localization of OCTs (**Table 4.10)** show that these transporters play a governing role in the excretion of toxic xenobiotic and endogenous organic cations. Their crucial involvement in drug disposition or drug response depicts tissue expression, substrate and inhibitors specificity of OCT family.

Table 4.10: Tissue expression and substrates of OCT family members

OCT	**Tissue expression**		**Substrates**	**Inhibitors**	**Reference**
	Apical	**Basolateral**			
OCT1	Lung epithelial cells	Hepatocytes, Rodents enterocytes and proximal tubule epithelial cells (rodents)	Acyclovir, famotidine, metformin etc.	Quinine, quinidine, disopyramide	[122, 387, 409, 420-423]
OCT2	Lung epithelial cells	Distal convoluted tubules	Cimetidin, dopamine, metformin etc.	Cimetidine, pilsicainide, cetirizine, testosterone, quinidine	[122, 387, 410, 411, 420, 422, 424]

OCT3	Lung epithelial cells and enterocytes	Hepatocytes, and trophoblasts	Cimetidine, histamine, serotonin etc.	β-Estradiol, Corticosterone, Deoxycorticosterone, Progesterone	[387, 410, 411, 422, 425-428]
OCTN 1	Renal epithelial cells (rodents), intestinal epithelial cells and lung epithelial cells	-	-	-	[30, 387]
OCTN 2	Renal proximal tubules, syncytiotrophoblasts in placenta and lung epithelial cells	-	-	-	[31, 387, 429]

Sodium Dependent Multivitamin Transporter (SMVT)

SMVT is an important plasma membrane protein which facilitates the cellular uptake of vitamins and other essential cofactors such as biotin, pantothenic acid and lipoic acid. SMVT primarily facilitates the cellular uptake of biotin (vitamin B7) and is a highly sodium dependent specific vitamin carrier system. It has been referred as sodium dependent multivitamin transporter because of its sodium and substrate specificity. SMVT protein encodes for 635 amino acids and has 12 transmembrane domains. The expression of SMVT has been reported in various tissues such as placenta, intestine, brain, liver, lung, kidney, cornea, retina and heart. Biotin has been utilized in drug delivery by covalently attaching or by surface modification of various therapeutic molecules [430]. Russel-Jones et al. reported enhanced tumor accumulation of biotinylated fluorescently-labelled N-(2-hydroxypropyl) methacrylamide (HPMA) polymers following intravenous administration in mice [431]. Biotin has also been employed as a target moiety to deliver large peptides orally by varying the absorptive transport pathways and improving intestinal permeability. Ramanathan et al. demonstrated enhanced cellular accumulation of biotinylated PEG-based conjugates of Tat9 via SMVT in Caco-2 and transfected CHO cells. The 29 kDa

peptide-loaded bioconjugate [PEG:(R.I-Cys-K(biotin)-Tat9)8] and biotin-PEG-3400 interact with human SMVT to enhance the cellular accumulation of these large molecules. This strategy of conjugating high molecular weight compounds with targeting moiety enhances the intestinal absorption and oral bioavailability of macromolecules [430, 432]. Biotin-ganciclovir (B-GCV) uptake mediated by SMVT was substantially higher compared to ganciclovir in both ARPE-19 cells and rabbit retina [433]. This study secularizes the intravitreal pharmacokinetics of GCV and B-GCV by an ocular microdialysis technique. The AUC of Biotin-GCV (17.5 ± 1.38 mg*min*mL^{-1}) was significantly higher than GCV (10.6 ± 1.27 mg*min*mL^{-1}) and no statistically significant difference was observed between half-lives of GCV and B-GCV [434]. The tissue distribution and kinetic parameters of SMVT are presented in the **Table 4.11**.

Table 4.11: An overview of tissue distribution and kinetic parameters of SMVT on cellular accumulation

Cells/ Tissue	**Michaelis – Menten Kinetic Parameters**		**Reference**
	K_m	**V_{max}**	
Bovine brain microvessel endothelial cells (BMEC)	49.1 μM	313.2 pmoles/mg protein/min	[435]
Human colonic epithelial cells (NCM460)	19.7 μM	38.8 pmoles/mg protein/3min	[436]
Human derived prostate cancer cells (PC-3)	19 μM	23 pmoles/min/mg protein	[437]
Human corneal Epithelial (HCE) cells	296.23 μM	77.23 pmol/mgprotein/min	[438]
Human retinal pigmented epithelial cells (ARPE-19 and D407)	138.25 μM (ARPE-19) and 863.81 μM (D407)	38.85 pmoles/mg protein/min (ARPE-19) and 308.26 pmol/mgprotein/min (D407)	[434, 438]
Canine kidney cells (MDCK-MDR1) transfected with human *MDR1* gene	13 μM	21.5 pmoles/mg protein/min	[439]

Human retinoblastoma cells (Y-79)	8.53 μM	14.12 pmoles/mg protein/min	[440]
Human placental brush border membrane	21 μM	4.5 nmoles/mg protein/min	[441]
Rabbit corneal epithelial cells (rPCEC)	32.52 μM	10.43 pmoles/mg protein/min	[433]
Rat retinal capillary endothelial cells (TR-iBRB2)	146 μM	0.223 nmoles/mg protein/min	[442]
Human proximal tubular epithelial cells (HK-2)	12.16 μM	14.4 pmoles/mg protein/7 min	[443]
Human intestinal cells (Caco-2)	9.5 μM	520 pmoles/mg protein/min	[444]
Human kidney cortex brush border membrane	31 μM	82 nmoles/mg protein/30 sec	[445]
Human liver basolateral membrane vesicles	1.22 μM	4.76 pmoles/mg protein/10 sec	[446]
Human intestinal brush border membrane (BBM)	5.26 μM	13.47 pmoles/mg protein/20 sec	[447]
Human rat kidney cortex brush-border membrane vesicles	55 μM	217 pmoles/mg protein/sec	[448]

Sodium-dependent vitamin C transporters (SVCT1 and SVCT2)

Ascorbic acid (AA or, vitamin C) is an essential nutrient required for cellular function, wound healing and immunity. Sodium-dependent vitamin C transporters (SVCT1 and SVCT2) have been cloned recently from human and rat DNA libraries [449-451]. Both isoforms have similar function and can mediate L-AA transport. This transporter is present in many tissues such as intestine [452, 453], kidney [454, 455], brain [456, 457], eye [458, 459], bone [460], and skin [461]. Luo et al. [462] reported the presence of SVCT1 and SVCT2 in MDCK cells. While SVCT1 expresses mainly on the apical membrane, SVCT2 is present on both the apical and basolateral membrane. Uptake of ascorbic acid in MDCK-MDR1 cells appears to be saturable and concentration dependent process in a range with K_m of 83.2 μM and 7.27 μM for SVCT1 and

SVCT2 respectively. Analysis of deduced primary amino acid sequence of hSVCT1 and hSVCT2 suggests the presence of five putative PKC phosphorylation sites while SVCT1 possess an additional PKA site [463].Various inter and intra cellular stimuli (hormones, paracrine factors, signaling molecules, etc.) are engaged in the expression of SVCT [464].

Conclusion

Complex nature of disease and presence of barrier in ocular and cancerous tissues provides a significant challenge for the treatment of ocular and other diseases. Identification and characterization of novel influx transporters and exploring them in terms of drug delivery helps in partially meeting these challenges in drug delivery to ocular or various tissues. Lower side effects with significant improvement in bioavailability are the major advantages provided by targeting specific transporters in specific tissues. Drug delivery has been revolutionized by development of non-invasive or less invasive drug delivery techniques. New polymers and polymeric drug delivery systems have been examined and evaluated for the purpose of controlled and sustained delivery for treating vision-threatening diseases and cancer. Progress in nanotechnology, influx transporter and non-invasive drug delivery techniques will lead the race for development of new and novel drug delivery systems.

CHAPTER 5

NOVEL PENTABLOCK COPOLYMER BASED NANOPARTICLES CONTAINING PAZOPANIB: A POTENTIAL THERAPY FOR OCULAR NEOVASCULARIZATION

Rationale

Several pathologic conditions such as infection, trauma, and loss of the limbal stem cells result in invasion of vessels from the limbal arcade to normally avascular cornea leading to corneal neovascularization (CNV) [465-467]. It leads to loss of ocular immunity due to induction of allo-immunity which ultimately leads to penetrating keratoplasty [465, 468-471]. Furthermore, graft rejection is also triggered due to ingrowth of neovessels into avascular recipient tissue following corneal surgery [465, 472]. Apart from CNV, one of the most common cause of vision loss is choroidal neovascularization (ChNV). It is mostly associated with age-related macular degeneration (AMD) leading to pathological myopia, ocular histoplasmosis, angioid streaks, and several other diseases. Limited information is available regarding the pathogenesis of neovascularization (NV). However understanding the role of vascular endothelial growth factor (VEGF) in development of neovessels is considered to be major advancement [473, 474]. Intraocular injections of ranibizumab, an anti-VEGF agent that binds with all isoforms of VEGF-A demonstrated substantial vision improvement in 34% to 40% of patients with ChNV [475, 476]. Also, bevacizumab (anti-VEGF agent that binds with all isoforms of VEGF-A) has shown positive indication in patients with ChNV from AMD [477-483]. Reduction in subretinal and intraretinal fluid accompanied by improvement in visual acuity was observed following administrations of ranibizumab and bevacizumab (antagonists of VEGF-A). However, monthly injections of ranibizumab only halted growth of ChNV and did not cause any significant effect on the regression of existing ChNV, possibly due to the involvement of factors other than VEGF-A [475]. These

factors are responsible for endothelial cell survival and once the levels of ranibizumab reaches below the critical level, onset of vascular leakage and growth of CNV is noted. Apart from VEGF family members, several factors such as pericytes, are platelet derived growth factor B (PDGF-B) are also responsible for survival of endothelial cells [484].

As mentioned above, neovascularization is triggered by a cascade of cellular and molecular events [485-487]. Development of neovessels is mainly triggered by VEGF such as VEGF-A, B, C and D [488]. Retinal pigmented epithelial cells, vascular endothelial cells, macrophages, fibroblasts and corneal epithelial cells are the main source of VEGF in cornea and retina respectively [489]. Expression of VEGF is highly upregulated in inflamed and vascularized cornea. Accelerated growth, migration, and survival of the endothelial cells are attributed to VEGF-triggered effects mediated via tyrosine kinase receptors (VEGFR1, 2, 3) [490, 491]. Tyrosine kinases selectively phosphorylate tyrosine residues by binding to extracellular domain of receptors that induce receptor dimerization of VEGF and VEGFR. This induction leads to tyrosine kinase activation and transcription of VEGF. Blockage of VEGF not only inhibits CNV but also promotes corneal graft survival [492-494]. VEGF transcription is also stimulated by PDGF via tyrosine kinase PDGF receptors (α and β) which play a vital role in recruitment of pericytes to neovessels. Growth of pericyte and endothelial cells are interdependent. Pericyte recruitment can be disrupted by inhibition of PDGF signaling pathways. PDGF is secreted by endothelial cells. Pericytes express PDGFR-β and the resulting signal stmulates pericyte growth. By inhibiting PDGF signaling pathways, endothelial cells undergo apoptosis because of lack of pericyte support and absence of VEGF signaling [484, 494-500]. From this information, it can be postulated that modulation of VEGF and PDGF may provide better therapeutic outcome in ocular NV [501].

Pazopanib, a small molecule tyrosine kinase inhibitor, not only inhibits VEGF but also targets PDGF receptors inhibiting angiogenesis [502, 503]. It has been approved by U.S. FDA for the treatment of renal cell carcinoma and soft tissue sarcoma [195, 504]. In preclinical studies, pazopanib exhibited proven beneficial effect in ocular complications. Following oral administration, pazopanib induced inhibition of VEGF and PDGF pathways leading to lowering of laser induced ChNV [505]. In rats, topical eye drops of pazopanib causes inhibition of laser induced ChNV, diabetic retinal vascular leukostasis, and leakage [506, 507].

Recently, Csaky G *et al* have reported that in phase 2B clinical trial no statistically significant differences were observed between pazopanib eye drops and monthly ranibizumab with regard to optical coherence tomography (OCT) parameter, including retinal morphology and CNV lesion size (abstract presented at Annual meeting of the American Academy of Ophthalmology, Louisiana, 2013). Expression of efflux transports on corneal epithelium and blood-retina barrier (i.e. retinal capillaries and retinal pigment epithelium (RPE) has been reported. These efflux transporters play a significant role in ocular pharmacokinetics and drug disposition [508]. Pazopanib is a substrate of efflux transporters which can limit uptake into the target tissue [152, 153, 509]. Thus by inhibiting or bypassing the efflux transporters, pazoapanib tissue penetration can be improved. However, inhibitors or specific efflux modulators may lead to systemic toxicity at doses required to modulate efflux activity. Hence, we have developed pazopanib encapsulated nanoparticles (NP) which not only eliminates efflux inhibitor related toxicity but also enhances tissue penetration of pazopanib along with controlled drug release. In this study, we have examined a novel pentablock copolymer (PB) composed of FDA approved polymer blocks such as PEG, PCL, and PLA/PGA. We have prepared a PB copolymer with block arrangements of PLA_{3000}-PCL_{7000}-PEG_{2000}-PCL_{7000}-PLA_{3000}. This polymer was utilized to prepare pazopanib loaded NP for

the treatment of ocular neovascularization. Characterization of PB polymer has been carried out with NMR, GPC, X-ray diffraction, cytotoxicity and biocompatibility studies. Also, several NP parameters such as entrapment efficiency, drug loading, *in vitro* drug release and effect of pazopanib NP in evading efflux transporters were studied.

Material And Methods

Materials

PEG (2 kDa), stannous octoate, ε-caprolactone, poly (vinyl alcohol) (PVA), lipopolysaccharide were procured from Sigma-Aldarich (St. Louis, MO; USA). L-lactide was purchased from Acros organics (Morris Plains, NJ; USA). Mouse TNF-α, IL-6 and IL-1β (Ready-Set-Go) ELISA kits were obtained from eBioscience Inc. Lactate dehydrogenase estimation kit and CellTiter 96® AQueous non-radioactive cell proliferation assay (MTS) kit were obtained from Takara Bio Inc. and Promega Corp., respectively. [^{3}H] Digoxin (specific activity 35.4 Ci/mmol) and [^{3}H] Abacavir (specific activity 0.1 Ci/mmol) were procured from Perkin Elmer (Boston, MA, USA). All other reagents utilized in this study were of analytical grade. Human conjunctival (CCL 20.2) and mouse leukaemic monocyte macrophage cells (RAW-264.7) were procured from American Type Culture Collection (ATCC). Human corneal epithelial (HCEC) and human retinal pigmental cells (D407) were generous gifts from Dr. Araki-Sasaki (Kinki Central Hospital, Japan) and Dr. Richard Hunt (University or South Carolina, Columbia, SC, USA), respectively.

Synthesis Of TB And PB Copolymers

Triblock (TB) and pentablock (PB) copolymers were synthesized by ring-opening bulk copolymerization [510]. Briefly, PCL-PEG-PCL copolymers (TB) were synthesized by copolymerization of ε-caprolactone on the hydroxyl ends of PEG (2kDa). In this reaction, PEG was used as a macro-initiator and stannous octoate (0.5wt%) as catalyst. To synthesize PCL-PEG-

PCL, pre-determined amount of PEG was vacuum-dried for 4 h followed by addition of ε-caprolactone and catalyst. The reaction was carried out in close vessel under nitrogen environment, at 130°C for 36 h. The reaction mixture was solubilized in DCM followed by precipitation in ice-cold diethyl ether. Precipitated polymer was vacuum-dried to remove any residual solvent and characterized to evaluate the reaction yield. Structure and molecular weight of TB copolymers were confirmed by ^{1}H-NMR and GPC.

In order to synthesize PB copolymers, predetermined amount of TB copolymer was employed as a macro-initiator and stannous octoate (0.5wt%) as catalyst. For the synthesis of PB, L-lactide was polymerized on the hydroxyl ends of TB copolymer. Reaction was carried out at 130°C for 36 h. In order to remove catalyst and unreacted monomers. The reaction mixture was dissolved in DCM and precipitated by addition of ice-cold diethyl ether. Polymers were vacuum-dried and characterized for structure and polydispersity by employing ^{1}H-NMR and GPC as analytical techniques. Purified polymers were stored at -20 °C until further use. Reaction scheme for the synthesis of TB and PB are described in **Fig.5.1**

Characterization Of Polymers

^{1}H-NMR and GPC analysis were performed to characterize polymers for purity, molecular weight and polydispersity. Further, XRD studies were performed to understand the crystalline nature of polymers.

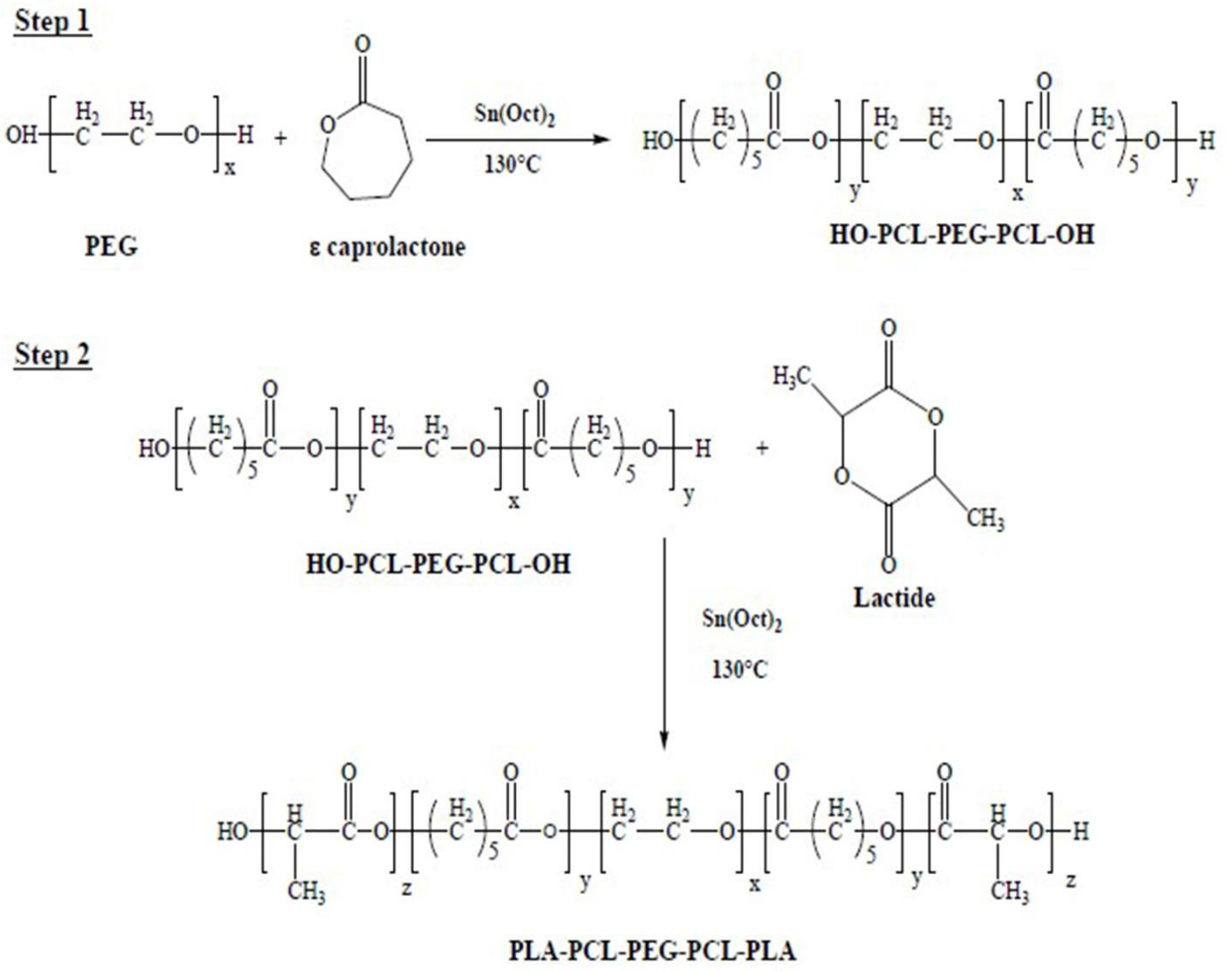

Fig.5.1: Synthesis scheme for triblock (TB) and pentablock (PB) copolymers

^{1}H-NMR

For ^{1}H-NMR spectroscopy, polymeric material was dissolved in deuterated chloroform ($CDCl_3$) and analyzed via Varian-400 NMR spectrometer. Using ^{1}H-NMR, purity and molecular weight (Mn) of the polymers were confirmed.

Gel Permeation Chromatography (GPC) Analysis

Purity of polymer is further confirmed by analyzing molecular weight and polydispersity.Five mg of polymeric material was dissolved in tetrahydrofuran (THF). It was utilized as eluting solvent at the flow rate of 1 mL/min whereas separation was performed on

Styragel HR-3 column. Polystyrene samples with narrow molecular weight distribution were employed as standards.

X-Ray Diffraction (XRD) Analysis Of Copolymers

Diffraction patterns of samples were analyzed in order to understand the effects of polymer composition (TB vs PB) on the crystallinity of copolymers. MiniFlex automated X-ray diffractometer (Rigaku, The Woodlands, Texas) with Ni-filtered Cu-kα radiation (30 kV and 15 mA) was employed to obtain diffraction patterns. XRD analysis was performed at room temperature.

In Vitro Cytotoxicity Studies

Cell Culture

RAW-264.7 cells were cultured and maintained in Dubelcco's modified Eagle medium (DMEM) supplemented with 10% FBS, 100 mg/L of streptomycin and 100 U/L of penicillin. HCEC cells were cultured according to previously published protocol [511-513]. Cells of passage numbers between 25 and 30 were cultured at 37°C, humidified 5% CO_2/95% air atmosphere in a DMEM/F-12 culture medium supplemented with 15% (v/v) FBS (heat inactivated), 15 mM HEPES, 22 mM $NaHCO_3$, 100 mg of penicillin and streptomycin each, 5 μg/ml insulin, and 10 ng/ml of human epidermal growth factor. D407 cells (passage numbers between 75 and 80) were grown at 37°C, humidified 5% CO_2/95% air atmosphere in a DMEM culture medium supplemented with 10% (v/v) FBS (heat inactivated), 29 mM $NaHCO_3$, 20 mM HEPES, 100 mg of penicillin and streptomycin each, and 1% nonessential amino acids at pH 7.4 [514, 515]. Chang's conjunctival cell line (CCL 20.2) were grown at 37°C, humidified 5% CO_2/95% air atmosphere in a Medium 199 containing Earle's BSS supplemented with 10% (v/v) FBS (heat inactivated), 29

mM $NaHCO_3$, 20 mM HEPES, 100 mg of penicillin and streptomycin each, and 1% nonessential amino acids at pH 7.4.

Lactate Dehydrogenase (LDH) Assay

Cytotoxicity of PB copolymer was evaluated according to previously published protocol with minor modifications [516]. Briefly, different concentrations (1-20 mg/mL) of PB copolymer were prepared in acetonitrile (ACN). A 100µL of solutions was aliquoted in each well of 96-well cell culture plates. In order to evaporate ACN and to sterilize block copolymers, cell culture plates were exposed overnight under UV light in a hood with laminar flow. Once the ACN is evaporated, 1.0 x 10^4 of HCEC cells were seeded in each well on the film of PB polymer formed after evaporation of ACN and incubated for 48 h at 37°C and 5% CO_2 in humidified atmosphere. After appropriate incubation time, LDH assay kit was utilized to analyze the supernatant for the levels of LDH. LDH assay was performed according to the supplier's protocol. Samples were analyzed using 96-well plate reader at 450 nm. Amount of released LDH is directly proportional to cytotoxicity of the polymers. In this study, LDH release >10% was considered as cytotoxic. To evaluate toxicity of block copolymers on or retinal and conjunctival cells, similar experiment was performed with D407 and CCL 20.2 cells. LDH release (%) was calculated by utilizing following equation:

$$\boldsymbol{LDH\ release}\ (\%) = \frac{\boldsymbol{Abs.of\ sample - Abs.of\ negative\ control}}{\boldsymbol{Abs.of\ positive\ control\ -\ Abs.of\ negative\ control}} * \mathbf{100}$$

MTS Assay

In vitro cell viability (MTS) assay was performed in order to confirm the safety of PB copolymer. MTS assay was carried out according to previously published protocol with minor modifications [517]. Four different concentrations of block copolymer solutions were prepared, aliquoted and sterilized according to the previously mentioned procedure. After sterilization,

HCEC cells at the density of 1.0 x 10^4 cells per well were seeded in 96-well plate. Cells were incubated for 48 h at 37°C and 5% CO_2 in humidified atmosphere. After incubation, cell culture medium was replaced with 100µL of serum free medium containing 20µL of MTS solution. Cells were further incubated for 4h at 37°C and 5% CO_2. Absorbance of each well was determined at 450 nm. Polymer concentrations at which viability of cell is > 90% was observed, were considered as non-toxic. Percent cell viability was estimated by the following equation. The similar experiment was repeated with CCL 20.2 and D407 cells.

$$\textbf{\textit{Cell viability}}\ (\%) = \frac{\textbf{\textit{Abs. of sample}} - \textbf{\textit{Abs. of negative control}}}{\textbf{\textit{Abs. of positive control}} - \textbf{\textit{Abs. of negative control}}} * \mathbf{100}$$

***In Vitro* Biocompatibility Studies**

Different concentrations (1-20 mg/mL) of block copolymer solutions were prepared in ACN and were added (200µl) in each well of 48-well cell culture plate. These plates were incubated overnight under UV light in a laminar flow hood for sterilization as well as for evaporation of ACN. After sterilization, RAW-264.7 cells were plated at the cell density of 5.0 x 10^4 per well. Cells were exposed to polymer for 48 h at 37 °C and 5% CO_2. After appropriate incubation time, cell supernatant was analyzed for the quantification of three different cytokines, i.e., TNF-α, IL-6 and IL-1β. ELISA method was employed to estimate the levels of cytokines. ELISA was performed according to the manufacturer's instruction. Calibration curves for TNF-α, IL-6 and IL-1β were prepared in the range of 10-750 pg/mL, 5-500 pg/mL and 10-500 pg/mL, respectively.

Preparation Of Nanoparticles

Nanoparticles were prepared using PB copolymer. An earlier published process (spontaneous emulsion solvent diffusion method) was adopted with minor modifications for the preparation of nanoparticles [518]. Briefly, 1 mg of pazopanib and 5mg of PB copolymer (1:5)

was dissolved in 1 ml of DMSO. This solution was added drop wise from a syringe into 5 ml of 1% poloxamer solution under constant stirring. Nanoparticles were formed instantaneously on mixing of both the solutions. Prepared nanoparticles were stirred for 1 hr followed by centrifugation. Finally, nanoparticles were washed two times with DDW to remove surface bound pazopanib, poloxamer, and DMSO. Several batches of nanoparticles were prepared with different ratios of pazopanib to PB copolymer (1:5 and 1:10). NPs were freeze-dried in 5% mannitol solution and stored at -20 °C until further characterization. NPs were prepared utilizing two different drug to polymer ratios i.e., 1:5 and 1:10. Freeze-dried NPs were characterized for particle size, entrapment efficiency (EE), drug loading (DL) and *in vitro* drug release behavior. This study was carried out in triplicate. Blank nanoparticles were also prepared by employing only polymer in similar amounts.

Characterization Of NPs

Particle size

NPs (1 mg/mL) suspended in DDW were subjected to particle size analysis. NPs mean size was evaluated at room temperature and 90° scattering angel utilizing Zeta sizer (Zetasizer Nano ZS, Malvern Instruments Ltd, Worcestershire, UK). All the samples were analyzed in triplicate. The size analysis consisted of 30 measurements per sample, and the results are expressed as mean size ± SD.

Entrapment efficiency (EE %) and drug loading (DL %)

Pazopanib-loaded freeze-dried NPs were examined for the estimation of DL and EE. Supernatant collected during NP preparation were analyzed to evaluate EE utilizing Micro BCATM protein estimation kit. Two milligram equivalent of pazopanib-encapsulated NPs were dissolved in 200µL of DMSO in order to evaluate DL. Resulting solution was subjected for

estimation of pazopanib via UV absorbance spectroscopy at 275nm. Standard curve of pazopanib ranging from 0.97 to 1000µg/mL was prepared in DMSO. EE (%) and DL (%) were estimated as per to the following equations.

$$\%EE = \frac{Total\ amount\ of\ drug - Amount\ of\ drug\ in\ supernatant}{Total\ amount\ of\ drug} * 100$$

$$\%DL = \frac{Amount\ of\ drug\ in\ nanoparticles}{Total\ amount\ of\ drug\ and\ polymer} * 100$$

In Vitro Release Studies

Dialysis Bag Method

A volume of 0.6 mL of NP formulation (1:5) was put in a dialysis bag (3.8 cm in length). Dialysis tubing consisted of regenerated cellulose, a material chemically and physically treated to increase its resistance (Avg. flat width 9 mm (0.35 in.), MWCO 2000, Sigma Aldrich, MO, USA). Both ends were tied. The dialysis bag was suspended in 10 mL of 0.1M phosphate buffer saline (pH - 7.4) at 37°C. The tube containing dialysis bag was placed in a shaker with water bath at 37°C. At predetermined time intervals dialysis bag was exchanged into a tube containing 10 mL of fresh 0.1M phosphate buffer saline (pH - 7.4) at 37°C. Drug concentrations were quantified using NanoDrop 2000c UV-Vis Spectrophotometer at 275nm and all experiments were conducted in triplicate

Release Kinetics

Release data were fitted in various kinetic models described below for the investigation of release mechanism of pazopanib from PB NPs.

Korsmeyer-Peppas Equation

$$\frac{Mt}{M\infty} = kt^n$$

Where k is the kinetic constant and n is the diffusion exponent describes release mechanism.

Mt and M∞ represent the cumulative pazopanib release at time t and at the equilibrium, respectively.

Higuchi Equation

$Q_t = Kt^{1/2}$

K denotes the Higuchi rate kinetic constant, Qt is the amount of released pazopanib at time t, and t is time (hour).

Hixon-Crowell Equation

$C_0^{1/3} - C_t^{1/3} = kt$

C_0 and C_t represents the initial amount and remaining amount of pazopanib, respectively. k is the constant incorporating surface-volume relation and t is time in hour.

First Order Equation

$LogC = LogC_0^{-Kt/2.303}$

K denotes the first order rate constant, C_0 is the initial pazopanib concentration and t represents time in hour.

Zero Order Equation

$C = K_0 t$

K_0 is the zero-order rate constant and t is time in hour.

***In Vitro* Cellular Accumulation Studies**

Twelve well polyester plates (Coaster Corning, NY) were utilized to conduct cellular accumulation studies. Following media removal, MDCK-MDR1 cells were rinsed thrice for 5 min

each with 1–2 ml of Dulbecco's phosphate-buffered saline (DPBS) containing 140 mM NaCl, 0.03 mM KCl, 7.5 mM Na_2HPO_4, 1.5 mM KH_2PO_4, 1 mM $CaCl_2$, 0.5 mM $MgSO_4$, 20 mM HEPES, and 5 mM glucose maintained at pH 7.4. Uptake studies were initiated by adding 250µl of solution containing 0.25 µCi/ml of [^{3}H] Digoxin (probe radiolabelled substrate for P-gp) in the absence and presence of GF 120918, pazopanib and pazopanib NPs. Following incubation, the solution was removed and uptake was terminated with 2 ml of ice-cold stop solution containing 200 mM KCl and 2 mM HEPES. The cell monolayer was washed thrice, 5 min each and 1ml of lysis buffer (0.1% Triton-X solution in 0.3% NaOH) was added to each well and plates were stored overnight at room temperature. Subsequently, the cell lysate (400µl) from each well was transferred to scintillation vials containing 3 ml of scintillation cocktail (Fisher Scientific, Fairlawn, NJ, USA). Samples were quantified by measuring the radioactivity using liquid scintillation spectrophotometer coulter (Beckman Instruments Inc., Fullerton, CA, USA, model LS-6500). Protein content of each sample was estimated by BioRad Protein Estimation Kit (BioRad Protein Estimation Kit, Hercules, CA, USA). Similarly, experiment was repeated in MDCK-Bcrp1 cells by utilizing 0.25 µCi/ml of [^{3}H] Abacavir (probe radiolabelled substrate for Bcrp1).

Results And Discussion

Inhibition of VEGFR and PDGFR tyrosine kinases has been explored as a new target for treatment of ocular neovascularization. In a recently concluded Phase 2b trial, pazopanib failed to demonstrate any significant effect on neovascularization lesion size over the control arm (ranibizumab) (abstract presented at Annual meeting of the American Academy of Ophthalmology, Louisiana, 2013). Expression and functional role of active efflux at the ocular tissues has been very well established [508]. Such efflux transporters may vary the ocular pharmacokinetics of the therapeutic agent. Higher affinity of efflux transporters (P-gp and BCRP)

toward this particular class of molecularly targeted agents has been reported before **[152, 153, 509]**. Reason behind failure of pazopanib in the treatment of ocular neovascularization has not been clearly revealed so far.

In this study, we have prepared novel PB copolymers which are composed of FDA approved polymer blocks such as PEG, PCL, and PLA. Each block plays a vital role such as presence of Stability of NPs is improved by incorporating PEG which ultimately reduces NP aggregation and helps in escaping phagocytosis by macrophages resulting in improved half-life. Sustain drug release can be improved by incorporating PCL, which is a slow degrading semi-crystalline polymer. Extremely slow degradation profile of polymer is not advantageous if the formulation is administered via intravitreal route. Synchronization of polymer degradation profile with the drug release profile is an important aspect to be considered by formulation scientists in order to avoid accumulation of empty formulation in limited vitreous cavity. As per previously published reports, reduction in the crystallinity of PCL may improve its hydrolytic and enzymatic degradation, since poor degradation of PCL has been attributed to its crystalline nature [519]. According to Huang *et al*, crystallinity of PCL can be significantly reduced by conjugation of PLA to PCL which will result in faster degradation of PCL [520]. The final formulation (pazopanib loaded NPs) will not only help in evading efflux transporters but will also exhibit sustain release of pazopanib from NPs.

Synthesis And Characterization Of TB And PB Copolymers

We have synthesized various PB copolymers with different molecular weights of PEG/PCL. For this whole study we have only utilized the PB copolymer with highest PCL content out of the various PB copolymers. Since one of our main goal was to sustain release of pazopanib

from formulation, that's the reason we utilized the PB copolymer having highest PCL content which imparts enhanced hydrophobicity to the polymer.

Ring-opening bulk copolymerization of ε-caprolactone, and L-lactide leads to successful synthesis of TB and PB copolymers. First step involves synthesis of TB copolymers (PCL-PEG-PCL) with different molecular weight of PEG/PCL utilizing PEG (4kDa) as macroinitiator and stannous octoate as catalyst. Purified TB copolymer was employed as macroinitiator for the synthesis of PB copolymers. Molecular weight (Mn) and purity of TB and PB copolymers were confirmed by ^{1}H-NMR spectroscopy. As described in **Fig.5.2**, typical ^{1}H-NMR characteristic peaks of PCL units were observed at 1.40, 1.65, 2.30 and 4.06 δ ppm representing methylene protons of -$(CH_2)_3$-, -OCO-CH_2-, and -CH_2OOC-, respectively. A sharp proton peak observed at 3.65 δ ppm was attributed to methylene protons (-CH_2CH_2O-) of PEG. ^{1}H-NMR spectrograms of PB copolymers with PLA as terminals (PB-A, PB-B, PB-D and PB-E) exhibited two additional peaks at 1.50 (-CH_3) and 5.17 (-CH-) δ ppm **(Fig.5.3)**.

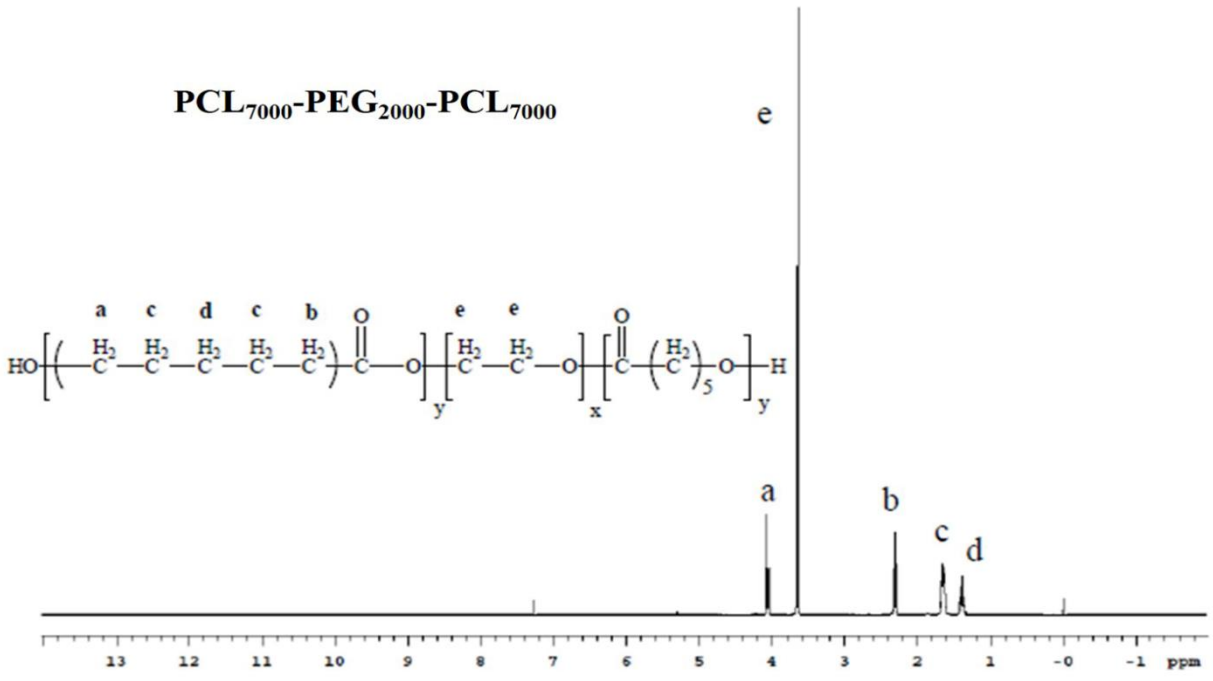

Fig.5.2: ^{1}H-NMR of TB in $CDCl_3$ (PCL_{7000}-PEG_{2000}-PCL_{7000})

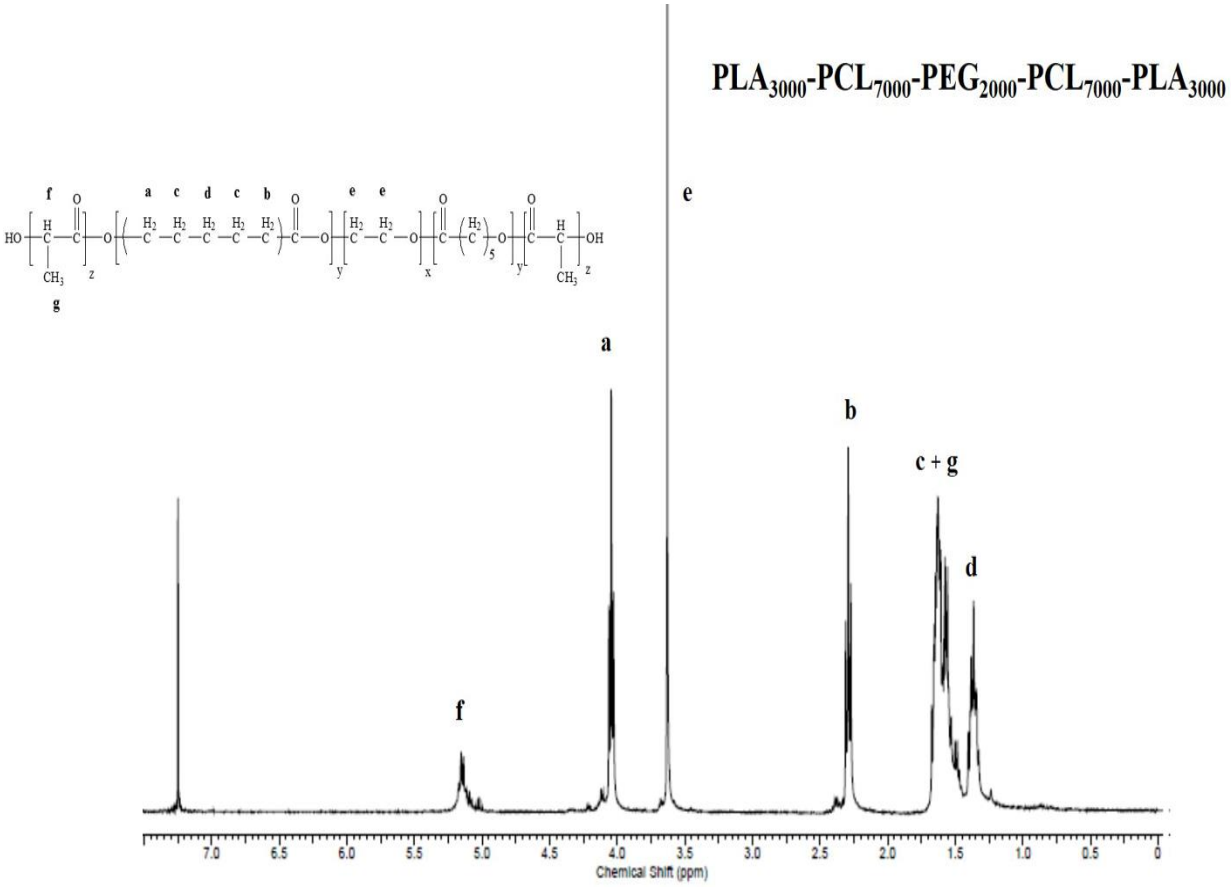

Fig.5.3: ^{1}H-NMR of PB $CDCl_3$ (PLA_{3000}-PCL_{7000}-PEG_{2000}-PCL_{7000}-PLA_{3000})

Molecular weight and purity of the TB and PB block copolymers were further confirmed by GPC analysis. Mono-distribution of molecular weight was exhibited by block copolymers along with absence of any other homopolymers such as PEG, PCL or PLA. Narrow distribution of molecular weights were observed since the calculated molecular weights were very close to the feed ratio and polydispersity of block copolymers. **Table 5.1** represents theoretical molecular weights, calculated molecular weights (^{1}H-NMR and GPC) and polydispersity. The Mn values obtained from GPC analysis were markedly lower relative to the Mn values observed from ^{1}H-NMR. Difference in hydrodynamic diameter of block copolymers in comparison to parent homopolymers can be attributed as a cause of difference in Mn values from GPC and ^{1}H-NMR analysis. As reported in **Table 5.1**, observed molecular weights were very similar to theoretical

molecular weights. For the future reference in the text, theoretical molecular weights will be mentioned instead of calculated molecular weights.

Table 5.1: Characterization of TB and PB copolymers

Polymer Structure	**Total Mn[a] (theoretical)**	**Total Mn[b] (calculated)**	**Total Mn[c] (calculated)**	***Mw*[c] (GPC)**	**PD[c]**
PCL_{7000}-PEG_{2000}-PCL_{7000}	16000	14654	12560	16520	1.31
$PL(L)A_{3000}$-PCL_{7000}-PEG_{2000}-PCL_{7000}-$PL(L)A_{3000}$	22000	20780	17250	24020	1.39

a. Theoretical value, calculated according to the feed ratio

b. Calculated from 1H-NMR results

c. Determined by GPC analysis

Covalent conjugation between PLA and PCL, significantly reduces crystallinity of PCL [521-524]. In order to confirm this, we carried out XRD studies for TB and PB copolymers. PLA with L-lactide is a semi-crystalline in nature [520]. XRD patterns of TB and PB copolymer has been described in **Fig.5.4**. TB-A shows two strong characteristic crystalline peaks of PCL blocks at diffraction angle (2θ) 21.5° and 23.8° in **Fig.5.4**. Conjugation of PLA (L-lactide) significantly diminished the crystallinity of TB which is confirmed by demonstration of reduced intensity of PCL peaks in PB copolymer containing L-lactide.

In Vitro Cytotoxicity Studies

LDH assay

On rupture of cell membrane, Lactate dehydrogenase (LDH) (a cytosolic enzyme) is screted in the culture medium. Measurement of LDH release is an ideal way to estimate the membrane damage and cytotoxicity of polymer as the cell membrane act as a potential site for polymer-cell interaction. As described in **Fig.5.5** (D407, CCL 20.2 and HCEC cells), LDH release on exposure of 4 different concentration of PB copolymers was comparable with negative control and less than 10% at any given concentrations indicating negligible or no toxicity.

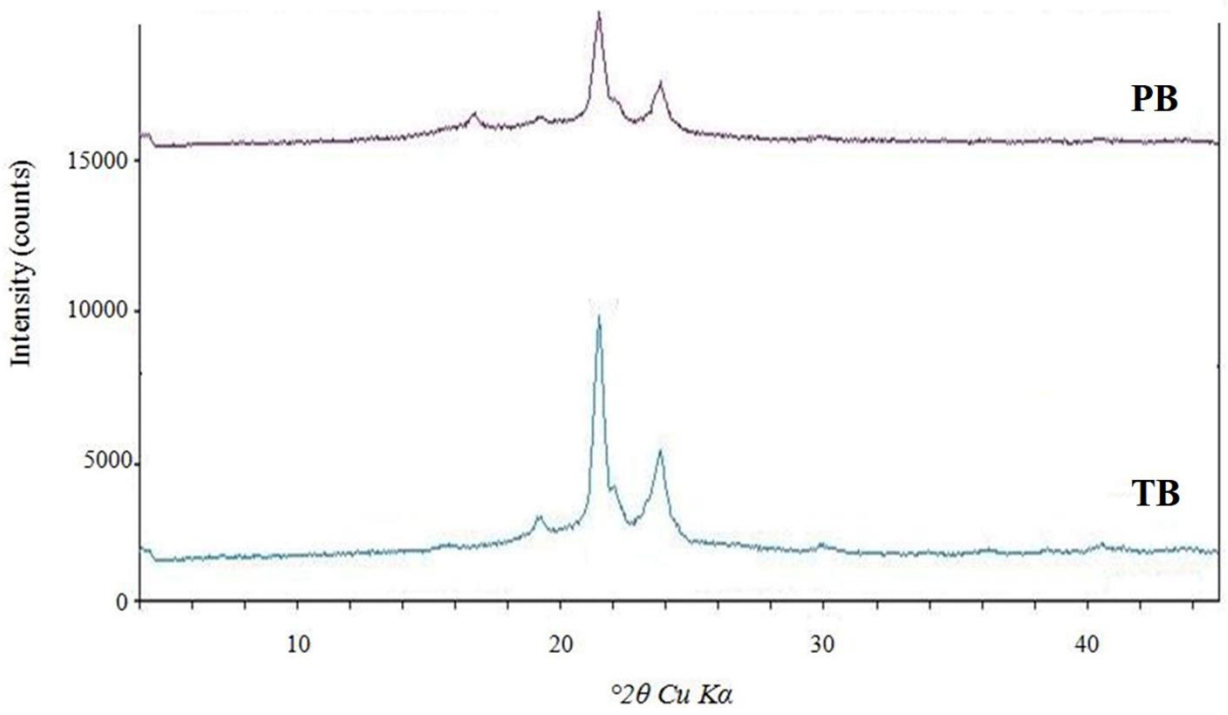

Fig.5.4: XRD patterns of TB and PB copolymers

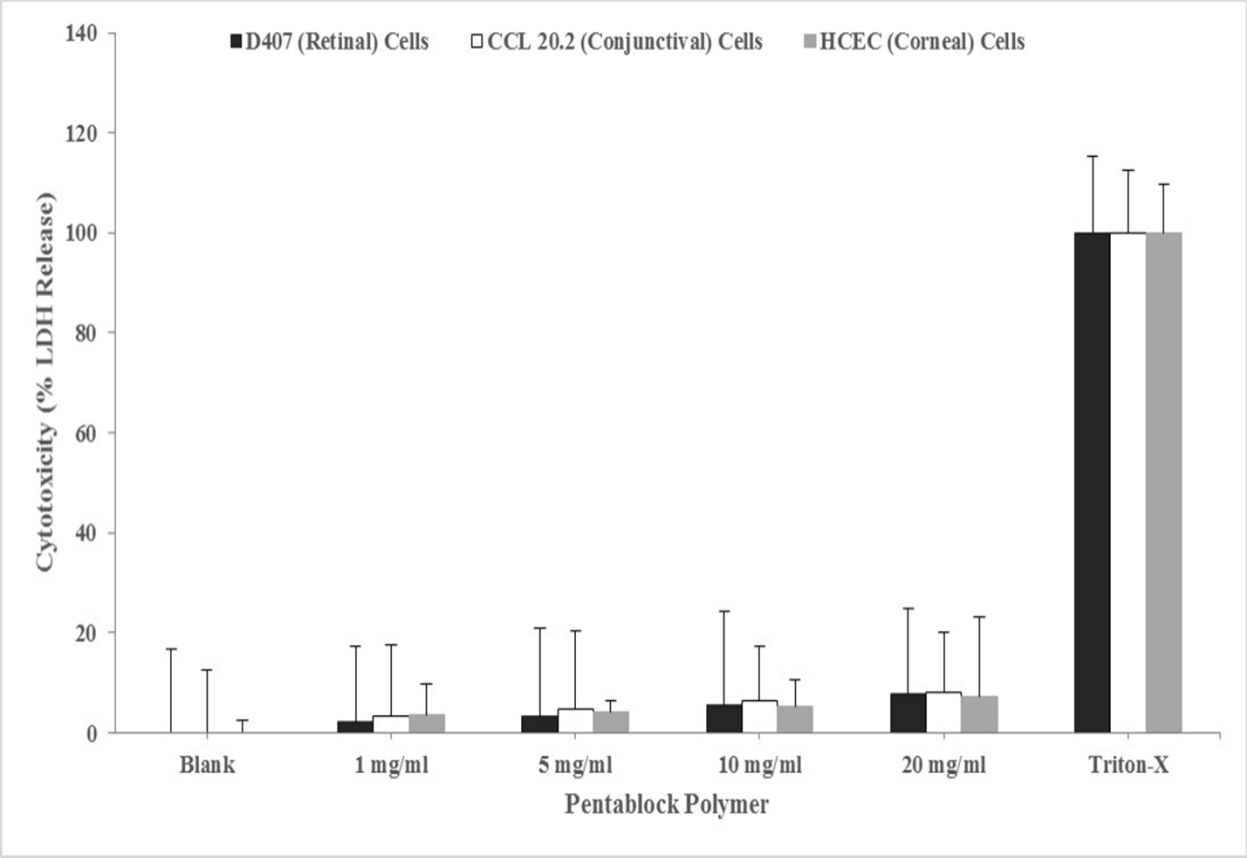

Fig.5.5: *In vitro* cytotoxicity (LDH) assay of PB copolymer at different concentrations were performed on D407, CCL 20.2 and HCEC cells

MTS Assay

In order to further confirm the results observed in cytotoxicity (LDH assay) studies, cytotoxic nature of PB copolymer were further evaluated by MTS assay. On exposure to various concentrations ranging from 1-20 mg/mL PB copolymer exhibited greater than 90% cell viability **(Fig.5.6)**. Moreover, results obtained were comparable to the negative control indicating lack of toxicity of PB copolymer. Results observed in LDH and MTS assays clearly indicated that PB block is safe for ocular application.

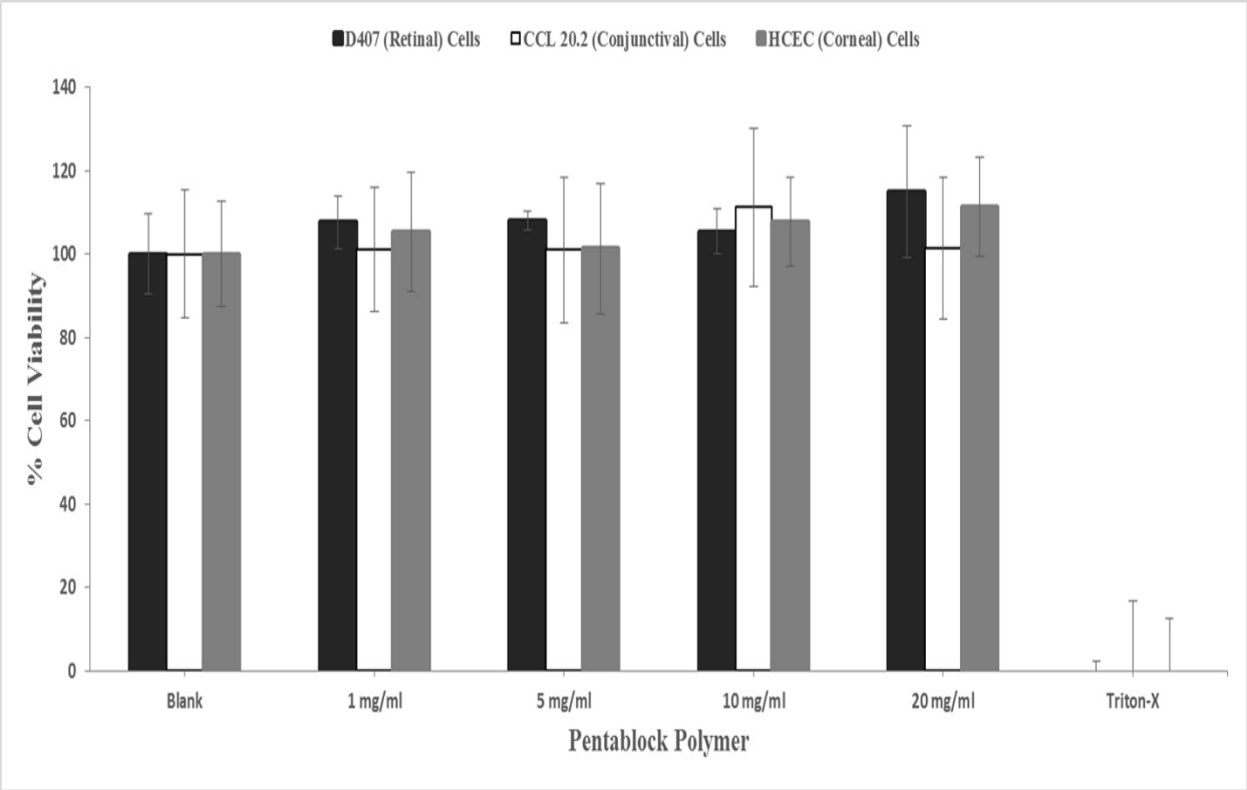

Fig.5.6: *In vitro* cytotoxicity (MTS) assay of PB copolymer at different concentrations were performed on D407, CCL 20.2 and HCEC cells

***In Vitro* Biocompatibility Studies**

It is also important to confirm that newly synthesized PB copolymer is not producing any inflammatory responses on administration via ocular route. A quick, cost effective and reliable technique to examine biocompatibility of polymers is via carrying out *in vitro* assessment for release of cytokines upon exposure to polymer. To study inflammatory responses of polymers intended for human applications RAW-264.7 cells (a well-established *in vitro* cell culture model) was employed. Negligible release of TNFα, IL-6 and IL-1β upon 24 h exposure to different concentrations of PB copolymer ranging from 1-20 mg/mL were observed in **(Fig.5.7)**. Release of any cytokines from PB copolymer was not significantly different relative to negative control indicating excellent biocompatibility of PB copolymer for ocular applications.

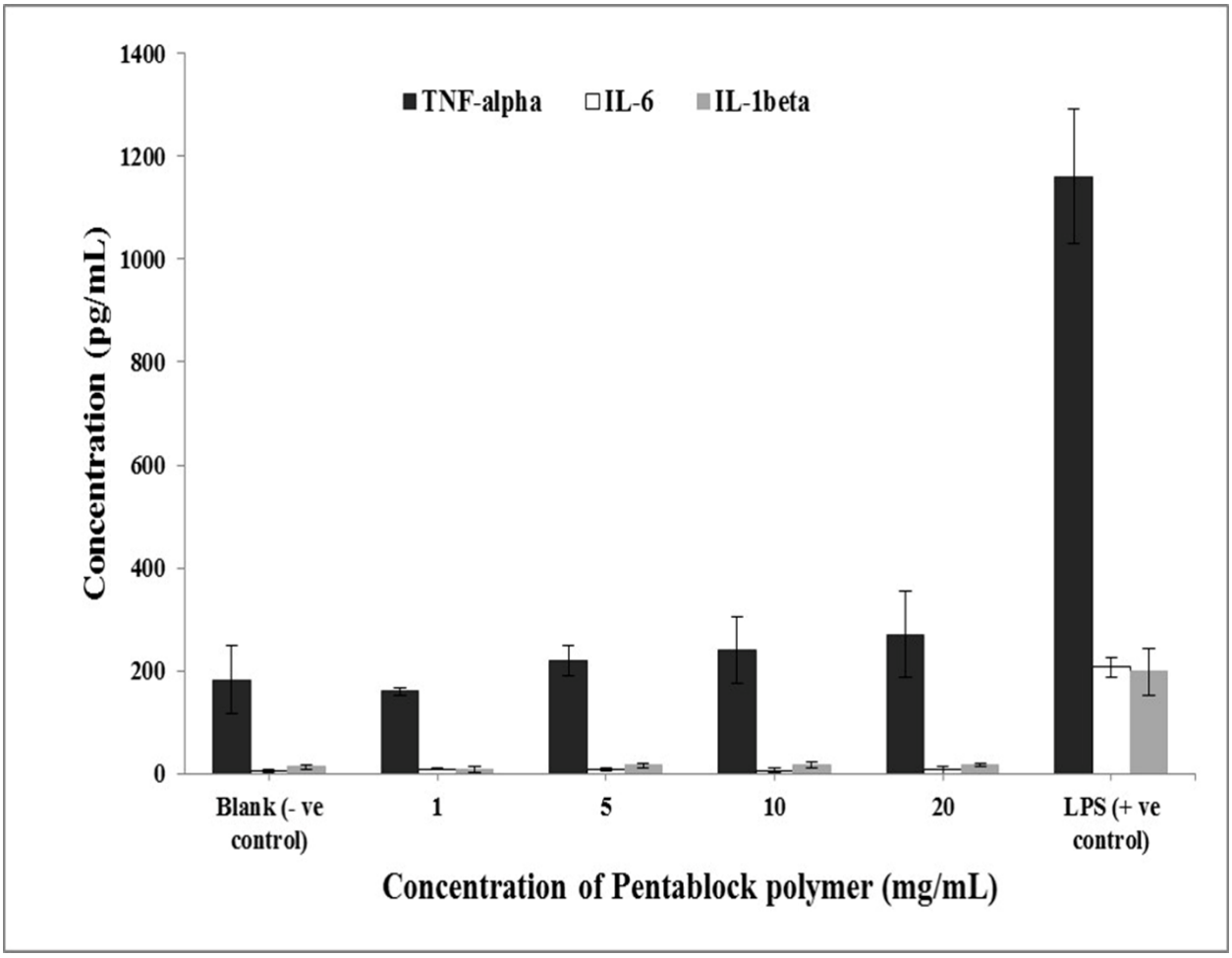

Fig.5.7: *In vitro* biocompatibility of PB copolymer were evaluated by estimating the levels of TNF-α, IL-6 and IL-1β in the supernatants of polymer treated RAW 264.7 cells

Characterization Of NPs

Particle Size

Pazopanib loaded PB NPs were prepared by spontaneous emulsion solvent diffusion method. As described in **Table 5.2**, size of NPs were between 420 nm to 515 nm. In order to understand the effect of drug to polymer ratio on particle size, we have prepared NPs with two distinct drug to polymer ratios i.e., 1:5 and 1:10. Interestingly, we observed significant increase in the size of nanoparticles, as we employed higher amounts of PB copolymer to prepare pazopanib NPs. These results suggest that particle size is highly influenced polymer:drug ratio.

Entrapment efficiency (EE) and drug loading (DL)

This work also studied the entrapment efficiency of pazopanib in two different batches of nanoparticles. We observed the higher entrapment of the pazopanib as we increased the amount of PB copolymer used in the preparation of nanoparticles. When the ratios of pazopanib to PB copolymer were 1:5 and 1:10, entrapment efficiencies of pazopanib in NPs were 85.6±9.05 and 92.9±7.9% respectively **(Table 5.2)**. It is possible that higher polymer content leads to enhanced hydrophobic interactions with pazopanib. This could be the explanation for higher entrapment of pazopanib in NPs with higher polymer content. The DL % was found to be 13.09±1.05 and 8.36±0.58% for pazopanib loaded NP batches 1:5 and 1:10 respectively.

Table 5.2: Characterization of pazopanib loaded PB copolymer NPs

Ratio of Drug:Polymer	**Entrapment Efficiency (%)**	**Drug Loading (%)**	**Particle Size (nm)**
1:5	85.6±9.05	13.09±1.05	423.5±15.9
1:10	92.9±7.9	8.36±0.58	514.2±10.3

***In Vitro* Release Studies**

Finally, we studied the release of pazopanib from NPs (ratio of pazopanib:PB 1:5). NPs demonstrated bi-phasic release profile i.e., initial burst release phase followed by a phase of sustained release **(Fig.5.8)**. Sustained release of pazopanib from nanoparticles was observed over ~100 days with minimal burst effect (≈ 7% in first 2 days). Releases of a drug molecule from PB nanoparticles involve various phases. Burst effect was observed due to initial release of drug adsorbed on the surface of nanoparticles. After this phase, drug is released from NPs by following a slower diffusion phase. Due to different rate of diffusion of pazopanib from NPs, variation in

drug release was observed. Pazopanib demonstrates slow release rate from NPs because of hydrophobicity and low crystallinity of PB copolymer. Therefore, PB copolymer NPs are valuable relative to existing PLGA-based and other TB polymers which show very high burst release **[520, 525]**. An advantage associated with this sustained release formulation (pazopanib loaded NPs) is higher residence time of drug molecule at the site of absorption. This sustained release profile of NPs will help in overcoming the flaws associated with current therapeutic regimen i.e. frequent intravitreal injection to maintain therapeutic levels at retina/choroid. Also, potential complications like endophthalmitis, retinal detachment, retinal hemorrhage, and patient non-compliance has been widely associated as adverse effects with frequent intravitreal injections. This approach will eventually eliminate the potential complications linked with current therapy and may lower cost of treatment.

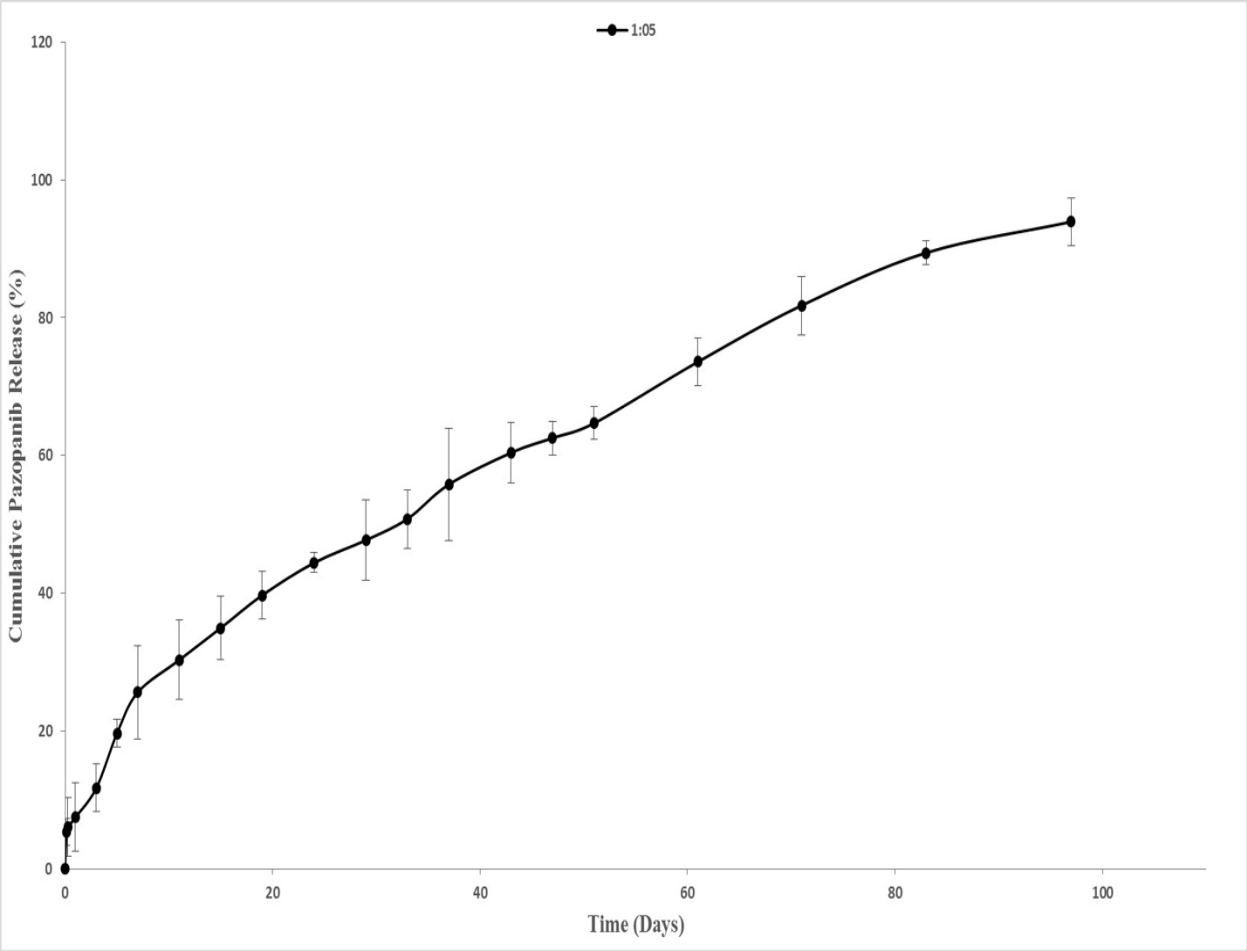

Fig.5.8: *In vitro* release of pazopanib from NPs prepared with PB copolymer

Drug Release Kinetics

Diffusion/degradation or a combination of diffusion and degradation mediated release phenomena is usually followed by drug released from NPs [526]. On fitting the data in in five different release kinetic models i.e., Korsmeyer-Peppas, Higuchi, Hixon-Crowell, zero-order and first-order (**Table 5.3)**, data was correlated well with Korsmeyer-Peppas with R^2 value of 0.9945. Also, n values in Korsmeyer-Peppas model for release of pazopanib from PB NPs were below 0.45 indicating controlled release diffussion (Fickian diffusion). These results suggests that drug release from PB NPs is controlled by diffusion of pazopanib from the NPs instead of degradation process of the PB copolymer.

Table 5.3: Coefficient of determination (R^2) for various kinetic models for *in vitro* release of pazopanib from PB copolymer NPs

	Korsmeyer-Peppas model		**Hixson-Crowell model**	**Higuchi Model**	**Zero Order**	**First order**	**Best Fit Model**
	R^2	n	R^2	R^2	R^2	R^2	
1:5	0.9945	0.4482	0.9785	0.9643	0.9488	0.9842	**Korsmeyer-Peppas model**

In Vitro Cellular Accumulation Studies

Intracellular accumulation of [^{3}H] digoxin was studied in MDCK-MDR1 overexpressing cells. On incubating the MDCK-MDR1 cells with GF 102918 (2µM) and pazopanib (0.1µM), enhanced intracellular accumulation of [^{3}H] digoxin by 2.1 and 1.5 fold respectively was observed. Further incubating the pazopanib NPs (containing pazopanib equivalent to 0.1µM), no effect on the intracellular accumulation of [^{3}H] digoxin was observed **(Fig.5.9)**. Similarly, intracellular accumulation of [^{3}H] abacavir was studied in MDCK-Bcrp1 overexpressing cells. Increased intracellular accumulation of [^{3}H] abacavir (5.2 and 3.5 fold) was observed on incubating the MDCK-Bcrp1 cells with GF 102918 (2µM) and pazopanib (0.1µM) respectively. On incubating the pazopanib NPs (containing pazopanib equivalent to 0.1µM), no effect on the intracellular accumulation of [^{3}H] abacavir was observed **(Fig.5.10)**. Presence of efflux transporters on corneal and retinal epithelial cells are known to limit the permeability fo drug across the ocular tissue [508]. These results confirms that pazopanib loaded polymeric PB copolymer NPs successfully prevent the P-gp and Bcrp1 mediated efflux of pazopanib. This evasion of drug efflux may help in achieving enhanced permeability and bioavailability of pazopanib across ocular tissue. The exact

mechanism by which these nanoparticles helps in evading efflux transporters needs to be fully explored.

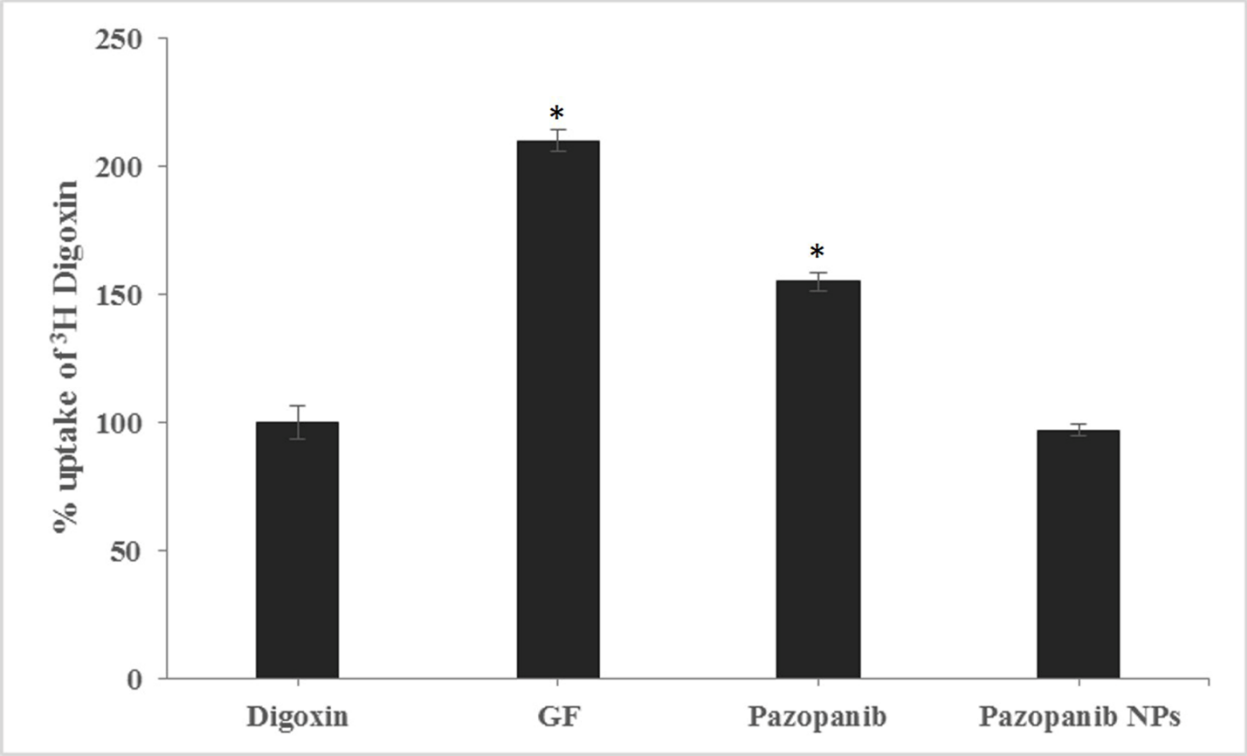

Fig.5.9: Intracellular accumulation of [^{3}H] digoxin in absence and presence of GF 102918 (2µM), pazopanib (0.1µM) and pazopanib NPs (containing pazopanib equivalent to 0.1µM) in MDCK-MDR1 cells. Results are expressed as mean±S.D. n = 4 (*$p < 0.05$)

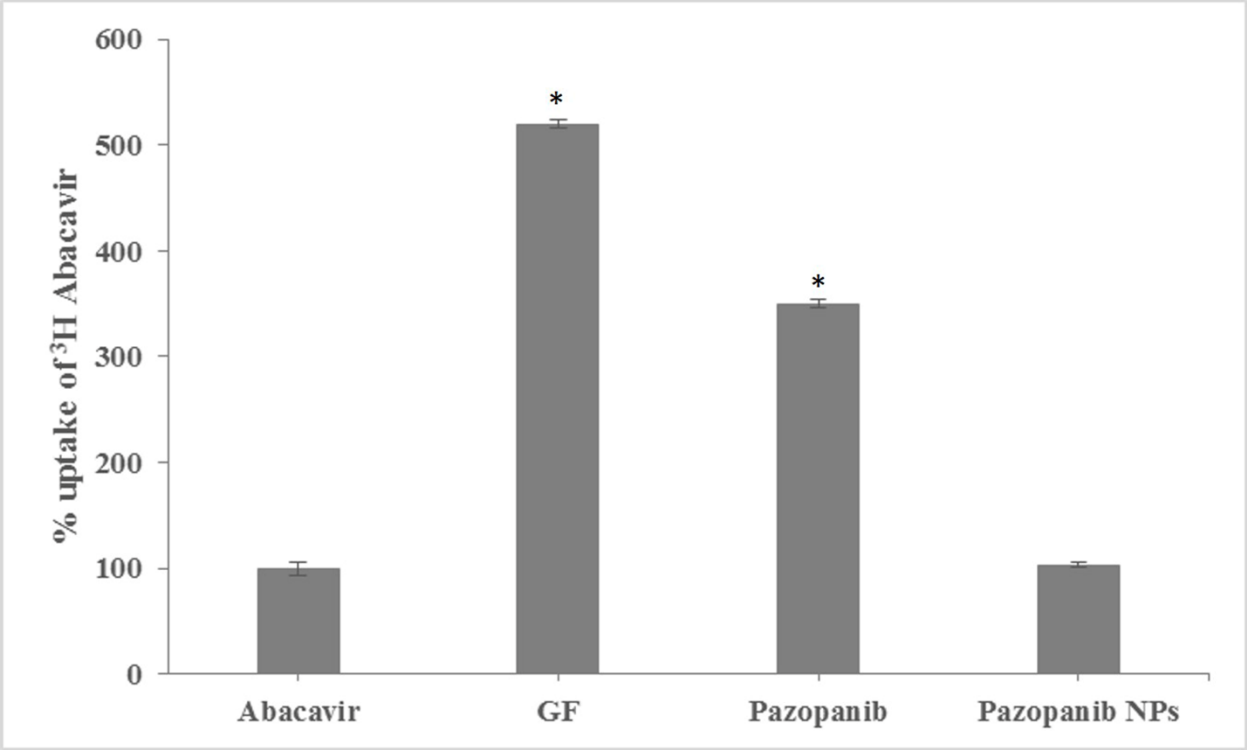

Fig.5.10: Intracellular accumulation of [^{3}H] abacavir in absence and presence of GF 102918 (2µM), pazopanib (0.1µM) and pazopanib NPs (containing pazopanib equivalent to 0.1µM) in MDCK-Bcrp1 cells. Results are expressed as mean±S.D. n = 4 (*$p < 0.05$)

Conclusion

We have successfully synthesized and characterized novel PB copolymer. These PB copolymers were studied for the development of pazopanib loaded NPs in the treatment of ocular neovascularization. Our results demonstrate that the synthesized PB polymers does not exhibit any cytotoxicity on ocular cell lines. Also, *in vitro* inflammatory studies confirmed that PB copolymer is an excellent biomaterial for the development of pazopanib loaded sustained delivery formulation for the treatment of ocular neovascularization. Pazopanib loaded PB NPs were successful in evading drug efflux. Nanoparticles prepared from PB copolymers had overcome the restrictions associated with existing PLGA or TB based copolymer NPs such as burst release effect and provided sustained release for longer duration. Novel PB copolymers are excellent biomaterials

and could serve as a vehicle not only for ocular drug delivery but also for other disorders where sustained levels of tyrosine kinase inhibitors is vital.

Acknowledgement

This work was supported by National Institutes of Health grant R01EY09171-16 and R01EY010659-14.

CHAPTER 6

FUNCTIONAL CHARACTERIZATION AND MOLECULAR IDENTIFICATION OF VITAMIN C TRANSPORTER (SVCT2) IN HUMAN CORNEAL EPITHELIAL (HCEC) AND RETINAL PIGMENT EPITHELIAL (D407) CELLS

Rationale

Ascorbic acid (AA, vitamin C) is an essential water-soluble vitamin required for various physiological and metabolic functions. It is a potent reducing agent that effectively quenches various reactive oxygen species (ROS), absorbs ultraviolet (UV) radiation and protects cornea, lens and other intraocular tissues against light-induced damage [458, 527]. Levels of antioxidant AA in aqueous humor plays an important role in the prevention of cataract. Human ocular tissues contain considerably higher amounts of ascorbic acid (1.33mg/g wet weight in corneal epithelium, 0.20mg/ml in aqueous humor, 23mg/100g in neural retina and 5mg/100mg in retinal pigment epithelium (RPE)/choroid) [458, 528]. Concentration of ascorbic acid in human tear fluid (23μM) is responsible for rapid wound healing and tear stability during ocular infections. Protective role of AA against various ocular infections and UV induced damage of ocular tissue suggests the need to scrutinize the mechanism of AA transport across ocular tissues (mainly, cornea and retina) [458].

Human and other primates cannot synthesize AA thus making this vitamin an essential dietary requirement. Therefore, AA is usually obtained from exogenous sources through the dietary intake [462]. AA uptake has already been reported in intestine [453], brain [457], kidney [454], skin [461], eye [458, 459] and bone [460] via specific transporter system. Human SLC23 family consists of two isoforms of sodium-dependent vitamin C transporters (SVCT) namely SVCT1 and SVCT2 [529]. Comparative analysis of two isoforms reveals that AA exhibits higher

affinity towards SVCT2 than SVCT1. Both SVCT1 and SVCT2 express close sequence homology and functional similarity but vary in distribution [458]. Structural and functional studies shows that transport of AA across various epithelial cells is mainly mediated via SVCT [458, 462].

In recent years, transporter targeted drug delivery has been widely employed to improve the drug absorption across biological membranes. In order to enhance drug permeation and absorption, active agent is chemically modified with transporter targeted moieties. Interaction between targeting moiety and the transporter will facilitate transport of conjugated drug across the cell membrane [437]. Many investigators have exploited SVCT2 as an important target for drug delivery across various membranes. AA conjugated saquinavir shows higher absorptive permeability and metabolic stability compared to saquinavir alone [530]. Conjugation of nipecotic, kynurenic and diclophenamic acids with AA has been utilized as an important tool in studying the mechanism of AA prodrugs interactions with vitamin C transporters across RPE cells. This approach has provided a new perspective for transporter/receptor targeted prodrug delivery by means of SVCT2 transporter system [531].

Hence, SVCT targeted drug delivery can be utilized as a vital strategy for enhancing intracellular accumulation of drugs in ocular complications. The aim of this study is to investigate the presence of a specialized carrier mediated transport system (SVCT2) across human corneal (HCEC) and retinal (D407) cells.

The presence of SVCT on rabbit cornea and Madin-Darby canine kidney cells has been previously reported from our laboratory [458, 462]. Variation in structural and biological properties between the rabbit and human eye suggest that the expression of transporters and receptors can highly differ. These anatomical and functional disparities among various species make it difficult to determine their impact on ocular drug absorption in human [438]. This

compelled us to study the practicality of human derived ocular cell lines as *in vitro* models for ocular drug absorption.

In the present study, we evaluated the ascorbic acid uptake process, kinetics as well as the expression, relative contribution, and regulation of the SVCT2 in HCEC and D407 cells. No information currently exists with regard to a comprehensive study of AA carrier mediated uptake across HCEC and D407 cells. Results obtained from this study may indicate involvement of a specific and high affinity carrier transport system (SVCT2) for translocation of AA.

Material And Methods

Materials

[^{14}C] Ascorbic acid ([^{14}C] AA specific activity 8.5 mCi/mM) was procured from Perkin Elmer (Boston, MA, USA). Unlabeled L-ascorbic acid, D-iso-ascorbic acid, dehydro-ascorbic acid (DHAA), glucose, para amino hippuric acid (PAHA), sodium azide, ouabain, 2,4-dinitrophenol, choline chloride, HEPES, bovine insulin, human epidermal growth factor, Triton X-100, phorbol-12-myristate-13-acetate (PMA), bisindolylmaleimide I (BIS), 3-isobutyl-1-methylxanthine (IBMX), 4,4'-di-isothiocyanatostilbene- 2,2'-disulphonic acid (DIDS), 4-acetamido-4'-isothiocyanostilbene-2,2'-disulfonic acid (SITC), and D-glucose were purchased from Sigma Chemical Co (St. Louis, MO, USA). Dulbecco's modified Eagle's medium (DMEM) and Dulbecco's Modified Eagle Medium: Nutrient Mixture F-12 (DMEM/F-12) were purchased from Invitrogen (Carlsbad, CA, USA). Fetal bovine serum (FBS) was obtained from Atlanta biologicals (Lawrenceville, GA, USA). Culture flasks (75 cm^2 growth area) and uptake plates (3.8 cm^2 growth area) were obtained from Corning Costar Corp. (Cambridge, MA, USA). The buffers for cDNA synthesis and amplification (oligodT, dNTP, MgCl2, M-MLV reverse transcriptase and Taq polymerase) were procured from Promega Corporation (Madison, WI, USA). Light Cycler 480®

SYBR I green master mix was obtained from Roche Applied Science (Indianapolis, IN, USA). Qualitative and quantitative primers used in the study were custom-designed and obtained from Invitrogen Life Technologies (Carlsbad, CA, USA). All other chemicals were obtained from Fisher Scientific Co. (Fair Lawn, NJ, USA) and utilized without further purification.

Cell Culture

HCEC and D407 cells were generous gifts from Dr.Araki-Sasaki (Kinki Central Hospital, Japan) and Dr.Richard Hunt (University or South Carolina, Columbia, SC, USA), respectively. HCEC cells were cultured according to previously published protocol [511, 512] [513]. Cells of passage numbers between 25 and 30 were cultured at 37°C, humidified 5% CO_2/95% air atmosphere in a DMEM/F-12 culture medium supplemented with 15% (v/v) FBS (heat inactivated), 15 mM HEPES, 22 mM $NaHCO_3$, 100 mg of penicillin and streptomycin each, 5 μg/ml insulin, and 10 ng/ml of human epidermal growth factor.

D407 cells (passage numbers between 75 and 80) were grown at 37°C, humidified 5% CO_2/95% air atmosphere in a DMEM culture medium supplemented with 10% (v/v) FBS (heat inactivated), 29 mM $NaHCO_3$, 20 mM HEPES, 100 mg of penicillin and streptomycin each, and 1% nonessential amino acids at pH 7.4 [514, 515]. The growth medium was changed every alternate day. Both HCEC and D407 cells were cultured in 75 cm^2 flasks, harvested at 80–90% confluency with TrypLE™ Express (Invitrogen, Carlsbad, CA, USA). Cells were then plated in 24-well uptake plates at a density of 300,000 cells/well. Cells were grown in a similar way as mentioned above and utilized for additional studies.

Uptake Studies

Confluent HCEC and D407 cells were utilized for uptake experiments. Following media removal, cells were rinsed thrice for 5 min each with 1–2 ml of Dulbecco's phosphate-buffered

saline (DPBS) containing 130 mM NaCl, 0.03 mM KCl, 7.5 mM Na_2HPO_4, 1.5 mM KH_2PO_4, 1 mM $CaCl_2$, 0.5 mM $MgSO_4$, 20 mM HEPES, and 5 mM glucose maintained at pH 7.4. Uptake studies were initiated by adding 250µl of solution containing 0.25 µCi/ml of [^{14}C] AA in the presence and absence of various competing substrates. Following incubation, the solution was removed and uptake was terminated with 2 ml of ice-cold stop solution containing 200 mM KCl and 2 mM HEPES. The cell monolayer was washed thrice, 5 min each and 1ml of lysis buffer (0.1% Triton-X solution in 0.3% NaOH) was added to each well and plates were stored overnight at room temperature. Subsequently, the cell lysate (400µl) from each well was transferred to scintillation vials containing 3 ml of scintillation cocktail (Fisher Scientific, Fairlawn, NJ, USA). Samples were quantified by measuring the radioactivity using liquid scintillation counter (Beckman Instruments Inc., Fullerton, CA, USA, model LS-6500). Protein content of each sample was estimated by BioRad Protein Estimation Kit (BioRad Protein Estimation Kit, Hercules, CA, USA).

Time And Temperature Dependency

Optimum time for [^{14}C] AA uptake was determined by performing the uptake studies over various time points (5, 10, 15, 30, 45 and 60 min). The uptake study was conducted according to previously published protocol [511-513].

The effect of temperature on [^{14}C] AA uptake was determined by carrying out the uptake study at different temperatures i.e. 4ºC, 25ºC and 37ºC.

pH And Ion Dependency

The effect of pH on [^{14}C] AA uptake was observed by adjusting the buffer pH to 5, 6, 6.5, 7.4 and 8. For delineating the role of sodium ions on [^{14}C] AA uptake, sodium chloride (NaCl) and sodium phosphate dibasic (Na_2HPO_4) in DPBS were substituted with equimolar quantities of

choline chloride and potassium phosphate dibasic (KH_2PO_4), respectively. Hill coefficient for AA uptake, as function of Na^+ was determined. In a similar way, buffer solution containing sodium (130 mM), potassium (0.03 mM), and calcium (1 mM) chlorides were replaced with equimolar quantities of sodium phosphate, potassium phosphate, and calcium acetate, respectively.

In another study, cells were pre-incubated with 1 mM amiloride (sodium channel inhibitor) and the uptake study was carried out as mentioned earlier.

Concentration Dependency

Several working concentrations of L-AA were prepared ranging from (0.12µM - 1000µM) in DPBS (pH 7.4) spiked with [^{14}C] AA (0.25µCi/ml). The data was fitted to Michaelis -Menten equation and the maximum transport rate (V_{max}) and Michaelis-Menten constant (K_m) were calculated according to nonlinear least squares regression analysis program; GraphPad Prism version 5.

Role Of Metabolic And Membrane Transport Inhibitors

For energy dependency, simultaneous incubation of [^{14}C] AA along with metabolic inhibitors such as ouabain (Na^+/K^+ ATPase inhibitor), 2,4-dinitrophenol (intracellular ATP reducer) and sodium azide (oxidative phosphorylation inhibitor) was performed for 1h. In order to examine the effect of anionic membrane transport inhibitors, cells were pre-incubated with 1mM SITC, DIDS and probenecid for 1h.

Substrate Specificity

The substrate specificity for SVCT was delineated by carrying out [^{14}C] AA uptake in the presence of three different concentrations of (250, 500 and 1000µM) unlabeled L-AA and structural analogs such as D-Iso AA and DHAA. A similar study was carried out at three different

concentrations of (250, 500 and 1000µM) various structurally unrelated analogs such as glucose (Glucose transporter/GLUT substrate) and PAHA (organic anion transporter/OAT substrate).

Intracellular Regulation

The influence of various intracellular regulatory pathways such as Ca^{++}/calmodulin, PTK (protein tyrosine kinase), PKC (protein kinase C) and PKA (protein kinase A) pathway on [^{14}C] AA uptake was also investigated. Cells were pre-incubated with three different concentrations of modulators such as calmidazolium (CaM) and KN-62 to delineate if the process is dependent on Ca^{++}/calmodulin pathway or not. In order to examine the role of PTK pathway in [^{14}C] AA uptake, cells were pre-incubated with three different concentrations of genistin and tyrphostin A25. For studying the effect of PKC pathway, cells were pre-incubated with three different concentrations of BIS and PMA. The effect of PKA pathway was studied by incubating cells with three different concentrations of IBMX and forskolin. Uptake of [^{14}C] AA was then performed according to the procedure.

Reverse Transcription–Polymerase Chain Reaction

Reverse transcription– polymerase chain reaction (RT-PCR) analysis was employed to determine the expression of SVCT2 on HCEC and D407 at the molecular level. TRIzol® reagent (Invitrogen, USA) was used to carry out the cell lysis and chloroform was added to the lysate for phase separation. Following separation of aqueous phase containing RNA, isopropanol was added to precipitate RNA. Obtained RNA was rinsed twice with 75% ethanol followed by resuspension in RNase-DNase free water. The concentration and purity of RNA was determined using Nanodrop (Thermo Fisher Scientific, Wilmington, DE, USA). RNA was reverse-transcribed to obtain cDNA using oligodT as a template and M-MLV reverse transcriptase. The conditions for reverse transcription were: denaturation of the template RNA for 5 min at 70°C; reverse transcription for

60 min at 42°C followed by final extension at 72°C for 5 min. cDNA obtained was then subjected to PCR for amplification of SVCT with specific primers. The primers (5′→3′) designed for SVCT2 were: forward: CCAGCGGTGAGCAGGACAAT, reverse primer: TAGGGCCACCGTGGGTGTAA. These primers correspond to a 626 base pair (bp) product in human SVCT2 cDNA. The conditions of PCR amplification were: denaturation for 30 s at 94°C, annealing for 1 min at 56°C, and extension for 1 min at 72°C, for 45 cycles followed by a final extension for 5 min at 72°C. PCR product was analyzed by gel electrophoresis on 1.5% agarose in TAE buffer and visualized under UV [438].

Quantitative Real-Time PCR

Following reverse transcription, quantitative real-time PCR (qPCR) was performed with LightCycler® SYBR green technology (Roche). cDNA equivalent to 80 ng in each well was subjected to amplification with specific primers. Glyceraldehyde-3-phosphate dehydrogenase (GAPDH) was selected as an internal control to normalize the amount of cDNA in each well. The sequences of real-time primers (5′→3′) used for SVCT2 were: forward: CCAGCGGTGAGCAGGACAAT, reverse primer: TAGGGCCACCGTGGGTGTAA, GAPDH: forward—ATCCCTCCAAAATCAAGTGG and reverse—GTTGTCATGGATGACCTTGG. A preliminary experiment was performed to ensure that SVCT2 and GAPDH were amplified with equal efficiencies. The specificity of these primers was also confirmed with melting-curve analysis. The comparative threshold method was applied to calculate the relative amount of SVCT2 in HCEC and D407 cells [438, 532].

Data Analysis

Radioactive Sample Analysis

Uptake of [^{14}C] AA was calculated using disintegrations per minute (DPM) of sample and donor solutions as represented in Eq. 1

$$\boldsymbol{Csample = \frac{DPMsample * Cdonor}{DPMdonor}} \quad \textbf{Eq. 1}$$

DPM_{sample} and DPM_{donor} represent average values of DPM counts of sample and donor respectively (n=4); C_{donor} denotes concentration of donor used and C_{sample} represents the concentration of sample.

Calculation Of Michaelis-Menten Kinetic Parameters

In order to determine K_m and V_{max} associated with [^{14}C] AA uptake, concentration-dependency data was fitted to a modified Michaelis–Menten equation (Eq.2)

$$\boldsymbol{v = \frac{Vmax[C]}{Km + [C]} + Kd[C]} \quad \textbf{Eq. 2}$$

v represents the total uptake, V_{max} stands for the maximum uptake rate for the carrier-mediated process, K_m is Michaelis–Menten constant which represents the concentration at half saturation, K_d is a non-saturable diffusion rate constant and C is substrate concentration. In Eq. (2), (V_{max}*C)/(K_m+C) represents carrier mediated saturable process whereas K_d(C) gives the non-saturable diffusion component. Data was fitted to a non-linear least-square regression analysis program (GraphPad Prism 5.0). Michaelis Menten kinetic parameters were calculated to determine saturable and non-saturable component of the total uptake.

Calculation Of Hill Ratio

Na^+:L-Ascorbic acid coupling ratio was determined using the logarithmic form of the Hill equation (Eq. 3)

$$Log\left[\frac{v'}{Vmax} - v'\right] = nlog(S) - logK' \qquad \textbf{Eq. 3}$$

v' denotes initial velocity, V_{max} represents the maximal velocity, n is number of substrate binding sites, S denotes the substrate concentration, and K' is a constant comprising multiple interaction factors and intrinsic dissociation constant.

Statistical Analysis

All the experiments were conducted at least in quadruplicate (n=4) and the outcomes were expressed as mean±standard deviation (SD). To calculate statistical significance, student's t test was performed. Any difference between mean values is considered statistically significant for P value ≤0.05.

Results

Time And Temperature Dependency

Time dependent uptake of [^{14}C] AA (29.4µM) in HCEC and D407 cells is depicted in **Fig.6.1.** Linear uptake of [^{14}C] AA was noticed upto 60 min of incubation period. Therefore, 30 min uptake time was selected for further uptake experiments.

Effect of temperature on the uptake of AA by HCEC and D407 cells was studied. **Fig.6.2** clearly depicts that the uptake of [^{14}C] AA in HCEC and D407 cells was maximal at 37 °C. Uptake of [^{14}C] AA in HCEC shows 45% and 80% decrease when the temperature was reduced to 25°C and 4°C respectively. In D407 cells, uptake was reduced to 60% and 20% when measured at 25°C and 4°C respectively, suggesting that the process may be carrier mediated in both cell lines. Activation energy (E_a) was calculated by plotting the temperature dependent data i.e. Uptake rate Ln(v) vs. 1/T **(Fig.6.3)** E_a was calculated to be 7.80 kcal/mol and 7.23 kcal/mol in HCEC and D407 cells respectively.

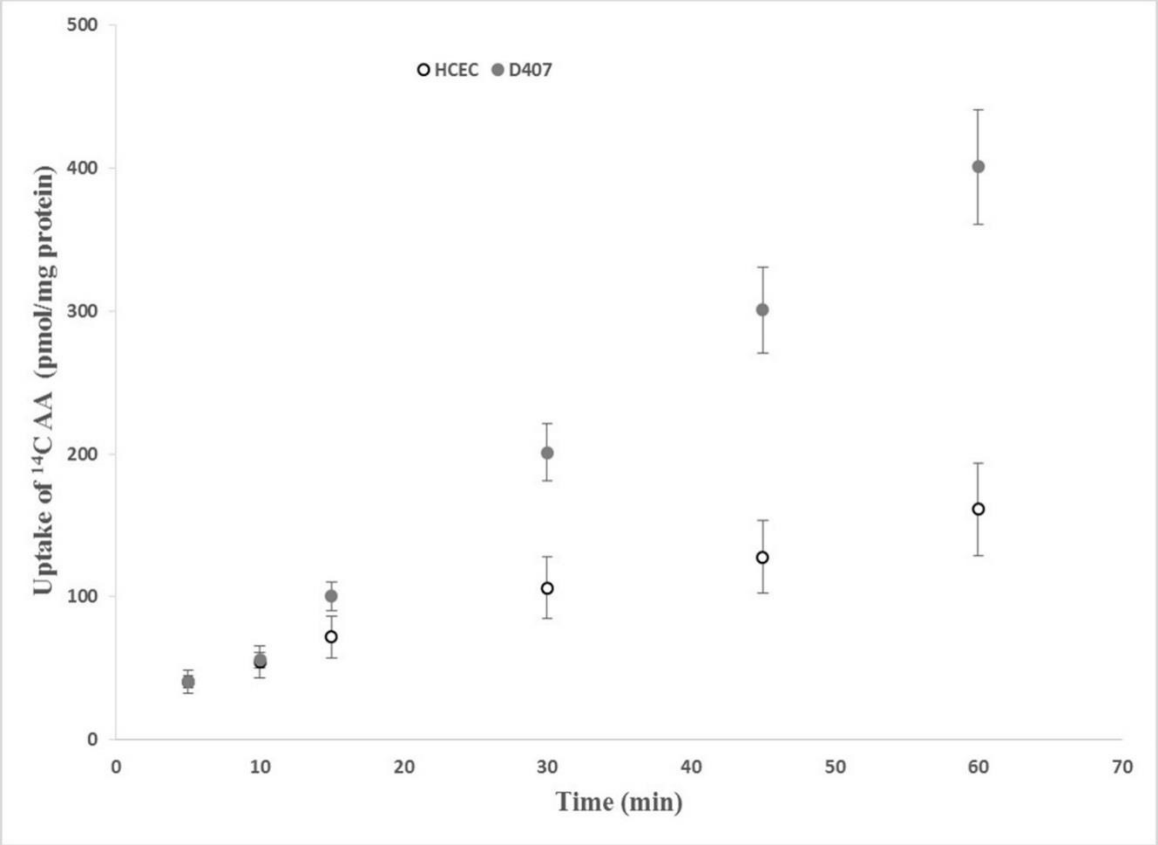

Fig.6.1: Time course of [^{14}C] AA uptake across HCEC and D407 cells. Uptake of [^{14}C] ascorbic acid ([^{14}C] AA) was measured in DPBS buffer (pH 7.4) at 37ºC. Data is shown as mean±S.D. n=4. S.D. means standard derivation.

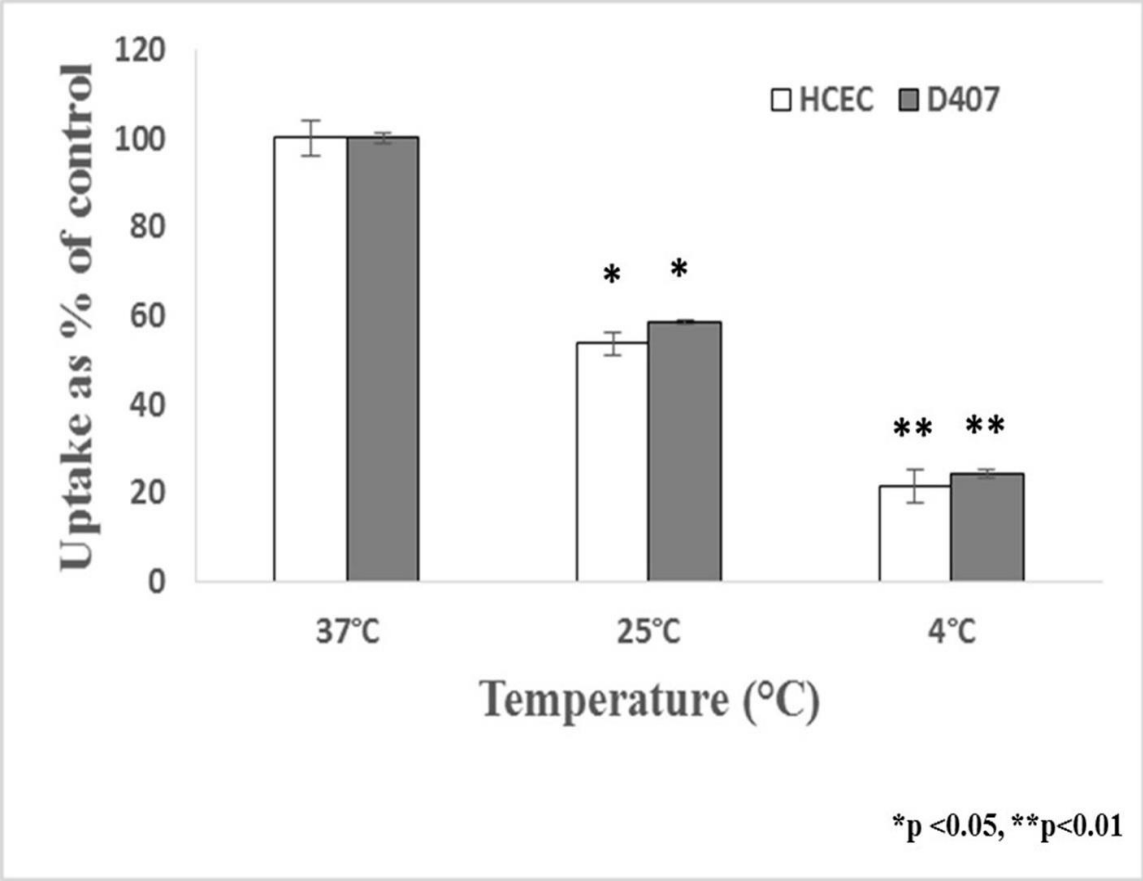

Fig.6.2: Temperature dependent uptake study of [^{14}C] AA uptake across HCEC and D407 cells in DPBS (pH 7.4). The uptake is expressed as percentage of control (37°C). Data is shown as mean±S.D. n=4. Asterisk (*) represents significant difference from the control (*p<0.05, **p<0.01).

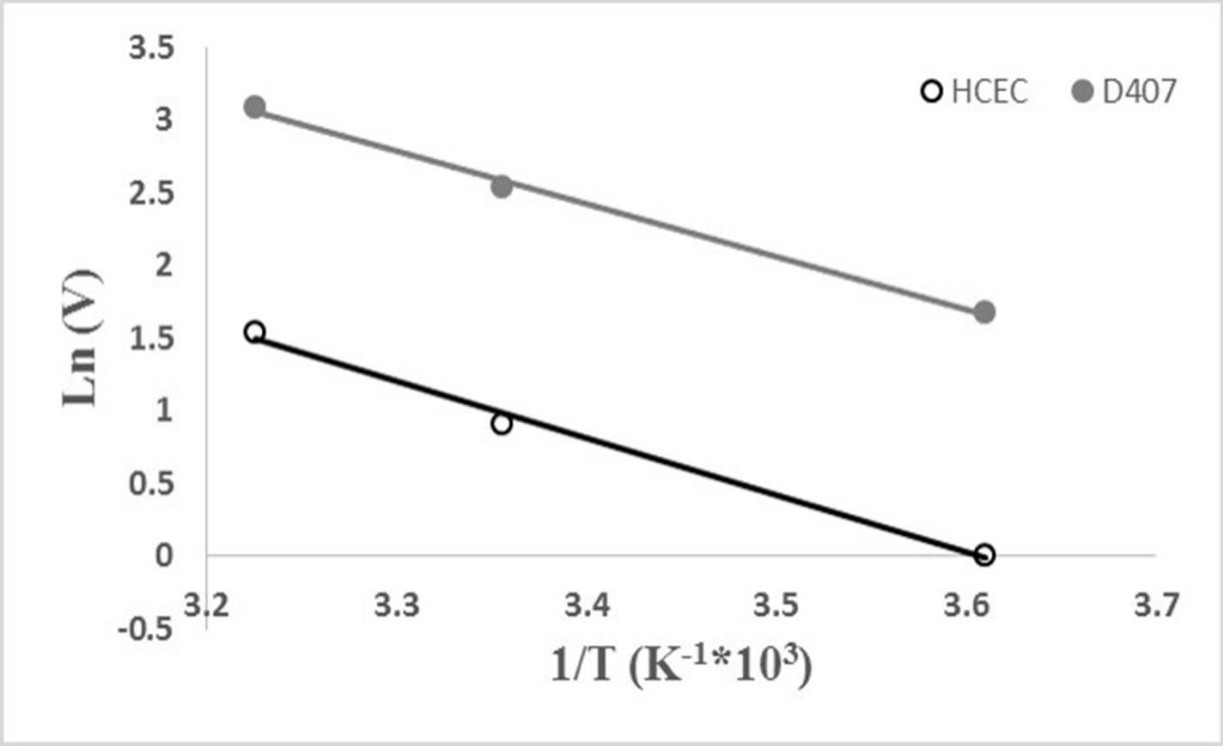

Fig.6.3: Arrhenius plot of the effect of temperature on [^{14}C] AA uptake across HCEC and D407 cells. Uptake of [^{14}C] AA was measured in DPBS buffer (pH 7.4) for 30min at 37, 25 and 4°C, across HCEC and D407 cells. Data is shown as mean±S.D. n=4

pH And Ion Dependency

In order to determine the role of an inward driven proton gradient for [^{14}C] AA uptake, the study was carried out at different pH ranging from 5-8 in HCEC and D407 cells. Uptake of [^{14}C] AA elevated with a rise in extracellular pH from 5 to 8 in both cell lines. Relative to pH 7.4, uptake of [^{14}C] AA diminshed to 40% and 50% at pH 5 and 6 respectively in HCEC and D407 cells **(Fig.6.4)**. Based on these results, further uptake studies were carried out at pH 7.4 with both the cell lines.

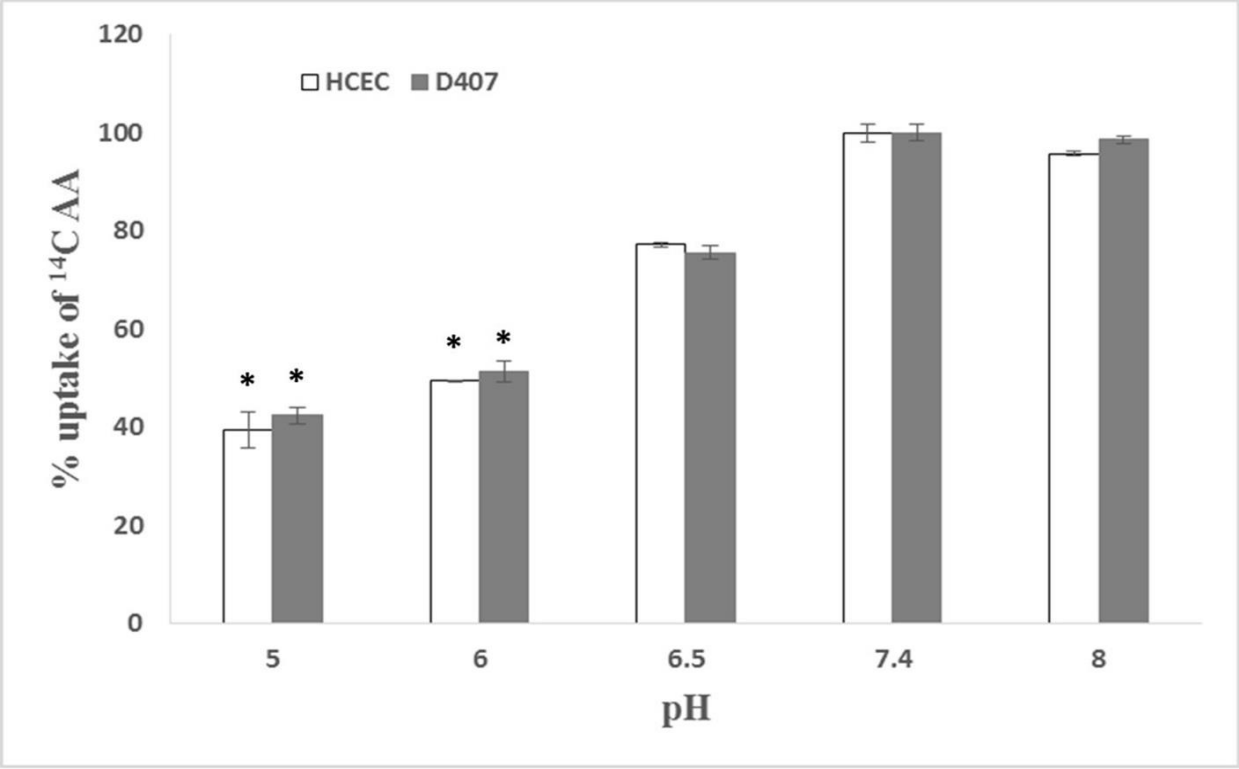

Fig.6.4: Effect of pH on [^{14}C] AA uptake across HCEC and D407cells. Uptake of [^{14}C] AA was determined in the presence of different pH (5.0, 6.0, 6.5, 7.4 and 8.0) at 37°C for 30 min across HCEC and D407 cells. The uptake is expressed as percentage of control (pH 7.4). Data is shown as mean±S.D. n=4. (*p<0.05, **p<0.01).

Uptake of [^{14}C] AA was reduced to 35% and 50% respectively, in HCEC and D407 cells, in the presence of sodium-free media. Similarly uptake of AA was also diminished to 50% and 60% in HCEC and D407 cells, in the presence of amiloride (Na^+ transport inhibitor) indicating possible involvement of sodium ions in the translocation of AA **(Fig.6.5).**

The effect of chloride ions was studied by replacing chloride ions with equimolar quantities of other monovalent cations in DPBS. A marked reduction (40% and 45%) in the uptake rate of [^{14}C] AA was observed in the absence of chloride ions in HCEC and D407 cells respectively. This

study clearly delineates the involvement of sodium and chloride ions in active transport of AA **(Fig.6.5).**

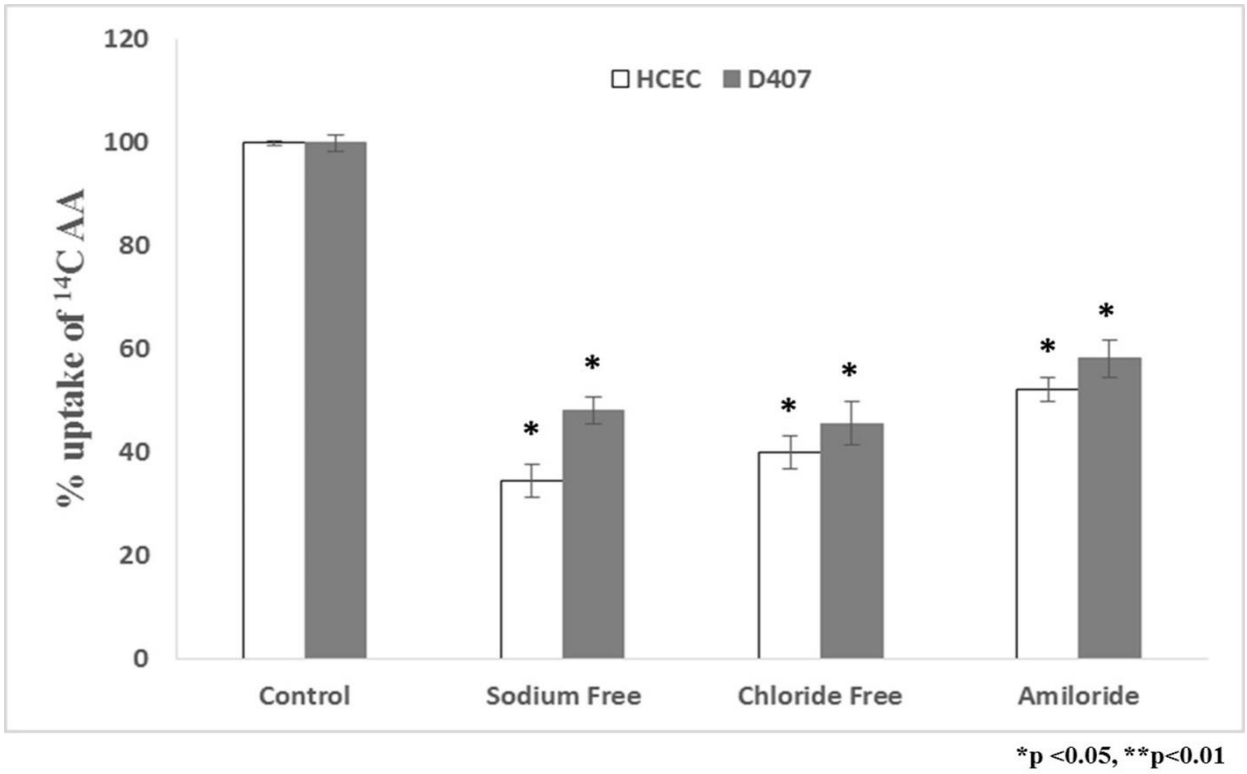

Fig.6.5: Uptake of [^{14}C] AA across HCEC and D407 cells in the presence of amiloride and absence of sodium and chloride ions in DPBS buffer (pH 7.4) at 37°C. (*p<0.05, **p<0.01).

Kinetics of AA in HCEC and D407 cells were also evaluated with various concentrations of sodium (0-140mM) in the DPBS. Elevated uptake of [^{14}C] AA was observed with higher Na^+ concentrations. Uptake data demonstrated saturation kinetics displaying the saturation of [^{14}C] AA uptake at about 70 mM of Na^+ concentration in both HCEC and D407 cells **(Fig.6.6)**. Hill transformation of the Na^+ saturation kinetics data showed 2:1 molar ratio of Na^+:AA coupling in both cell lines **(Fig.6.7).**

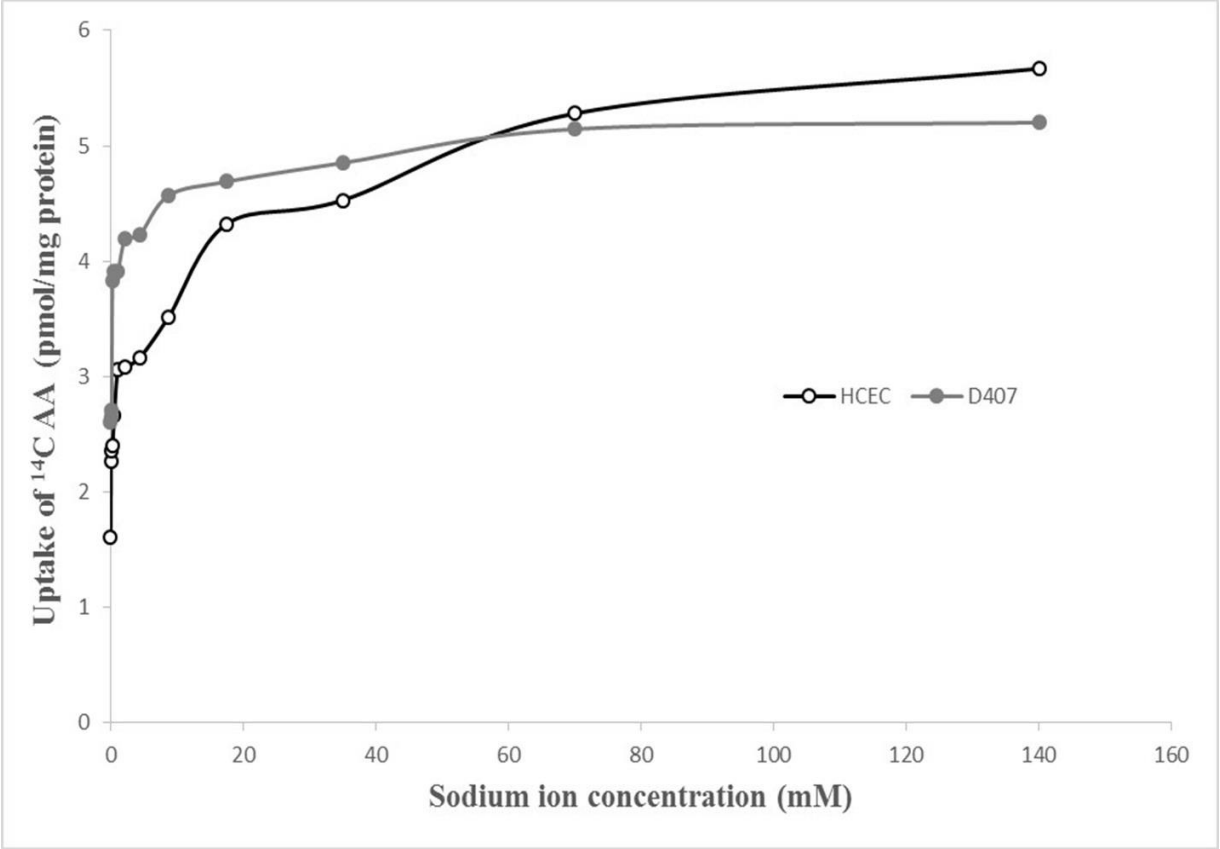

Fig.6.6: Uptake of [^{14}C] AA across HCEC and D407 cells as a function of sodium concentration in DPBS (pH 7.4) at 37°C. Data is shown as mean±S.D. n=4.

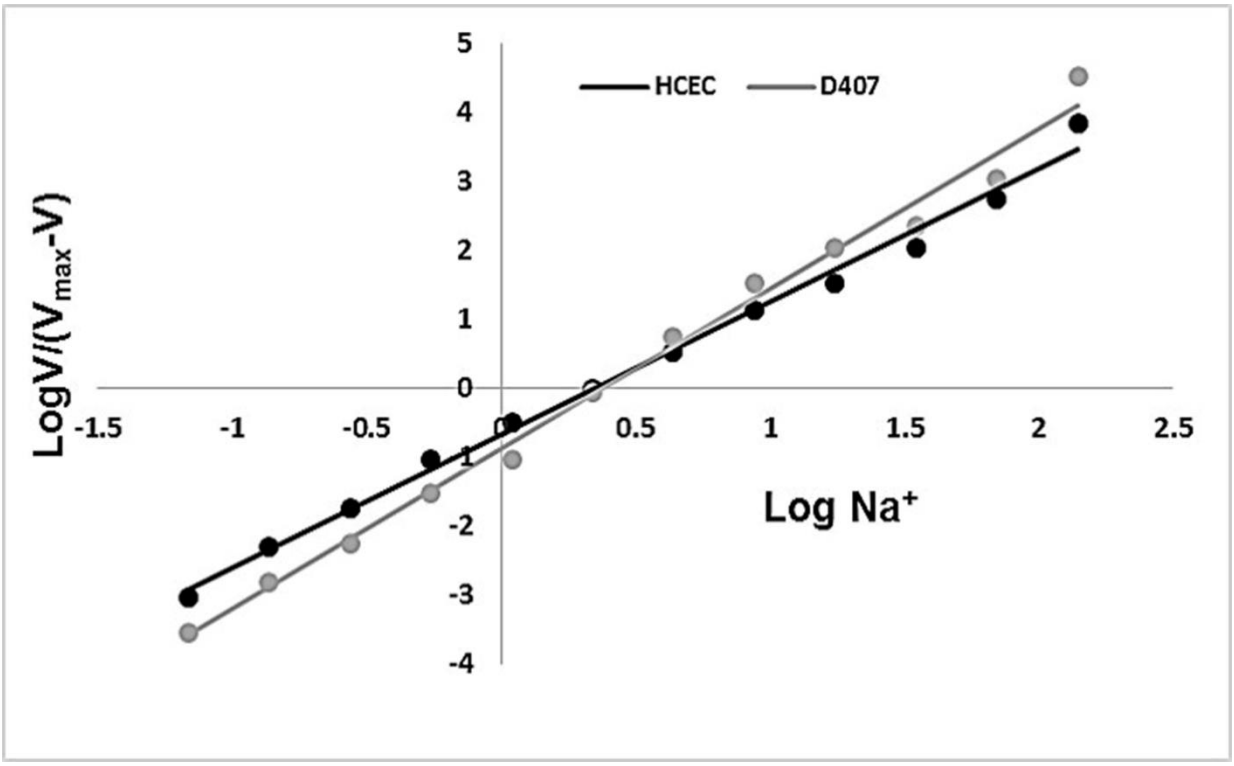

Fig.6.7: Hill plot of sodium-dependent uptake of [^{14}C] AA across HCEC and D407 cells.

Concentration Dependency

Michaelis Menten saturation kinetics of AA uptake were investigated by incubating HCEC and D407 cells with various concentrations (0.12-1000µM) of unlabeled AA for 30 min at 37°C. The uptake process involves both the saturable carrier mediated pathway and non-saturable diffusional process in both HCEC and D407 cells.

Uptake study performed at 4°C clearly delineated the passive diffusion component from the AA transport in both HCEC and D407 cells. The carrier mediated process of AA uptake in both the cell lines was plotted as the difference of total uptake of AA at 37°C and passive uptake of AA at 4°C. Uptake of [^{14}C] AA in HCEC cells was found to be concentration-dependent and saturable with K_m and V_{max} values of 46.14±6.03 µM and 17.34±0.58 pmol/mg protein/min, respectively **(Fig.6.8 and Table 6.1).**

The kinetic parameters (K_m and V_{max}) estimated for D407 cells were higher than those observed with HCEC, although similar saturation kinetics plot was observed in D407 cells. The K_m and V_{max} values obtained from the saturation kinetics plot for D407 cells were 47.26±3.24 μM and 31.86±0.56 pmol/mg protein/min, respectively **(Fig.6.9 and Table 6.1).**

Lineweaver-Burk (1/v vs. 1/[S]) plot, indicate the involvement of a single carrier in the uptake process of AA across HCEC and D407 cell lines **(Fig.6.10)**.

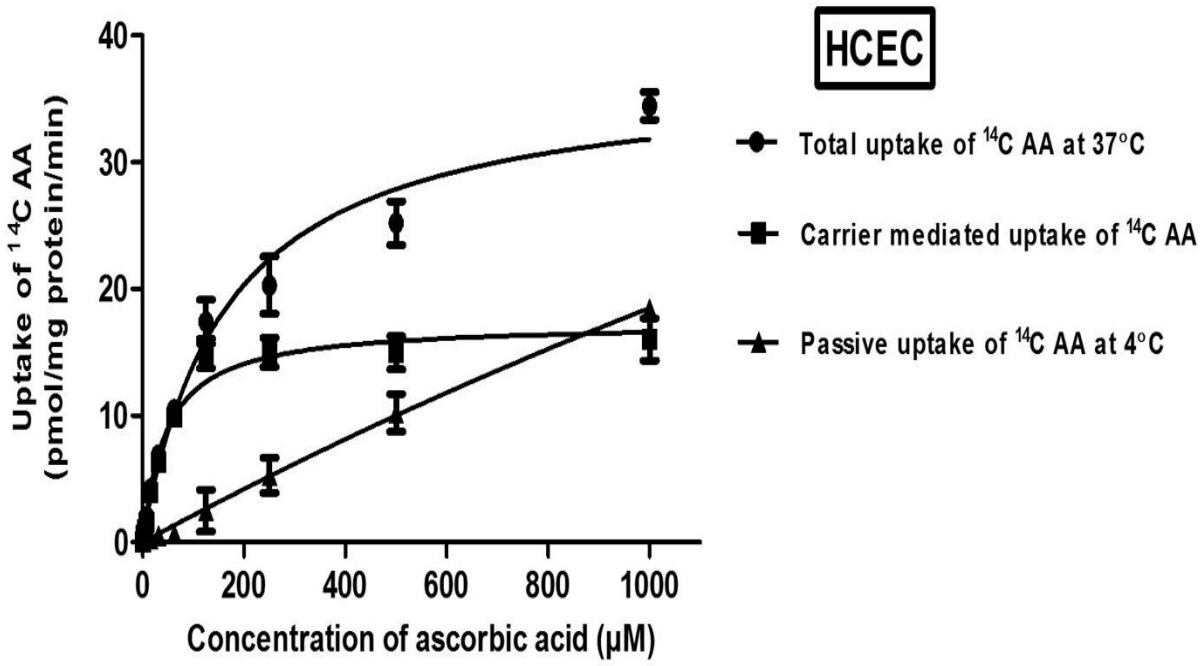

Fig.6.8: Concentration-dependent uptake of [^{14}C] AA across HCEC cells. Data is shown as mean±S.D. n=4 (● represents total uptake, ▲ represents passive uptake/non-saturable component and ■ represents carrier mediated uptake/saturable component)

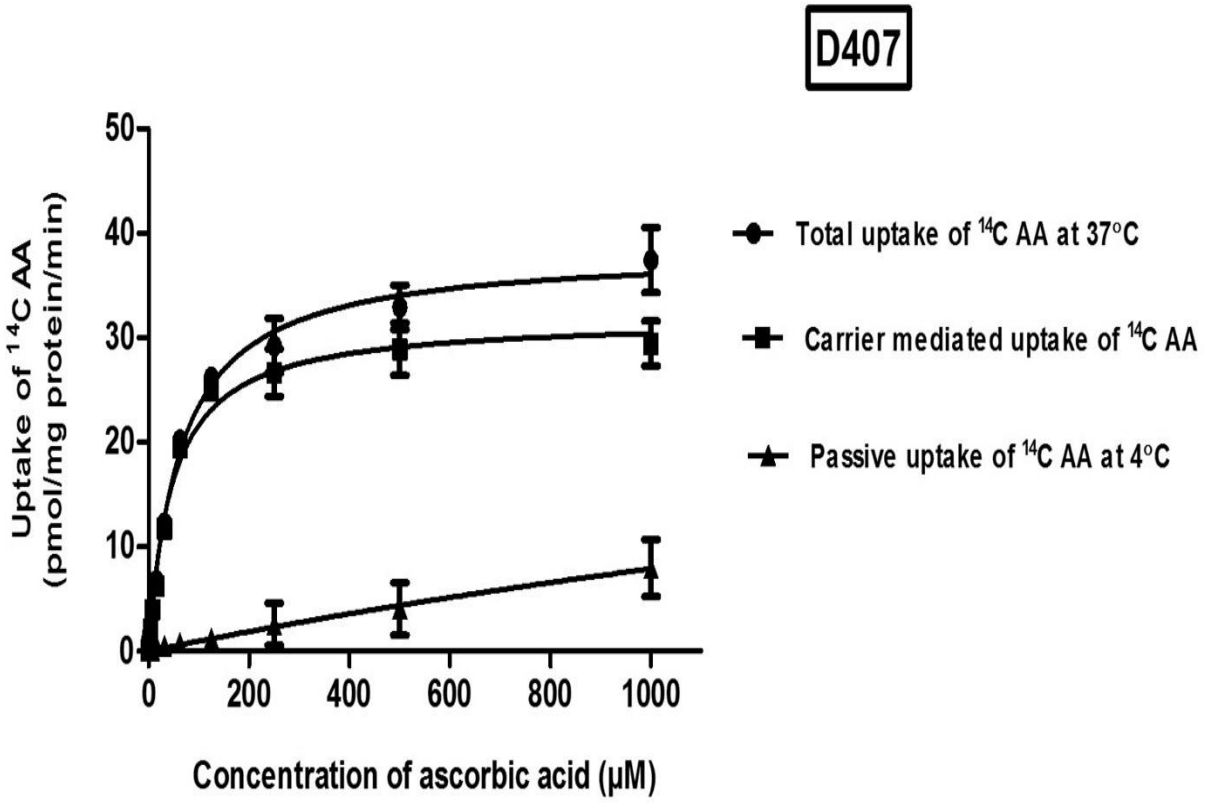

Fig.6.9: Concentration-dependent uptake of [^{14}C] AA across D407 cells. Data is shown as mean±S.D. n=4 (● represents total uptake, ▲ represents passive uptake/non-saturable component and ■ represents carrier mediated uptake/saturable component)

Table 6.1: Michaelis–Menten kinetic parameters (V_{max} and K_m) and catalytic efficiency (V_{max}/K_m) estimated for SVCT2 transporter system in HCEC and D407 cell lines. Units of K_m: micromolar (µM), V_{max}: pmoles/mg protein/min and V_{max}/K_m: µl/mg protein/min.

Kinetic Parameters of SVCT2	**HCEC**	**D407**
K_m	46.14±6.03	47.26±3.24
V_{max}	17.34±0.58	31.86±0.56
V_{max}/K_m	0.37	0.67

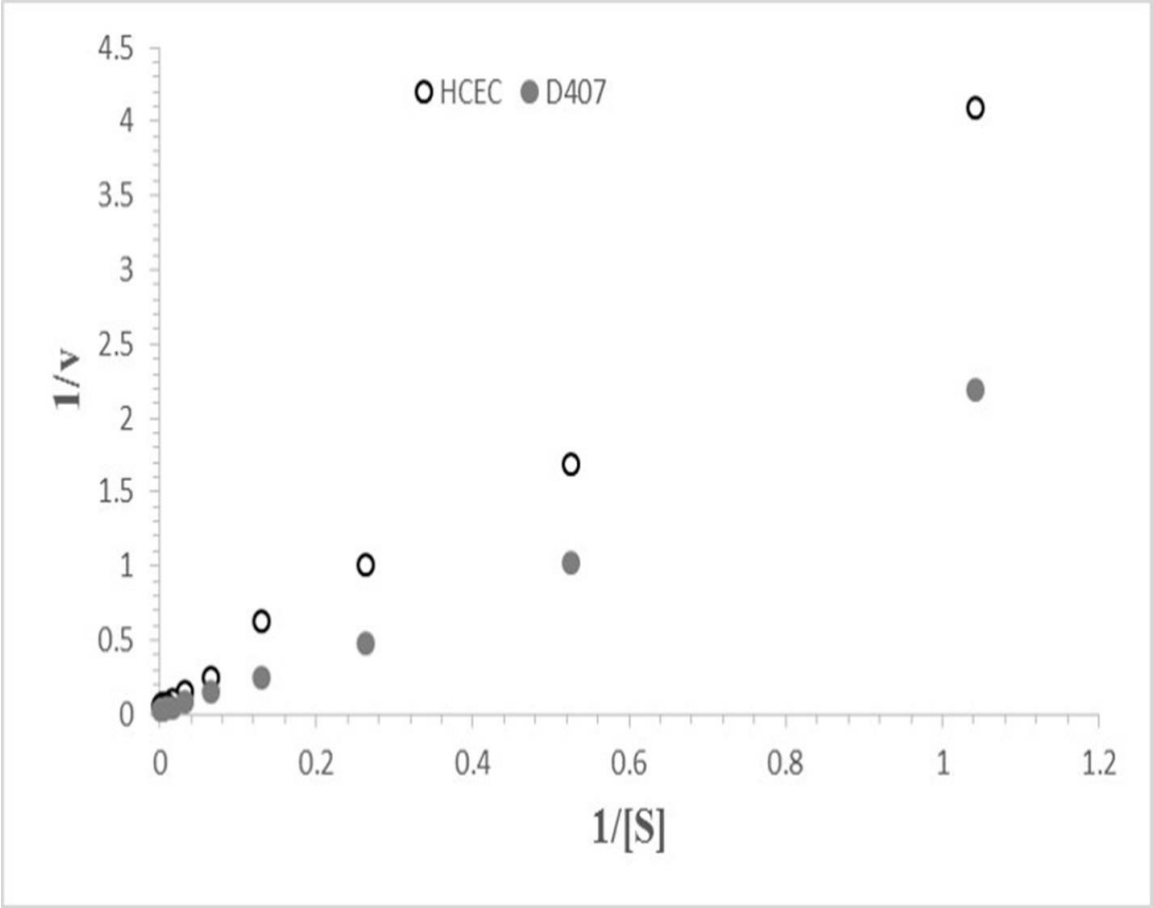

Fig.6.10: Lineweaver–Burk transformation of the data demonstrated involvement of a single carrier mediated process for the uptake of [^{14}C] AA across HCEC and D407 cells.

Role Of Metabolic And Membrane Transport Inhibitors

In order to delineate the effect of metabolic inhibitors on [^{14}C] AA uptake in both HCEC and D407 cells, uptake studies were carried out in the presence of metabolic inhibitors such as ouabain (Na^+/K^+ ATPase inhibitor), sodium azide (oxidative phosphorylation inhibitor), and 2,4-DNP (intracellular ATP reducer). In the presence of these metabolic inhibitors, a significant reduction (40 to 60%) in the uptake of [^{14}C] AA was observed **(Fig 6.11)**.

Further investigations were carried out in HCEC and D407 cells to investigate the effect of membrane inhibitors (SITC, DIDS and probenecid) on [^{14}C] AA uptake. AA uptake was reduced

to 40% in the presence of SITC, DIDS and probenecid, showing the involvement of an anion exchanger in carrier mediated transport of [^{14}C] AA **(Fig.6.12)**.

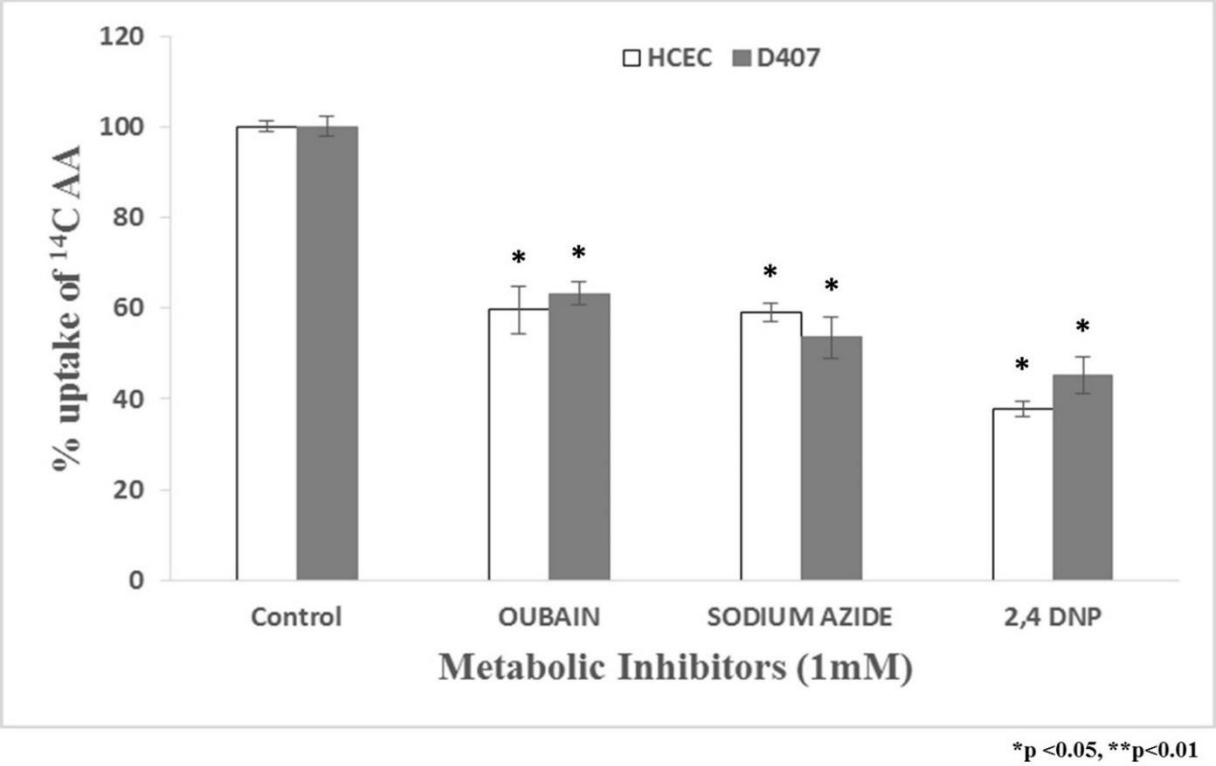

Fig.6.11: Uptake of [^{14}C] AA across HCEC and D407 cells in the presence of 1 mM concentrations of metabolic inhibitors: ouabain, sodium azide, and 2,4-DNP. [^{14}C] AA uptake was performed at 37°C with DPBS buffer (pH 7.4) for 30 min. Data is shown as mean±S.D. n=4. (*p<0.05, **p<0.01).

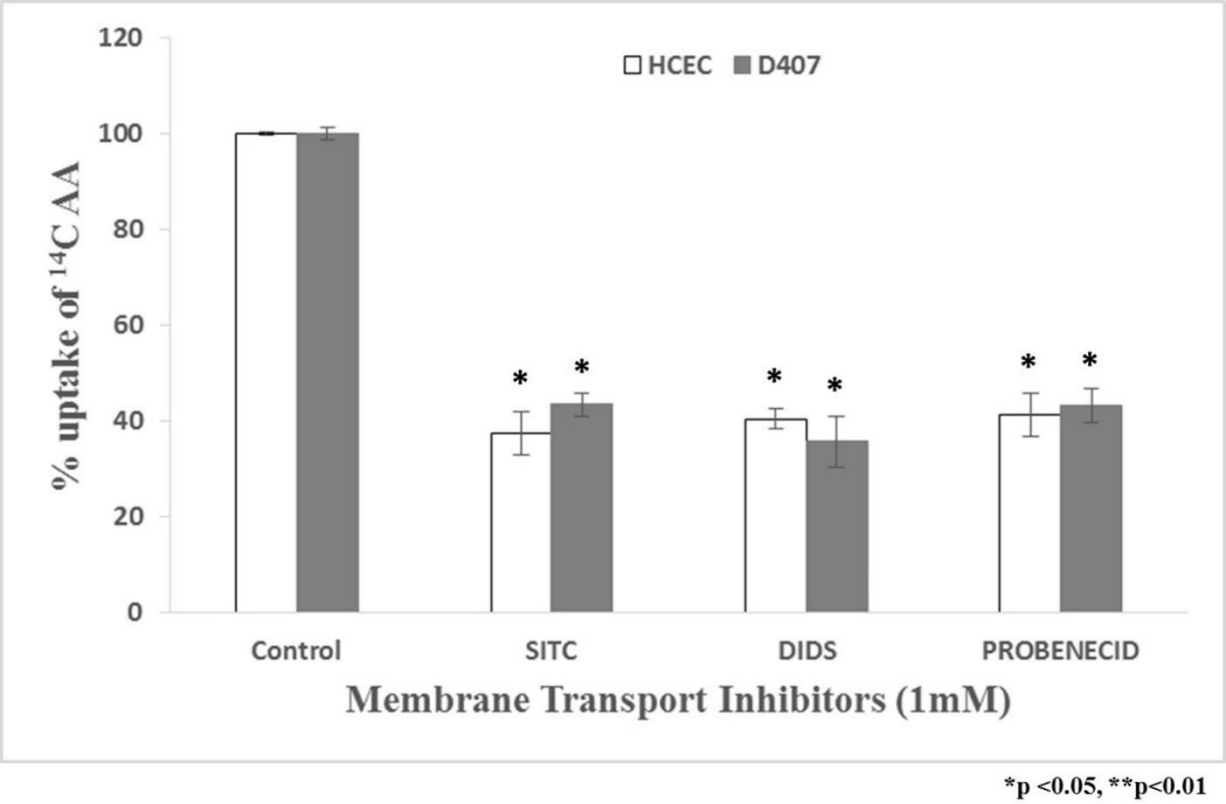

Fig.6.12. Uptake of [^{14}C] AA across HCEC and D407 cells in the presence of 1 mM concentrations of membrane inhibitors: SITC, DIDS and probenecid. [^{14}C] AA uptake was performed at 37°C with DPBS buffer (pH 7.4) for 30 min. Data is shown as mean±S.D. n=4. (*p<0.05, **p<0.01).

Substrate Specificity

With increasing concentration (250, 500 and 1000 µM) of AA structural analogs, [^{14}C] AA uptake in HCEC and D407 cells was significantly inhibited in the presence of L-AA and D-Iso AA whereas no significant change in the uptake of [^{14}C] AA was observed in DHAA. Also, no significant change in the uptake of [^{14}C] AA was observed in the presence of structurally unrelated analogs i.e. glucose and PAHA (250, 500 and 1000 µM) in both the cell lines **(Fig.6.13)**.

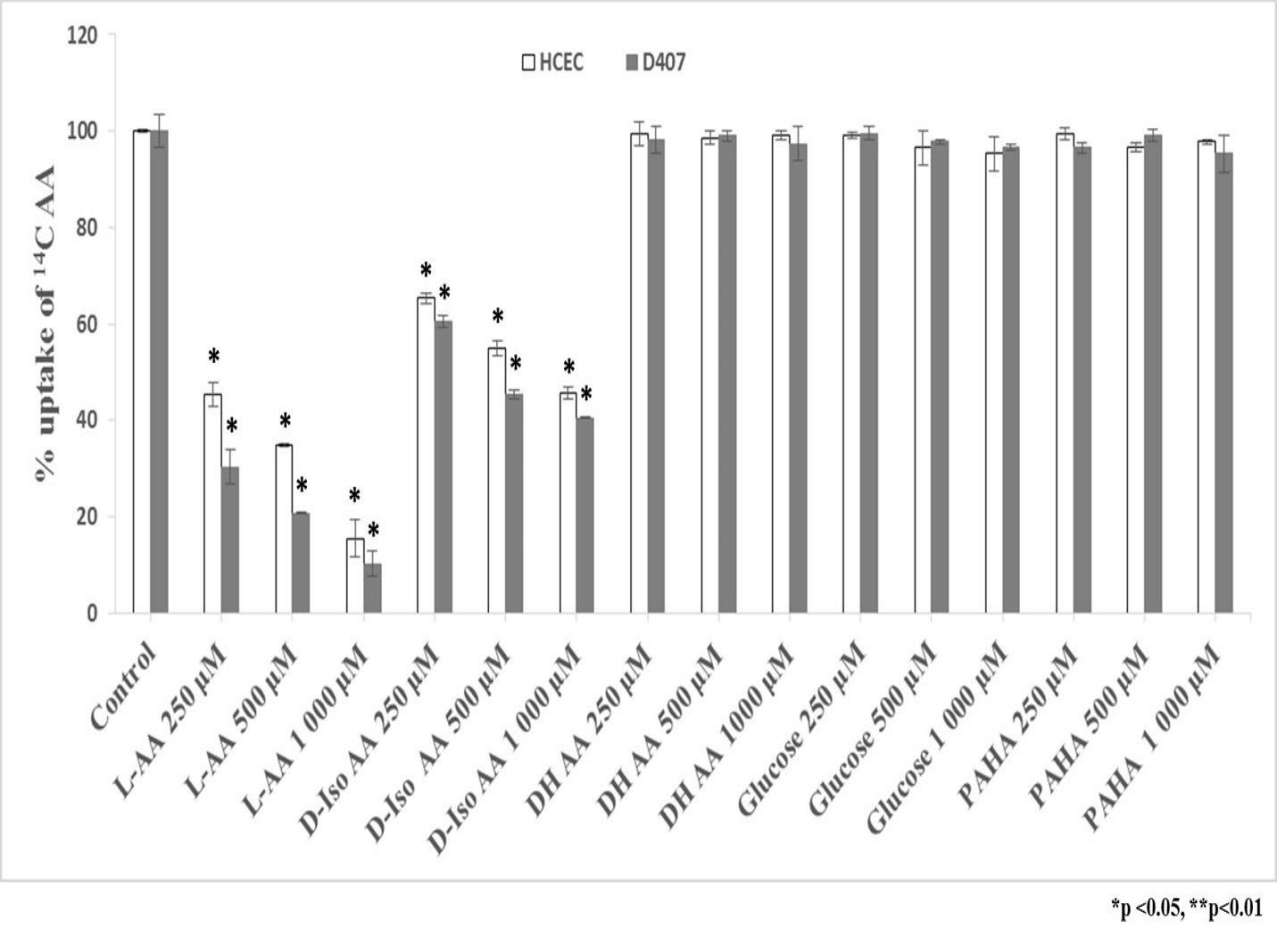

Fig.6.13. Uptake of [^{14}C] AA in presence of L-ascorbic acid (L-AA), D-isoascorbic acid (D-Iso AA), dehydro ascorbic acid (DHAA), D-glucose, and para-amino hippuric acid (PAHA) at three different concentrations across HCEC and D407 Cells. [^{14}C] AA uptake was performed at 37°C with DPBS buffer (pH 7.4) for 30 min. Data is shown as mean±S.D. n=4. (*p<0.05, **p<0.01).

Intracellular Regulation

The role of different cellular regulation pathways on [^{14}C] AA uptake was also investigated. With increasing concentrations of calmidazolium and KN-62 (modulators of Ca^{++}/calmodium (Ca^{++}/CaM) pathway), reduced uptake of [^{14}C] AA ranging from 25-41% and 27-41% respectively in HCEC, and, 20-47% and 20-40% respectively in D407 cells were observed. PKC activator, PMA (10-100 µM), significantly inhibited uptake of AA in the HCEC and D407

cells. Inhibitory effect of PMA was muted in both the cell lines by BIS (25-100 µM). Involvement of a PKA-mediated pathway in the regulation of [^{14}C] AA uptake was also examined by evaluating the effects of substrates at various concentrations. These compounds are known to induce intracellular cAMP levels (IBMX and forskolin) thus activating PKA in HCEC and D407 cells. Concentration dependent effect on the reduction of [^{14}C] AA uptake was evident in the presence of IBMX and forskolin, indicating the involvement of cAMP regulated PKA pathways in AA transport. Similarly, we examined the contribution of the PTK pathway on [^{14}C] AA uptake by incubating cells with genistein and tyrphostinA25 for 1 hour. Significant inhibition was observed on the uptake of AA with genistein and tyrphostinA25 (modulators of PTK-mediated pathway) across HCEC and D407 cells **(Table 6.2)**.

Table 6.2: Uptake of [^{14}C] AA across HCEC and D407 cells in the presence of various concentrations of Ca^{++}/calmodulin pathway, PKC pathway, PKA pathway and PTK pathway modulators in DPBS (pH 7.4) at 37 °C. The uptake is expressed as percentage of control (DPBS). Data is shown as mean±S.D. n=4. (*p<0.05, **p<0.01).

Pathways	**Modulators**	**Uptake as % of Control**	
		HCEC	**D407**
Ca^{++}/Calmodulin Pathway	Control	100±0.26	100±1.09
	CaM (10µM)	41.02±4.03**	47.31±1.43**
	CaM (50µM)	39.35±7.18**	35.43±3.91**
	CaM (100µM)	25.06±0.87**	20.54±2.28**
	KN-62 (0.1µM)	51.19±5.48**	40.43±5.22**
	KN-62 (1µM)	36.33±3.71**	30.92±4.78**
	KN-62 (10µM)	27.75±2.50**	20.42±2.76**

PKC Pathway	Control	100±4.25	100±4.91
	PMA (10µM)	50.19±5.56**	58.21±4.35**
	PMA (50µM)	46.47±3.83**	50.87±1.29**
	PMA (100µM)	45.43±17.43**	43.67±5.48**
	PMA (100µM) + BIS (25µM)	91.2±5.32	90.34±2.95
	PMA (100µM) + BIS (50µM)	93.85±3.49	92.69±3.45
	PMA (100µM) + BIS (100µM)	95.34±6.84	95.73±5.85
PKA Pathway	Control	100±3.24	100±2.65
	IBMX (0.1µM)	38.52±2.20**	43.67±3.12**
	IBMX (1µM)	34.42±3.16**	37.77±1.87**
	IBMX (5µM)	28.12±3.11**	30.43±5.21**
	Forskolin (1µM)	37.87±1.15**	35.63±2.35**
	Forkolin (10µM)	31.84±9.97**	33.22±4.98**
	Forskolin (50µM)	27.29±2.60**	30.87±3.65**
	Forskolin (100µM)	23.89±0.35**	20.89±5.44**
PTK Pathway	Control	100±3.24	100±2.65
	Genistein (10µM)	60.39±2.36*	53.41±2.43*
	Genistein (50µM)	48.47±4.83**	42.73±1.94**
	Genistein (100µM)	37.43±7.43**	33.47±3.68**
	Tyrphostin A25 (10µM)	55.23±6.59*	60.43±4.59*

Tyrphostin A25 (50µM)	44.85±1.84**	41.96±7.23**
Tyrphostin A25 (100µM)	32.34±5.39**	35.36±2.58**

Reverse Transcription–Polymerase Chain Reaction Analysis

For confirmation of the existence of AA transport system (SVCT) in HCEC and D407 cells, RT-PCR analysis was carried out. Agarose gel electrophoresis using ethidium bromide was employed to analyze the PCR product. PCR amplification of cDNA produced from total RNA was done with primers specific for a human SVCT system. The PCR product obtained at 626 bp confirms the expression of the AA transport system (SVCT2) on HCEC as well as D407 cells **(Fig.6.14)**.

Quantitative Real-Time PCR Analysis

RNA extraction and cDNA synthesis were carried out according to published protocol [333]. Quantitative estimates of the relative abundance of SVCT2 mRNA were obtained with qPCR analysis. mRNA levels of SVCT2 were analyzed in HCEC and D407 cells. Expression of SVCT2 mRNA in D407 was significantly higher relative to HCEC **(Fig 6.15)**.

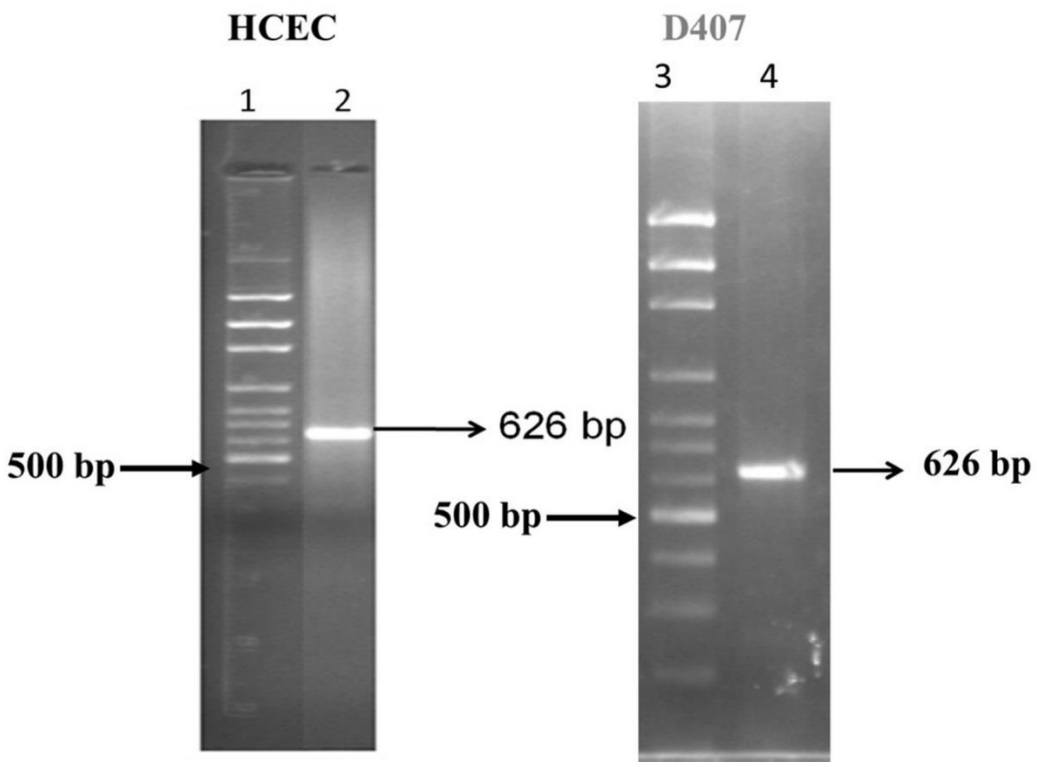

Fig.6.14: RT-PCR studies showing the molecular evidence of SVCT2 in HCEC and D407 cells. Lane 1 and 3 represents 100 bp molecular ladder and lane 2 and 4 represents 626 bp PCR product obtained from HCEC and D407 cells.

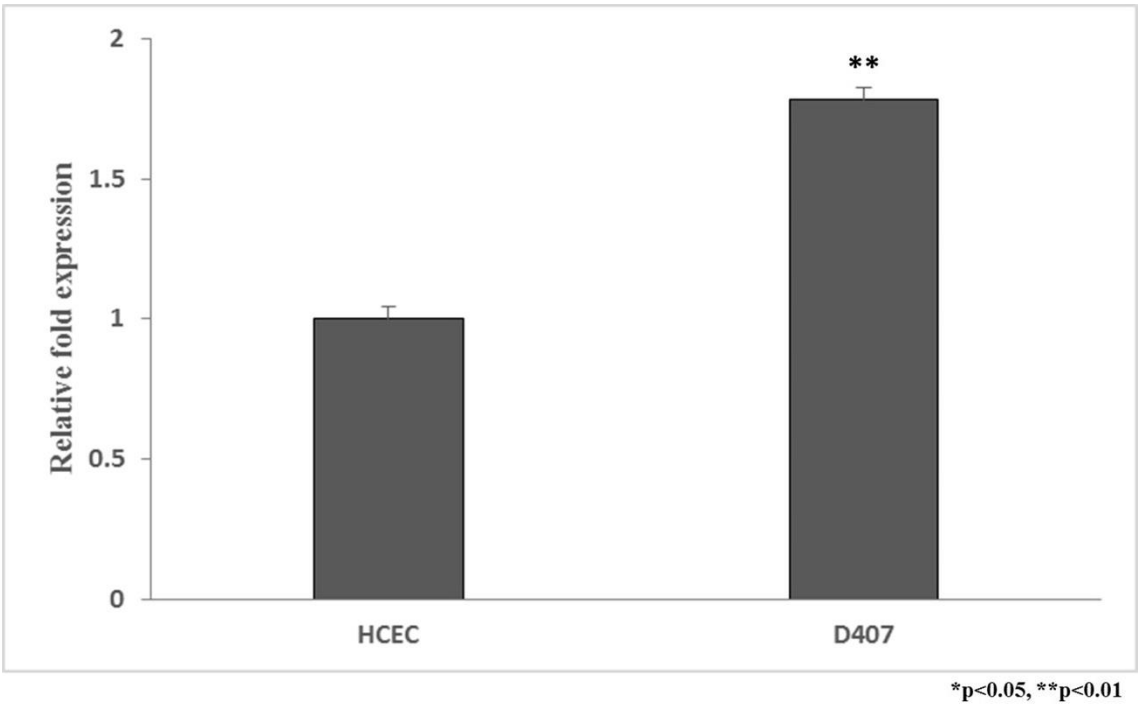

Fig.6.15: Real time-PCR comparing the expression of SVCT2 in HCEC and D407 cells. Data is shown as mean±S.D. n=4. (*p<0.05, **p<0.01).

Discussion

AA (vitamin C) is a vital cellular nutrient responsible for normal metabolic and physiological functions. Due to their biosynthetic limitation, distribution of AA between extra- and intra-cellular fluids in all cells is strictly reliant on absorption through functional vitamin C transporters [533]. AA is present in highest concentration in ocular tissues and aqueous humor to protect retinal cells and lens from the deleterious effects of sunlight [534]. AA is responsible for absorption of 99.96% of radiation even before it reaches the lens [527]. Anti-cataract role of ascorbic acid justifies the presence of high ascorbic acid levels in aqueous humor. All these biological progressions put emphasis on having a thorough understanding of the mechanism of AA transport in ocular tissues [535, 536].

In the present study, we have evaluated the AA uptake process, as well as the expression, contribution, and regulation of the SVCT2 across HCEC and D407 cells. Recently, *in vitro* culture models have been applied as prized tools to predict ocular drug permeation. These cell culture models have provided a platform for additional investigation on ocular drug delivery in lieu of *in vivo* studies. Evaluation of drug transport across ocular tissues has been traditionally done utilizing primary cultures of rabbit corneal (rPCEC) and human retinal pigment epithelial (ARPE-19). [537]. Unlike primary cultures, immortalized cell cultures can be subcultured many times without losing their metabolic and physiological characteristics including enzymatic activity and cytoskeletal polarization. These immortalized human ocular cell culture models have been utilized for cell biology, toxicity, ocular irritancy, drug delivery, drug permeability and transport studies [438, 537].

Time course of AA uptake showed the linear uptake till 60 min. Hence, an incubation time of 30 min is selected for further uptake studies in HCEC as well as D407 cells **(Fig.6.1)**. AA uptake process appears to be temperature dependent with significant rapid rate at physiological temperature (37ºC) in comparison to 25ºC and 4ºC. Rise in pH results in enhanced uptake of AA **(Figs. 6.2 & 6.3)**. Since the $pKa_{1\ of}$ AA is 4.17, it exists primarily in ascorbate form (-1 charge) above the pH range of 5.0. As a result AA enhanced uptake with increase in pH may not be due to the ionic state of AA. It can be concluded from pH dependency results that SVCT2 shows higher affinity towards ascorbate at higher pH **(Fig.6.4)** [451, 463]. Ion–ion and/or ion–polarity interactions between SVCT and its substrates are the major forces responsible for the binding of SVCT2 with the ionized form of AA. At lower pH, protonation of histidine residues reduces the binding affinity of SVCT2 with its substrates [463].

In the absence of sodium and chloride ions, lower A uptake was noticed confirming that SVCT2 transporter system may be highly sodium and chloride dependent **(Fig.6.5)**. Moreover, presence of amiloride (a Na^+ transport inhibitor) caused significant inhibition to AA uptake demonstrating that the transport system is highly sodium dependent **(Fig.6.5)**. Transmembrane sodium gradient as well as the membrane potential are responsible for the uphill transport of SVCT2 substrates [458]. Hence, we studied whether the carrier mediated transport of AA via SVCT2 is coupled with the electrochemical gradient of Na^+ ions in HCEC and D407 cells. In both cell lines, elevated uptake of AA was observed with rising concentrations of Na^+ in the uptake buffer and was found to be saturated at higher concentrations. This results suggest that AA is coupled to Na^+ and transported directly via SVCT2 **(Fig.6.6)**. The Hill ratio analysis indicates that approximately two sodium ions (1.9 for HCEC and 2.3 for D407) are required for translocation of each AA molecule **(Fig.6.7)**.

Concentration dependency of AA uptake clearly reveals that the carrier mediated process is saturable at higher concentrations of unlabeled AA. In order to distinguish the passive diffusion component from the active AA transport, uptake study was carried out at 4ºC in both HCEC and D407 cells. AA uptake was found to be saturable with K_m and V_{max} values of 46.14±6.03 μM and 17.34±0.58 pmol/mg protein/min, respectively in HCEC cells and K_m and V_{max} values of 47.26±3.24 μM and 31.86±0.56 pmol/mg protein/min, respectively in D407 cells **(Figs. 6.8 & 6.9)**. Michaelis Menten kinetic parameters (K_m and V_{max}) are two important parameters responsible for defining the functional and kinetic constants of a transporter. K_m defines the measure of apparent binding affinity of a substrate whereas V_{max} represents a measure of translocation capacity of the carrier-mediated process. On the basis of Michaelis Menten kinetics, the K_m value of SVCT2 was found to be similar in both HCEC and D407 cells, indicating a similar binding strength and affinity

of AA with both the cell lines. However comparison of V_{max} values of SVCT2 for both cell lines suggest that transport capacity of SVCT2 in D407 cells is higher relative to HCEC cells (31.86±0.56 vs 17.34±0.58 pmol/mg protein/min). Catalytic efficiency of SVCT2 was estimated by the ratio of Michaelis Menten kinetic parameters (V_{max}/K_m). A variation in V_{max} values results in higher transport efficiency (V_{max}/K_m) of SVCT2 for D407 (0.67 µl/mg protein/min) than HCEC (0.37 µl/mg protein/min) **(Table 6.1)**. These kinetic parameters indicate possible involvement of a carrier mediated transport system for the translocation of AA in HCEC and D407 cell lines. When the kinetic data was plotted in the form of Lineweaver-Burk (1/v vs. 1/[S]) plot, a single line was obtained for HCEC and D407 cell respectively, which suggests the involvement of a single transporter for the translocation of AA across human corneal and retinal cells **(Fig.6.10**). These Michaelis Menten kinetic parameters of SVCT2 in D407 cells were in accordance with previously published reports showing the presence of SVCT2 across human RPE cells [531].

AA uptake was significantly inhibited in HCEC and D407 cells in the presence of metabolic inhibitors such as sodium azide (oxidative phosphorylation inhibitor), 2,4-dinitrophenol (intracellular ATP reducer) and ouabain, (a known Na+/K+ ATPase inhibitor). These results confirms that the uptake of AA via SVCT2 is highly dependent on energy and directly coupled to ATP energy sources **(Fig.6.11)**. Uptake of AA was also significantly inhibited in the presence of various membrane/anion inhibitors such as DIDS, SITC, and probenecid **(Fig.6.12)**. Similar reports involving inhibition of AA uptake by membrane inhibitors has been published [460, 462]. These results indicate that uptake of AA is altered by the presence of specific anions and the site of the SVCT2 transport system may be the plasma membrane [460, 462].

In HCEC and D407 cells, concentration dependent inhibition in SVCT2 mediated AA uptake was revealed in the presence of structural analogs of AA i.e. L-AA and D-Iso AA. No

significant inhibition in the SVCT2 mediated AA uptake was observed in the presence of DHAA (structural analog and GLUT substrate), glucose (GLUT substrate) and PAHA (OAT substrate) **(Fig.6.13)**. Similar results with respect to substrate specificity have been published from our laboratory [462, 538]. These results in rabbit corneal epithelial cells corroborate our findings in HCEC and D407 cells. Due to a lack of 3D structure of SVCT2 transporter, it is difficult to postulate about structural requirements for the binding of SVCT2 with its substrates at this time and further investigations are required to address the issue.

Several intracellular regulatory pathways such as Ca^{++}/calmodulin, PKA, PTK and PKC are involved in the regulation of expression sodium-ascorbate cotransporters [462]. Five putative PKC phosphorylation sites in hSVCT1 and hSVCT2 and one additional PKA site in hSVCT1 have been identified based on the analysis of deduced primary amino acid sequence of SVCT [463]. It has also been reported that the uptake of AA mediated by SVCT2 expressed in COS-1 and MDCK-MDR1 cells was under the regulation of PKC-mediated pathway [462, 539]. For this reason, we investigated the regulation of AA uptake by inter- and intra-cellular protein kinase-mediated pathways. Significant inhibition in the presence of calmidazolium and KN-62 in HCEC and D407 cells was observed, leading to a hypothesis that the AA uptake process is under the regulation of Ca^{++}/CaM mediated pathway. Treating both the cell lines with PMA led to a significant lowering in AA uptake, indicating the role of PKC-mediated pathway on the regulation of AA uptake. Also, addition of BIS (PKC pathway inhibitor) reverses the inhibitory effect of PMA signifying the contribution of PKC pathway in controlling this uptake process.

On the other hand, significant inhibition on AA uptake by IBMX and forskolin treated HCEC and D407 cells confirms that PKA-mediated pathway plays a vital role in SVCT2 mediated uptake of AA. Significant inhibition was observed in presence of PTK pathway modulators

(genistein and tyrphostin A25) showing a possible role of PTK pathway in intracellular regulation of AA **(Table 6.2)**. Molecular mechanism by which the protein kinase and calmodulin pathway exert their effect on AA uptake process is yet to be fully established.

Finally, RT-PCR analysis confirms the molecular evidence of a vitamin C/AA specific carrier system in HCEC and D407 cells. The PCR product obtained at 626 bp is specific for the SVCT2 transporter system **(Fig.6.14)**. qPCR analysis revealed that the expression of SVCT2 was significantly higher in D407 in comparison to HCEC cells **(Fig.6.15).** Higher expression of SVCT2 in D407 provides the justification of greater catalytic transporter efficiency of SVCT2 in D407 relative to HCEC cells.

Conclusion

In summary, this study clearly delineates the detailed study of functional activity and molecular evidence as well as the expression, contribution, and regulation of the sodium-dependent vitamin C transporter 2 (SVCT2) across HCEC and D407 cell lines. AA uptake across HCEC and D407 cells involves a carrier-mediated active process that is modulated by both protein kinases as well as Ca^{++}/CaM mediated pathways. This transporter is highly pH dependent and requires coupling to an electrochemical Na^{+} gradient and ATP sources for cellular uptake of AA. This membrane transporter (SVCT2) can be utilized as a potential target for enhancing ocular bioavailability of AA conjugated prodrugs. This investigation demonstrates complete profiling of SVCT2 mediated AA uptake showing its dependence on calmodulin, protein kinases and intracellular ions. Also, HCEC and D407 cell line can be utilized as a valuable *in vitro* model than primary culture models to investigate ocular drug absorption of AA-conjugated therapeutics.

Acknowledgement

This work was supported by National Institutes of Health grant R01EY09171-16 and R01EY010659-14.

CHAPTER 7

MOLECULAR EXPRESSION AND FUNCTIONAL ACTIVITY OF VITAMIN C SPECIFIC TRANSPORT SYSTEM (SVCT2) IN HUMAN BREAST CANCER CELLS

Rationale

In United States, 1 in 8 women develop breast cancer during their lifespan. In 2013 about 232,340 new cases of breast cancer were diagnosed among American women. Breast cancer represents 14.1% of all new cancer cases in the U.S (cancer.gov-recent statistics). Although, chemotherapy has shown promising results in treating breast cancer, it frequently leads to systemic side effects. Also, acquired drug resistance has been reported due to the frequent use of multiple chemotherapeutic drugs during treatment of advanced breast cancer [77, 540]. During lactating period, breast epithelial cells are responsible for transport of amino acids and vitamins across cell membranes in order to meet the requirements of accelerated milk-protein synthesis. However, information is still limited with respect to transport of amino acids and vitamins across breast epithelial cells and its regulation in various biological and pathological progressions [541] [542, 543]. Presence of efflux transporter proteins i.e., P-glycoprotein (P-gp or MDR1), multidrug resistance proteins (MRPs) and breast cancer resistance protein (BCRP) render drug delivery to the breast cancer cells at therapeutic doses highly challenging [77, 543-548]. In cancer patients, overcoming multidrug resistance by exploring strategies such as evasion or modulation of these efflux transporters may play a vital role [153, 154, 543]. Several reports suggested high level expressions of influx/nutrient transporters, such as biotin [543], nucleoside/nucleobase [549, 550], glucose [551], monocarboxylic acid [552, 553], folate [554, 555], organic anion and cation transporters [556] on various breast cancer cells. This information, in turn, facilitates the rational

design of novel anti-cancer therapeutic targeting a specific carrier mediated transporter expressed in breast cancer cells [557].

Ascorbic acid (AA, vitamin C) is an essential water-soluble vitamin required for physiological and metabolic functions. It is an important nutrient required as a cofactor by various metabolic enzymes [558-561]. Efficacy of AA in cancer treatment has a controversial history [561, 562]. Many published reports described beneficial effects of AA in cancer treatment. AA has shown inhibitory effects on various cancer cells including breast, brain, prostate and stomach [561, 563-566]. Also, pharmacologic doses of AA, 10 g daily, showed effective results in the average survival of advanced cancer patients, improved patient well-being and reduced pain [561, 567-570]. In human breast carcinoma cells, AA appears to potentiate the antineoplastic activity of doxorubicin, cisplatin, and paclitaxel [571]. AA plays an important role in enhancing natural immunity and may cause lowest toxicity of all the vitamins [570].

AA cannot be synthesized by human and other primates, thus making this vitamin an essential dietary requirement. Therefore, AA is usually obtained from exogenous sources through the dietary intake [462]. AA uptake via specific transport system has already been reported in intestine [453], brain [457], kidney [454], skin [461], eye [458, 459] and bone [460]. Human *SLC23A2* family consists of two isoforms of sodium-dependent vitamin C transporters (SVCT) namely SVCT1 and SVCT2 [529]. A relative study of two isoforms discloses that AA exhibits higher structural and functional tropisms towards SVCT2 than SVCT1. Both SVCT1 and SVCT2 vary in distribution but express close sequence homology and functional similarity [458]. Structural and functional studies reveal that transport of AA across epithelial cells is primarily facilitated via SVCT [458, 462].

Transporter targeted drug delivery, in recent years, has been widely explored to improve targeted drug delivery across biological membranes. An active agent is chemically modified with transporter targeted moieties, this bioreversible conjugate enhances drug permeation and absorption. Facilitated transport of conjugated drug interacts with targeting moiety and the transporter resulting in elevated absorption [437]. SVCT2 has been exploited by many investigators as an important target for drug delivery across epithelial membranes. Higher absorptive permeability and metabolic stability compared to saquinavir alone has been observed with AA conjugated saquinavir [530]. Conjugation of nipecotic, kynurenic and diclophenamic acids with AA has been employed to enhance transport of therapeutic agents. This approach has provided a new perspective for transporter/receptor targeted prodrug design targeted to SVCT2 transporter [531]. Hence, SVCT targeted drug delivery can be utilized as a vital strategy for enhancing intracellular accumulation of anti-cancer in cancer cells. The aim of this study is to investigate the expression of a specialized carrier mediated transport system (SVCT2) on the epithelia of breast cancer cells (MDA-MB231, T47D and ZR-75-1).

The presence of SVCT on corneal cells and Madin-Darby canine kidney cells has been previously reported from our laboratory [458, 462]. Also, SVCT expression was shown on breast cancer epithelial cells (MDA-MB231 and T47D cells). However, no information currently exists regarding mechanistic and functional processes as well as molecular expression of AA carrier mediated uptake by breast cancer cells. In the present study, we evaluated the ascorbic acid uptake process, kinetics as well as expression, relative contribution, and regulation of SVCT2 in MDA-MB231, T47D and ZR-75-1 cells. Results obtained from this study may indicate involvement of a specific and high affinity carrier transport system (SVCT2) for translocation of AA.

Material And Methods

Materials

[^{14}C] Ascorbic acid ([^{14}C] AA specific activity 8.5 mCi/mM) was procured from Perkin Elmer (Boston, MA, USA). Unlabeled L-ascorbic acid, D-iso-ascorbic acid, dehydro-ascorbic acid (DHAA), glucose, para amino hippuric acid (PAHA), sodium azide, ouabain, 2,4-dinitrophenol, choline chloride, HEPES, bovine insulin, human epidermal growth factor, Triton X-100, phorbol-12-myristate-13-acetate (PMA), bisindolylmaleimide I (BIS), 3-isobutyl-1-methylxanthine (IBMX), 4,4'-di-isothiocyanatostilbene- 2,2'-disulphonic acid (DIDS), 4-acetamido-4'-isothiocyanostilbene-2,2'-disulfonic acid (SITC), and D-glucose were purchased from Sigma Chemical Co (St. Louis, MO, USA). Culture media (Dulbecco's modified Eagle's medium (DMEM), RPMI 1640 culture medium and DMEM/F-12) were procured from Invitrogen (Carlsbad, CA, USA). Fetal bovine serum (FBS) was obtained from Atlanta biologicals (Lawrenceville, GA, USA). Culture flasks (75 cm^2 growth area) and uptake plates (3.8 cm^2 growth area) were purchased from Corning Costar Corp. (Cambridge, MA, USA). The buffers for cDNA synthesis and amplification (oligodT, dNTP, MgCl2, M-MLV reverse transcriptase and Taq polymerase) were obtained from Promega Corporation (Madison, WI, USA). Light Cycler 480® SYBR I green master mix was obtained from Roche Applied Science (Indianapolis, IN, USA). Qualitative and quantitative primers used in the study were custom-designed and obtained from Invitrogen Life Technologies (Carlsbad, CA, USA). All other chemicals were obtained from Fisher Scientific Co. (Fair Lawn, NJ, USA) and utilized without further purification.

Cell Culture

T47D cells were obtained from American Type Culture Collection (ATCC). MDA-MB-231 and ZR-75-1 cells were generous gifts from Dr. Walter Jäger University of Vienna, Austria)

and Dr. A.J. van Agthoven (Josephine Nefkens Institute, Netherlands), respectively. T47D cells were cultured according to a previously published protocol [543]. Cells of passage numbers between 20 and 30 were cultured at 37°C, humidified 5% CO_2/95% air atmosphere in a DMEM culture medium supplemented with 10% (v/v) FBS (heat inactivated), 1% nonessential amino acids, 20 mM HEPES, 29 mM sodium bicarbonate, 100 mg of penicillin and streptomycin.

ZR-75-1 cells were cultured at 37°C, humidified 5% CO_2/95% air atmosphere in a RPMI 1640 culture medium supplemented with 10% (v/v) FBS (heat inactivated), 29 mM $NaHCO_3$, 20 mM HEPES, 100 mg of penicillin and streptomycin each, and 1 nM estradiol. (0.5 ml/ 500 ml medium) at pH 7.4 [514, 515]. The growth medium was changed every alternate day.

MDA-MB-231 cells were cultured at 37°C, humidified 5% CO_2/95% air atmosphere in a DMEM/F12 culture medium supplemented with 10% (v/v) FBS, 29 mM $NaHCO_3$, 20 mM HEPES, 100 mg of penicillin and streptomycin each.

All breast cancer cell lines were cultured in 75 cm^2 flasks, harvested at 80–90% confluency with TrypLE™ Express (Invitrogen, Carlsbad, CA, USA). Cells were then plated in 24-well uptake plates at a density of 300,000 cells/well. Cells were grown in a similar way as mentioned above and utilized for additional studies.

Uptake Studies

Confluent breast cancer cells were employed for uptake experiments. Following media removal, cells were rinsed thrice for 5 min each with 1–2 ml of Dulbecco's phosphate-buffered saline (DPBS) containing 140 mM NaCl, 0.03 mM KCl, 7.5 mM Na_2HPO_4, 1.5 mM KH_2PO_4, 1 mM $CaCl_2$, 0.5 mM $MgSO_4$, 20 mM HEPES, and 5 mM glucose maintained at pH 7.4. Uptake studies were initiated by adding 250µl of solution containing 0.25 µCi/ml (29.4µM) of [^{14}C] AA in the presence and absence of various competing substrates. Following specific period of

incubation, the solution was removed and uptake process was terminated with 2 ml of ice-cold stop solution containing 200 mM KCl and 2 mM HEPES. The cell monolayer was washed thrice, 5 min each and 1ml of lysis buffer (0.1% Triton-X solution in 0.3% NaOH) was added to each well and plates were stored overnight at room temperature. Subsequently, the cell lysate (400µl) from each well was transferred to scintillation vials containing 3 ml of scintillation cocktail (Fisher Scientific, Fairlawn, NJ, USA). Samples were quantified by measuring the radioactivity using liquid scintillation spectrophotometer coulter (Beckman Instruments Inc., Fullerton, CA, USA, model LS-6500). Protein content of each sample was estimated by BioRad Protein Estimation Kit (BioRad Protein Estimation Kit, Hercules, CA, USA).

Time And Temperature Dependency

The optimum time for uptake studies of [^{14}C] AA were determined by performing the uptake studies over various time points (5, 10, 15, 30, 45 and 60 min). The uptake study was conducted as per method described earlier.

The effect of temperature on [^{14}C] AA uptake was determined by carrying out the uptake study at different temperatures i.e. 4ºC, 25ºC and 37ºC. The buffer temperature was adjusted to 4ºC, 25ºC and 37ºC prior to the initiation of [^{14}C] AA uptake.

pH And Ion Dependency

The effect of pH on [^{14}C] AA uptake was observed by adjusting the pH to 5, 6, 6.5, 7.4 and 8. For delineating the role of sodium ions on [^{14}C] AA uptake, sodium chloride (NaCl) and sodium phosphate dibasic (Na_2HPO_4) in DPBS were substituted with equimolar quantities of choline chloride and potassium phosphate dibasic (KH_2PO_4), respectively. Hill coefficient for uptake of AA as function of Na^+ was determined. In a similar manner, buffer solution containing sodium

(140 mM), potassium (0.03 mM), and calcium (1 mM) chlorides were replaced with equimolar quantities of sodium phosphate, potassium phosphate, and calcium acetate, respectively.

In another study, cells were pre-incubated with 1 mM amiloride (sodium channel inhibitor) and the uptake study was carried out as mentioned earlier.

Concentration Dependency

Several concentrations of L-AA were prepared ranging from (0.12-2000µM) in DPBS (pH 7.4) and spiked with [^{14}C] AA (29.4µM). The uptake studies were performed according to a previously described method [543]. The data was fitted to Michaelis-Menten equation as shown in section 3.2 and the maximum transport rate (V_{max}) and Michaelis-Menten constant (K_m) were calculated according to nonlinear least squares regression analysis program; GraphPad Prism version 5.

Role Of Metabolic And Membrane Transport Inhibitors

For energy dependency studies, simultaneous incubation of [^{14}C] AA along with metabolic inhibitors such as ouabain (Na^+/K^+ ATPase inhibitor), 2,4-dinitrophenol (intracellular ATP reducer) and sodium azide (oxidative phosphorylation inhibitor) were performed for 1h. In order to examine the effect of anionic membrane transport inhibitors, cells were pre-incubated with 1mM SITC, DIDS and probenecid for 1h.

Substrate Specificity

The substrate specificity for SVCT was delineated by carrying out [^{14}C] AA uptake in the presence of three concentrations of (500, 1000 and 2000µM) unlabeled L-AA and structural analogs such as D-Iso AA and DHAA. A similar study was carried out at three different concentrations of (500, 1000 and 2000µM) of various structurally unrelated analogs such as

glucose (Glucose transporter/GLUT substrate) and PAHA (organic anion transporter/OAT substrate).

Intracellular Regulation

Involvement of various intracellular regulatory pathways such as Ca^{++}/calmodulin, PTK (protein tyrosine kinase), PKC (protein kinase C) and PKA (protein kinase A) pathway on [^{14}C] AA uptake was also investigated. Cells were pre-incubated with modulators such as calmidazolium (CaM) and KN-62 to delineate the process. In order to examine the role of PTK pathway in [^{14}C] AA uptake, cells were pre-incubated with genistin and tyrphostin A25. For studying the effect of PKC pathway, cells were pre-incubated with BIS and PMA (modulators of PKC pathway). The effect of PKA pathway was studied by incubating the cells with IBMX and forskolin (modulators of PKA pathway). Uptake of [^{14}C] AA was then performed according to the procedure as previously described.

Reverse Transcription–Polymerase Chain Reaction

Reverse transcription– polymerase chain reaction (RT-PCR) analysis was carried out to determine the expression of SVCT2 on T47D, MDA-MD-231 and ZR-75-1 at molecular level. TRIzol® reagent (Invitrogen, USA) was used to perform cell lysis. Chloroform was added to the lysate for phase separation. Following separation of aqueous phase containing RNA, isopropanol was added to precipitate RNA which was rinsed twice with 75% ethanol followed by resuspension in RNase-DNase free water. The concentration and purity of RNA was determined with Nanodrop (Thermo Fisher Scientific, Wilmington, DE, USA). RNA was reverse-transcribed to obtain cDNA using oligodT as a template and M-MLV reverse transcriptase. The conditions for reverse transcription were: denaturation of the template RNA for 5 min at 70°C; reverse transcription for 60 min at 42°C followed by final extension at 72°C for 5 min. cDNA obtained was then subjected

to PCR for amplification of SVCT using specific set of primers. Set of primers (5′→3′) designed for SVCT2 were: forward: CCAGCGGTGAGCAGGACAAT, reverse primer: TAGGGCCACCGTGGGTGTAA. These primers correspond to a 626 base pair (bp) product in human SVCT2 cDNA. The conditions of PCR amplification were: denaturation for 30 s at 94°C, annealing for 1 min at 56°C, and extension for 1 min at 72°C, for 45 cycles followed by a final extension for 5 min at 72°C. PCR product obtained was analyzed by gel electrophoresis on 1.5% agarose in TAE buffer and visualized under UV [438].

Quantitative Real-Time PCR

Following reverse transcription, quantitative real-time PCR (qPCR) was performed with LightCycler® SYBR green technology (Roche). cDNA equivalent to 80 ng in each well was subjected to amplification with specific primers. Glyceraldehyde-3-phosphate dehydrogenase (GAPDH) was used as an internal standard to normalize the amount of cDNA in each well. The sequences of real-time primers (5′→3′) used for SVCT2 were: forward: GCCAGCTAGGTCTTGACTCC, reverse primer: GATGTGGCGTAGACCTGTCC, GAPDH: forward—ATCCCTCCAAAATCAAGTGG and reverse—GTTGTCATGGATGACCTTGG. A preliminary experiment was performed to ensure that SVCT2 and GAPDH were amplified with equal efficiencies. The specificity of these primers was also confirmed by melting-curve analysis. The comparative threshold method was used to calculate the relative amount of SVCT2 in breast cancer cell lines [438, 532].

Data Analysis

Radioactive Sample Analysis

The uptake of [^{14}C] AA was calculated using disintegrations per minute (DPM) of sample and donor solutions as shown in Eq. 1

$$Csample = \frac{DPMsample * Cdonor}{DPMdonor} \quad \textbf{Eq. 1}$$

where, DPM_{sample} and DPM_{donor} represent average values of DPM counts of sample and donor (n=4) respectively; C_{donor} denotes the concentration of donor used and C_{sample} represents the concentration of sample.

Calculation of Michaelis-Menten Kinetic Parameters

In order to determine K_m and V_{max} associated with [^{14}C] AA uptake, concentration-dependency data was fitted in a modified Michaelis–Menten equation as shown in Eq.2

$$v = \frac{Vmax[C]}{Km + [C]} + Kd[C] \quad \textbf{Eq. 2}$$

v represents the total uptake, V_{max} stands for the maximum uptake rate for the carrier-mediated process, K_m is Michaelis–Menten constant which represents the concentration at half saturation, K_d is a non-saturable diffusion rate constant and C is substrate concentration. In Eq. (2), $(V_{max}*C)/(K_m+C)$ represents carrier mediated saturable process whereas $K_d(C)$ denotes the non-saturable component. Data was fitted to a non-linear least-square regression analysis program (GraphPad Prism 5.0). The Michaelis-Menten kinetic parameters were calculated to determine saturable and non-saturable component of the total uptake.

Calculation Of Hill Ratio

Na^+:L-Ascorbic acid coupling ratio was determined using the logarithmic form of the Hill equation (Eq. 3)

$$Log\left[\frac{v'}{Vmax} - v'\right] = nlog(S) - logK' \quad \textbf{Eq. 3}$$

v' denotes initial velocity, V_{max} represents the maximal velocity, n is number of substrate binding sites, S denotes the substrate concentration, and K' is a constant comprising multiple interaction factors and the intrinsic dissociation constant.

Statistical Analysis

All the experiments were conducted at least in quadruplicate (n=4) and the outcomes were expressed as mean±standard deviation (SD). To calculate statistical significance, student's t test was applied and the difference between mean values is considered statistically significant for P value ≤ 0.05.

Results

Time And Temperature Dependency

Time dependent uptake of [^{14}C] AA (29.4µM) in MDA-MB231, T47D and ZR-75-1 cells is depicted in **Fig.7.1.** Linear uptake of [^{14}C] AA was noticed upto 60 min of incubation period. Therefore, 30 min uptake time was selected for all uptake experiments.

Effect of temperature on the uptake of AA was studied on MDA-MB231, T47D and ZR-75-1 cells. Uptake of [^{14}C] AA in the three breast cancer cell lines was maximal at 37°C **(Fig.7.2)**. Uptake of [^{14}C] AA in MDA-MB231 showed ~40% and 70% decrease when the temperature was reduced to 25°C and 4°C respectively. In T47D cells, uptake was reduced to ~55% and 25% when measured at 25°C and 4°C respectively, whereas, in ZR-75-1 cells uptake of [^{14}C] AA diminished to ~50% and 20% respectively, at 25°C and 4°C, suggesting that the process may be carrier mediated in all the studied breast cancer cell lines. Activation energy (E_a) was calculated by plotting the temperature dependent data i.e. Uptake rate Ln(v) vs. 1/T **(Fig.7.3)** E_a was calculated to be 8.08, 9.71 and 9.99 kcal/mol in MDA-MB231, T47D and ZR-75-1 cells respectively.

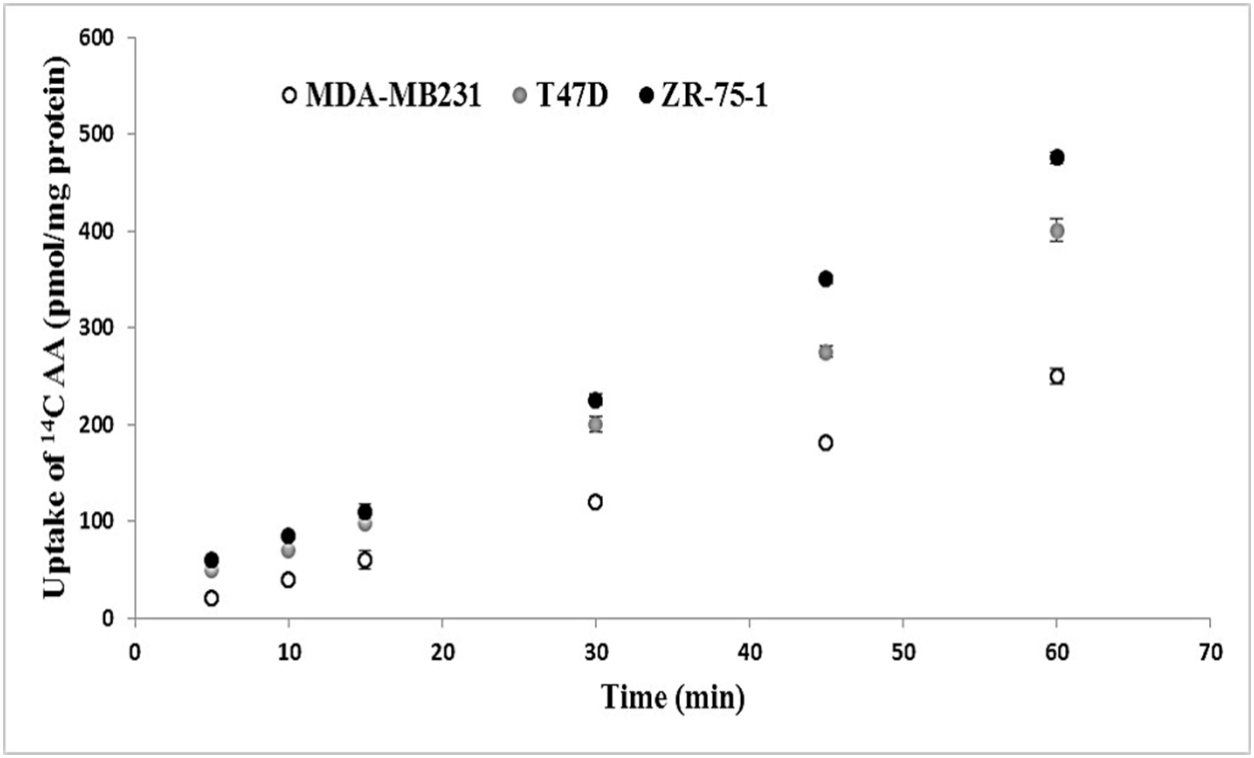

Fig.7.1: Time course of [^{14}C] AA uptake across MDA-MB231, T47D and ZR-75-1 cells. Uptake of [^{14}C] ascorbic acid ([^{14}C] AA) was measured in DPBS buffer (pH 7.4) at 37ºC. Data is shown as mean±S.D. n=4. S.D. means standard derivation.

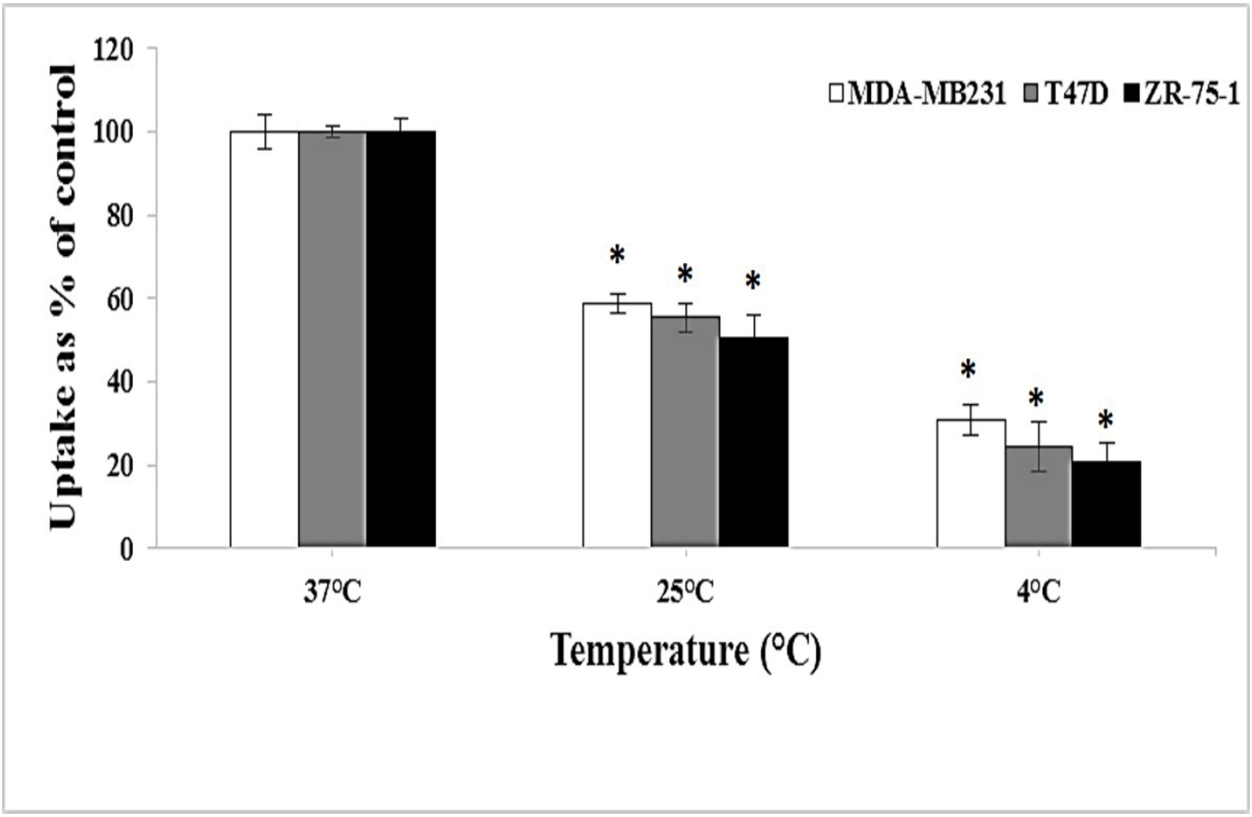

Fig.7.2: Temperature dependent uptake study of [^{14}C] AA uptake across MDA-MB231, T47D and ZR-75-1 cells in DPBS (pH 7.4). The uptake is expressed as percentage of control (37°C). Data is shown as mean±S.D. n=4. Asterisk (*) represents significant difference from the control (*$p<0.05$).

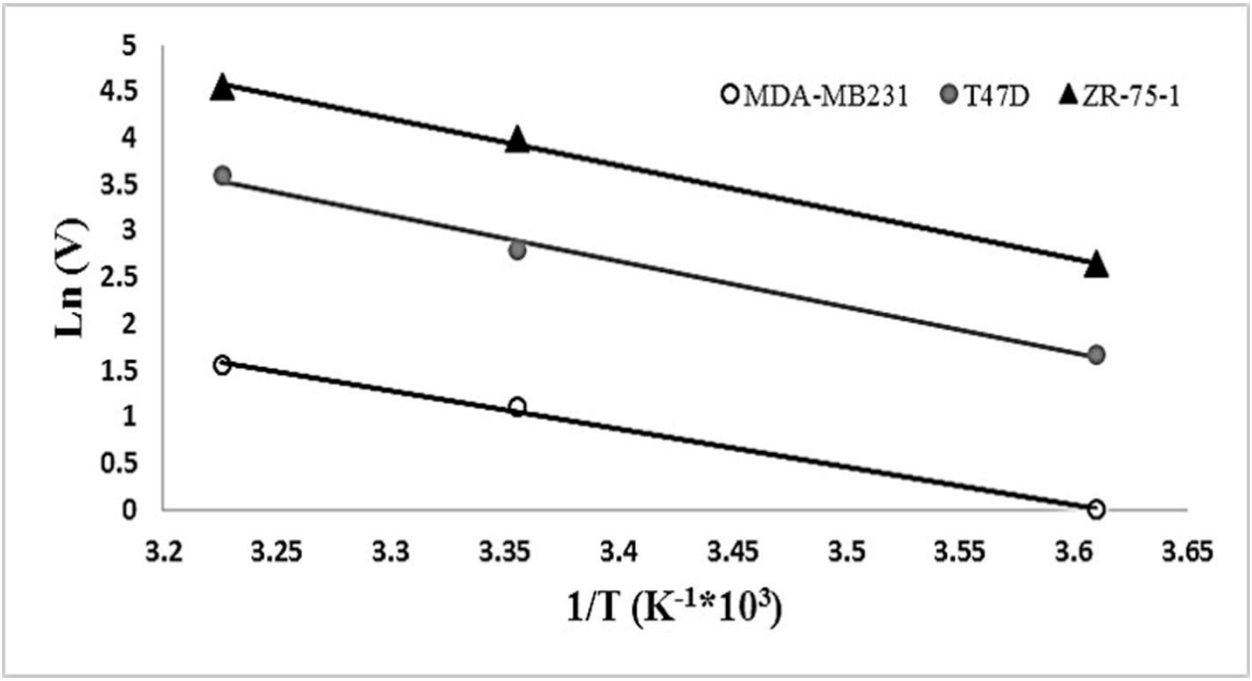

Fig.7.3: Arrhenius plot of the effect of temperature on [^{14}C] AA uptake across MDA-MB231, T47D and ZR-75-1 cells. Uptake of [^{14}C] AA was measured in DPBS buffer (pH 7.4) for 30min at 37, 25 and 4°C, across MDA-MB231, T47D and ZR-75-1 cells. Data is shown as mean±S.D. n=4

pH *And Ion Dependency*

In order to delineate the role of an inward driven proton gradient for [^{14}C] AA uptake, the study was carried out with pH ranging from 5-8 in MDA-MB231, T47D and ZR-75-1 cells. Uptake of [^{14}C] AA elevated with a rise in extracellular pH from 5 to 8 in all cell lines. In comparison to pH 7.4, uptake of [^{14}C] AA diminished to ~40% and 50% at pH 5 and 6 respectively in MDA-MB231, T47D and ZR-75-1 cells **(Fig.7.4)**. Based on these results, further uptake studies were carried out at pH 7.4 with all the cell lines.

In sodium free media, uptake of [^{14}C] AA was reduced to ~50%, 25% and 30% respectively, in MDA-MB231, T47D and ZR-75-1 cells **(Fig.7.5).** Similarly, uptake of AA was also diminished to ~%60, 50% and 50% in MDA-MB231, T47D and ZR-75-1 cells respectively

in the presence of amiloride (Na^+ transport inhibitor), indicating possible involvement of sodium ions in translocation of AA **(Fig.7.5).**

The effect of chloride ions was studied by replacing chloride ions with equimolar quantities of other monovalent cations in DPBS. A marked reduction (45%, 40% and 40%) in the uptake rate of [^{14}C] AA was observed in the absence of chloride ions in MDA-MB231, T47D and ZR-75-1 cells respectively. This study evidently defines the involvement of sodium and chloride ions in active transport of AA **(Fig.7.5).**

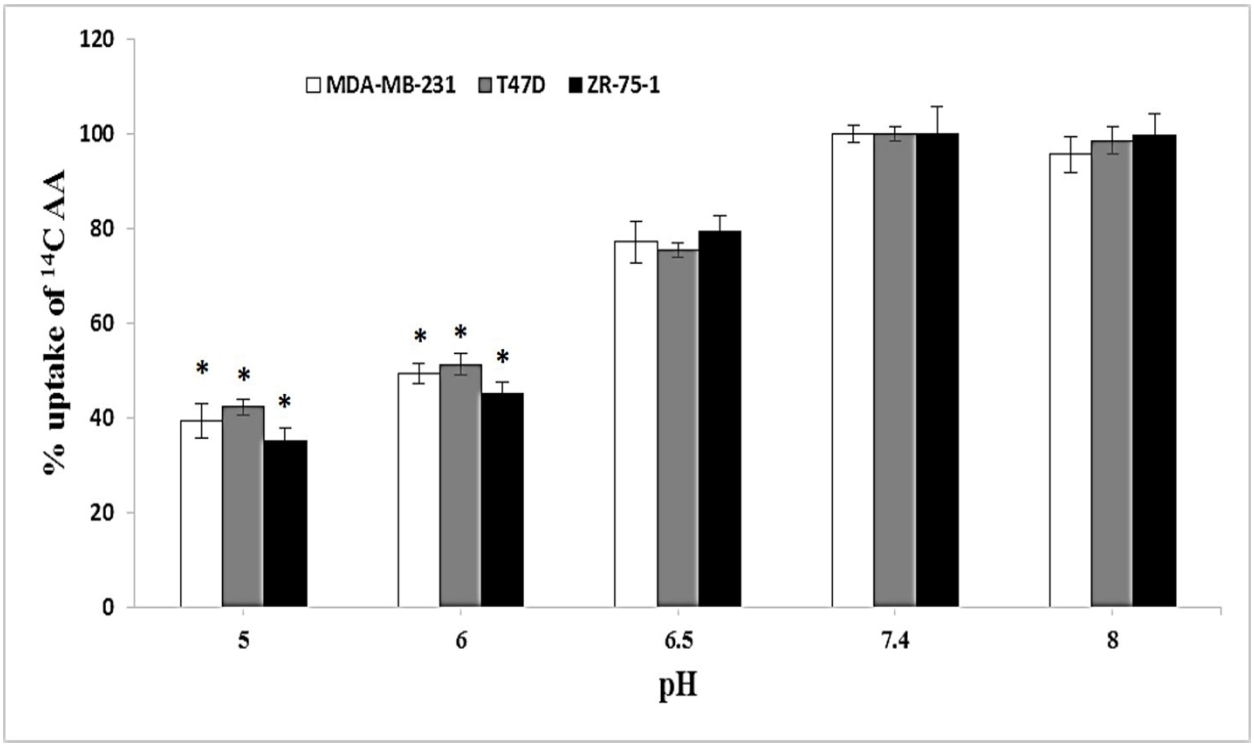

Fig.7.4: Effect of pH on [^{14}C] AA uptake across MDA-MB231, T47D and ZR-75-1 cells. Uptake of [^{14}C] AA was determined in the presence of different pH (5.0, 6.0, 6.5, 7.4 and 8.0) at 37°C for 30 min across MDA-MB231, T47D and ZR-75-1 cells. The uptake is expressed as percentage of control (pH 7.4). Data is shown as mean±S.D. n=4. (*$p<0.05$).

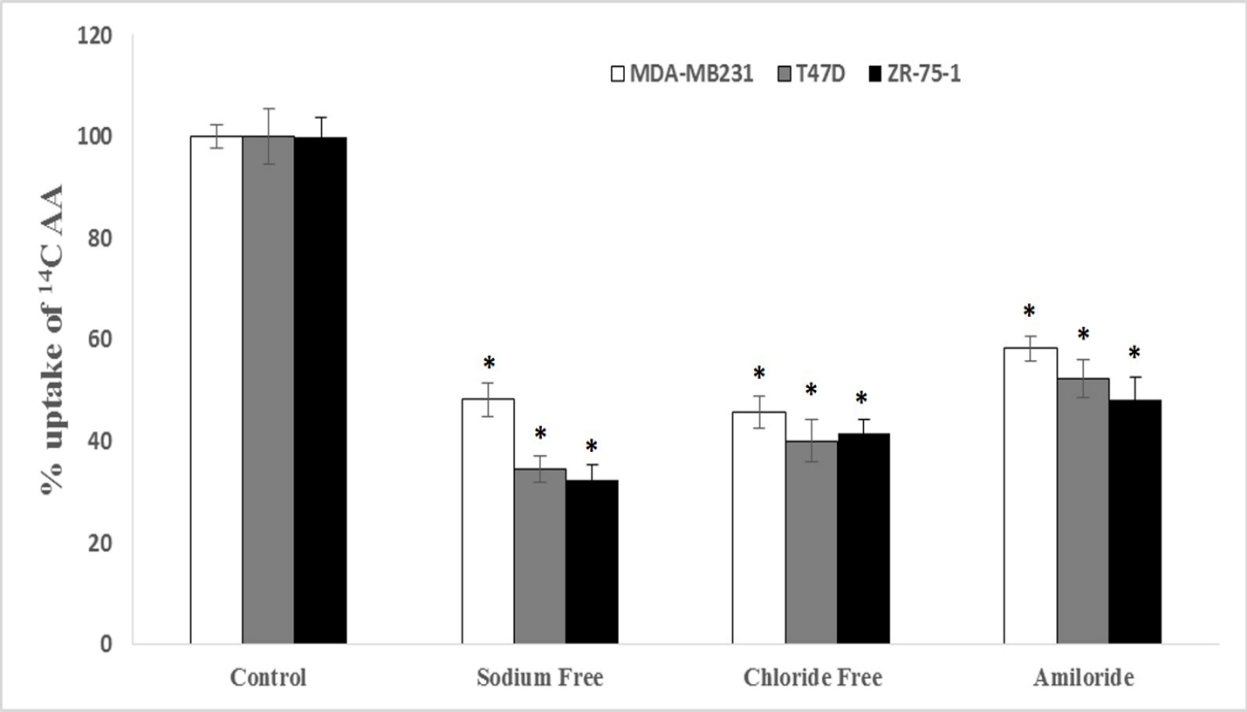

Fig.7.5: Uptake of [^{14}C] AA across MDA-MB231, T47D and ZR-75-1 cells in the presence of amiloride and absence of sodium and chloride ions in DPBS buffer (pH 7.4) at 37°C. (*$p<0.05$).

Role of sodium on AA absorption kinetics of AA was also evaluated with various concentrations of sodium (0-140mM) in the DPBS. Reduced uptake of [^{14}C] AA was observed with lower Na^+ concentrations. Uptake data displayed saturation kinetics of [^{14}C] AA uptake at about 70 mM of Na^+ concentration in MDA-MB231, T47D and ZR-75-1 cells **(Fig.7.6)**. Hill transformation of Na^+ saturation kinetics data showed 2:1 molar ratio of Na^+:AA coupling in these breast cancer cell lines **(Fig.7.7)**.

Concentration Dependency

Breast cancer cells were incubated with various concentrations (0.12-2000µM) of unlabeled AA for 30 min at 37°C, in order to investigate Michaelis-Menten saturation kinetics. The uptake process involves both the saturable carrier mediated pathway and non-saturable diffusional process in all three breast cancer cell lines. Uptake of [^{14}C] AA was reduced at 4°C

compared to 37°C indicating the role of passive diffusion component involved in AA transport in breast cancer cells. The carrier mediated process of AA uptake in breast cancer cell lines was plotted as the difference of total uptake of AA at 37°C and passive uptake of AA at 4°C. [^{14}C] AA uptake in MDA-MB231 cells was found to be concentration-dependent and saturable with K_m and V_{max} values of 53.85±6.24 μM and 18.45±0.50 pmol/mg protein/min, respectively **(Fig.7.8).** The kinetic parameters (K_m and V_{max}) estimated for T47D and ZR-75-1 cells were also concentration dependent and saturable with a relatively lower K_m and higher V_{max} than MDA-MB231 cells. K_m and V_{max} values obtained from the saturation kinetics plot for T47D cells were 49.69±2.83 μM and 32.50±0.43 pmol/mg protein/min **(Fig.7.9)**, and for ZR-75-1 cell were 45.44±3.16 μM and 33.25±0.53 pmol/mg protein/min respectively **(Fig.7.10).** Lineweaver-Burk (1/v vs. 1/[S]) plot, indicate the involvement of a single carrier in the uptake process of AA across these breast cancer cell lines (data not shown).

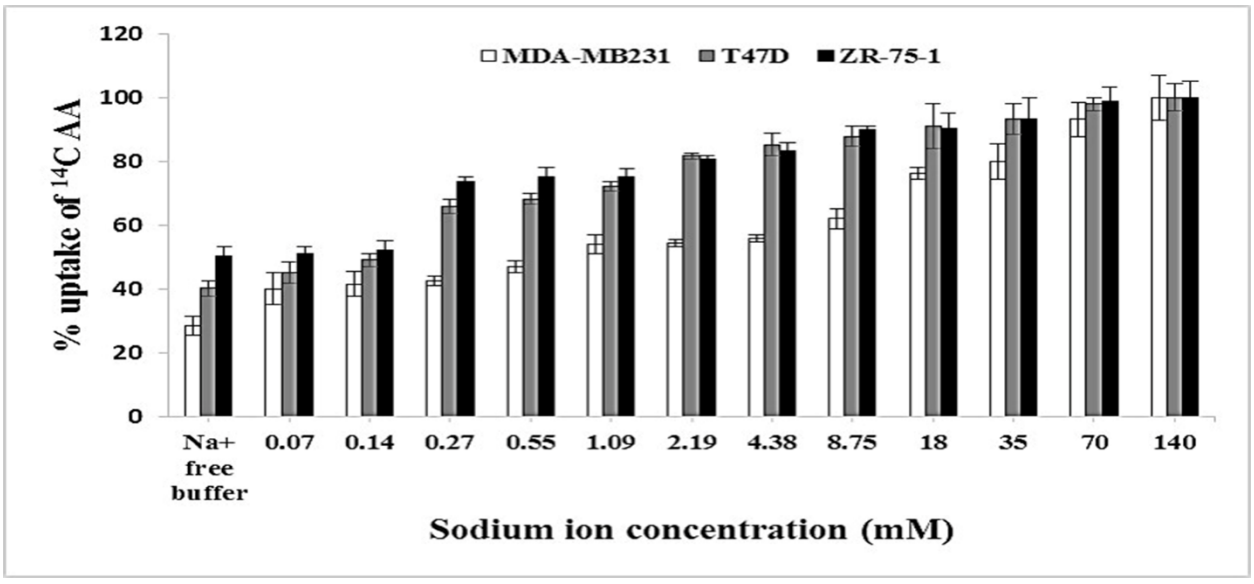

Fig.7.6: Uptake of [^{14}C] AA across MDA-MB231, T47D and ZR-75-1 cells as a function of sodium concentration in DPBS (pH 7.4) at 37°C. Data is shown as mean±S.D. n=4.

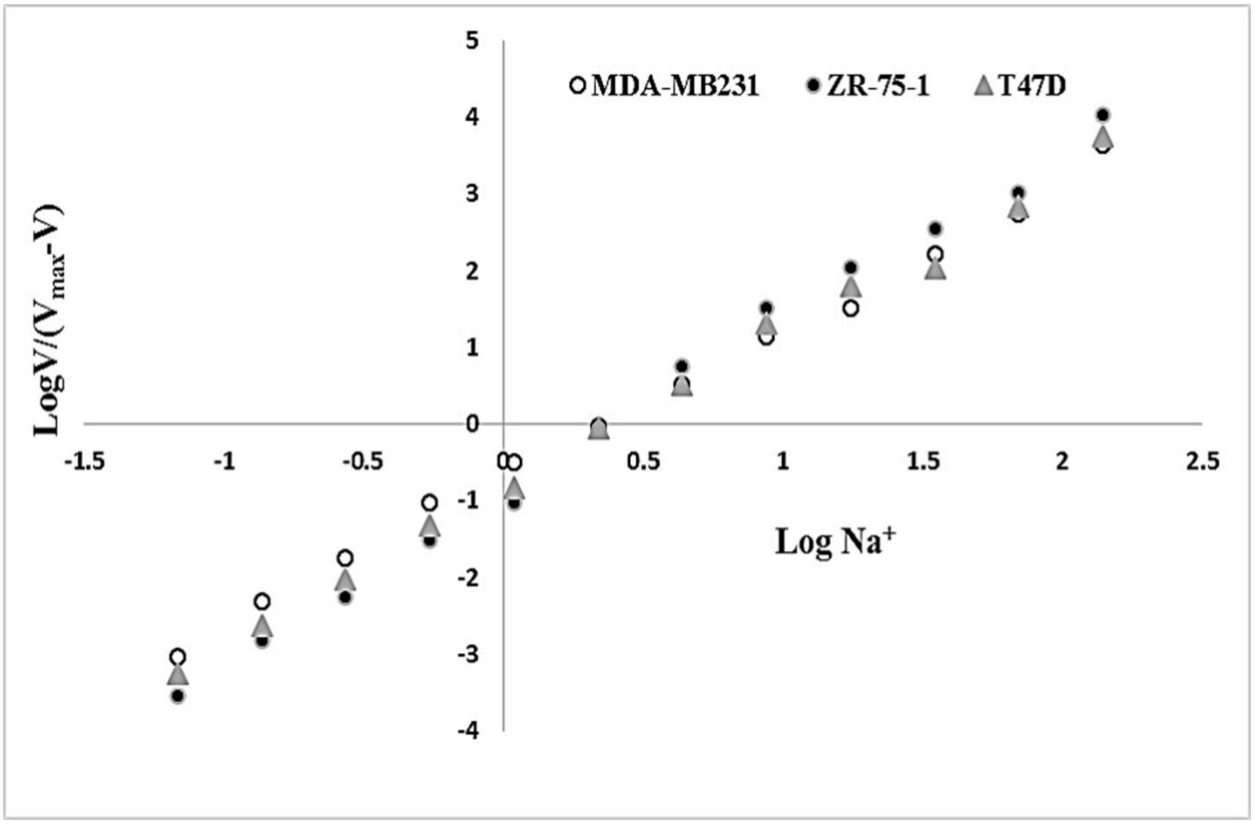

Fig.7.7: Hill plot of sodium-dependent uptake of [^{14}C] AA across MDA-MB231, T47D and ZR-75-1 cells.

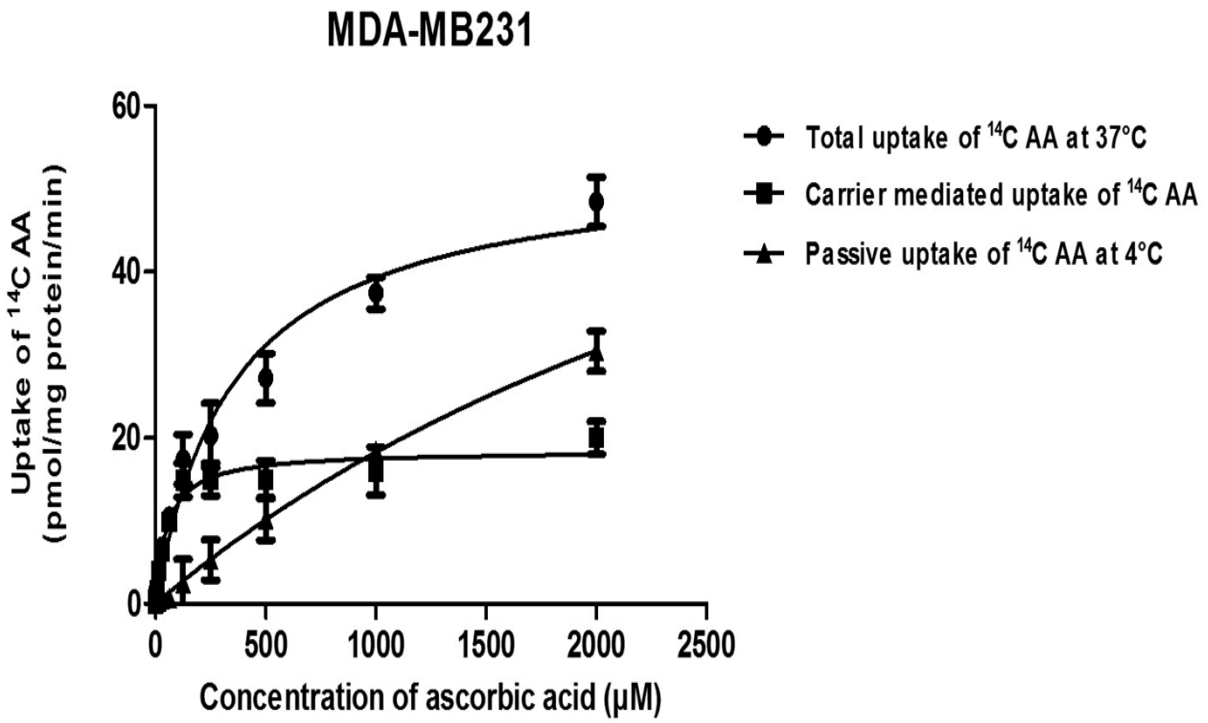

Fig.7.8: Concentration-dependent uptake of [^{14}C] AA across MDA-MB231 cells. Data is shown as mean±S.D. n=4 (● represents total uptake, ▲ represents passive uptake/non-saturable component and ■ represents carrier mediated uptake/saturable component)

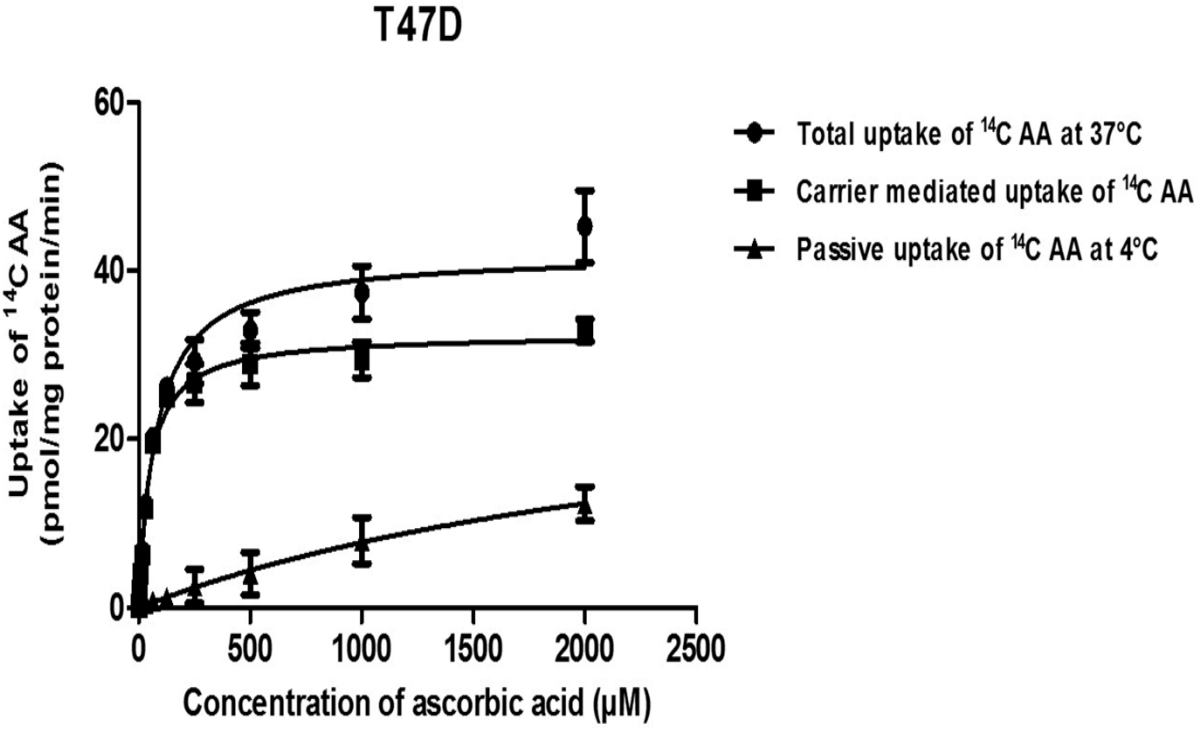

Fig.7.9: Concentration-dependent uptake of [^{14}C] AA across T47D cells. Data is shown as mean±S.D. n=4 (● represents total uptake, ▲ represents passive uptake/non-saturable component and ■ represents carrier mediated uptake/saturable component)

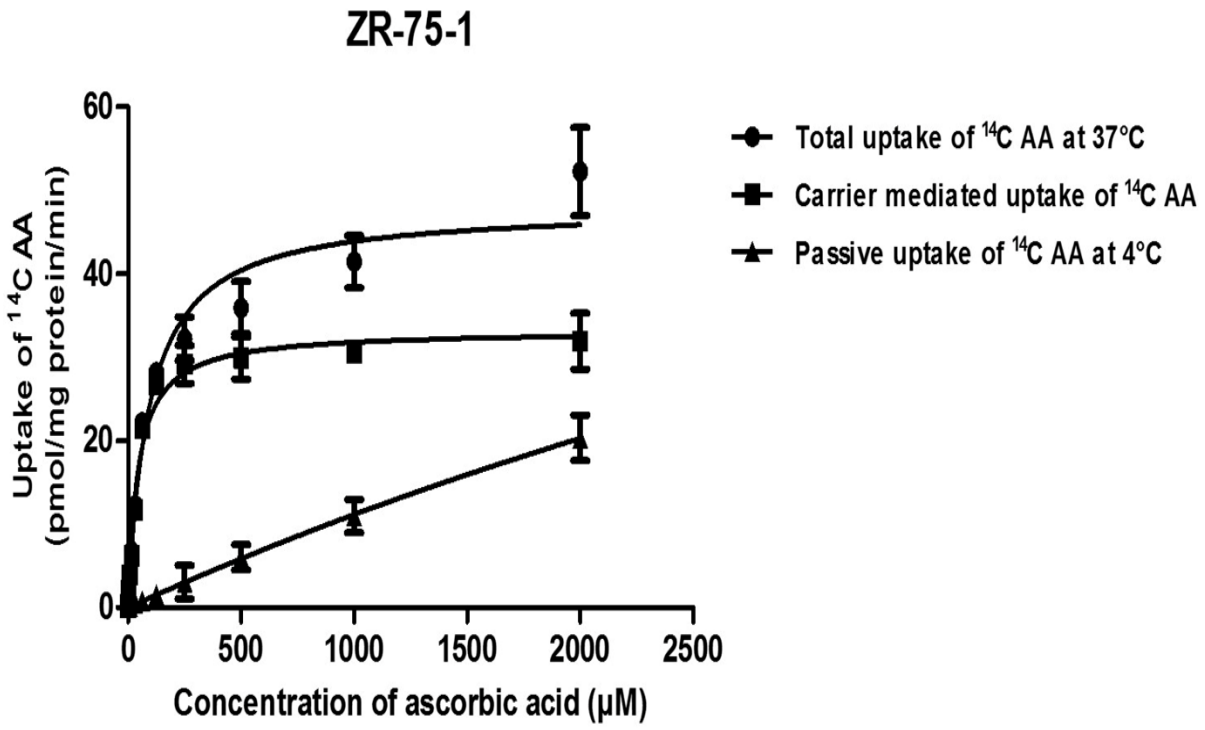

Fig.7.10: Concentration-dependent uptake of [^{14}C] AA across ZR-75-1 cells. Data is shown as mean±S.D. n=4 (● represents total uptake, ▲ represents passive uptake/non-saturable component and ■ represents carrier mediated uptake/saturable component)

Role Of Metabolic And Membrane Transport Inhibitors

Uptake studies were carried out in the presence of metabolic inhibitors such as ouabain (Na^+/K^+ ATPase inhibitor), sodium azide (oxidative phosphorylation inhibitor), and 2,4-DNP (intracellular ATP reducer) in MDA-MB231, T47D and ZR-75-1 cells to delineate the effect of metabolic inhibitors on [^{14}C] AA uptake. These metabolic inhibitors caused significant reduction (50% to 60%) in the uptake of [^{14}C] AA was observed **(Fig.7.11)**.

Additional studies were carried out to investigate the effect of membrane inhibitors (SITC, DIDS and probenecid). AA uptake was also reduced to 35% to 45% in the presence of SITC, DIDS

and probenecid, suggesting a role of an anion exchanger in carrier mediated transport of [^{14}C] AA **(Fig.7.12)**.

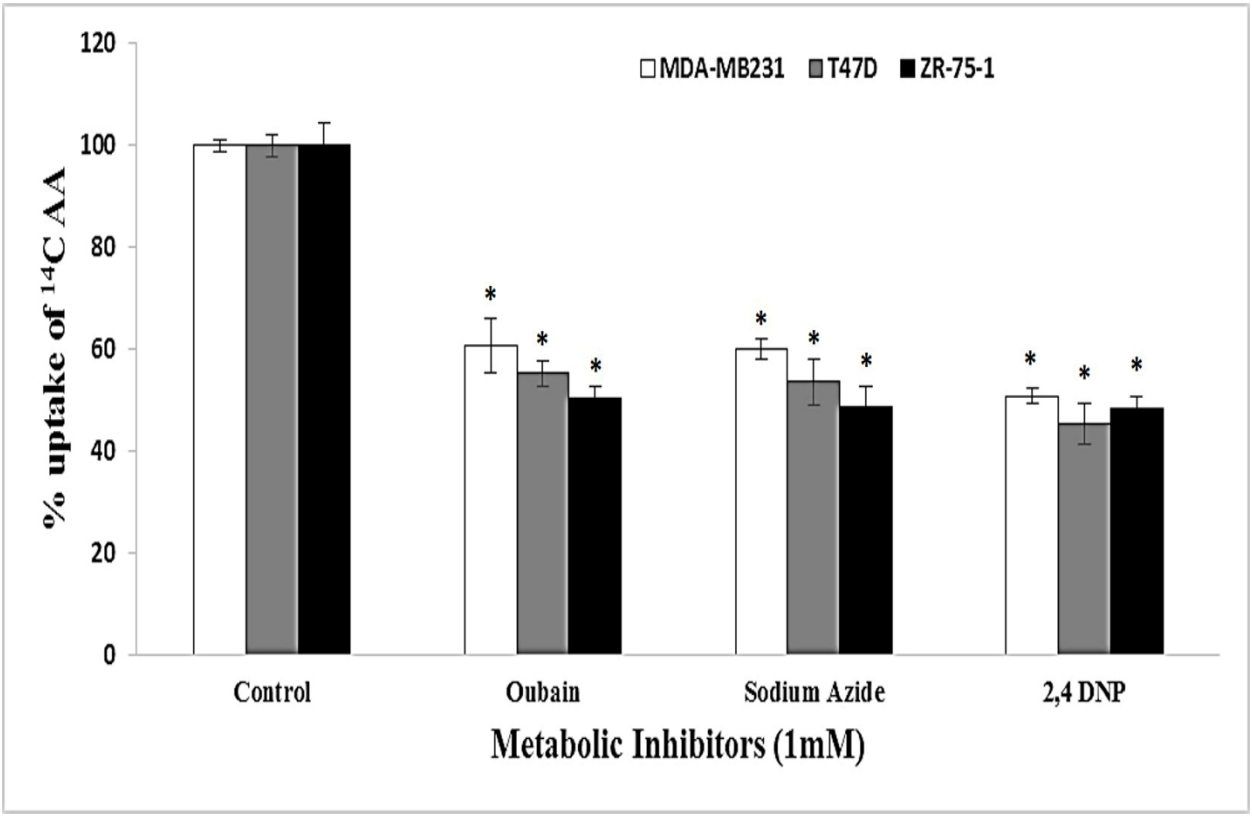

Fig.7.11: Uptake of [^{14}C] AA across MDA-MB231, T47D and ZR-75-1 cells in the presence of metabolic inhibitors (ouabain, sodium azide, and 2,4-DNP). [^{14}C] AA uptake was performed at 37°C with DPBS buffer (pH 7.4) for 30 min. Data is shown as mean±S.D. n=4. (*$p<0.05$).

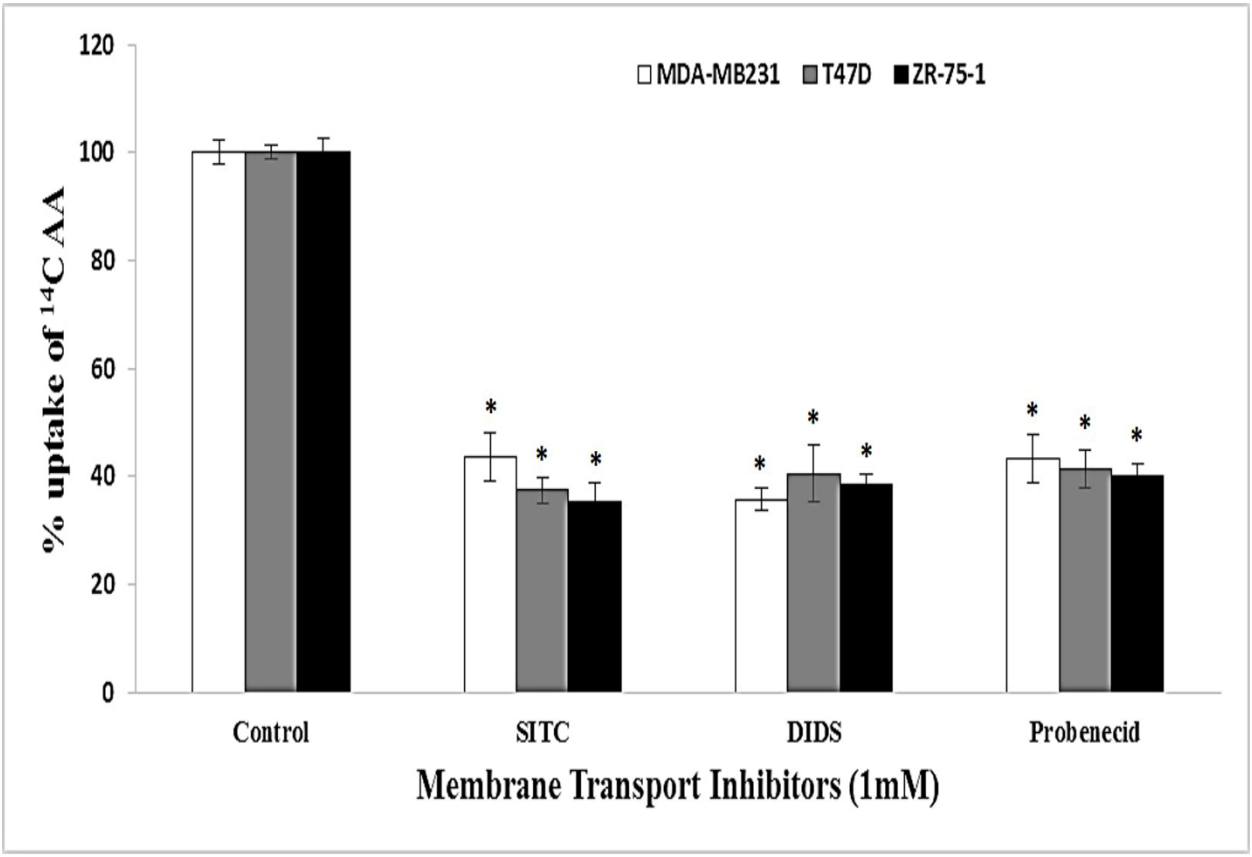

Fig.7.12. Uptake of [^{14}C] AA across MDA-MB231, T47D and ZR-75-1 cells in the presence of membrane inhibitors (SITC, DIDS and probenecid). [^{14}C] AA uptake was performed at 37°C with DPBS buffer (pH 7.4) for 30 min. Data is shown as mean±S.D. n=4. (*$p<0.05$).

Substrate Specificity

[^{14}C] AA uptake in these breast cancer cells was significantly inhibited in the presence of increasing concentration (500, 1000 and 2000µM) of structural analogs (L-AA and D-Iso AA) whereas no substantial alteration in the uptake was observed with DHAA. Also, presence of structurally unrelated analogs i.e. glucose and PAHA (500, 1000 and 2000µM) did not change the uptake of [^{14}C] AA significantly **(Fig.7.13)**.

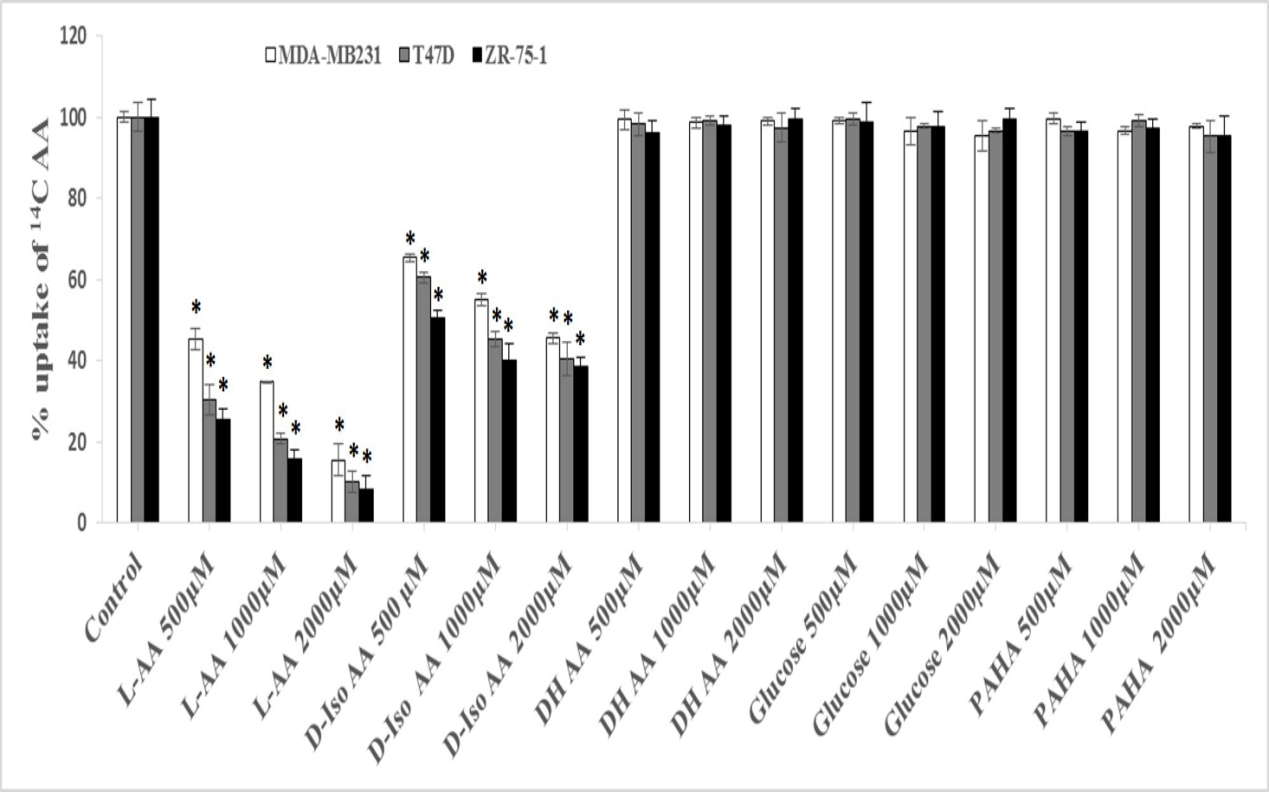

Fig.7.13. Uptake of [^{14}C] AA in presence of L-ascorbic acid (L-AA), D-isoascorbic acid (D-Iso AA), dehydro ascorbic acid (DHAA), D-glucose, and para-amino hippuric acid (PAHA) at three different concentrations across MDA-MB231, T47D and ZR-75-1 cells. [^{14}C] AA uptake was performed at 37°C with DPBS buffer (pH 7.4) for 30 min. Data is shown as mean±S.D. n=4. (*$p<0.05$).

Intracellular Regulation

The role of different intracellular regulation pathways on [^{14}C] AA uptake was also investigated. With higher concentrations of calmidazolium and KN-62 (modulators of Ca^{++}/calmodium (Ca^{++}/CaM) pathway), significantly reduced uptake of [^{14}C] AA was observed in breast cancer cells. PKC activator, PMA (10-100 μM) also caused significant inhibition of AA uptake in all breast cancer cell lines. Inhibitory effect of PMA was muted by BIS (25-100 μM) across all breast cancer cells **(Table 7.1).**

Involvement of a PKA-mediated pathway in the regulation of [^{14}C] AA uptake was examined by evaluating the effects of substrates at various concentrations. These compounds are known to induce intracellular cAMP levels (IBMX and forskolin) thus activating PKA in these cells. Concentration dependent effect on the reduction of [^{14}C] AA uptake was evident with IBMX and forskolin, indicating the involvement of cAMP regulated PKA pathways in AA transport. Similarly, we examined the contribution of the PTK pathway on [^{14}C] AA uptake by incubating cells with genistein and tyrphostinA25 for 1 hour. Significantly diminished uptake was observed in the presence of genistein and tyrphostinA25 (modulators of PTK-mediated pathway) across these cell lines **(Table 7.1).**

Table 7.1: Uptake of [^{14}C] AA across MDA-MB231, T47D and ZR-75-1 cells in the presence of various concentrations of Ca^{++}/calmodulin pathway, PKC pathway, PKA pathway and PTK pathway modulators in DPBS (pH 7.4) at 37 °C. The uptake is expressed as percentage of control (DPBS). Data is shown as mean±S.D. n=4. (*$p<0.05$).

Pathways	**Modulators**	**Uptake as % of Control**		
		MDA-MB231	**T47D**	**ZR-75-1**
Ca^{++}/Calmodulin Pathway	Control	100 ± 1.57	100 ± 2.89	100 ± 4.12
	CaM (10µM)	38.55 ± 3.56*	32.89 ± 2.48*	31.49 ± 1.56*
	CaM (50µM)	35.18 ± 2.15*	27.69 ± 4.25*	25.78 ± 3.53*
	CaM (100µM)	24.45 ± 3.18*	18.46± 3.85*	15.63± 2.17*
	KN-62 (0.1µM)	48.68 ± 2.89*	38.14 ± 2.59*	40.14 ± 3.19*
	KN-62 (1µM)	38.45 ± 4.51*	25.91± 4.21*	28.76± 1.05*
	KN-62 (10µM)	25.26 ± 6.72*	21.83± 2.43*	19.45± 2.35*

	Control	100 ± 5.52	100 ± 3.19	100 ± 2.69
	PMA (10µM)	52.35 ± 4.65*	54.82 ± 3.54*	55.46 ± 2.89*
	PMA (50µM)	50.23 ± 2.38*	47.61 ± 2.19*	50.12 ± 3.67*
PKC Pathway	PMA (100µM)	44.98 ± 6.34*	40.75 ± 4.85*	42.15 ± 5.48*
	PMA (100µM) + BIS (25µM)	89.23 ± 6.35	90.25 ± 5.92	88.68 ± 7.89
	PMA (100µM) + BIS (50µM)	92.85 ± 4.39	92.68 ± 3.45	93.63 ± 5.67
	PMA (100µM) + BIS (100µM)	95.34 ± 3.48	93.15 ± 4.85	94.19 ± 2.11
	Control	100 ± 3.24	100 ± 2.65	100 ± 6.32
	IBMX (0.1µM)	36.23 ± 4.21*	40.13 ± 4.21*	39.65 ± 2.12*
	IBMX (1µM)	30.64 ± 2.87*	35.84 ± 2.78*	36.48 ± 5.87*
PKA Pathway	IBMX (5µM)	25.96 ± 5.12*	32.67 ± 4.51*	30.76 ± 2.15*
	Forskolin (1µM)	33.14 ± 4.29*	38.21 ± 3.53*	40.12 ± 5.33*
	Forkolin (10µM)	30.97 ± 7.19*	32.49 ± 7.89*	38.94 ± 6.98*
	Forskolin (50µM)	25.73 ± 4.28*	31.96 ± 4.56*	35.69 ± 3.65*
	Forskolin (100µM)	22.81 ± 2.16*	25.78 ± 2.55*	30.87 ± 5.22*
	Control	100 ± 5.52	100 ± 3.19	100 ± 2.69
	Genistein (10µM)	52.35 ± 4.65*	54.82 ± 3.54*	55.46 ± 2.89*
	Genistein (50µM)	50.23 ± 2.38*	47.61 ± 2.19*	50.12 ± 3.67*
PTK Pathway	Genistein (100µM)	44.98 ± 6.34*	40.75 ± 4.85*	42.15 ± 5.48*
	Tyrphostin A25 (10µM)	54.65 ± 6.35*	50.25 ± 5.92*	48.68 ± 7.89*
	Tyrphostin A25 (50µM)	45.78 ± 4.39*	42.68 ± 3.45*	43.63 ± 5.67*

Tyrphostin A25 (100µM)	33.21 ± 3.48*	36.15 ± 4.85*	34.19 ± 2.11*

Reverse Transcription–Polymerase Chain Reaction Analysis

RT-PCR analysis was carried out for the confirmation of AA transport system (SVCT2) in all three breast cancer cell lines. Agarose gel electrophoresis using ethidium bromide was employed to analyze the PCR product. PCR amplification of cDNA from total RNA was performed with a set of primers specific for a human SVCT2 system. The PCR product obtained at 626 bp confirms the expression of the AA transport system (SVCT2) on MDA-MB231, T47D and ZR-75-1 cells. Higher intensity of 626 bp was detected in ZR-75-1 and T47D cell lines relative to MDA-MB231 cells **(Fig.7.14)**.

Quantitative Real-Time PCR Analysis

Quantitative estimates of the relative abundance of SVCT2 mRNA were obtained with qPCR analysis. mRNA levels of SVCT2 were also analyzed in MDA-MB231, T47D and ZR-75-1 cells. Average C_t values for SVCT2 were around 38-42 and the average C_t values for GAPDH were observed to be 16-19. Significantly higher expression of SVCT2 mRNA in T47D and ZR-75-1 cells was observed relative to MDA-MB231 cells **(Fig.15)**.

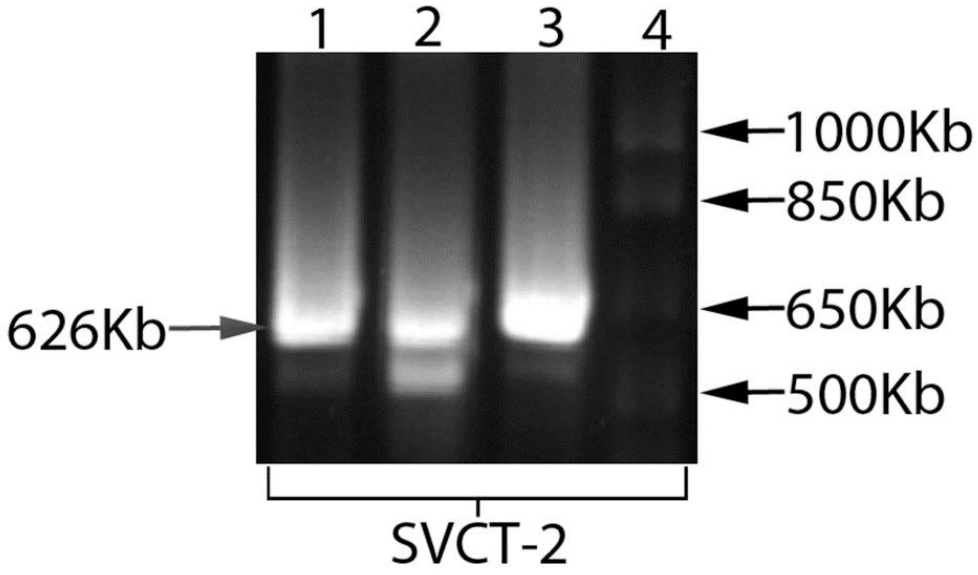

Fig.7.14: RT-PCR studies showing the molecular evidence of SVCT2 in MDA-MB231, T47D and ZR-75-1 cells. Lane 1 represents ZR-75-1, lane 2: T47D, lane 3: MDA-MB231 and lane 4: 1 Kb molecular ladder.

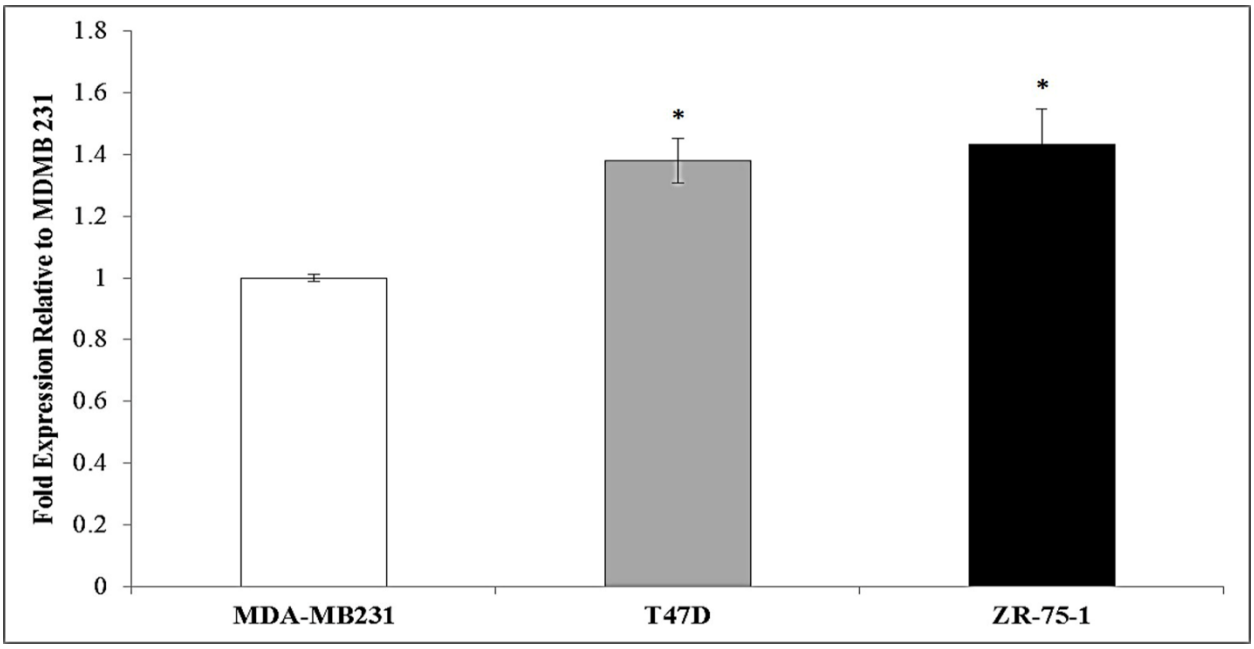

Fig.7.15: Real time-PCR comparing the expression of SVCT2 in MDA-MB231, T47D and ZR-75-1 cells. Data is shown as mean±S.D. n=4. (*$p<0.05$).

Discussion

AA (vitamin C) is a vital cellular nutrient responsible for normal metabolic and physiological functions. Due to biosynthetic limitation, distribution of AA between extra- and intra-cellular fluids in cells is highly dependent on absorption through functional vitamin C transporters [533]. Due to its antioxidant nature causing neutralization of free radicals, AA has been postulated to inhibit cancer initiation and promotion [572]. Several reports have suggested the cytotoxic action of vitamin C against cancer cells [573, 574]. Also, the evidence from various epidemiologic studies cited the role of vitamin C as controversial in breast cancer [572]. All these biological progressions put emphasis on having a thorough understanding of the mechanism of AA transport in breast cancer cell lines. The main goal of this study was to investigate the functional and molecular expression of SVCT2 in human derived breast cancer cells (MDA-MB231, T47D and ZR-75-1). We have selected these cell lines as an *in vitro* cell culture model because of their aggressive phenotype [575, 576]. Hence, in this study we have investigated the functional and molecular aspects of carrier mediated system responsible for AA uptake on these breast carcinoma cells. Another purpose was to delineate the mechanism of uptake and intracellular regulation.

Since time course of AA uptake showed the linear uptake till 60 min, an incubation time of 30 min was selected for all AA uptake studies in MDA-MB231, T47D and ZR-75-1 cells **(Fig.7.1)**. AA uptake appears to be temperature dependent with significant rapid rate at physiological temperature (37ºC) relative to 25ºC and 4ºC **(Figs.7.2 & 7.3)**. Rise in pH resulted in enhanced AA uptake **(Fig.7.4)**. Since the $pKa_{1\ of}$ AA is 4.17, it exists primarily in ascorbate form (-1 charge) above the pH 5.0. As a consequence, enhanced AA uptake observed with rise in pH may not be due to the ionic state of AA. It can be concluded from pH dependency results that SVCT2 shows

higher affinity towards ascorbate at higher pH **(Fig.7.4)** [451, 463]. The major forces between SVCT2 and its substrates, responsible for the binding of SVCT2 with the ionized form of AA are ion–ion and/or ion–polarity interactions. At lower pH, protonation of histidine residues reduces the binding affinity of SVCT2 [463].

In the absence of sodium and chloride ions, lower AA uptake was noticed confirming that SVCT2 transporter system may be highly sodium and chloride dependent **(Fig.7.5)**. Additionally, significant inhibition to AA uptake was observed in the presence of amiloride (a Na^+ transport inhibitor) demonstrating that the transport system is highly sodium dependent **(Fig.7.5)**. Transmembrane sodium gradient as well as the membrane potential are responsible for the uphill transport of SVCT2 substrates [458]. Therefore, we studied whether the carrier mediated transport via SVCT2 is coupled with the electrochemical gradient of Na^+ ions in MDA-MB231, T47D and ZR-75-1 cells. In all these breast cancer cell lines, diminished uptake of AA was observed with decreasing concentrations of Na^+ in the uptake buffer and was found to be saturated at higher concentrations. These results suggest that AA is coupled to Na^+ and transported directly via SVCT2 **(Fig.7.6)**. The Hill ratio analysis indicates that approximately two sodium ions (1.90 for MDA-MB231, 2.05 for T47D and 2.27 for ZR-75-1) are required for translocation of each AA molecule **(Fig.7.7)**.

Concentration dependent uptake of AA clearly reveals that a carrier mediated saturable process is present. In order to distinguish the passive diffusion component from the active AA transport, uptake study was carried out at 4ºC in all the breast carcinoma cells. [^{14}C] AA uptake at 4ºC was significantly lower than that at 37ºC. This suggest the involvement of passive diffusion of AA in thse cell lines. AA uptake was found to be saturable with K_m values of 53.85±6.24, 49.69±2.83 and 45.44±3.16 μM and V_{max} values of 18.45±0.50, 32.50±0.43 and 33.25±0.53

pmol/mg protein/min in MDA-MB231, T47D and ZR-75-1 cells, respectively **(Figs.7.8, 7.9 & 7.10)**. Michaelis-Menten kinetic parameters (K_m and V_{max}) are two vital parameters accountable for functional and kinetic constants of a transporter. K_m defines the measure of apparent binding affinity of a substrate whereas V_{max} represents a measure of translocation capacity of the carrier-mediated process. On the basis of Michaelis-Menten kinetics, the K_m value of SVCT2 was found to be higher in MDA-MB231 in comparison to T47D and ZR-75-1 cells, indicating a higher binding strength and affinity of AA for MDA-MB231 cells. However comparison of V_{max} values of SVCT2 suggest that transport capacity of SVCT2 in T47D and ZR-75-1 is higher relative to MDA-MB231 cells (32.50±0.43 and 33.25±0.53 vs 18.45±0.50 pmol/mg protein/min). Catalytic efficiency of SVCT2 was estimated by the ratio of Michaelis- Menten kinetic parameters (V_{max}/K_m). A variation in V_{max} values results in higher transport efficiency (V_{max}/K_m) of SVCT2 for T47D and ZR-75-1 (0.65 and 0.73 µl/mg protein/min, respectively) than MDA-MB231 (0.34 µl/mg protein/min). These kinetic parameters indicate possible involvement of a carrier mediated transport system for the translocation of AA in MDA-MB231, T47D and ZR-75-1 cell lines. When the kinetic data was plotted in the form of Lineweaver-Burk (1/v vs. 1/[S]) plot, a single line was obtained for MDA-MB231, T47D and ZR-75-1 cells respectively, which suggests possible involvement of a single transporter for the translocation of AA across breast carcinoma cells **(data not shown)**. These Michaelis-Menten kinetic parameters of SVCT2 in MDA-MB231, T47D and ZR-75-1 cells were in accordance with previously published reports showing the presence of SVCT2 across human retinal cells [531].

AA uptake was significantly inhibited in all breast cancer cells in the presence of metabolic inhibitors such as sodium azide (oxidative phosphorylation inhibitor), 2,4-dinitrophenol (intracellular ATP reducer) and ouabain, (a known Na+/K+ ATPase inhibitor). This result suggest

that uptake of AA via SVCT2 is highly dependent on energy and directly coupled to ATP energy sources **(Fig.7.11)**. Uptake of AA was also significantly inhibited in the presence of various membrane/anion inhibitors such as DIDS, SITC, and probenecid **(Fig.7.12)**. Similar reports involving inhibition of AA uptake by membrane inhibitors has been published [460, 462]. These results suggest that AA uptake is altered by the presence of specific anions and the site of the SVCT2 transport system may be the plasma membrane [460, 462].

In MDA-MB231, T47D and ZR-75-1 cells, concentration dependent inhibition of AA uptake mediated via SVCT2 was evident in the presence of structural analogs of AA (L-AA and D-Iso AA). No statistically significant inhibition in the AA uptake via SVCT2 was found in the presence of DHAA (structural analog and GLUT substrate), glucose (GLUT substrate) and PAHA (OAT substrate) (Fig.13). Similar results with respect to substrate specificity have been reported previously from our laboratory [462, 538]. Due to a lack of 3D structure of SVCT2 transporter, it is difficult to postulate about structural requirements for the binding of SVCT2 with its substrates and further investigations are required to address the issue.

Several intracellular regulatory pathways such as Ca^{++}/calmodulin, PKA, PTK and PKC are known to be involved in the regulation of AA transport system [462]. Five putative PKC phosphorylation sites in hSVCT1 and hSVCT2 and one additional PKA site in hSVCT1 have been identified based on the analysis of primary amino acid sequence of SVCT [463]. It has also been reported that AA uptake by SVCT2 expressed in COS-1 and MDCK-MDR1 cells was under the regulation of PKC-mediated pathway [462, 539]. For the same reason, we investigated the regulation of AA uptake by inter- and intra-cellular protein kinase-mediated pathways. Significant inhibition of AA uptake in the presence of calmidazolium and KN-62 was observed in these cell lines suggesting that the AA uptake process is under the regulation of Ca^{++}/CaM mediated

pathway. Cell tretament with PMA led to a significant lowering in AA uptake, indicating the role of PKC-mediated pathway on the regulation of AA uptake. Conversely, addition of BIS (PKC pathway inhibitor) reverses the inhibitory effect of PMA signifying the contribution of PKC pathway in controlling this uptake process **(Table.7.1)**.

On the other hand, significant inhibition on AA uptake by IBMX and forskolin treated breast cancer cells confirms that PKA-mediated pathway plays a vital role in SVCT2 mediated. Significant inhibition was observed in presence of genistein and tyrphostin A25 (PTK pathway modulators) showing a possible role of PTK pathway in intracellular regulation of AA **(Table.7.1)**. Molecular mechanism by which the protein kinase and calmodulin pathway exert their effect on AA uptake process is yet to be fully delineated.

Finally, RT-PCR analysis confirms the molecular evidence of a vitamin C/AA specific carrier system in MDA-MB231, T47D and ZR-75-1 cells. An expression of SVCT2 on breast carcinoma cell lines were verified by a specific primer set for the gene. The expression was confirmed by the presence of strong bands of desired size. The PCR product obtained at 626 bp is specific for the SVCT2 transporter system **(Fig.7.14)**. There was a non-specific band of a slightly lower molecular weight observed in the primer set for T47D. qPCR analysis revealed that the expression of SVCT2 was significantly higher in T47D and ZR-75-1 cells in comparison to MDA-MB231 cells **(Fig.7.15).** Higher expression of SVCT2 in T47D and ZR-75-1 provides the justification of greater catalytic transporter efficiency of SVCT2 in T47D and ZR-75-1 relative to MDA-MB231 cells.

Conclusion

In summary, this work clearly delineates the functional activity and molecular evidence as well as the expression, contribution, and regulation of the sodium-dependent vitamin C transporter

2 (SVCT2) across MDA-MB231, T47D and ZR-75-1 cell lines. AA uptake across MDA-MB231, T47D and ZR-75-1 cells involves a carrier-mediated active process which is controlled by both Ca^{++}/CaM mediated as well as protein kinases pathways. This transporter is highly pH dependent and requires coupling to an electrochemical Na^{+} gradient and ATP sources for cellular uptake. This membrane transporter (SVCT2) can be utilized as a potential target for enhancing permeability and bioavailability of highly potent anti-cancer drugs. Our investigation demonstrates complete profiling of SVCT2 mediated AA uptake and its dependence on calmodulin, protein kinases and intracellular ions. Demarcation of AA uptake and transport mechanism by SVCT2 can aid in achieving therapeutic drug concentrations at the target site. The results may help in providing cancer chemotherapy by evasion of efflux pumps in cancer cells and overcoming chemotherapeutic resistance which is an obstacle in the treatment of breast cancer. Also, MDA-MB231, T47D and ZR-75-1 cell lines can be utilized as a valuable *in vitro* model to investigate absorption and permeability of AA-conjugated chemotherapeutics.

Acknowledgement

This work was supported by National Institutes of Health grant 1R01 AI071199. The authors highly appreciate Dr. Walter Jäger University of Vienna, Austria) and Dr. A.J. van Agthoven (Josephine Nefkens Institute, Netherlands) for their generous gift of MDA-MB231 and ZR-75-1 cell lines.

CHAPTER 8

SUMMARY AND RECOMMENDATIONS

Summary

Currently, hepatic transport processes has been recognized as a vital factor in determining drug disposition. Hence, evaluation of the hepatic transport and biliary excretion properties of prospective drug candidates plays a major role in drug development process. This information provides understanding of any altered hepatic disposition of therapeutic agents due to drug interactions and diseased states. Translocation of drug molecules across the sinusoidal membrane is mediated via basolateral transport system, whereas the biliary excretion of therapeutic agents and metabolites is mediated via active canalicular transport. Basolateral transport proteins consist of several membrane transporters including organic anion transporting polypeptides [OATPs (SLCO family)], organic anion and cation transporters [OATs, OCTs (SLC22A family)], Na^+-taurocholate co-transporting polypeptide [NTCP (SLC10A1)] and multidrug resistance-associated proteins [MRPs (ABCC family)]. P-glycoprotein (ABCB1), MRP2 (ABCC2), breast cancer resistance protein [BCRP (ABCG2)] and the bile salt export pump [BSEP (ABCB11)] forms the active canalicular transport system [1].

Metabolism of tyrosine kinase inhibitors (TKIs) is mainly mediated via hepatic route, but the mechanism responsible for their hepatocellular accumulation is still unknown. This study was designed to understand the contribution of organic anion transporting polypeptides (OATPs) in the hepatic uptake of selected TKIs - pazopanib, canertinib, erlotinib, vandetanib and nilotinib (Chapter 2). Michaelis-Menten (MM) kinetic parameters for TKIs were determined by concentration dependent cellular accumulation of selected TKIs using Chinese Hamster Ovary (CHO) cells - wild type as well as transfected with humanized OATP-1B1 and OATP-1B3

transporter proteins. The MM constant, K_m values of OATP-1B1 for nilotinib and vandetanib are 10.14±1.91 and 2.72±0.25μM respectively and V_{max} values of OATP-1B1 for nilotinib and vandetanib were 6.95±0.47 and 75.95±1.99 nmoles/mg protein/min respectively. Likewise, K_m values of OATP-1B3 for canertinib, nilotinib and vandetanib were 12.18±3.32, 7.84±1.43 and 4.37±0.79μM respectively and V_{max} values of OATP-1B3 for canertinib, nilotinib and vandetanib were 15.34±1.59, 6.75±0.42 and 194.64±10.58 nmoles/mg protein/min respectively. Canertinib did not exhibit any substrate specificity towards OATP-1B1. Also, erlotinib and pazopanib did not exhibit any substrate specificity towards OATP-1B1 and -1B3. Since selected TKIs are the substrates of OATP-1B1 and -1B3 expressed in hepatic tissue, these compounds can be regarded as molecular targets for transporter mediated DDIs. Any alteration in the function of these hepatic OATPs might account for the pharmacokinetic variability of TKIs.

The potential of tyrosine kinase inhibitors (TKIs) as interacting drugs through hepatic uptake transporter inhibition has not been fully exploited in drug-drug interactions (DDIs). This study was designed to estimate the half maximal inhibitory concentration (IC_{50}) values of 5 small molecule TKIs (pazopanib, nilotinib, vandetanib, canertinib and erlotinib) for organic anion transporting polypeptides (OATPs): OATP-1B1 and -1B3 (Chapter 3). The half maximal inhibitory concentration (IC_{50}) values of TKIs and rifampicin (positive control) were determined by concentration dependent inhibition of TKIs on cellular accumulation of probe radiolabelled substrates [^{3}H] ES and [^{3}H] CCK-8. Chinese Hamster Ovary (CHO) cells transfected with humanized OATP-1B1 and OATP-1B3 transporter proteins, respectively, were utilized to carry out these studies. Pazopanib and nilotinib shows its inhibitory activity on OATP-1B1 transporter protein. The IC_{50} values for rifampicin, pazopanib and nilotinib were 10.46±1.15, 3.89±1.21 and 2.78±1.13 μM respectively for OATP-1B1 transporter. Vandetanib, canertinib and erlotinib did

not exhibit any inhibitory potency towards OATP-1B1 transporter protein. Only vandetanib showed tis inhibitory potential towards OATP-1B3 transporter proteins out of the 5 selected TKIs. The IC_{50} values for rifampicin and vandetanib for OATP-1B3 transporter inhibition were 3.67±1.20 and 18.13±1.21 μM respectively. No significant inhibition in the presence of increasing concentrations of pazopanib, nilotinib, canertinib and erlotinib were observed towards OATP-1B3 transporter. Since selected TKIs are the inhibitors of OATP-1B1 and -1B3 expressed in hepatic tissue, these compounds can be regarded as molecular targets for transporter mediated DDIs. These finding provide the basis of further pre-clinical and clinical studies investigating the transporter based DDI potential of TKIs.

Expression of drug transporters across various tissues like brain, ocular, liver, kidney and intestine has been reported before. These membrane transporters play an important role in drug absorption, distribution, metabolism and excretion. Also, the functionality of these transporters can be exploited and explored in terms of drug delivery in order to improve the absorption and permeation of drug across membrane by targeting specific transporter proteins [577]. Corneal epithelium and blood-retina barrier (i.e. retinal capillaries and retinal pigment epithelium (RPE)) acts as vital membranes governing the admittance of xenobiotics into the ocular tissues. Following topical administration, corneal epithelium limits the absorption of drug from the lacrimal fluid into the anterior chamber, while restriction of drug entry from systemic circulation to the posterior segment is regulated via blood-retina barrier. Involvement of membrane transporters for translocating drug across the membranes is quite limited relative to passive diffusion. However, after revelation of functionality of these membrane transporters, it has been attributed that these transporters play a vital role in modulating the pharmacokinetics of the therapeutic agent. Many drugs are known substrates of the transporters, however, the understanding about studies involving

expression and functionality of these transporters in ocular tissues is limited. Hence, these transporters have a vital role in regulating the ocular pharmacokinetics of a drug molecule [508].

The main aim of this study was to design novel pentablock (PB) (PLA–PCL–PEG–PCL–PLA) polymer to prepare nanoparticles (NP) in order to achieve sustain delivery of pazopanib with minimal burst effect for the treatment of ocular neovascularization. Another purpose was to evaluate the effect of pazopanib loaded NP to bypass drug efflux (Chapter 5). PB copolymer was successfully synthesized using ring opening polymerization reaction mechanism and characterized using ^{1}H NMR, GPC and XRD analysis. Synthesized PB copolymer was found to non-cytotoxic, non-immunogenic and biocompatible with ocular cell lines. Also, several parameters such as entrapment efficiency, drug loading, *in vitro* drug release profiling and effect of pazopanib NP in evading efflux transporters were examined. PB copolymer-based NP exhibited continuous release of pazopanib. It can be utilized to achieve continuous first order delivery of pazopanib upto 100 days from nanoparticles without any significant burst effect. Pazopanib loaded NP were successful in evading drug efflux mediated via efflux transporters. This formulation can be employed to circumvent ocular barriers without altering ocular protective mechanisms. Our results indicated that PB copolymer based drug delivery systems can serve as a platform technology for the development of sustained release therapy for the treatment of ocular neovascularization. This drug delivery system can also be applicable for other ocular complications.

Ascorbic Acid (AA, Vitamin C) is an essential vitamin responsible for normal cellular growth and physiological and metabolic functions**.** AA act as an anti-oxidant and absorbs the UV radiation, thus protecting the cornea, retina and other intraocular tissues against radiation induced damage. AA relieves the oxidative stress accompanying various eye infections. However, the uptake mechanism of AA in human corneal and retinal cells along with its cellular translocation

and intracellular trafficking are poorly understood. The main goal of this study is to investigate the existence of sodium dependent vitamin C transport system (SVCT2) and to define time dependent uptake mechanism and intracellular regulation of AA in human corneal epithelial (HCEC) and human retinal pigment epithelial (D407) cells (Chapter 6). Uptake of [^{14}C] AA was observed to be sodium, chloride, temperature, pH and energy dependent in both cell lines. [^{14}C] AA uptake was found to be saturable, with K_m values of 46.14±6.03 and 47.26±3.24 μM and V_{max} values of 17.34±0.58 and 31.86±0.56 pmol/min/mg protein, across HCEC and D407 cells, respectively. The process is inhibited by structural analogs (L-AA and D-Iso AA) but not by structurally unrelated substrates (glucose and PAHA). Ca^{++}/calmodulin and protein kinase C (PKC) pathways play an important role in modulating uptake of AA. A 626 bp band corresponding to a vitamin C transporter (SVCT2) has been identified by RT-PCR analysis in both the cell lines. This study reports the ascorbic acid uptake mechanism, kinetics, and regulation by sodium dependent vitamin C transporter (SVCT2) in HCEC and D407 cells. Also, SVCT2 can be utilized for targeted delivery in enhancing ocular permeation and bioavailability of highly potent ophthalmic drugs.

The main goal of this study is to investigate the existence of sodium dependent vitamin C transport system (SVCT2) and to define uptake mechanism and intracellular regulation of ascorbic acid (AA) in human breast cancer cells (MDA-MB231, T47D and ZR-75-1) (Chapter 7). Uptake of [^{14}C] AA was studied in MDA-MB231, T47D and ZR-75-1 cells. Functional aspects of [^{14}C] AA uptake were studied in the presence of different concentrations of unlabeled AA, pH, temperature, metabolic inhibitors, substrates and structural analogs. Molecular identification of SVCT2 was examined with reverse transcription–polymerase chain reaction (RT-PCR). Uptake of [^{14}C] AA was observed to be sodium, chloride, temperature, pH and energy dependent in all the breast cancer cell lines. [^{14}C] AA uptake was found to be saturable, with K_m values of 53.85±6.24,

49.69±2.83 and 45.44±3.16 μM and V_{max} values of 18.45±0.50, 32.50±0.43 and 33.25±0.53 pmol/min/mg protein, across MDA-MB231, T47D and ZR-75-1, respectively. The process is inhibited by structural analogs (L-AA and D-Iso AA) but not by structurally unrelated substrates (glucose and PAHA). Ca^{++}/calmodulin and protein kinase pathways were found to play a crucial role in modulating uptake of AA. A 626 bp band corresponding to a vitamin C transporter (SVCT2) based on the primer design was observed by RT-PCR analysis in all the breast cancer cell lines. This study reports AA uptake mechanism, kinetics, and regulation by sodium dependent vitamin C transporter (SVCT2) in MDA-MB231, T47D and ZR-75-1 cells. Also, SVCT2 can be utilized for designing targeted delivery to circumvent efflux and enhance permeation and bioavailability of highly potent chemotherapeutic drugs.

Recommendations

The above studies aimed at understanding the disposition of tyrosine kinase inhibitors (TKIs) on interaction with hepatic OATP-1B1 and -1B3. A few recommendations that can be made based on the results obtained from the above studies are:

- To study transcellular transport of TKIs across a double-transfected MDCKII cell monolayer expressing both Human OATP and MRP2. This study can help in delineating the role of hepatic uptake and efflux transporters in governing disposition of TKIs.
- To study transcellular transport of TKIs across a double-transfected MDCKII cell monolayer expressing both Human OATP and CYP3A4. This study can help in delineating the role of hepatic uptake and metabolizing enzymes in governing disposition of TKIs.
- These are proof of concept studies performed on *in vitro* transfected cell culture model. Further *in vivo* studies on transgenic mouse model are required for better understanding of

the contribution of OATP-1B1 and/or -1B3 transporter proteins in the hepatic disposition of TKIs and for predicting any adverse drug reactions associated with DDIs.

The other project was aimed at enhancing the bioavailability of therapeutic agents by evading drug efflux by formulating into NPs. The influx transporters were also characterized across ocular and breast cancer cells. These transporters can be utilized as a target for designing of better therapeutic agents.

- A novel approach of a NPs embedded in thermosensitive gel can be utilized to further sustain the release of small and macromolecules and it will also imparts stability to the drug molecule.
- Since Pazopanib is a substrate for efflux transporter. Surface modified NPs can be utilized for targeted drug delivery. Ascorbic acid surface modified PB NPs might be recognized by vitamin C transporter (SVCT2) located on the apical site of the corneal and retinal pigment epithelial cells. Hence via surface modification approach, uptake of NPs across target site can be enhanced. Our composite formulation approach may serve as a platform technology for the delivery of small and macro molecules in the treatment of ocular diseases.
- Also, these surface modified PB NPs can be utilized to target breast cancer cells expressing vitamin C transporter (SVCT2). Targeted delivery to SVCT2 will not only circumvent efflux but also enhance permeation and bioavailability of highly potent chemotherapeutic drugs.
- Ascorbic acid prodrugs of pazopanib can be synthesized to circumvent efflux. These ascorbic acid conjugated pazopanib may enhance permeability and bioavailability of pazopanib across targeted tissue.

APPENDIX

SPRINGER LICENSE
TERMS AND CONDITIONS

Feb 26, 2014

This is a License Agreement between Varun Khurana ("You") and Springer ("Springer") provided by Copyright Clearance Center ("CCC"). The license consists of your order details, the terms and conditions provided by Springer, and the payment terms and conditions.

All payments must be made in full to CCC. For payment instructions, please see information listed at the bottom of this form.

License Number	3336751045590
License date	Feb 26, 2014
Licensed content publisher	Springer
Licensed content publication	Springer eBook
Licensed content title	Uptake Transporters of the Human OATP Family
Licensed content author	Jörg König
Licensed content date	Jan 1, 2011
Type of Use	Thesis/Dissertation
Portion	Full text
Number of copies	50
Author of this Springer article	No
Order reference number	
Title of your thesis / dissertation	Role of membrane transporters in drug delivery, drug disposition and drug–drug interactions
Expected completion date	May 2014
Estimated size(pages)	200
Total	0.00 USD

SPRINGER LICENSE
TERMS AND CONDITIONS

Feb 26, 2014

This is a License Agreement between Varun Khurana ("You") and Springer ("Springer") provided by Copyright Clearance Center ("CCC"). The license consists of your order details, the terms and conditions provided by Springer, and the payment terms and conditions.

All payments must be made in full to CCC. For payment instructions, please see information listed at the bottom of this form.

License Number	3336750790954
License date	Feb 26, 2014
Licensed content publisher	Springer
Licensed content publication	Pharmaceutical Research
Licensed content title	The Complexities of Hepatic Drug Transport: Current Knowledge and Emerging Concepts
Licensed content author	Priyamvada Chandra
Licensed content date	Jan 1, 2004
Volume number	21
Issue number	5
Type of Use	Thesis/Dissertation
Portion	Full text
Number of copies	50
Author of this Springer article	No
Order reference number	
Title of your thesis / dissertation	Role of membrane transporters in drug delivery, drug disposition and drug-drug interactions
Expected completion date	May 2014
Estimated size(pages)	200
Total	0.00 USD

ELSEVIER LICENSE
TERMS AND CONDITIONS

Feb 26, 2014

This is a License Agreement between Varun Khurana ("You") and Elsevier ("Elsevier") provided by Copyright Clearance Center ("CCC"). The license consists of your order details, the terms and conditions provided by Elsevier, and the payment terms and conditions.

All payments must be made in full to CCC. For payment instructions, please see information listed at the bottom of this form.

Supplier	Elsevier Limited The Boulevard,Langford Lane Kidlington,Oxford,OX5 1GB,UK
Registered Company Number	1982084
Customer name	Varun Khurana
Customer address	UMKC, School of Pharmacy, Kansas City, MO 64108
License number	3336751470670
License date	Feb 26, 2014
Licensed content publisher	Elsevier
Licensed content publication	Advanced Drug Delivery Reviews
Licensed content title	PLGA nanoparticles containing various anticancer agents and tumour delivery by EPR effect
Licensed content author	Sarbari Acharya,Sanjeeb K. Sahoo
Licensed content date	18 March 2011
Licensed content volume number	63
Licensed content issue number	3
Number of pages	14
Start Page	170
End Page	183
Type of Use	reuse in a thesis/dissertation
Intended publisher of new work	other
Portion	full article
Format	both print and electronic
Are you the author of this Elsevier article?	No

Will you be translating?	No
Title of your thesis/dissertation	Role of membrane transporters in drug delivery, drug disposition and drug-drug interactions
Expected completion date	May 2014
Estimated size (number of pages)	200
Elsevier VAT number	GB 494 6272 12
Permissions price	0.00 USD
VAT/Local Sales Tax	0.00 USD / 0.00 GBP
Total	0.00 USD

RE: Republication/Electronic Request Form

Wiley Global Permissions <permissions@wiley.com>

Tue 2/25/2014 3:43 AM

To:Khurana, Varun (UMKC-Student) <varunkhurana@mail.umkc.edu>;

Dear VARUN KHURANA

Thank you for your request.

Permission is granted for you to use the material requested for your thesis/dissertation subject to the usual acknowledgements and on the understanding that you will reapply for permission if you wish to distribute or publish your thesis/dissertation commercially.

Permission is granted solely for use in conjunction with the thesis, and the article may not be posted online separately.

Any third party material is expressly excluded from this permission. If any material appears within the article with credit to another source, authorisation from that source must be obtained.

Yours sincerely

Duncan James
Associate Permissions Manager
John Wiley & Sons Ltd
The Atrium
Southern Gate, Chichester
West Sussex, PO19 8SQ
UK

——Original Message——
From: PermissionsUS@wiley.com on www.wiley.com [mailto:webmaster@wiley.com]
Sent: Saturday, 15 February, 2014 3:35 AM
To: Permissions - US
Subject: Republication/Electronic Request Form

A01_First_Name: VARUN
A02_Last_Name: KHURANA
A03_Company_Name: UNIVERSITY OF MISSOURI KANSAS CITY
A04_Address: 2464 CHARLOTTE STREET, HSB 5258,
A05_City: KANSAS CITY
A06_State: MO
A07_Zip: 64108
A08_Country: USA
A09_Contact_Phone_Number: 8167699305
A10_Fax:
A11_Emails: varunkhurana@mail.umkc.edu
A12_Reference:
A13_Book_Title: Advanced Drug Delivery

A40_Book_or_Journal: Book
A14_Book_Author: ASHIM K MITRA
A15_Book_ISBN: 978-1-118-02266-5
A16_Journal_Month:
A17_Journal_Year:
A18_Journal_Volume:
A19_Journal_Issue_Number:
A20_Copy_Pages: FULL TEXT
A21_Maximum_Copies: 50
A22_Your_Publisher: University of Missouri Kansas City
A23_Your_Title: Role of membrane transporters in drug delivery, drug disposition and drug-drug interactions
A24_Publication_Date: May 2014
A25_Format: print,E-Book
A41_Ebook_Reader_Type: Adobe Acrobat
A26_If_WWW_URL:
A27_If_WWW_From_Adopted_Book:
A28_If_WWW_Password_Access:
A45_WWW_Users:
A29_If_WWW_Material_Posted_From:
A30_If_WWW_Material_Posted_To:
A42_If_Intranet_URL:
A32_If_Intranet_From_Adopted_Book:
A33_If_Intranet_Password_Access:
A48_Intranet_Users:
A34_If_Intranet_Material_Posted_From:
A35_If_Intranet_Material_Posted_To:
A50_If_Software_Print_Type:
A60_If_Other_Type:
A37_Comments_For_Request: I am the leading/first author of the chapter for which I am requesting permission to reprint. I want to reuse/reprint Chapter 3: The Role of Transporters and the Efflux System in Drug Delivery (Page 47) in my thesis/dissertation.

Thanks and Regards
Varun Khurana

License Details

Thank you very much for your order.

This is a License Agreement between Varun Khurana ("You") and Elsevier ("Elsevier"). The license consists of your order details, the terms and conditions provided by Elsevier, and the payment terms and conditions.

Get the printable license.

License Number	3337250585992
License date	Feb 27, 2014
Licensed content publisher	Elsevier
Licensed content publication	Advanced Drug Delivery Reviews
Licensed content title	Drug transport proteins in the liver
Licensed content author	Klaas Nico Faber,Michael Müller,Peter L.M Jansen
Licensed content date	21 January 2003
Licensed content volume number	55
Licensed content issue number	1
Number of pages	18
Type of Use	reuse in a thesis/dissertation
Portion	full article
Format	both print and electronic
Are you the author of this Elsevier article?	No
Will you be translating?	No
Title of your thesis/dissertation	Role of membrane transporters in drug delivery, drug disposition and drug-drug interactions
Expected completion date	May 2014
Estimated size (number of pages)	200
Elsevier VAT number	GB 494 6272 12
Permissions price	0.00 USD
VAT/Local Sales Tax	0.00 USD / 0.00 GBP
Total	**0.00 USD**

Order Completed

Thank you very much for your order.

This is a License Agreement between Varun Khurana ("You") and Elsevier ("Elsevier"). The license consists of your order details, the terms and conditions provided by Elsevier, and the payment terms and conditions.

Get the printable license.

License Number	3337250669807
License date	Feb 27, 2014
Licensed content publisher	Elsevier
Licensed content publication	Advanced Drug Delivery Reviews
Licensed content title	Drug transport in corneal epithelium and blood–retina barrier: Emerging role of transporters in ocular pharmacokinetics
Licensed content author	Eliisa Mannermaa,Kati-Sisko Vellonen,Arto Urtti
Licensed content date	15 November 2006
Licensed content volume number	58
Licensed content issue number	11
Number of pages	28
Type of Use	reuse in a thesis/dissertation
Portion	full article
Format	both print and electronic
Are you the author of this Elsevier article?	No
Will you be translating?	No
Title of your thesis/dissertation	Role of membrane transporters in drug delivery, drug disposition and drug-drug interactions
Expected completion date	May 2014
Estimated size (number of pages)	200
Elsevier VAT number	GB 494 6272 12
Permissions price	0.00 USD
VAT/Local Sales Tax	0.00 USD / 0.00 GBP
Total	0.00 USD

LIST OF REFERENCES

1. Chandra P, Brouwer KL. The complexities of hepatic drug transport: current knowledge and emerging concepts. Pharm Res. 2004;21719-35.
2. Hagenbuch B, Stieger B, Foguet M, Lubbert H, Meier PJ. Functional expression cloning and characterization of the hepatocyte Na+/bile acid cotransport system. Proc Natl Acad Sci U S A. 1991;8810629-33.
3. Meier PJ, Eckhardt U, Schroeder A, Hagenbuch B, Stieger B. Substrate specificity of sinusoidal bile acid and organic anion uptake systems in rat and human liver. Hepatology. 1997;261667-77.
4. Kullak-Ublick GA, Ismair MG, Kubitz R, Schmitt M, Haussinger D, Stieger B, et al. Stable expression and functional characterization of a Na+-taurocholate cotransporting green fluorescent protein in human hepatoblastoma HepG2 cells. Cytotechnology. 2000;341-9.
5. Friesema EC, Docter R, Moerings EP, Stieger B, Hagenbuch B, Meier PJ, et al. Identification of thyroid hormone transporters. Biochem Biophys Res Commun. 1999;254497-501.
6. Li L, Lee TK, Meier PJ, Ballatori N. Identification of glutathione as a driving force and leukotriene C4 as a substrate for oatp1, the hepatic sinusoidal organic solute transporter. J Biol Chem. 1998;27316184-91.
7. Hagenbuch B, Gui C. Xenobiotic transporters of the human organic anion transporting polypeptides (OATP) family. Xenobiotica. 2008;38778-801.
8. Konig J. Uptake transporters of the human OATP family: molecular characteristics, substrates, their role in drug-drug interactions, and functional consequences of polymorphisms. Handb Exp Pharmacol. 20111-28.
9. Kullak-Ublick GA, Ismair MG, Stieger B, Landmann L, Huber R, Pizzagalli F, et al. Organic anion-transporting polypeptide B (OATP-B) and its functional comparison with three other OATPs of human liver. Gastroenterology. 2001;120525-33.
10. Tamai I, Nezu J, Uchino H, Sai Y, Oku A, Shimane M, et al. Molecular identification and characterization of novel members of the human organic anion transporter (OATP) family. Biochem Biophys Res Commun. 2000;273251-60.
11. Kullak-Ublick GA, Hagenbuch B, Stieger B, Wolkoff AW, Meier PJ. Functional characterization of the basolateral rat liver organic anion transporting polypeptide. Hepatology. 1994;20411-6.
12. Cattori V, van Montfoort JE, Stieger B, Landmann L, Meijer DK, Winterhalter KH, et al. Localization of organic anion transporting polypeptide 4 (Oatp4) in rat liver and comparison of its substrate specificity with Oatp1, Oatp2 and Oatp3. Pflugers Arch. 2001;443188-95.
13. Fujiwara K, Adachi H, Nishio T, Unno M, Tokui T, Okabe M, et al. Identification of thyroid hormone transporters in humans: different molecules are involved in a tissue-specific manner. Endocrinology. 2001;1422005-12.
14. Tirona RG, Kim RB. Pharmacogenomics of organic anion-transporting polypeptides (OATP). Adv Drug Deliv Rev. 2002;541343-52.
15. Sekine T, Cha SH, Tsuda M, Apiwattanakul N, Nakajima N, Kanai Y, et al. Identification of multispecific organic anion transporter 2 expressed predominantly in the liver. FEBS Lett. 1998;429179-82.

16. Kusuhara H, Sekine T, Utsunomiya-Tate N, Tsuda M, Kojima R, Cha SH, et al. Molecular cloning and characterization of a new multispecific organic anion transporter from rat brain. J Biol Chem. 1999;27413675-80.
17. Kullak-Ublick GA, Beuers U, Paumgartner G. Hepatobiliary transport. J Hepatol. 2000;323-18.
18. Sun W, Wu RR, van Poelje PD, Erion MD. Isolation of a family of organic anion transporters from human liver and kidney. Biochem Biophys Res Commun. 2001;283417-22.
19. Enomoto A, Takeda M, Shimoda M, Narikawa S, Kobayashi Y, Kobayashi Y, et al. Interaction of human organic anion transporters 2 and 4 with organic anion transport inhibitors. J Pharmacol Exp Ther. 2002;301797-802.
20. Kimura H, Takeda M, Narikawa S, Enomoto A, Ichida K, Endou H. Human organic anion transporters and human organic cation transporters mediate renal transport of prostaglandins. J Pharmacol Exp Ther. 2002;301293-8.
21. Babu E, Takeda M, Narikawa S, Kobayashi Y, Yamamoto T, Cha SH, et al. Human organic anion transporters mediate the transport of tetracycline. Jpn J Pharmacol. 2002;8869-76.
22. Khamdang S, Takeda M, Noshiro R, Narikawa S, Enomoto A, Anzai N, et al. Interactions of human organic anion transporters and human organic cation transporters with nonsteroidal anti-inflammatory drugs. J Pharmacol Exp Ther. 2002;303534-9.
23. Takeda M, Khamdang S, Narikawa S, Kimura H, Kobayashi Y, Yamamoto T, et al. Human organic anion transporters and human organic cation transporters mediate renal antiviral transport. J Pharmacol Exp Ther. 2002;300918-24.
24. Takeda M, Khamdang S, Narikawa S, Kimura H, Hosoyamada M, Cha SH, et al. Characterization of methotrexate transport and its drug interactions with human organic anion transporters. J Pharmacol Exp Ther. 2002;302666-71.
25. Babu E, Takeda M, Narikawa S, Kobayashi Y, Enomoto A, Tojo A, et al. Role of human organic anion transporter 4 in the transport of ochratoxin A. Biochim Biophys Acta. 2002;159064-75.
26. Grundemann D, Gorboulev V, Gambaryan S, Veyhl M, Koepsell H. Drug excretion mediated by a new prototype of polyspecific transporter. Nature. 1994;372549-52.
27. Zhang L, Dresser MJ, Gray AT, Yost SC, Terashita S, Giacomini KM. Cloning and functional expression of a human liver organic cation transporter. Mol Pharmacol. 1997;51913-21.
28. Meyer-Wentrup F, Karbach U, Gorboulev V, Arndt P, Koepsell H. Membrane localization of the electrogenic cation transporter rOCT1 in rat liver. Biochem Biophys Res Commun. 1998;248673-8.
29. Hayer-Zillgen M, Bruss M, Bonisch H. Expression and pharmacological profile of the human organic cation transporters hOCT1, hOCT2 and hOCT3. Br J Pharmacol. 2002;136829-36.
30. Tamai I, Yabuuchi H, Nezu J, Sai Y, Oku A, Shimane M, et al. Cloning and characterization of a novel human pH-dependent organic cation transporter, OCTN1. FEBS Lett. 1997;419107-11.
31. Wu X, Prasad PD, Leibach FH, Ganapathy V. cDNA sequence, transport function, and genomic organization of human OCTN2, a new member of the organic cation transporter family. Biochem Biophys Res Commun. 1998;246589-95.
32. Borst P, Evers R, Kool M, Wijnholds J. The multidrug resistance protein family. Biochim Biophys Acta. 1999;1461347-57.

33. Roelofsen H, Muller M, Jansen PL. Regulation of organic anion transport in the liver. Yale J Biol Med. 1997;70435-45.
34. Flens MJ, Zaman GJ, van der Valk P, Izquierdo MA, Schroeijers AB, Scheffer GL, et al. Tissue distribution of the multidrug resistance protein. Am J Pathol. 1996;1481237-47.
35. Loe DW, Deeley RG, Cole SP. Characterization of vincristine transport by the M(r) 190,000 multidrug resistance protein (MRP): evidence for cotransport with reduced glutathione. Cancer Res. 1998;585130-6.
36. Hirohashi T, Suzuki H, Sugiyama Y. Characterization of the transport properties of cloned rat multidrug resistance-associated protein 3 (MRP3). J Biol Chem. 1999;27415181-5.
37. Hirohashi T, Suzuki H, Takikawa H, Sugiyama Y. ATP-dependent transport of bile salts by rat multidrug resistance-associated protein 3 (Mrp3). J Biol Chem. 2000;2752905-10.
38. Xiong H, Turner KC, Ward ES, Jansen PL, Brouwer KL. Altered hepatobiliary disposition of acetaminophen glucuronide in isolated perfused livers from multidrug resistance-associated protein 2-deficient TR(-) rats. J Pharmacol Exp Ther. 2000;295512-8.
39. Ogawa K, Suzuki H, Hirohashi T, Ishikawa T, Meier PJ, Hirose K, et al. Characterization of inducible nature of MRP3 in rat liver. Am J Physiol Gastrointest Liver Physiol. 2000;278G438-46.
40. Konig J, Rost D, Cui Y, Keppler D. Characterization of the human multidrug resistance protein isoform MRP3 localized to the basolateral hepatocyte membrane. Hepatology. 1999;291156-63.
41. Reid G, Wielinga P, Zelcer N, De Haas M, Van Deemter L, Wijnholds J, et al. Characterization of the transport of nucleoside analog drugs by the human multidrug resistance proteins MRP4 and MRP5. Mol Pharmacol. 2003;631094-103.
42. Chen ZS, Lee K, Kruh GD. Transport of cyclic nucleotides and estradiol 17-beta-D-glucuronide by multidrug resistance protein 4. Resistance to 6-mercaptopurine and 6-thioguanine. J Biol Chem. 2001;27633747-54.
43. Jedlitschky G, Burchell B, Keppler D. The multidrug resistance protein 5 functions as an ATP-dependent export pump for cyclic nucleotides. J Biol Chem. 2000;27530069-74.
44. Chen ZS, Lee K, Walther S, Raftogianis RB, Kuwano M, Zeng H, et al. Analysis of methotrexate and folate transport by multidrug resistance protein 4 (ABCC4): MRP4 is a component of the methotrexate efflux system. Cancer Res. 2002;623144-50.
45. Schuetz JD, Connelly MC, Sun D, Paibir SG, Flynn PM, Srinivas RV, et al. MRP4: A previously unidentified factor in resistance to nucleoside-based antiviral drugs. Nat Med. 1999;51048-51.
46. Zelcer N, Reid G, Wielinga P, Kuil A, van der Heijden I, Schuetz JD, et al. Steroid and bile acid conjugates are substrates of human multidrug-resistance protein (MRP) 4 (ATP-binding cassette C4). Biochem J. 2003;371361-7.
47. Schuetz EG, Strom S, Yasuda K, Lecureur V, Assem M, Brimer C, et al. Disrupted bile acid homeostasis reveals an unexpected interaction among nuclear hormone receptors, transporters, and cytochrome P450. J Biol Chem. 2001;27639411-8.
48. Madon J, Hagenbuch B, Landmann L, Meier PJ, Stieger B. Transport function and hepatocellular localization of mrp6 in rat liver. Mol Pharmacol. 2000;57634-41.
49. Kool M, van der Linden M, de Haas M, Baas F, Borst P. Expression of human MRP6, a homologue of the multidrug resistance protein gene MRP1, in tissues and cancer cells. Cancer Res. 1999;59175-82.

50. Hopper E, Belinsky MG, Zeng H, Tosolini A, Testa JR, Kruh GD. Analysis of the structure and expression pattern of MRP7 (ABCC10), a new member of the MRP subfamily. Cancer Lett. 2001;162181-91.
51. Chen ZS, Hopper-Borge E, Belinsky MG, Shchaveleva I, Kotova E, Kruh GD. Characterization of the transport properties of human multidrug resistance protein 7 (MRP7, ABCC10). Mol Pharmacol. 2003;63351-8.
52. Bera TK, Lee S, Salvatore G, Lee B, Pastan I. MRP8, a new member of ABC transporter superfamily, identified by EST database mining and gene prediction program, is highly expressed in breast cancer. Mol Med. 2001;7509-16.
53. Guo Y, Kotova E, Chen ZS, Lee K, Hopper-Borge E, Belinsky MG, et al. MRP8, ATP-binding cassette C11 (ABCC11), is a cyclic nucleotide efflux pump and a resistance factor for fluoropyrimidines 2',3'-dideoxycytidine and 9'-(2'-phosphonylmethoxyethyl)adenine. J Biol Chem. 2003;27829509-14.
54. Hyde SC, Emsley P, Hartshorn MJ, Mimmack MM, Gileadi U, Pearce SR, et al. Structural model of ATP-binding proteins associated with cystic fibrosis, multidrug resistance and bacterial transport. Nature. 1990;346362-5.
55. Gerloff T, Stieger B, Hagenbuch B, Madon J, Landmann L, Roth J, et al. The sister of P-glycoprotein represents the canalicular bile salt export pump of mammalian liver. J Biol Chem. 1998;27310046-50.
56. Strautnieks SS, Bull LN, Knisely AS, Kocoshis SA, Dahl N, Arnell H, et al. A gene encoding a liver-specific ABC transporter is mutated in progressive familial intrahepatic cholestasis. Nat Genet. 1998;20233-8.
57. Jansen PL, Strautnieks SS, Jacquemin E, Hadchouel M, Sokal EM, Hooiveld GJ, et al. Hepatocanalicular bile salt export pump deficiency in patients with progressive familial intrahepatic cholestasis. Gastroenterology. 1999;1171370-9.
58. Konig J, Nies AT, Cui Y, Leier I, Keppler D. Conjugate export pumps of the multidrug resistance protein (MRP) family: localization, substrate specificity, and MRP2-mediated drug resistance. Biochim Biophys Acta. 1999;1461377-94.
59. Jansen PL, Groothuis GM, Peters WH, Meijer DF. Selective hepatobiliary transport defect for organic anions and neutral steroids in mutant rats with hereditary-conjugated hyperbilirubinemia. Hepatology. 1987;771-6.
60. Paulusma CC, Bosma PJ, Zaman GJ, Bakker CT, Otter M, Scheffer GL, et al. Congenital jaundice in rats with a mutation in a multidrug resistance-associated protein gene. Science. 1996;2711126-8.
61. Ito K, Suzuki H, Hirohashi T, Kume K, Shimizu T, Sugiyama Y. Molecular cloning of canalicular multispecific organic anion transporter defective in EHBR. Am J Physiol. 1997;272G16-22.
62. Hirohashi T, Suzuki H, Ito K, Ogawa K, Kume K, Shimizu T, et al. Hepatic expression of multidrug resistance-associated protein-like proteins maintained in eisai hyperbilirubinemic rats. Mol Pharmacol. 1998;531068-75.
63. Pastan I, Gottesman M. Multiple-drug resistance in human cancer. N Engl J Med. 1987;3161388-93.
64. Oude Elferink RP, Meijer DK, Kuipers F, Jansen PL, Groen AK, Groothuis GM. Hepatobiliary secretion of organic compounds; molecular mechanisms of membrane transport. Biochim Biophys Acta. 1995;1241215-68.

65. Schmid D, Ecker G, Kopp S, Hitzler M, Chiba P. Structure-activity relationship studies of propafenone analogs based on P-glycoprotein ATPase activity measurements. Biochem Pharmacol. 1999;581447-56.
66. Smit JW, Schinkel AH, Muller M, Weert B, Meijer DK. Contribution of the murine mdr1a P-glycoprotein to hepatobiliary and intestinal elimination of cationic drugs as measured in mice with an mdr1a gene disruption. Hepatology. 1998;271056-63.
67. Smit JW, Weert B, Schinkel AH, Meijer DK. Heterologous expression of various P-glycoproteins in polarized epithelial cells induces directional transport of small (type 1) and bulky (type 2) cationic drugs. J Pharmacol Exp Ther. 1998;286321-7.
68. Matheny CJ, Lamb MW, Brouwer KR, Pollack GM. Pharmacokinetic and pharmacodynamic implications of P-glycoprotein modulation. Pharmacotherapy. 2001;21778-96.
69. Ekins S, Kim RB, Leake BF, Dantzig AH, Schuetz EG, Lan LB, et al. Application of three-dimensional quantitative structure-activity relationships of P-glycoprotein inhibitors and substrates. Mol Pharmacol. 2002;61974-81.
70. Ekins S, Kim RB, Leake BF, Dantzig AH, Schuetz EG, Lan LB, et al. Three-dimensional quantitative structure-activity relationships of inhibitors of P-glycoprotein. Mol Pharmacol. 2002;61964-73.
71. Stouch TR, Gudmundsson O. Progress in understanding the structure-activity relationships of P-glycoprotein. Adv Drug Deliv Rev. 2002;54315-28.
72. Lee YM, Song IS, Kim SG, Lee MG, Chung SJ, Shim CK. The suppressed expression and functional activity of hepatic P-glycoprotein in rats with protein-calorie malnutrition. J Pharm Sci. 2003;921323-30.
73. Patel VA, Dunn MJ, Sorokin A. Regulation of MDR-1 (P-glycoprotein) by cyclooxygenase-2. J Biol Chem. 2002;27738915-20.
74. Sukhai M, Piquette-Miller M. Regulation of the multidrug resistance genes by stress signals. J Pharm Pharm Sci. 2000;3268-80.
75. McRae MP, Brouwer KL, Kashuba AD. Cytokine regulation of P-glycoprotein. Drug Metab Rev. 2003;3519-33.
76. Smith AJ, van Helvoort A, van Meer G, Szabo K, Welker E, Szakacs G, et al. MDR3 P-glycoprotein, a phosphatidylcholine translocase, transports several cytotoxic drugs and directly interacts with drugs as judged by interference with nucleotide trapping. J Biol Chem. 2000;27523530-9.
77. Doyle LA, Yang W, Abruzzo LV, Krogmann T, Gao Y, Rishi AK, et al. A multidrug resistance transporter from human MCF-7 breast cancer cells. Proc Natl Acad Sci U S A. 1998;9515665-70.
78. Suzuki M, Suzuki H, Sugimoto Y, Sugiyama Y. ABCG2 transports sulfated conjugates of steroids and xenobiotics. J Biol Chem. 2003;27822644-9.
79. Maliepaard M, Scheffer GL, Faneyte IF, van Gastelen MA, Pijnenborg AC, Schinkel AH, et al. Subcellular localization and distribution of the breast cancer resistance protein transporter in normal human tissues. Cancer Res. 2001;613458-64.
80. Houssin D, Capron M, Celier C, Cresteil T, Demaugre F, Beaune P. Evaluation of isolated human hepatocytes. Life Sci. 1983;331805-9.
81. Tee LB, Seddon T, Boobis AR, Davies DS. Drug metabolising activity of freshly isolated human hepatocytes. Br J Clin Pharmacol. 1985;19279-94.
82. Groothuis GM, Hulstaert CE, Kalicharan D, Hardonk MJ. Plasma membrane specialization and intracellular polarity of freshly isolated rat hepatocytes. Eur J Cell Biol. 1981;2643-51.

83. Ihrke G, Neufeld EB, Meads T, Shanks MR, Cassio D, Laurent M, et al. WIF-B cells: an in vitro model for studies of hepatocyte polarity. J Cell Biol. 1993;1231761-75.
84. Sai Y, Nies AT, Arias IM. Bile acid secretion and direct targeting of mdr1-green fluorescent protein from Golgi to the canalicular membrane in polarized WIF-B cells. J Cell Sci. 1999;112 (Pt 24)4535-45.
85. Zegers MM, Hoekstra D. Mechanisms and functional features of polarized membrane traffic in epithelial and hepatic cells. Biochem J. 1998;336 (Pt 2)257-69.
86. Dranoff JA, McClure M, Burgstahler AD, Denson LA, Crawford AR, Crawford JM, et al. Short-term regulation of bile acid uptake by microfilament-dependent translocation of rat ntcp to the plasma membrane. Hepatology. 1999;30223-9.
87. Liu X, LeCluyse EL, Brouwer KR, Lightfoot RM, Lee JI, Brouwer KL. Use of Ca2+ modulation to evaluate biliary excretion in sandwich-cultured rat hepatocytes. J Pharmacol Exp Ther. 1999;2891592-9.
88. Liu X, Chism JP, LeCluyse EL, Brouwer KR, Brouwer KL. Correlation of biliary excretion in sandwich-cultured rat hepatocytes and in vivo in rats. Drug Metab Dispos. 1999;27637-44.
89. Liu X, LeCluyse EL, Brouwer KR, Gan LS, Lemasters JJ, Stieger B, et al. Biliary excretion in primary rat hepatocytes cultured in a collagen-sandwich configuration. Am J Physiol. 1999;277G12-21.
90. Smith NF, Figg WD, Sparreboom A. Role of the liver-specific transporters OATP1B1 and OATP1B3 in governing drug elimination. Expert Opin Drug Metab Toxicol. 2005;1429-45.
91. Tamai I, Nakanishi T. OATP transporter-mediated drug absorption and interaction. Curr Opin Pharmacol. 2013;13859-63.
92. Muller M. Transcriptional control of hepatocanalicular transporter gene expression. Semin Liver Dis. 2000;20323-37.
93. Denson LA, Sturm E, Echevarria W, Zimmerman TL, Makishima M, Mangelsdorf DJ, et al. The orphan nuclear receptor, shp, mediates bile acid-induced inhibition of the rat bile acid transporter, ntcp. Gastroenterology. 2001;121140-7.
94. Denson LA, Auld KL, Schiek DS, McClure MH, Mangelsdorf DJ, Karpen SJ. Interleukin-1beta suppresses retinoid transactivation of two hepatic transporter genes involved in bile formation. J Biol Chem. 2000;2758835-43.
95. Jung D, Podvinec M, Meyer UA, Mangelsdorf DJ, Fried M, Meier PJ, et al. Human organic anion transporting polypeptide 8 promoter is transactivated by the farnesoid X receptor/bile acid receptor. Gastroenterology. 2002;1221954-66.
96. Staudinger JL, Madan A, Carol KM, Parkinson A. Regulation of drug transporter gene expression by nuclear receptors. Drug Metab Dispos. 2003;31523-7.
97. Xiong H, Yoshinari K, Brouwer KL, Negishi M. Role of constitutive androstane receptor in the in vivo induction of Mrp3 and CYP2B1/2 by phenobarbital. Drug Metab Dispos. 2002;30918-23.
98. Ananthanarayanan M, Balasubramanian N, Makishima M, Mangelsdorf DJ, Suchy FJ. Human bile salt export pump promoter is transactivated by the farnesoid X receptor/bile acid receptor. J Biol Chem. 2001;27628857-65.
99. Kauffmann HM, Pfannschmidt S, Zoller H, Benz A, Vorderstemann B, Webster JI, et al. Influence of redox-active compounds and PXR-activators on human MRP1 and MRP2 gene expression. Toxicology. 2002;171137-46.
100. Kast HR, Goodwin B, Tarr PT, Jones SA, Anisfeld AM, Stoltz CM, et al. Regulation of multidrug resistance-associated protein 2 (ABCC2) by the nuclear receptors pregnane X receptor,

farnesoid X-activated receptor, and constitutive androstane receptor. J Biol Chem. 2002;2772908-15.
101. Kliewer SA, Moore JT, Wade L, Staudinger JL, Watson MA, Jones SA, et al. An orphan nuclear receptor activated by pregnanes defines a novel steroid signaling pathway. Cell. 1998;9273-82.
102. Geick A, Eichelbaum M, Burk O. Nuclear receptor response elements mediate induction of intestinal MDR1 by rifampin. J Biol Chem. 2001;27614581-7.
103. Synold TW, Dussault I, Forman BM. The orphan nuclear receptor SXR coordinately regulates drug metabolism and efflux. Nat Med. 2001;7584-90.
104. Kok T, Bloks VW, Wolters H, Havinga R, Jansen PL, Staels B, et al. Peroxisome proliferator-activated receptor alpha (PPARalpha)-mediated regulation of multidrug resistance 2 (Mdr2) expression and function in mice. Biochem J. 2003;369539-47.
105. Boyer JL, Soroka CJ. Vesicle targeting to the apical domain regulates bile excretory function in isolated rat hepatocyte couplets. Gastroenterology. 1995;1091600-11.
106. Mukhopadhayay S, Ananthanarayanan M, Stieger B, Meier PJ, Suchy FJ, Anwer MS. cAMP increases liver Na+-taurocholate cotransport by translocating transporter to plasma membranes. Am J Physiol. 1997;273G842-8.
107. Kipp H, Arias IM. Intracellular trafficking and regulation of canalicular ATP-binding cassette transporters. Semin Liver Dis. 2000;20339-51.
108. Durand-Schneider AM, Bouanga JC, Feldmann G, Maurice M. Microtubule disruption interferes with the structural and functional integrity of the apical pole in primary cultures of rat hepatocytes. Eur J Cell Biol. 1991;56260-8.
109. Oude Elferink RP, Bakker CT, Roelofsen H, Middelkoop E, Ottenhoff R, Heijn M, et al. Accumulation of organic anion in intracellular vesicles of cultured rat hepatocytes is mediated by the canalicular multispecific organic anion transporter. Hepatology. 1993;17434-44.
110. Roelofsen H, Soroka CJ, Keppler D, Boyer JL. Cyclic AMP stimulates sorting of the canalicular organic anion transporter (Mrp2/cMoat) to the apical domain in hepatocyte couplets. J Cell Sci. 1998;111 (Pt 8)1137-45.
111. Kubitz R, D'Urso D, Keppler D, Haussinger D. Osmodependent dynamic localization of the multidrug resistance protein 2 in the rat hepatocyte canalicular membrane. Gastroenterology. 1997;1131438-42.
112. Gatmaitan ZC, Nies AT, Arias IM. Regulation and translocation of ATP-dependent apical membrane proteins in rat liver. Am J Physiol. 1997;272G1041-9.
113. Glavy JS, Wu SM, Wang PJ, Orr GA, Wolkoff AW. Down-regulation by extracellular ATP of rat hepatocyte organic anion transport is mediated by serine phosphorylation of oatp1. J Biol Chem. 2000;2751479-84.
114. Shitara Y, Itoh T, Sato H, Li AP, Sugiyama Y. Inhibition of transporter-mediated hepatic uptake as a mechanism for drug-drug interaction between cerivastatin and cyclosporin A. J Pharmacol Exp Ther. 2003;304610-6.
115. Muck W, Mai I, Fritsche L, Ochmann K, Rohde G, Unger S, et al. Increase in cerivastatin systemic exposure after single and multiple dosing in cyclosporine-treated kidney transplant recipients. Clin Pharmacol Ther. 1999;65251-61.
116. Angelin B, Arvidsson A, Dahlqvist R, Hedman A, Schenck-Gustafsson K. Quinidine reduces biliary clearance of digoxin in man. Eur J Clin Invest. 1987;17262-5.
117. Horio M, Gottesman MM, Pastan I. ATP-dependent transport of vinblastine in vesicles from human multidrug-resistant cells. Proc Natl Acad Sci U S A. 1988;853580-4.

118. Booth CL, Brouwer KR, Brouwer KL. Effect of multidrug resistance modulators on the hepatobiliary disposition of doxorubicin in the isolated perfused rat liver. Cancer Res. 1998;583641-8.
119. van Asperen J, van Tellingen O, Beijnen JH. The role of mdr1a P-glycoprotein in the biliary and intestinal secretion of doxorubicin and vinblastine in mice. Drug Metab Dispos. 2000;28264-7.
120. Riley J, Styles J, Verschoyle RD, Stanley LA, White IN, Gant TW. Association of tamoxifen biliary excretion rate with prior tamoxifen exposure and increased mdr1b expression. Biochem Pharmacol. 2000;60233-9.
121. Fattinger K, Funk C, Pantze M, Weber C, Reichen J, Stieger B, et al. The endothelin antagonist bosentan inhibits the canalicular bile salt export pump: a potential mechanism for hepatic adverse reactions. Clin Pharmacol Ther. 2001;69223-31.
122. Giacomini KM, Huang SM, Tweedie DJ, Benet LZ, Brouwer KL, Chu X, et al. Membrane transporters in drug development. Nat Rev Drug Discov. 2010;9215-36.
123. Wacher VJ, Wu CY, Benet LZ. Overlapping substrate specificities and tissue distribution of cytochrome P450 3A and P-glycoprotein: implications for drug delivery and activity in cancer chemotherapy. Mol Carcinog. 1995;13129-34.
124. Huang L, Wring SA, Woolley JL, Brouwer KR, Serabjit-Singh C, Polli JW. Induction of P-glycoprotein and cytochrome P450 3A by HIV protease inhibitors. Drug Metab Dispos. 2001;29754-60.
125. Schuetz EG, Beck WT, Schuetz JD. Modulators and substrates of P-glycoprotein and cytochrome P4503A coordinately up-regulate these proteins in human colon carcinoma cells. Mol Pharmacol. 1996;49311-8.
126. Schuetz EG, Schinkel AH, Relling MV, Schuetz JD. P-glycoprotein: a major determinant of rifampicin-inducible expression of cytochrome P4503A in mice and humans. Proc Natl Acad Sci U S A. 1996;934001-5.
127. Salphati L, Benet LZ. Modulation of P-glycoprotein expression by cytochrome P450 3A inducers in male and female rat livers. Biochem Pharmacol. 1998;55387-95.
128. Yasuda K, Lan LB, Sanglard D, Furuya K, Schuetz JD, Schuetz EG. Interaction of cytochrome P450 3A inhibitors with P-glycoprotein. J Pharmacol Exp Ther. 2002;303323-32.
129. Wu CY, Benet LZ. Disposition of tacrolimus in isolated perfused rat liver: influence of troleandomycin, cyclosporine, and gg918. Drug Metab Dispos. 2003;311292-5.
130. Schuetz EG, Umbenhauer DR, Yasuda K, Brimer C, Nguyen L, Relling MV, et al. Altered expression of hepatic cytochromes P-450 in mice deficient in one or more mdr1 genes. Mol Pharmacol. 2000;57188-97.
131. Lan LB, Dalton JT, Schuetz EG. Mdr1 limits CYP3A metabolism in vivo. Mol Pharmacol. 2000;58863-9.
132. Iida A, Saito S, Sekine A, Mishima C, Kondo K, Kitamura Y, et al. Catalog of 258 single-nucleotide polymorphisms (SNPs) in genes encoding three organic anion transporters, three organic anion-transporting polypeptides, and three NADH:ubiquinone oxidoreductase flavoproteins. J Hum Genet. 2001;46668-83.
133. Nozawa T, Nakajima M, Tamai I, Noda K, Nezu J, Sai Y, et al. Genetic polymorphisms of human organic anion transporters OATP-C (SLC21A6) and OATP-B (SLC21A9): allele frequencies in the Japanese population and functional analysis. J Pharmacol Exp Ther. 2002;302804-13.

134. Michalski C, Cui Y, Nies AT, Nuessler AK, Neuhaus P, Zanger UM, et al. A naturally occurring mutation in the SLC21A6 gene causing impaired membrane localization of the hepatocyte uptake transporter. J Biol Chem. 2002;27743058-63.
135. Tirona RG, Leake BF, Merino G, Kim RB. Polymorphisms in OATP-C: identification of multiple allelic variants associated with altered transport activity among European- and African-Americans. J Biol Chem. 2001;27635669-75.
136. Nishizato Y, Ieiri I, Suzuki H, Kimura M, Kawabata K, Hirota T, et al. Polymorphisms of OATP-C (SLC21A6) and OAT3 (SLC22A8) genes: consequences for pravastatin pharmacokinetics. Clin Pharmacol Ther. 2003;73554-65.
137. Conrad S, Kauffmann HM, Ito K, Leslie EM, Deeley RG, Schrenk D, et al. A naturally occurring mutation in MRP1 results in a selective decrease in organic anion transport and in increased doxorubicin resistance. Pharmacogenetics. 2002;12321-30.
138. Ito S, Ieiri I, Tanabe M, Suzuki A, Higuchi S, Otsubo K. Polymorphism of the ABC transporter genes, MDR1, MRP1 and MRP2/cMOAT, in healthy Japanese subjects. Pharmacogenetics. 2001;11175-84.
139. Germain DP, Remones V, Perdu J, Jeunemaitre X. Identification of two polymorphisms (c189G>C; c190T>C) in exon 2 of the human MRP6 gene (ABCC6) by screening of Pseudoxanthoma elasticum patients: possible sequence correction? Hum Mutat. 2000;16449.
140. Dubin IN, Johnson FB. Chronic idiopathic jaundice with unidentified pigment in liver cells; a new clinicopathologic entity with a report of 12 cases. Medicine (Baltimore). 1954;33155-97.
141. Kartenbeck J, Leuschner U, Mayer R, Keppler D. Absence of the canalicular isoform of the MRP gene-encoded conjugate export pump from the hepatocytes in Dubin-Johnson syndrome. Hepatology. 1996;231061-6.
142. Keitel V, Kartenbeck J, Nies AT, Spring H, Brom M, Keppler D. Impaired protein maturation of the conjugate export pump multidrug resistance protein 2 as a consequence of a deletion mutation in Dubin-Johnson syndrome. Hepatology. 2000;321317-28.
143. Hashimoto K, Uchiumi T, Konno T, Ebihara T, Nakamura T, Wada M, et al. Trafficking and functional defects by mutations of the ATP-binding domains in MRP2 in patients with Dubin-Johnson syndrome. Hepatology. 2002;361236-45.
144. Shimizu M, Fuse K, Okudaira K, Nishigaki R, Maeda K, Kusuhara H, et al. Contribution of OATP (organic anion-transporting polypeptide) family transporters to the hepatic uptake of fexofenadine in humans. Drug Metab Dispos. 2005;331477-81.
145. Hagenbuch B, Meier PJ. Organic anion transporting polypeptides of the OATP/ SLC21 family: phylogenetic classification as OATP/ SLCO superfamily, new nomenclature and molecular/functional properties. Pflugers Arch. 2004;447653-65.
146. Barton HA, Lai Y, Goosen TC, Jones HM, El-Kattan AF, Gosset JR, et al. Model-based approaches to predict drug-drug interactions associated with hepatic uptake transporters: preclinical, clinical and beyond. Expert Opin Drug Metab Toxicol. 2013;9459-72.
147. Shitara Y, Maeda K, Ikejiri K, Yoshida K, Horie T, Sugiyama Y. Clinical significance of organic anion transporting polypeptides (OATPs) in drug disposition: their roles in hepatic clearance and intestinal absorption. Biopharm Drug Dispos. 2013;3445-78.
148. Zimmerman EI, Hu S, Roberts JL, Gibson AA, Orwick SJ, Li L, et al. Contribution of OATP1B1 and OATP1B3 to the disposition of sorafenib and sorafenib-glucuronide. Clin Cancer Res.191458-66.

149. Pearson MA, Fabbro D. Targeting protein kinases in cancer therapy: a success? Expert Rev Anticancer Ther. 2004;41113-24.
150. Undevia SD, Gomez-Abuin G, Ratain MJ. Pharmacokinetic variability of anticancer agents. Nat Rev Cancer. 2005;5447-58.
151. van Erp NP, Gelderblom H, Guchelaar HJ. Clinical pharmacokinetics of tyrosine kinase inhibitors. Cancer Treat Rev. 2009;35692-706.
152. Minocha M, Khurana V, Mitra AK. Determination of pazopanib (GW-786034) in mouse plasma and brain tissue by liquid chromatography-tandem mass spectrometry (LC/MS-MS). J Chromatogr B Analyt Technol Biomed Life Sci.90185-92.
153. Minocha M, Khurana V, Qin B, Pal D, Mitra AK. Enhanced brain accumulation of pazopanib by modulating P-gp and Bcrp1 mediated efflux with canertinib or erlotinib. Int J Pharm.436127-34.
154. Minocha M, Khurana V, Qin B, Pal D, Mitra AK. Co-administration strategy to enhance brain accumulation of vandetanib by modulating P-glycoprotein (P-gp/Abcb1) and breast cancer resistance protein (Bcrp1/Abcg2) mediated efflux with m-TOR inhibitors. Int J Pharm.434306-14.
155. Gotze L, Hegele A, Metzelder SK, Renz H, Nockher WA. Development and clinical application of a LC-MS/MS method for simultaneous determination of various tyrosine kinase inhibitors in human plasma. Clin Chim Acta. 2012;413143-9.
156. Lankheet NA, Hillebrand MJ, Rosing H, Schellens JH, Beijnen JH, Huitema AD. Method development and validation for the quantification of dasatinib, erlotinib, gefitinib, imatinib, lapatinib, nilotinib, sorafenib and sunitinib in human plasma by liquid chromatography coupled with tandem mass spectrometry. Biomed Chromatogr. 2013;27466-76.
157. Zimmerman EI, Hu S, Roberts JL, Gibson AA, Orwick SJ, Li L, et al. Contribution of OATP1B1 and OATP1B3 to the disposition of sorafenib and sorafenib-glucuronide. Clin Cancer Res. 2013;191458-66.
158. Kalliokoski A, Niemi M. Impact of OATP transporters on pharmacokinetics. Br J Pharmacol. 2009;158693-705.
159. Konig J, Cui Y, Nies AT, Keppler D. Localization and genomic organization of a new hepatocellular organic anion transporting polypeptide. J Biol Chem. 2000;27523161-8.
160. De Bruyn T, van Westen GJ, Ijzerman AP, Stieger B, de Witte P, Augustijns PF, et al. Structure-based identification of OATP1B1/3 inhibitors. Mol Pharmacol. 2013;831257-67.
161. Gui C, Obaidat A, Chaguturu R, Hagenbuch B. Development of a cell-based high-throughput assay to screen for inhibitors of organic anion transporting polypeptides 1B1 and 1B3. Curr Chem Genomics. 2010;41-8.
162. Nozawa T, Minami H, Sugiura S, Tsuji A, Tamai I. Role of organic anion transporter OATP1B1 (OATP-C) in hepatic uptake of irinotecan and its active metabolite, 7-ethyl-10-hydroxycamptothecin: in vitro evidence and effect of single nucleotide polymorphisms. Drug Metab Dispos. 2005;33434-9.
163. Agarwal S, Mittapalli RK, Zellmer DM, Gallardo JL, Donelson R, Seiler C, et al. Active efflux of Dasatinib from the brain limits efficacy against murine glioblastoma: broad implications for the clinical use of molecularly targeted agents. Mol Cancer Ther.112183-92.
164. Agarwal S, Elmquist WF. Insight into the cooperation of P-glycoprotein (ABCB1) and breast cancer resistance protein (ABCG2) at the blood-brain barrier: a case study examining sorafenib efflux clearance. Mol Pharm.9678-84.
165. Wang T, Agarwal S, Elmquist WF. Brain distribution of cediranib is limited by active efflux at the blood-brain barrier. J Pharmacol Exp Ther.341386-95.

166. Agarwal S, Sane R, Gallardo JL, Ohlfest JR, Elmquist WF. Distribution of gefitinib to the brain is limited by P-glycoprotein (ABCB1) and breast cancer resistance protein (ABCG2)-mediated active efflux. J Pharmacol Exp Ther.334147-55.
167. Seithel A, Eberl S, Singer K, Auge D, Heinkele G, Wolf NB, et al. The influence of macrolide antibiotics on the uptake of organic anions and drugs mediated by OATP1B1 and OATP1B3. Drug Metab Dispos. 2007;35779-86.
168. Backman JT, Kyrklund C, Neuvonen M, Neuvonen PJ. Gemfibrozil greatly increases plasma concentrations of cerivastatin. Clin Pharmacol Ther. 2002;72685-91.
169. Backman JT, Kyrklund C, Kivisto KT, Wang JS, Neuvonen PJ. Plasma concentrations of active simvastatin acid are increased by gemfibrozil. Clin Pharmacol Ther. 2000;68122-9.
170. Fahrmayr C, Fromm MF, Konig J. Hepatic OATP and OCT uptake transporters: their role for drug-drug interactions and pharmacogenetic aspects. Drug Metab Rev.42380-401.
171. Romaine SP, Bailey KM, Hall AS, Balmforth AJ. The influence of SLCO1B1 (OATP1B1) gene polymorphisms on response to statin therapy. Pharmacogenomics J.101-11.
172. Hu S, Franke RM, Filipski KK, Hu C, Orwick SJ, de Bruijn EA, et al. Interaction of imatinib with human organic ion carriers. Clin Cancer Res. 2008;143141-8.
173. Burger H, van Tol H, Brok M, Wiemer EA, de Bruijn EA, Guetens G, et al. Chronic imatinib mesylate exposure leads to reduced intracellular drug accumulation by induction of the ABCG2 (BCRP) and ABCB1 (MDR1) drug transport pumps. Cancer Biol Ther. 2005;4747-52.
174. Burger H, van Tol H, Boersma AW, Brok M, Wiemer EA, Stoter G, et al. Imatinib mesylate (STI571) is a substrate for the breast cancer resistance protein (BCRP)/ABCG2 drug pump. Blood. 2004;1042940-2.
175. Hamada A, Miyano H, Watanabe H, Saito H. Interaction of imatinib mesilate with human P-glycoprotein. J Pharmacol Exp Ther. 2003;307824-8.
176. Shitara Y, Maeda K, Ikejiri K, Yoshida K, Horie T, Sugiyama Y. Clinical significance of organic anion transporting polypeptides (OATPs) in drug disposition: their roles in hepatic clearance and intestinal absorption. Biopharm Drug Dispos.3445-78.
177. Kim RB. Organic anion-transporting polypeptide (OATP) transporter family and drug disposition. Eur J Clin Invest. 2003;33 Suppl 21-5.
178. Duckett DR, Cameron MD. Metabolism considerations for kinase inhibitors in cancer treatment. Expert Opin Drug Metab Toxicol. 2010;61175-93.
179. Choi MK, Jin QR, Choi YL, Ahn SH, Bae MA, Song IS. Inhibitory effects of ketoconazole and rifampin on OAT1 and OATP1B1 transport activities: considerations on drug-drug interactions. Biopharm Drug Dispos.32175-84.
180. Koenen A, Kroemer HK, Grube M, Meyer zu Schwabedissen HE. Current understanding of hepatic and intestinal OATP-mediated drug-drug interactions. Expert Rev Clin Pharmacol.4729-42.
181. Muller F, Fromm MF. Transporter-mediated drug-drug interactions. Pharmacogenomics.121017-37.
182. Niemi M. Role of OATP transporters in the disposition of drugs. Pharmacogenomics. 2007;8787-802.
183. Keitel V, Burdelski M, Warskulat U, Kuhlkamp T, Keppler D, Haussinger D, et al. Expression and localization of hepatobiliary transport proteins in progressive familial intrahepatic cholestasis. Hepatology. 2005;411160-72.
184. Oswald M, Kullak-Ublick GA, Paumgartner G, Beuers U. Expression of hepatic transporters OATP-C and MRP2 in primary sclerosing cholangitis. Liver. 2001;21247-53.

185. Wlcek K, Svoboda M, Riha J, Zakaria S, Olszewski U, Dvorak Z, et al. The analysis of organic anion transporting polypeptide (OATP) mRNA and protein patterns in primary and metastatic liver cancer. Cancer Biol Ther.11801-11.
186. Vavricka SR, Jung D, Fried M, Grutzner U, Meier PJ, Kullak-Ublick GA. The human organic anion transporting polypeptide 8 (SLCO1B3) gene is transcriptionally repressed by hepatocyte nuclear factor 3beta in hepatocellular carcinoma. J Hepatol. 2004;40212-8.
187. Cui Y, Konig J, Nies AT, Pfannschmidt M, Hergt M, Franke WW, et al. Detection of the human organic anion transporters SLC21A6 (OATP2) and SLC21A8 (OATP8) in liver and hepatocellular carcinoma. Lab Invest. 2003;83527-38.
188. Di Gion P, Kanefendt F, Lindauer A, Scheffler M, Doroshyenko O, Fuhr U, et al. Clinical pharmacokinetics of tyrosine kinase inhibitors: focus on pyrimidines, pyridines and pyrroles. Clin Pharmacokinet.50551-603.
189. Feng B, Xu JJ, Bi YA, Mireles R, Davidson R, Duignan DB, et al. Role of hepatic transporters in the disposition and hepatotoxicity of a HER2 tyrosine kinase inhibitor CP-724,714. Toxicol Sci. 2009;108492-500.
190. Khurana V, Minocha M, Pal D, Mitra AK. Role of OATP-1B1 and/or OATP-1B3 in hepatic disposition of tyrosine kinase inhibitors. Drug Metabol Drug Interact. 2014.
191. Minematsu T, Giacomini KM. Interactions of tyrosine kinase inhibitors with organic cation transporters and multidrug and toxic compound extrusion proteins. Mol Cancer Ther. 2011;10531-9.
192. Hartmann JT, Haap M, Kopp HG, Lipp HP. Tyrosine kinase inhibitors - a review on pharmacology, metabolism and side effects. Curr Drug Metab. 2009;10470-81.
193. Teo YL, Ho HK, Chan A. Risk of tyrosine kinase inhibitors-induced hepatotoxicity in cancer patients: a meta-analysis. Cancer Treat Rev. 2013;39199-206.
194. Xu CF, Reck BH, Xue Z, Huang L, Baker KL, Chen M, et al. Pazopanib-induced hyperbilirubinemia is associated with Gilbert's syndrome UGT1A1 polymorphism. Br J Cancer. 2010;1021371-7.
195. Sternberg CN, Davis ID, Mardiak J, Szczylik C, Lee E, Wagstaff J, et al. Pazopanib in locally advanced or metastatic renal cell carcinoma: results of a randomized phase III trial. J Clin Oncol. 2010;281061-8.
196. Swift B, Nebot N, Lee JK, Han T, Proctor WR, Thakker DR, et al. Sorafenib hepatobiliary disposition: mechanisms of hepatic uptake and disposition of generated metabolites. Drug Metab Dispos. 2013;411179-86.
197. Minocha M, Khurana V, Qin B, Pal D, Mitra AK. Co-administration strategy to enhance brain accumulation of vandetanib by modulating P-glycoprotein (P-gp/Abcb1) and breast cancer resistance protein (Bcrp1/Abcg2) mediated efflux with m-TOR inhibitors. Int J Pharm. 2012;434306-14.
198. Karlgren M, Vildhede A, Norinder U, Wisniewski JR, Kimoto E, Lai Y, et al. Classification of inhibitors of hepatic organic anion transporting polypeptides (OATPs): influence of protein expression on drug-drug interactions. J Med Chem. 2012;554740-63.
199. Shitara Y. Clinical importance of OATP1B1 and OATP1B3 in drug-drug interactions. Drug Metab Pharmacokinet. 2011;26220-7.
200. Hu S, Mathijssen RH, de Bruijn P, Baker SD, Sparreboom A. Inhibition of OATP1B1 by tyrosine kinase inhibitors: in vitro-in vivo correlations. Br J Cancer. 2014;110894-8.
201. Hagenbuch B, Meier PJ. The superfamily of organic anion transporting polypeptides. Biochim Biophys Acta. 2003;16091-18.

202. Abe T, Unno M, Onogawa T, Tokui T, Kondo TN, Nakagomi R, et al. LST-2, a human liver-specific organic anion transporter, determines methotrexate sensitivity in gastrointestinal cancers. Gastroenterology. 2001;1201689-99.
203. Muto M, Onogawa T, Suzuki T, Ishida T, Rikiyama T, Katayose Y, et al. Human liver-specific organic anion transporter-2 is a potent prognostic factor for human breast carcinoma. Cancer Sci. 2007;981570-6.
204. Smith NF, Acharya MR, Desai N, Figg WD, Sparreboom A. Identification of OATP1B3 as a high-affinity hepatocellular transporter of paclitaxel. Cancer Biol Ther. 2005;4815-8.
205. de Graan AJ, Lancaster CS, Obaidat A, Hagenbuch B, Elens L, Friberg LE, et al. Influence of polymorphic OATP1B-type carriers on the disposition of docetaxel. Clin Cancer Res. 2012;184433-40.
206. Yamazaki M, Suzuki H, Sugiyama Y. Recent advances in carrier-mediated hepatic uptake and biliary excretion of xenobiotics. Pharm Res. 1996;13497-513.
207. Shitara Y, Horie T, Sugiyama Y. Transporters as a determinant of drug clearance and tissue distribution. Eur J Pharm Sci. 2006;27425-46.
208. Asberg A, Hartmann A, Fjeldsa E, Bergan S, Holdaas H. Bilateral pharmacokinetic interaction between cyclosporine A and atorvastatin in renal transplant recipients. Am J Transplant. 2001;1382-6.
209. Hedman M, Neuvonen PJ, Neuvonen M, Holmberg C, Antikainen M. Pharmacokinetics and pharmacodynamics of pravastatin in pediatric and adolescent cardiac transplant recipients on a regimen of triple immunosuppression. Clin Pharmacol Ther. 2004;75101-9.
210. Nakagomi-Hagihara R, Nakai D, Tokui T, Abe T, Ikeda T. Gemfibrozil and its glucuronide inhibit the hepatic uptake of pravastatin mediated by OATP1B1. Xenobiotica. 2007;37474-86.
211. Kyrklund C, Backman JT, Neuvonen M, Neuvonen PJ. Gemfibrozil increases plasma pravastatin concentrations and reduces pravastatin renal clearance. Clin Pharmacol Ther. 2003;73538-44.
212. Whitfield LR, Porcari AR, Alvey C, Abel R, Bullen W, Hartman D. Effect of gemfibrozil and fenofibrate on the pharmacokinetics of atorvastatin. J Clin Pharmacol. 2011;51378-88.
213. Liu X, Huang J, Sun Y, Zhan K, Zhang Z, Hong M. Identification of multiple binding sites for substrate transport in bovine organic anion transporting polypeptide 1a2. Drug Metab Dispos. 2013;41602-7.
214. Weaver YM, Hagenbuch B. Several conserved positively charged amino acids in OATP1B1 are involved in binding or translocation of different substrates. J Membr Biol. 2010;236279-90.
215. Tan AR, Dowlati A, Jones SF, Infante JR, Nishioka J, Fang L, et al. Phase I study of pazopanib in combination with weekly paclitaxel in patients with advanced solid tumors. Oncologist. 2010;151253-61.
216. Jang SH, Wientjes MG, Au JL. Kinetics of P-glycoprotein-mediated efflux of paclitaxel. J Pharmacol Exp Ther. 2001;2981236-42.
217. Kemper EM, van Zandbergen AE, Cleypool C, Mos HA, Boogerd W, Beijnen JH, et al. Increased penetration of paclitaxel into the brain by inhibition of P-Glycoprotein. Clin Cancer Res. 2003;92849-55.
218. Singer JB, Shou Y, Giles F, Kantarjian HM, Hsu Y, Robeva AS, et al. UGT1A1 promoter polymorphism increases risk of nilotinib-induced hyperbilirubinemia. Leukemia. 2007;212311-5.
219. Khurana V, Minocha M, Pal D, Mitra AK. Inhibition of OATP-1B1 and OATP-1B3 by tyrosine kinase inhibitors. Drug Metabol Drug Interact. 2014.

220. Giacomini KM, Sugiyama Y. Membrane Transporters and Drug Response: Introduction. In: Brunton LL CB, Knollmann BC, editor. Brunton LL, Chabner BA, Knollmann BC. 12e ed. New York: The McGraw-Hill Companies; 2011.
221. Borst P, Elferink RO. Mammalian ABC transporters in health and disease. Annu Rev Biochem. 2002;71537-92.
222. Ambudkar SV, Kimchi-Sarfaty C, Sauna ZE, Gottesman MM. P-glycoprotein: from genomics to mechanism. Oncogene. 2003;227468-85.
223. Gottesman MM. Mechanisms of cancer drug resistance. Annu Rev Med. 2002;53615-27.
224. Lin JH, Yamazaki M. Clinical relevance of P-glycoprotein in drug therapy. Drug Metab Rev. 2003;35417-54.
225. Juliano RL, Ling V. A surface glycoprotein modulating drug permeability in Chinese hamster ovary cell mutants. Biochim Biophys Acta. 1976;455152-62.
226. Kessel D, Bosmann HB. Effects of L-asparaginase on protein and glycoprotein synthesis. FEBS Lett. 1970;1085-8.
227. Biedler JL, Riehm H. Cellular resistance to actinomycin D in Chinese hamster cells in vitro: cross-resistance, radioautographic, and cytogenetic studies. Cancer Res. 1970;301174-84.
228. Higgins CF. ABC transporters: from microorganisms to man. Annu Rev Cell Biol. 1992;867-113.
229. Tusnady GE, Bakos E, Varadi A, Sarkadi B. Membrane topology distinguishes a subfamily of the ATP-binding cassette (ABC) transporters. FEBS Lett. 1997;4021-3.
230. Kast C, Canfield V, Levenson R, Gros P. Membrane topology of P-glycoprotein as determined by epitope insertion: transmembrane organization of the N-terminal domain of mdr3. Biochemistry. 1995;344402-11.
231. Locher KP, Borths E. ABC transporter architecture and mechanism: implications from the crystal structures of BtuCD and BtuF. FEBS Lett. 2004;564264-8.
232. Kerr ID. Structure and association of ATP-binding cassette transporter nucleotide-binding domains. Biochim Biophys Acta. 2002;156147-64.
233. Dean M, Rzhetsky A, Allikmets R. The human ATP-binding cassette (ABC) transporter superfamily. Genome Res. 2001;111156-66.
234. Linton KJ, Higgins CF. The Escherichia coli ATP-binding cassette (ABC) proteins. Mol Microbiol. 1998;285-13.
235. Hrycyna CA, Airan LE, Germann UA, Ambudkar SV, Pastan I, Gottesman MM. Structural flexibility of the linker region of human P-glycoprotein permits ATP hydrolysis and drug transport. Biochemistry. 1998;3713660-73.
236. Sauna ZE, Nandigama K, Ambudkar SV. Exploiting reaction intermediates of the ATPase reaction to elucidate the mechanism of transport by P-glycoprotein (ABCB1). J Biol Chem. 2006;28126501-11.
237. Zaitseva J, Jenewein S, Oswald C, Jumpertz T, Holland IB, Schmitt L. A molecular understanding of the catalytic cycle of the nucleotide-binding domain of the ABC transporter HlyB. Biochem Soc Trans. 2005;33990-5.
238. Jones PM, George AM. The ABC transporter structure and mechanism: perspectives on recent research. Cell Mol Life Sci. 2004;61682-99.
239. Hulot JS, Villard E, Maguy A, Morel V, Mir L, Tostivint I, et al. A mutation in the drug transporter gene ABCC2 associated with impaired methotrexate elimination. Pharmacogenet Genomics. 2005;15277-85.

240. Letourneau IJ, Bowers RJ, Deeley RG, Cole SP. Limited modulation of the transport activity of the human multidrug resistance proteins MRP1, MRP2 and MRP3 by nicotine glucuronide metabolites. Toxicol Lett. 2005;1579-19.
241. Huisman MT, Smit JW, Crommentuyn KM, Zelcer N, Wiltshire HR, Beijnen JH, et al. Multidrug resistance protein 2 (MRP2) transports HIV protease inhibitors, and transport can be enhanced by other drugs. AIDS. 2002;162295-301.
242. Naruhashi K, Tamai I, Inoue N, Muraoka H, Sai Y, Suzuki N, et al. Involvement of multidrug resistance-associated protein 2 in intestinal secretion of grepafloxacin in rats. Antimicrob Agents Chemother. 2002;46344-9.
243. Bakos E, Evers R, Sinko E, Varadi A, Borst P, Sarkadi B. Interactions of the human multidrug resistance proteins MRP1 and MRP2 with organic anions. Mol Pharmacol. 2000;57760-8.
244. Wacher VJ, Silverman JA, Zhang Y, Benet LZ. Role of P-glycoprotein and cytochrome P450 3A in limiting oral absorption of peptides and peptidomimetics. J Pharm Sci. 1998;871322-30.
245. Sharom FJ. The P-glycoprotein efflux pump: how does it transport drugs? J Membr Biol. 1997;160161-75.
246. Pal D, Kwatra D, Minocha M, Paturi DK, Budda B, Mitra AK. Efflux transporters- and cytochrome P-450-mediated interactions between drugs of abuse and antiretrovirals. Life Sci. 2011;88959-71.
247. Pal D, Mitra AK. MDR- and CYP3A4-mediated drug-herbal interactions. Life Sci. 2006;782131-45.
248. Borst P, Evers R, Kool M, Wijnholds J. A family of drug transporters: the multidrug resistance-associated proteins. J Natl Cancer Inst. 2000;921295-302.
249. Borst P, Schinkel AH, Smit JJ, Wagenaar E, Van Deemter L, Smith AJ, et al. Classical and novel forms of multidrug resistance and the physiological functions of P-glycoproteins in mammals. Pharmacol Ther. 1993;60289-99.
250. Gottesman MM, Pastan I. Biochemistry of multidrug resistance mediated by the multidrug transporter. Annu Rev Biochem. 1993;62385-427.
251. Ueda K, Okamura N, Hirai M, Tanigawara Y, Saeki T, Kioka N, et al. Human P-glycoprotein transports cortisol, aldosterone, and dexamethasone, but not progesterone. J Biol Chem. 1992;26724248-52.
252. Mechetner EB, Roninson IB. Efficient inhibition of P-glycoprotein-mediated multidrug resistance with a monoclonal antibody. Proc Natl Acad Sci U S A. 1992;895824-8.
253. Hofsli E, Nissen-Meyer J. Reversal of drug resistance by erythromycin: erythromycin increases the accumulation of actinomycin D and doxorubicin in multidrug-resistant cells. Int J Cancer. 1989;44149-54.
254. Roninson IB, Abelson HT, Housman DE, Howell N, Varshavsky A. Amplification of specific DNA sequences correlates with multi-drug resistance in Chinese hamster cells. Nature. 1984;309626-8.
255. Bech-Hansen NT, Till JE, Ling V. Pleiotropic phenotype of colchicine-resistant CHO cells: cross-resistance and collateral sensitivity. J Cell Physiol. 1976;8823-31.
256. Takano M, Yumoto R, Murakami T. Expression and function of efflux drug transporters in the intestine. Pharmacol Ther. 2006;109137-61.

257. Miller DS, Nobmann SN, Gutmann H, Toeroek M, Drewe J, Fricker G. Xenobiotic transport across isolated brain microvessels studied by confocal microscopy. Mol Pharmacol. 2000;581357-67.
258. Park S, Sinko PJ. P-glycoprotein and mutlidrug resistance-associated proteins limit the brain uptake of saquinavir in mice. J Pharmacol Exp Ther. 2005;3121249-56.
259. Schinkel AH, Jonker JW. Mammalian drug efflux transporters of the ATP binding cassette (ABC) family: an overview. Adv Drug Deliv Rev. 2003;553-29.
260. Staud F, Pavek P. Breast cancer resistance protein (BCRP/ABCG2). Int J Biochem Cell Biol. 2005;37720-5.
261. Zhang Z, Wu JY, Hait WN, Yang JM. Regulation of the stability of P-glycoprotein by ubiquitination. Mol Pharmacol. 2004;66395-403.
262. Sarkadi B, Ozvegy-Laczka C, Nemet K, Varadi A. ABCG2 -- a transporter for all seasons. FEBS Lett. 2004;567116-20.
263. Haimeur A, Conseil G, Deeley RG, Cole SP. The MRP-related and BCRP/ABCG2 multidrug resistance proteins: biology, substrate specificity and regulation. Curr Drug Metab. 2004;521-53.
264. Abbott BL. ABCG2 (BCRP) expression in normal and malignant hematopoietic cells. Hematol Oncol. 2003;21115-30.
265. Doyle LA, Ross DD. Multidrug resistance mediated by the breast cancer resistance protein BCRP (ABCG2). Oncogene. 2003;227340-58.
266. Ejendal KF, Hrycyna CA. Multidrug resistance and cancer: the role of the human ABC transporter ABCG2. Curr Protein Pept Sci. 2002;3503-11.
267. Hoffmeyer S, Burk O, von Richter O, Arnold HP, Brockmoller J, Johne A, et al. Functional polymorphisms of the human multidrug-resistance gene: multiple sequence variations and correlation of one allele with P-glycoprotein expression and activity in vivo. Proc Natl Acad Sci U S A. 2000;973473-8.
268. Fellay J, Marzolini C, Meaden ER, Back DJ, Buclin T, Chave JP, et al. Response to antiretroviral treatment in HIV-1-infected individuals with allelic variants of the multidrug resistance transporter 1: a pharmacogenetics study. Lancet. 2002;35930-6.
269. Chowbay B, Zhou S, Lee EJ. An interethnic comparison of polymorphisms of the genes encoding drug-metabolizing enzymes and drug transporters: experience in Singapore. Drug Metab Rev. 2005;37327-78.
270. Fung KL, Gottesman MM. A synonymous polymorphism in a common MDR1 (ABCB1) haplotype shapes protein function. Biochim Biophys Acta. 2009;1794860-71.
271. Nakamura T, Okamura N, Yagi M, Omatsu H, Yamamori M, Kuwahara A, et al. Effects of ABCB1 3435C>T genotype on serum levels of cortisol and aldosterone in women with normal menstrual cycles. Genet Mol Res. 2009;8397-403.
272. Lamba J, Strom S, Venkataramanan R, Thummel KE, Lin YS, Liu W, et al. MDR1 genotype is associated with hepatic cytochrome P450 3A4 basal and induction phenotype. Clin Pharmacol Ther. 2006;79325-38.
273. Seelig A. A general pattern for substrate recognition by P-glycoprotein. Eur J Biochem. 1998;251252-61.
274. Ambudkar SV, Dey S, Hrycyna CA, Ramachandra M, Pastan I, Gottesman MM. Biochemical, cellular, and pharmacological aspects of the multidrug transporter. Annu Rev Pharmacol Toxicol. 1999;39361-98.

275. Schinkel AH. Pharmacological insights from P-glycoprotein knockout mice. Int J Clin Pharmacol Ther. 1998;369-13.
276. Agarwal S, Hartz AM, Elmquist WF, Bauer B. Breast cancer resistance protein and P-glycoprotein in brain cancer: two gatekeepers team up. Curr Pharm Des. 2011;172793-802.
277. Mayer U, Wagenaar E, Dorobek B, Beijnen JH, Borst P, Schinkel AH. Full blockade of intestinal P-glycoprotein and extensive inhibition of blood-brain barrier P-glycoprotein by oral treatment of mice with PSC833. J Clin Invest. 1997;1002430-6.
278. Kiso S, Cai SH, Kitaichi K, Furui N, Takagi K, Nabeshima T, et al. Inhibitory effect of erythromycin on P-glycoprotein-mediated biliary excretion of doxorubicin in rats. Anticancer Res. 2000;202827-34.
279. Song S, Suzuki H, Kawai R, Sugiyama Y. Effect of PSC 833, a P-glycoprotein modulator, on the disposition of vincristine and digoxin in rats. Drug Metab Dispos. 1999;27689-94.
280. Harker WG, Bauer D, Etiz BB, Newman RA, Sikic BI. Verapamil-mediated sensitization of doxorubicin-selected pleiotropic resistance in human sarcoma cells: selectivity for drugs which produce DNA scission. Cancer Res. 1986;462369-73.
281. Inaba M, Kobayashi H, Sakurai Y, Johnson RK. Active efflux of daunorubicin and adriamycin in sensitive and resistant sublines of P388 leukemia. Cancer Res. 1979;392200-3.
282. Kuhl JS, Sikic BI, Blume KG, Chao NJ. Use of etoposide in combination with cyclosporin for purging multidrug-resistant leukemic cells from bone marrow in a mouse model. Exp Hematol. 1992;201048-54.
283. Eliason JF, Ramuz H, Kaufmann F. Human multi-drug-resistant cancer cells exhibit a high degree of selectivity for stereoisomers of verapamil and quinidine. Int J Cancer. 1990;46113-7.
284. Sehested M, Jensen PB, Skovsgaard T, Bindslev N, Demant EJ, Friche E, et al. Inhibition of vincristine binding to plasma membrane vesicles from daunorubicin-resistant Ehrlich ascites cells by multidrug resistance modulators. Br J Cancer. 1989;60809-14.
285. Ozols RF, Cunnion RE, Klecker RW, Jr., Hamilton TC, Ostchega Y, Parrillo JE, et al. Verapamil and adriamycin in the treatment of drug-resistant ovarian cancer patients. J Clin Oncol. 1987;5641-7.
286. Jonsson B, Nilsson K, Nygren P, Larsson R. SDZ PSC-833--a novel potent in vitro chemosensitizer in multiple myeloma. Anticancer Drugs. 1992;3641-6.
287. Pirker R, FitzGerald DJ, Raschack M, Frank Z, Willingham MC, Pastan I. Enhancement of the activity of immunotoxins by analogues of verapamil. Cancer Res. 1989;494791-5.
288. Giaccone G, Linn SC, Welink J, Catimel G, Stieltjes H, van der Vijgh WJ, et al. A dose-finding and pharmacokinetic study of reversal of multidrug resistance with SDZ PSC 833 in combination with doxorubicin in patients with solid tumors. Clin Cancer Res. 1997;32005-15.
289. Wilson WH, Jamis-Dow C, Bryant G, Balis FM, Klecker RW, Bates SE, et al. Phase I and pharmacokinetic study of the multidrug resistance modulator dexverapamil with EPOCH chemotherapy. J Clin Oncol. 1995;131985-94.
290. Lum BL, Gosland MP. MDR expression in normal tissues. Pharmacologic implications for the clinical use of P-glycoprotein inhibitors. Hematol Oncol Clin North Am. 1995;9319-36.
291. Dantzig AH, Shepard RL, Cao J, Law KL, Ehlhardt WJ, Baughman TM, et al. Reversal of P-glycoprotein-mediated multidrug resistance by a potent cyclopropyldibenzosuberane modulator, LY335979. Cancer Res. 1996;564171-9.
292. Dale IL, Tuffley W, Callaghan R, Holmes JA, Martin K, Luscombe M, et al. Reversal of P-glycoprotein-mediated multidrug resistance by XR9051, a novel diketopiperazine derivative. Br J Cancer. 1998;78885-92.

293. Hyafil F, Vergely C, Du Vignaud P, Grand-Perret T. In vitro and in vivo reversal of multidrug resistance by GF120918, an acridonecarboxamide derivative. Cancer Res. 1993;534595-602.
294. Dantzig AH, Law KL, Cao J, Starling JJ. Reversal of multidrug resistance by the P-glycoprotein modulator, LY335979, from the bench to the clinic. Curr Med Chem. 2001;839-50.
295. Ruff P, Vorobiof DA, Jordaan JP, Demetriou GS, Moodley SD, Nosworthy AL, et al. A randomized, placebo-controlled, double-blind phase 2 study of docetaxel compared to docetaxel plus zosuquidar (LY335979) in women with metastatic or locally recurrent breast cancer who have received one prior chemotherapy regimen. Cancer Chemother Pharmacol. 2009;64763-8.
296. Lancet JE, Baer MR, Duran GE, List AF, Fielding R, Marcelletti JF, et al. A phase I trial of continuous infusion of the multidrug resistance inhibitor zosuquidar with daunorubicin and cytarabine in acute myeloid leukemia. Leuk Res. 2009;331055-61.
297. Morschhauser F, Zinzani PL, Burgess M, Sloots L, Bouafia F, Dumontet C. Phase I/II trial of a P-glycoprotein inhibitor, Zosuquidar.3HCl trihydrochloride (LY335979), given orally in combination with the CHOP regimen in patients with non-Hodgkin's lymphoma. Leuk Lymphoma. 2007;48708-15.
298. Sandler A, Gordon M, De Alwis DP, Pouliquen I, Green L, Marder P, et al. A Phase I trial of a potent P-glycoprotein inhibitor, zosuquidar trihydrochloride (LY335979), administered intravenously in combination with doxorubicin in patients with advanced malignancy. Clin Cancer Res. 2004;103265-72.
299. Kruijtzer CM, Beijnen JH, Rosing H, ten Bokkel Huinink WW, Schot M, Jewell RC, et al. Increased oral bioavailability of topotecan in combination with the breast cancer resistance protein and P-glycoprotein inhibitor GF120918. J Clin Oncol. 2002;202943-50.
300. Cisternino S, Mercier C, Bourasset F, Roux F, Scherrmann JM. Expression, up-regulation, and transport activity of the multidrug-resistance protein Abcg2 at the mouse blood-brain barrier. Cancer Res. 2004;643296-301.
301. Patel J, Buddha B, Dey S, Pal D, Mitra AK. In vitro interaction of the HIV protease inhibitor ritonavir with herbal constituents: changes in P-gp and CYP3A4 activity. Am J Ther. 2004;11262-77.
302. Di Pietro A, Conseil G, Perez-Victoria JM, Dayan G, Baubichon-Cortay H, Trompier D, et al. Modulation by flavonoids of cell multidrug resistance mediated by P-glycoprotein and related ABC transporters. Cell Mol Life Sci. 2002;59307-22.
303. Zhang L, Lin G, Kovacs B, Jani M, Krajcsi P, Zuo Z. Mechanistic study on the intestinal absorption and disposition of baicalein. Eur J Pharm Sci. 2007;31221-31.
304. Zhang S, Yang X, Coburn RA, Morris ME. Structure activity relationships and quantitative structure activity relationships for the flavonoid-mediated inhibition of breast cancer resistance protein. Biochem Pharmacol. 2005;70627-39.
305. Zhang S, Yang X, Morris ME. Combined effects of multiple flavonoids on breast cancer resistance protein (ABCG2)-mediated transport. Pharm Res. 2004;211263-73.
306. Imai Y, Tsukahara S, Asada S, Sugimoto Y. Phytoestrogens/flavonoids reverse breast cancer resistance protein/ABCG2-mediated multidrug resistance. Cancer Res. 2004;644346-52.
307. Yamagata T, Kusuhara H, Morishita M, Takayama K, Benameur H, Sugiyama Y. Improvement of the oral drug absorption of topotecan through the inhibition of intestinal xenobiotic efflux transporter, breast cancer resistance protein, by excipients. Drug Metab Dispos. 2007;351142-8.

308. Batrakova EV, Miller DW, Li S, Alakhov VY, Kabanov AV, Elmquist WF. Pluronic P85 enhances the delivery of digoxin to the brain: in vitro and in vivo studies. J Pharmacol Exp Ther. 2001;296551-7.
309. Jain R, Agarwal S, Majumdar S, Zhu X, Pal D, Mitra AK. Evasion of P-gp mediated cellular efflux and permeability enhancement of HIV-protease inhibitor saquinavir by prodrug modification. Int J Pharm. 2005;3038-19.
310. Agarwal S, Boddu SH, Jain R, Samanta S, Pal D, Mitra AK. Peptide prodrugs: improved oral absorption of lopinavir, a HIV protease inhibitor. Int J Pharm. 2008;3597-14.
311. Jain R, Majumdar S, Nashed Y, Pal D, Mitra AK. Circumventing P-glycoprotein-mediated cellular efflux of quinidine by prodrug derivatization. Mol Pharm. 2004;1290-9.
312. Fenske DB, Cullis PR. Liposomal nanomedicines. Expert Opin Drug Deliv. 2008;525-44.
313. Acharya S, Sahoo SK. PLGA nanoparticles containing various anticancer agents and tumour delivery by EPR effect. Adv Drug Deliv Rev. 2011;63170-83.
314. Dong X, Mattingly CA, Tseng MT, Cho MJ, Liu Y, Adams VR, et al. Doxorubicin and paclitaxel-loaded lipid-based nanoparticles overcome multidrug resistance by inhibiting P-glycoprotein and depleting ATP. Cancer Res. 2009;693918-26.
315. Naito M, Watanabe T, Tsuge H, Koyama T, Oh-hara T, Tsuruo T. Potentiation of the reversal activity of SDZ PSC833 on multi-drug resistance by an anti-P-glycoprotein monoclonal antibody MRK-16. Int J Cancer. 1996;67435-40.
316. Pearson JW, Fogler WE, Volker K, Usui N, Goldenberg SK, Gruys E, et al. Reversal of drug resistance in a human colon cancer xenograft expressing MDR1 complementary DNA by in vivo administration of MRK-16 monoclonal antibody. J Natl Cancer Inst. 1991;831386-91.
317. Haus-Cohen M, Assaraf YG, Binyamin L, Benhar I, Reiter Y. Disruption of P-glycoprotein anticancer drug efflux activity by a small recombinant single-chain Fv antibody fragment targeted to an extracellular epitope. Int J Cancer. 2004;109750-8.
318. Gaudana R, Ananthula HK, Parenky A, Mitra AK. Ocular drug delivery. AAPS J. 2010;12348-60.
319. Nakanishi T. Drug transporters as targets for cancer chemotherapy. Cancer Genomics Proteomics. 2007;4241-54.
320. Rubio-Aliaga I, Daniel H. Mammalian peptide transporters as targets for drug delivery. Trends Pharmacol Sci. 2002;23434-40.
321. Kramer W. Transporters, Trojan horses and therapeutics: suitability of bile acid and peptide transporters for drug delivery. Biol Chem. 2011;39277-94.
322. Balimane PV, Tamai I, Guo A, Nakanishi T, Kitada H, Leibach FH, et al. Direct evidence for peptide transporter (PepT1)-mediated uptake of a nonpeptide prodrug, valacyclovir. Biochem Biophys Res Commun. 1998;250246-51.
323. Ganapathy ME, Huang W, Wang H, Ganapathy V, Leibach FH. Valacyclovir: a substrate for the intestinal and renal peptide transporters PEPT1 and PEPT2. Biochem Biophys Res Commun. 1998;246470-5.
324. Sugawara M, Huang W, Fei YJ, Leibach FH, Ganapathy V, Ganapathy ME. Transport of valganciclovir, a ganciclovir prodrug, via peptide transporters PEPT1 and PEPT2. J Pharm Sci. 2000;89781-9.
325. Santos C, Morais J, Gouveia L, de Clercq E, Pannecouque C, Nielsen CU, et al. Dipeptide derivatives of AZT: synthesis, chemical stability, activation in human plasma, hPEPT1 affinity, and antiviral activity. ChemMedChem. 2008;3970-8.

326. Tsume Y, Vig BS, Sun J, Landowski CP, Hilfinger JM, Ramachandran C, et al. Enhanced absorption and growth inhibition with amino acid monoester prodrugs of floxuridine by targeting hPEPT1 transporters. Molecules. 2008;131441-54.
327. Rubio-Aliaga I, Daniel H. Peptide transporters and their roles in physiological processes and drug disposition. Xenobiotica. 2008;381022-42.
328. Tamai I, Nakanishi T, Nakahara H, Sai Y, Ganapathy V, Leibach FH, et al. Improvement of L-dopa absorption by dipeptidyl derivation, utilizing peptide transporter PepT1. J Pharm Sci. 1998;871542-6.
329. Ogihara H, Saito H, Shin BC, Terado T, Takenoshita S, Nagamachi Y, et al. Immuno-localization of H+/peptide cotransporter in rat digestive tract. Biochem Biophys Res Commun. 1996;220848-52.
330. Shen H, Smith DE, Yang T, Huang YG, Schnermann JB, Brosius FC, 3rd. Localization of PEPT1 and PEPT2 proton-coupled oligopeptide transporter mRNA and protein in rat kidney. Am J Physiol. 1999;276F658-65.
331. Knutter I, Rubio-Aliaga I, Boll M, Hause G, Daniel H, Neubert K, et al. H+-peptide cotransport in the human bile duct epithelium cell line SK-ChA-1. Am J Physiol Gastrointest Liver Physiol. 2002;283G222-9.
332. Bockman DE, Ganapathy V, Oblak TG, Leibach FH. Localization of peptide transporter in nuclei and lysosomes of the pancreas. Int J Pancreatol. 1997;22221-5.
333. Zhang T, Xiang CD, Gale D, Carreiro S, Wu EY, Zhang EY. Drug transporter and cytochrome P450 mRNA expression in human ocular barriers: implications for ocular drug disposition. Drug Metab Dispos. 2008;361300-7.
334. Berger UV, Hediger MA. Distribution of peptide transporter PEPT2 mRNA in the rat nervous system. Anat Embryol (Berl). 1999;199439-49.
335. Groneberg DA, Doring F, Nickolaus M, Daniel H, Fischer A. Expression of PEPT2 peptide transporter mRNA and protein in glial cells of rat dorsal root ganglia. Neurosci Lett. 2001;304181-4.
336. Groneberg DA, Nickolaus M, Springer J, Doring F, Daniel H, Fischer A. Localization of the peptide transporter PEPT2 in the lung: implications for pulmonary oligopeptide uptake. Am J Pathol. 2001;158707-14.
337. Groneberg DA, Doring F, Theis S, Nickolaus M, Fischer A, Daniel H. Peptide transport in the mammary gland: expression and distribution of PEPT2 mRNA and protein. Am J Physiol Endocrinol Metab. 2002;282E1172-9.
338. Bretschneider B, Brandsch M, Neubert R. Intestinal transport of beta-lactam antibiotics: analysis of the affinity at the H+/peptide symporter (PEPT1), the uptake into Caco-2 cell monolayers and the transepithelial flux. Pharm Res. 1999;1655-61.
339. Daniel H, Adibi SA. Transport of beta-lactam antibiotics in kidney brush border membrane. Determinants of their affinity for the oligopeptide/H+ symporter. J Clin Invest. 1993;922215-23.
340. Ganapathy ME, Prasad PD, Mackenzie B, Ganapathy V, Leibach FH. Interaction of anionic cephalosporins with the intestinal and renal peptide transporters PEPT 1 and PEPT 2. Biochim Biophys Acta. 1997;1324296-308.
341. Ocheltree SM, Shen H, Hu Y, Xiang J, Keep RF, Smith DE. Mechanisms of cefadroxil uptake in the choroid plexus: studies in wild-type and PEPT2 knockout mice. J Pharmacol Exp Ther. 2004;308462-7.

342. Boll M, Markovich D, Weber WM, Korte H, Daniel H, Murer H. Expression cloning of a cDNA from rabbit small intestine related to proton-coupled transport of peptides, beta-lactam antibiotics and ACE-inhibitors. Pflugers Arch. 1994;429146-9.
343. Ganapathy ME, Brandsch M, Prasad PD, Ganapathy V, Leibach FH. Differential recognition of beta -lactam antibiotics by intestinal and renal peptide transporters, PEPT 1 and PEPT 2. J Biol Chem. 1995;27025672-7.
344. Fei YJ, Kanai Y, Nussberger S, Ganapathy V, Leibach FH, Romero MF, et al. Expression cloning of a mammalian proton-coupled oligopeptide transporter. Nature. 1994;368563-6.
345. Wenzel U, Gebert I, Weintraut H, Weber WM, Clauss W, Daniel H. Transport characteristics of differently charged cephalosporin antibiotics in oocytes expressing the cloned intestinal peptide transporter PepT1 and in human intestinal Caco-2 cells. J Pharmacol Exp Ther. 1996;277831-9.
346. Doring F, Walter J, Will J, Focking M, Boll M, Amasheh S, et al. Delta-aminolevulinic acid transport by intestinal and renal peptide transporters and its physiological and clinical implications. J Clin Invest. 1998;1012761-7.
347. Saito H, Terada T, Okuda M, Sasaki S, Inui K. Molecular cloning and tissue distribution of rat peptide transporter PEPT2. Biochim Biophys Acta. 1996;1280173-7.
348. Landowski CP, Vig BS, Song X, Amidon GL. Targeted delivery to PEPT1-overexpressing cells: acidic, basic, and secondary floxuridine amino acid ester prodrugs. Mol Cancer Ther. 2005;4659-67.
349. Tsuda M, Terada T, Irie M, Katsura T, Niida A, Tomita K, et al. Transport characteristics of a novel peptide transporter 1 substrate, antihypotensive drug midodrine, and its amino acid derivatives. J Pharmacol Exp Ther. 2006;318455-60.
350. Han H, de Vrueh RL, Rhie JK, Covitz KM, Smith PL, Lee CP, et al. 5'-Amino acid esters of antiviral nucleosides, acyclovir, and AZT are absorbed by the intestinal PEPT1 peptide transporter. Pharm Res. 1998;151154-9.
351. Watanabe C, Kato Y, Ito S, Kubo Y, Sai Y, Tsuji A. Na+/H+ exchanger 3 affects transport property of H+/oligopeptide transporter 1. Drug Metab Pharmacokinet. 2005;20443-51.
352. Shu C, Shen H, Hopfer U, Smith DE. Mechanism of intestinal absorption and renal reabsorption of an orally active ace inhibitor: uptake and transport of fosinopril in cell cultures. Drug Metab Dispos. 2001;291307-15.
353. Zhu T, Chen XZ, Steel A, Hediger MA, Smith DE. Differential recognition of ACE inhibitors in Xenopus laevis oocytes expressing rat PEPT1 and PEPT2. Pharm Res. 2000;17526-32.
354. Sekine T, Miyazaki H, Endou H. Molecular physiology of renal organic anion transporters. Am J Physiol Renal Physiol. 2006;290F251-61.
355. Konig J, Seithel A, Gradhand U, Fromm MF. Pharmacogenomics of human OATP transporters. Naunyn Schmiedebergs Arch Pharmacol. 2006;372432-43.
356. Obaidat A, Roth M, Hagenbuch B. The expression and function of organic anion transporting polypeptides in normal tissues and in cancer. Annu Rev Pharmacol Toxicol. 2012;52135-51.
357. Ho RH, Tirona RG, Leake BF, Glaeser H, Lee W, Lemke CJ, et al. Drug and bile acid transporters in rosuvastatin hepatic uptake: function, expression, and pharmacogenetics. Gastroenterology. 2006;1301793-806.

358. Su Y, Zhang X, Sinko PJ. Human organic anion-transporting polypeptide OATP-A (SLC21A3) acts in concert with P-glycoprotein and multidrug resistance protein 2 in the vectorial transport of Saquinavir in Hep G2 cells. Mol Pharm. 2004;149-56.
359. Lee W, Glaeser H, Smith LH, Roberts RL, Moeckel GW, Gervasini G, et al. Polymorphisms in human organic anion-transporting polypeptide 1A2 (OATP1A2): implications for altered drug disposition and central nervous system drug entry. J Biol Chem. 2005;2809610-7.
360. Cvetkovic M, Leake B, Fromm MF, Wilkinson GR, Kim RB. OATP and P-glycoprotein transporters mediate the cellular uptake and excretion of fexofenadine. Drug Metab Dispos. 1999;27866-71.
361. Kullak-Ublick GA, Hagenbuch B, Stieger B, Schteingart CD, Hofmann AF, Wolkoff AW, et al. Molecular and functional characterization of an organic anion transporting polypeptide cloned from human liver. Gastroenterology. 1995;1091274-82.
362. Lau YY, Huang Y, Frassetto L, Benet LZ. effect of OATP1B transporter inhibition on the pharmacokinetics of atorvastatin in healthy volunteers. Clin Pharmacol Ther. 2007;81194-204.
363. Liu L, Cui Y, Chung AY, Shitara Y, Sugiyama Y, Keppler D, et al. Vectorial transport of enalapril by Oatp1a1/Mrp2 and OATP1B1 and OATP1B3/MRP2 in rat and human livers. J Pharmacol Exp Ther. 2006;318395-402.
364. Yamashiro W, Maeda K, Hirouchi M, Adachi Y, Hu Z, Sugiyama Y. Involvement of transporters in the hepatic uptake and biliary excretion of valsartan, a selective antagonist of the angiotensin II AT1-receptor, in humans. Drug Metab Dispos. 2006;341247-54.
365. Briz O, Serrano MA, MacIas RI, Gonzalez-Gallego J, Marin JJ. Role of organic anion-transporting polypeptides, OATP-A, OATP-C and OATP-8, in the human placenta-maternal liver tandem excretory pathway for foetal bilirubin. Biochem J. 2003;371897-905.
366. Cui Y, Konig J, Leier I, Buchholz U, Keppler D. Hepatic uptake of bilirubin and its conjugates by the human organic anion transporter SLC21A6. J Biol Chem. 2001;2769626-30.
367. Letschert K, Faulstich H, Keller D, Keppler D. Molecular characterization and inhibition of amanitin uptake into human hepatocytes. Toxicol Sci. 2006;91140-9.
368. Hirano M, Maeda K, Shitara Y, Sugiyama Y. Contribution of OATP2 (OATP1B1) and OATP8 (OATP1B3) to the hepatic uptake of pitavastatin in humans. J Pharmacol Exp Ther. 2004;311139-46.
369. Tirona RG, Leake BF, Wolkoff AW, Kim RB. Human organic anion transporting polypeptide-C (SLC21A6) is a major determinant of rifampin-mediated pregnane X receptor activation. J Pharmacol Exp Ther. 2003;304223-8.
370. Vavricka SR, Van Montfoort J, Ha HR, Meier PJ, Fattinger K. Interactions of rifamycin SV and rifampicin with organic anion uptake systems of human liver. Hepatology. 2002;36164-72.
371. Pizzagalli F, Hagenbuch B, Stieger B, Klenk U, Folkers G, Meier PJ. Identification of a novel human organic anion transporting polypeptide as a high affinity thyroxine transporter. Mol Endocrinol. 2002;162283-96.
372. Kraft ME, Glaeser H, Mandery K, Konig J, Auge D, Fromm MF, et al. The prostaglandin transporter OATP2A1 is expressed in human ocular tissues and transports the antiglaucoma prostanoid latanoprost. Invest Ophthalmol Vis Sci. 2010;512504-11.
373. Treiber A, Schneiter R, Hausler S, Stieger B. Bosentan is a substrate of human OATP1B1 and OATP1B3: inhibition of hepatic uptake as the common mechanism of its interactions with cyclosporin A, rifampicin, and sildenafil. Drug Metab Dispos. 2007;351400-7.

374. Noe J, Portmann R, Brun ME, Funk C. Substrate-dependent drug-drug interactions between gemfibrozil, fluvastatin and other organic anion-transporting peptide (OATP) substrates on OATP1B1, OATP2B1, and OATP1B3. Drug Metab Dispos. 2007;351308-14.
375. Nozawa T, Imai K, Nezu J, Tsuji A, Tamai I. Functional characterization of pH-sensitive organic anion transporting polypeptide OATP-B in human. J Pharmacol Exp Ther. 2004;308438-45.
376. Huber RD, Gao B, Sidler Pfandler MA, Zhang-Fu W, Leuthold S, Hagenbuch B, et al. Characterization of two splice variants of human organic anion transporting polypeptide 3A1 isolated from human brain. Am J Physiol Cell Physiol. 2007;292C795-806.
377. Adachi H, Suzuki T, Abe M, Asano N, Mizutamari H, Tanemoto M, et al. Molecular characterization of human and rat organic anion transporter OATP-D. Am J Physiol Renal Physiol. 2003;285F1188-97.
378. Mikkaichi T, Suzuki T, Onogawa T, Tanemoto M, Mizutamari H, Okada M, et al. Isolation and characterization of a digoxin transporter and its rat homologue expressed in the kidney. Proc Natl Acad Sci U S A. 2004;1013569-74.
379. Meyer zu Schwabedissen HE, Tirona RG, Yip CS, Ho RH, Kim RB. Interplay between the nuclear receptor pregnane X receptor and the uptake transporter organic anion transporter polypeptide 1A2 selectively enhances estrogen effects in breast cancer. Cancer Res. 2008;689338-47.
380. Ballestero MR, Monte MJ, Briz O, Jimenez F, Gonzalez-San Martin F, Marin JJ. Expression of transporters potentially involved in the targeting of cytostatic bile acid derivatives to colon cancer and polyps. Biochem Pharmacol. 2006;72729-38.
381. Miki Y, Suzuki T, Kitada K, Yabuki N, Shibuya R, Moriya T, et al. Expression of the steroid and xenobiotic receptor and its possible target gene, organic anion transporting polypeptide-A, in human breast carcinoma. Cancer Res. 2006;66535-42.
382. Tsuboyama T, Onishi H, Kim T, Akita H, Hori M, Tatsumi M, et al. Hepatocellular carcinoma: hepatocyte-selective enhancement at gadoxetic acid-enhanced MR imaging--correlation with expression of sinusoidal and canalicular transporters and bile accumulation. Radiology. 2010;255824-33.
383. Wlcek K, Svoboda M, Riha J, Zakaria S, Olszewski U, Dvorak Z, et al. The analysis of organic anion transporting polypeptide (OATP) mRNA and protein patterns in primary and metastatic liver cancer. Cancer Biol Ther. 2011;11801-11.
384. Holla VR, Backlund MG, Yang P, Newman RA, DuBois RN. Regulation of prostaglandin transporters in colorectal neoplasia. Cancer Prev Res (Phila). 2008;193-9.
385. Wlcek K, Svoboda M, Thalhammer T, Sellner F, Krupitza G, Jaeger W. Altered expression of organic anion transporter polypeptide (OATP) genes in human breast carcinoma. Cancer Biol Ther. 2008;71450-5.
386. Liedauer R, Svoboda M, Wlcek K, Arrich F, Ja W, Toma C, et al. Different expression patterns of organic anion transporting polypeptides in osteosarcomas, bone metastases and aneurysmal bone cysts. Oncol Rep. 2009;221485-92.
387. Roth M, Obaidat A, Hagenbuch B. OATPs, OATs and OCTs: the organic anion and cation transporters of the SLCO and SLC22A gene superfamilies. Br J Pharmacol. 2012;1651260-87.
388. Pao SS, Paulsen IT, Saier MH, Jr. Major facilitator superfamily. Microbiol Mol Biol Rev. 1998;621-34.
389. Ren Q, Kang KH, Paulsen IT. TransportDB: a relational database of cellular membrane transport systems. Nucleic Acids Res. 2004;32D284-8.

390. Saier MH, Jr., Beatty JT, Goffeau A, Harley KT, Heijne WH, Huang SC, et al. The major facilitator superfamily. J Mol Microbiol Biotechnol. 1999;1257-79.
391. Reizer J, Finley K, Kakuda D, MacLeod CL, Reizer A, Saier MH, Jr. Mammalian integral membrane receptors are homologous to facilitators and antiporters of yeast, fungi, and eubacteria. Protein Sci. 1993;220-30.
392. Eraly SA, Bush KT, Sampogna RV, Bhatnagar V, Nigam SK. The molecular pharmacology of organic anion transporters: from DNA to FDA? Mol Pharmacol. 2004;65479-87.
393. Cha SH, Sekine T, Kusuhara H, Yu E, Kim JY, Kim DK, et al. Molecular cloning and characterization of multispecific organic anion transporter 4 expressed in the placenta. J Biol Chem. 2000;2754507-12.
394. Ljubojevic M, Balen D, Breljak D, Kusan M, Anzai N, Bahn A, et al. Renal expression of organic anion transporter OAT2 in rats and mice is regulated by sex hormones. Am J Physiol Renal Physiol. 2007;292F361-72.
395. Sykes D, Sweet DH, Lowes S, Nigam SK, Pritchard JB, Miller DS. Organic anion transport in choroid plexus from wild-type and organic anion transporter 3 (Slc22a8)-null mice. Am J Physiol Renal Physiol. 2004;286F972-8.
396. Alebouyeh M, Takeda M, Onozato ML, Tojo A, Noshiro R, Hasannejad H, et al. Expression of human organic anion transporters in the choroid plexus and their interactions with neurotransmitter metabolites. J Pharmacol Sci. 2003;93430-6.
397. Takeda M, Noshiro R, Onozato ML, Tojo A, Hasannejad H, Huang XL, et al. Evidence for a role of human organic anion transporters in the muscular side effects of HMG-CoA reductase inhibitors. Eur J Pharmacol. 2004;483133-8.
398. Motohashi H, Sakurai Y, Saito H, Masuda S, Urakami Y, Goto M, et al. Gene expression levels and immunolocalization of organic ion transporters in the human kidney. J Am Soc Nephrol. 2002;13866-74.
399. Pritchard JB, Sweet DH, Miller DS, Walden R. Mechanism of organic anion transport across the apical membrane of choroid plexus. J Biol Chem. 1999;27433382-7.
400. Hosoyamada M, Sekine T, Kanai Y, Endou H. Molecular cloning and functional expression of a multispecific organic anion transporter from human kidney. Am J Physiol. 1999;276F122-8.
401. Burckhardt G. Drug transport by Organic Anion Transporters (OATs). Pharmacol Ther. 2012;136106-30.
402. Enomoto A, Takeda M, Shimoda M, Narikawa S, Kobayashi Y, Yamamoto T, et al. Interaction of human organic anion transporters 2 and 4 with organic anion transport inhibitors. J Pharmacol Exp Ther. 2002;301797-802.
403. Cha SH, Sekine T, Fukushima JI, Kanai Y, Kobayashi Y, Goya T, et al. Identification and characterization of human organic anion transporter 3 expressing predominantly in the kidney. Mol Pharmacol. 2001;591277-86.
404. Ekaratanawong S, Anzai N, Jutabha P, Miyazaki H, Noshiro R, Takeda M, et al. Human organic anion transporter 4 is a renal apical organic anion/dicarboxylate exchanger in the proximal tubules. J Pharmacol Sci. 2004;94297-304.
405. Ugele B, St-Pierre MV, Pihusch M, Bahn A, Hantschmann P. Characterization and identification of steroid sulfate transporters of human placenta. Am J Physiol Endocrinol Metab. 2003;284E390-8.

406. Asif AR, Steffgen J, Metten M, Grunewald RW, Muller GA, Bahn A, et al. Presence of organic anion transporters 3 (OAT3) and 4 (OAT4) in human adrenocortical cells. Pflugers Arch. 2005;45088-95.
407. Shin HJ, Anzai N, Enomoto A, He X, Kim do K, Endou H, et al. Novel liver-specific organic anion transporter OAT7 that operates the exchange of sulfate conjugates for short chain fatty acid butyrate. Hepatology. 2007;451046-55.
408. Enomoto A, Kimura H, Chairoungdua A, Shigeta Y, Jutabha P, Cha SH, et al. Molecular identification of a renal urate anion exchanger that regulates blood urate levels. Nature. 2002;417447-52.
409. Koepsell H. Polyspecific organic cation transporters: their functions and interactions with drugs. Trends Pharmacol Sci. 2004;25375-81.
410. Jonker JW, Schinkel AH. Pharmacological and physiological functions of the polyspecific organic cation transporters: OCT1, 2, and 3 (SLC22A1-3). J Pharmacol Exp Ther. 2004;3082-9.
411. Dresser MJ, Leabman MK, Giacomini KM. Transporters involved in the elimination of drugs in the kidney: organic anion transporters and organic cation transporters. J Pharm Sci. 2001;90397-421.
412. Wright SH. Role of organic cation transporters in the renal handling of therapeutic agents and xenobiotics. Toxicol Appl Pharmacol. 2005;204309-19.
413. Wright SH, Dantzler WH. Molecular and cellular physiology of renal organic cation and anion transport. Physiol Rev. 2004;84987-1049.
414. Koepsell H, Endou H. The SLC22 drug transporter family. Pflugers Arch. 2004;447666-76.
415. Koepsell H, Schmitt BM, Gorboulev V. Organic cation transporters. Rev Physiol Biochem Pharmacol. 2003;15036-90.
416. Koepsell H, Gorboulev V, Arndt P. Molecular pharmacology of organic cation transporters in kidney. J Membr Biol. 1999;167103-17.
417. Takeda Y, Inoue H. [Polyamines and cell multiplication]. Horumon To Rinsho. 1975;23111-9.
418. Choi MK, Song IS. Organic cation transporters and their pharmacokinetic and pharmacodynamic consequences. Drug Metab Pharmacokinet. 2008;23243-53.
419. Dresser MJ, Gray AT, Giacomini KM. Kinetic and selectivity differences between rodent, rabbit, and human organic cation transporters (OCT1). J Pharmacol Exp Ther. 2000;2921146-52.
420. Kimura N, Masuda S, Tanihara Y, Ueo H, Okuda M, Katsura T, et al. Metformin is a superior substrate for renal organic cation transporter OCT2 rather than hepatic OCT1. Drug Metab Pharmacokinet. 2005;20379-86.
421. Bourdet DL, Pritchard JB, Thakker DR. Differential substrate and inhibitory activities of ranitidine and famotidine toward human organic cation transporter 1 (hOCT1; SLC22A1), hOCT2 (SLC22A2), and hOCT3 (SLC22A3). J Pharmacol Exp Ther. 2005;3151288-97.
422. Lips KS, Volk C, Schmitt BM, Pfeil U, Arndt P, Miska D, et al. Polyspecific cation transporters mediate luminal release of acetylcholine from bronchial epithelium. Am J Respir Cell Mol Biol. 2005;3379-88.
423. Karbach U, Kricke J, Meyer-Wentrup F, Gorboulev V, Volk C, Loffing-Cueni D, et al. Localization of organic cation transporters OCT1 and OCT2 in rat kidney. Am J Physiol Renal Physiol. 2000;279F679-87.

424. Gorboulev V, Ulzheimer JC, Akhoundova A, Ulzheimer-Teuber I, Karbach U, Quester S, et al. Cloning and characterization of two human polyspecific organic cation transporters. DNA Cell Biol. 1997;16871-81.
425. Nies AT, Koepsell H, Winter S, Burk O, Klein K, Kerb R, et al. Expression of organic cation transporters OCT1 (SLC22A1) and OCT3 (SLC22A3) is affected by genetic factors and cholestasis in human liver. Hepatology. 2009;501227-40.
426. Muller J, Lips KS, Metzner L, Neubert RH, Koepsell H, Brandsch M. Drug specificity and intestinal membrane localization of human organic cation transporters (OCT). Biochem Pharmacol. 2005;701851-60.
427. Sata R, Ohtani H, Tsujimoto M, Murakami H, Koyabu N, Nakamura T, et al. Functional analysis of organic cation transporter 3 expressed in human placenta. J Pharmacol Exp Ther. 2005;315888-95.
428. Wu X, Kekuda R, Huang W, Fei YJ, Leibach FH, Chen J, et al. Identity of the organic cation transporter OCT3 as the extraneuronal monoamine transporter (uptake2) and evidence for the expression of the transporter in the brain. J Biol Chem. 1998;27332776-86.
429. Masuda S, Terada T, Yonezawa A, Tanihara Y, Kishimoto K, Katsura T, et al. Identification and functional characterization of a new human kidney-specific H+/organic cation antiporter, kidney-specific multidrug and toxin extrusion 2. J Am Soc Nephrol. 2006;172127-35.
430. Vadlapudi AD, Vadlapatla RK, Mitra AK. Sodium dependent multivitamin transporter (SMVT): a potential target for drug delivery. Curr Drug Targets. 2012;13994-1003.
431. Russell-Jones G, McTavish K, McEwan J, Rice J, Nowotnik D. Vitamin-mediated targeting as a potential mechanism to increase drug uptake by tumours. J Inorg Biochem. 2004;981625-33.
432. Ramanathan S, Qiu B, Pooyan S, Zhang G, Stein S, Leibowitz MJ, et al. Targeted PEG-based bioconjugates enhance the cellular uptake and transport of a HIV-1 TAT nonapeptide. J Control Release. 2001;77199-212.
433. Janoria KG, Hariharan S, Paturi D, Pal D, Mitra AK. Biotin uptake by rabbit corneal epithelial cells: role of sodium-dependent multivitamin transporter (SMVT). Curr Eye Res. 2006;31797-809.
434. Janoria KG, Boddu SH, Wang Z, Paturi DK, Samanta S, Pal D, et al. Vitreal pharmacokinetics of biotinylated ganciclovir: role of sodium-dependent multivitamin transporter expressed on retina. J Ocul Pharmacol Ther. 2009;2539-49.
435. Park S, Sinko PJ. The blood-brain barrier sodium-dependent multivitamin transporter: a molecular functional in vitro-in situ correlation. Drug Metab Dispos. 2005;331547-54.
436. Said HM, Ortiz A, McCloud E, Dyer D, Moyer MP, Rubin S. Biotin uptake by human colonic epithelial NCM460 cells: a carrier-mediated process shared with pantothenic acid. Am J Physiol. 1998;275C1365-71.
437. Patel M, Vadlapatla RK, Shah S, Mitra AK. Molecular expression and functional activity of sodium dependent multivitamin transporter in human prostate cancer cells. Int J Pharm. 2012;436324-31.
438. Vadlapudi AD, Vadlapatla RK, Pal D, Mitra AK. Functional and Molecular Aspects of Biotin Uptake via SMVT in Human Corneal Epithelial (HCEC) and Retinal Pigment Epithelial (D407) Cells. AAPS J. 2012.
439. Luo S, Kansara VS, Zhu X, Mandava NK, Pal D, Mitra AK. Functional characterization of sodium-dependent multivitamin transporter in MDCK-MDR1 cells and its utilization as a target for drug delivery. Mol Pharm. 2006;3329-39.

440. Kansara V, Luo S, Balasubrahmanyam B, Pal D, Mitra AK. Biotin uptake and cellular translocation in human derived retinoblastoma cell line (Y-79): a role of hSMVT system. Int J Pharm. 2006;31243-52.
441. Grassl SM. Human placental brush-border membrane Na(+)-biotin cotransport. J Biol Chem. 1992;26717760-5.
442. Ohkura Y, Akanuma S, Tachikawa M, Hosoya K. Blood-to-retina transport of biotin via Na+-dependent multivitamin transporter (SMVT) at the inner blood-retinal barrier. Exp Eye Res. 2010;91387-92.
443. Balamurugan K, Vaziri ND, Said HM. Biotin uptake by human proximal tubular epithelial cells: cellular and molecular aspects. Am J Physiol Renal Physiol. 2005;288F823-31.
444. Ma TY, Dyer DL, Said HM. Human intestinal cell line Caco-2: a useful model for studying cellular and molecular regulation of biotin uptake. Biochim Biophys Acta. 1994;118981-8.
445. Baur B, Baumgartner ER. Na(+)-dependent biotin transport into brush-border membrane vesicles from human kidney cortex. Pflugers Arch. 1993;422499-505.
446. Said HM, Hoefs J, Mohammadkhani R, Horne DW. Biotin transport in human liver basolateral membrane vesicles: a carrier-mediated, Na+ gradient-dependent process. Gastroenterology. 1992;1022120-5.
447. Said HM, Redha R, Nylander W. A carrier-mediated, Na+ gradient-dependent transport for biotin in human intestinal brush-border membrane vesicles. Am J Physiol. 1987;253G631-6.
448. Baur B, Wick H, Baumgartner ER. Na(+)-dependent biotin transport into brush-border membrane vesicles from rat kidney. Am J Physiol. 1990;258F840-7.
449. Daruwala R, Song J, Koh WS, Rumsey SC, Levine M. Cloning and functional characterization of the human sodium-dependent vitamin C transporters hSVCT1 and hSVCT2. FEBS Lett. 1999;460480-4.
450. Wang H, Dutta B, Huang W, Devoe LD, Leibach FH, Ganapathy V, et al. Human Na(+)-dependent vitamin C transporter 1 (hSVCT1): primary structure, functional characteristics and evidence for a non-functional splice variant. Biochim Biophys Acta. 1999;14611-9.
451. Tsukaguchi H, Tokui T, Mackenzie B, Berger UV, Chen XZ, Wang Y, et al. A family of mammalian Na+-dependent L-ascorbic acid transporters. Nature. 1999;39970-5.
452. Said HM, Mohammed ZM. Intestinal absorption of water-soluble vitamins: an update. Curr Opin Gastroenterol. 2006;22140-6.
453. Maulen NP, Henriquez EA, Kempe S, Carcamo JG, Schmid-Kotsas A, Bachem M, et al. Up-regulation and polarized expression of the sodium-ascorbic acid transporter SVCT1 in post-confluent differentiated CaCo-2 cells. J Biol Chem. 2003;2789035-41.
454. Bowers-Komro DM, McCormick DB. Characterization of ascorbic acid uptake by isolated rat kidney cells. J Nutr. 1991;12157-64.
455. Rose RC. Ascorbic acid transport in mammalian kidney. Am J Physiol. 1986;250F627-32.
456. Astuya A, Caprile T, Castro M, Salazar K, Garcia Mde L, Reinicke K, et al. Vitamin C uptake and recycling among normal and tumor cells from the central nervous system. J Neurosci Res. 2005;79146-56.
457. Castro M, Caprile T, Astuya A, Millan C, Reinicke K, Vera JC, et al. High-affinity sodium-vitamin C co-transporters (SVCT) expression in embryonic mouse neurons. J Neurochem. 2001;78815-23.
458. Talluri RS, Katragadda S, Pal D, Mitra AK. Mechanism of L-ascorbic acid uptake by rabbit corneal epithelial cells: evidence for the involvement of sodium-dependent vitamin C transporter 2. Curr Eye Res. 2006;31481-9.

459. Garland DL. Ascorbic acid and the eye. Am J Clin Nutr. 1991;541198S-202S.
460. Dixon SJ, Kulaga A, Jaworski EM, Wilson JX. Ascorbate uptake by ROS 17/2.8 osteoblast-like cells: substrate specificity and sensitivity to transport inhibitors. J Bone Miner Res. 1991;6623-9.
461. Padh H, Aleo JJ. Characterization of the ascorbic acid transport by 3T6 fibroblasts. Biochim Biophys Acta. 1987;901283-90.
462. Luo S, Wang Z, Kansara V, Pal D, Mitra AK. Activity of a sodium-dependent vitamin C transporter (SVCT) in MDCK-MDR1 cells and mechanism of ascorbate uptake. Int J Pharm. 2008;358168-76.
463. Liang WJ, Johnson D, Jarvis SM. Vitamin C transport systems of mammalian cells. Mol Membr Biol. 2001;1887-95.
464. Wilson JX. Regulation of vitamin C transport. Annu Rev Nutr. 2005;25105-25.
465. Amparo F, Sadrai Z, Jin Y, Alfonso-Bartolozzi B, Wang H, Shikari H, et al. Safety and efficacy of the multitargeted receptor kinase inhibitor pazopanib in the treatment of corneal neovascularization. Invest Ophthalmol Vis Sci. 2013;54537-44.
466. Chang JH, Gabison EE, Kato T, Azar DT. Corneal neovascularization. Curr Opin Ophthalmol. 2001;12242-9.
467. Epstein RJ, Stulting RD, Hendricks RL, Harris DM. Corneal neovascularization. Pathogenesis and inhibition. Cornea. 1987;6250-7.
468. Hajrasouliha AR, Funaki T, Sadrai Z, Hattori T, Chauhan SK, Dana R. Vascular endothelial growth factor-C promotes alloimmunity by amplifying antigen-presenting cell maturation and lymphangiogenesis. Invest Ophthalmol Vis Sci. 2012;531244-50.
469. Niederkorn JY. Immune privilege and immune regulation in the eye. Adv Immunol. 1990;48191-226.
470. Dana MR, Streilein JW. Loss and restoration of immune privilege in eyes with corneal neovascularization. Invest Ophthalmol Vis Sci. 1996;372485-94.
471. Maguire MG, Stark WJ, Gottsch JD, Stulting RD, Sugar A, Fink NE, et al. Risk factors for corneal graft failure and rejection in the collaborative corneal transplantation studies. Collaborative Corneal Transplantation Studies Research Group. Ophthalmology. 1994;1011536-47.
472. Bachmann BO, Bock F, Wiegand SJ, Maruyama K, Dana MR, Kruse FE, et al. Promotion of graft survival by vascular endothelial growth factor a neutralization after high-risk corneal transplantation. Arch Ophthalmol. 2008;12671-7.
473. Kwak N, Okamoto N, Wood JM, Campochiaro PA. VEGF is major stimulator in model of choroidal neovascularization. Invest Ophthalmol Vis Sci. 2000;413158-64.
474. Krzystolik MG, Afshari MA, Adamis AP, Gaudreault J, Gragoudas ES, Michaud NA, et al. Prevention of experimental choroidal neovascularization with intravitreal anti-vascular endothelial growth factor antibody fragment. Arch Ophthalmol. 2002;120338-46.
475. Rosenfeld PJ, Brown DM, Heier JS, Boyer DS, Kaiser PK, Chung CY, et al. Ranibizumab for neovascular age-related macular degeneration. N Engl J Med. 2006;3551419-31.
476. Brown DM, Michels M, Kaiser PK, Heier JS, Sy JP, Ianchulev T, et al. Ranibizumab versus verteporfin photodynamic therapy for neovascular age-related macular degeneration: Two-year results of the ANCHOR study. Ophthalmology. 2009;11657-65 e5.
477. Michels S, Rosenfeld PJ, Puliafito CA, Marcus EN, Venkatraman AS. Systemic bevacizumab (Avastin) therapy for neovascular age-related macular degeneration twelve-week results of an uncontrolled open-label clinical study. Ophthalmology. 2005;1121035-47.

478. Nguyen QD, Shah S, Tatlipinar S, Do DV, Anden EV, Campochiaro PA. Bevacizumab suppresses choroidal neovascularisation caused by pathological myopia. Br J Ophthalmol. 2005;891368-70.
479. Avery RL, Pearlman J, Pieramici DJ, Rabena MD, Castellarin AA, Nasir MA, et al. Intravitreal bevacizumab (Avastin) in the treatment of proliferative diabetic retinopathy. Ophthalmology. 2006;1131695 e1-15.
480. Laud K, Spaide RF, Freund KB, Slakter J, Klancnik JM, Jr. Treatment of choroidal neovascularization in pathologic myopia with intravitreal bevacizumab. Retina. 2006;26960-3.
481. Spaide RF, Laud K, Fine HF, Klancnik JM, Jr., Meyerle CB, Yannuzzi LA, et al. Intravitreal bevacizumab treatment of choroidal neovascularization secondary to age-related macular degeneration. Retina. 2006;26383-90.
482. Nguyen QD, Shah SM, Hafiz G, Do DV, Haller JA, Pili R, et al. Intravenous bevacizumab causes regression of choroidal neovascularization secondary to diseases other than age-related macular degeneration. Am J Ophthalmol. 2008;145257-66.
483. Sakaguchi H, Ikuno Y, Gomi F, Kamei M, Sawa M, Tsujikawa M, et al. Intravitreal injection of bevacizumab for choroidal neovascularisation associated with pathological myopia. Br J Ophthalmol. 2007;91161-5.
484. Lindblom P, Gerhardt H, Liebner S, Abramsson A, Enge M, Hellstrom M, et al. Endothelial PDGF-B retention is required for proper investment of pericytes in the microvessel wall. Genes Dev. 2003;171835-40.
485. Risau W. Mechanisms of angiogenesis. Nature. 1997;386671-4.
486. Nehls V, Denzer K, Drenckhahn D. Pericyte involvement in capillary sprouting during angiogenesis in situ. Cell Tissue Res. 1992;270469-74.
487. Naldini A, Carraro F. Role of inflammatory mediators in angiogenesis. Curr Drug Targets Inflamm Allergy. 2005;43-8.
488. Folkman J. Angiogenesis in cancer, vascular, rheumatoid and other disease. Nat Med. 1995;127-31.
489. Azar DT. Corneal angiogenic privilege: angiogenic and antiangiogenic factors in corneal avascularity, vasculogenesis, and wound healing (an American Ophthalmological Society thesis). Trans Am Ophthalmol Soc. 2006;104264-302.
490. Amano S, Rohan R, Kuroki M, Tolentino M, Adamis AP. Requirement for vascular endothelial growth factor in wound- and inflammation-related corneal neovascularization. Invest Ophthalmol Vis Sci. 1998;3918-22.
491. Philipp W, Speicher L, Humpel C. Expression of vascular endothelial growth factor and its receptors in inflamed and vascularized human corneas. Invest Ophthalmol Vis Sci. 2000;412514-22.
492. Cursiefen C, Cao J, Chen L, Liu Y, Maruyama K, Jackson D, et al. Inhibition of hemangiogenesis and lymphangiogenesis after normal-risk corneal transplantation by neutralizing VEGF promotes graft survival. Invest Ophthalmol Vis Sci. 2004;452666-73.
493. Dastjerdi MH, Saban DR, Okanobo A, Nallasamy N, Sadrai Z, Chauhan SK, et al. Effects of topical and subconjunctival bevacizumab in high-risk corneal transplant survival. Invest Ophthalmol Vis Sci. 2010;512411-7.
494. Song S, Ewald AJ, Stallcup W, Werb Z, Bergers G. PDGFRbeta+ perivascular progenitor cells in tumours regulate pericyte differentiation and vascular survival. Nat Cell Biol. 2005;7870-9.

495. Finkenzeller G, Marme D, Weich HA, Hug H. Platelet-derived growth factor-induced transcription of the vascular endothelial growth factor gene is mediated by protein kinase C. Cancer Res. 1992;524821-3.
496. Abramsson A, Lindblom P, Betsholtz C. Endothelial and nonendothelial sources of PDGF-B regulate pericyte recruitment and influence vascular pattern formation in tumors. J Clin Invest. 2003;1121142-51.
497. Jain RK, Booth MF. What brings pericytes to tumor vessels? J Clin Invest. 2003;1121134-6.
498. Hasumi Y, Klosowska-Wardega A, Furuhashi M, Ostman A, Heldin CH, Hellberg C. Identification of a subset of pericytes that respond to combination therapy targeting PDGF and VEGF signaling. Int J Cancer. 2007;1212606-14.
499. Erber R, Thurnher A, Katsen AD, Groth G, Kerger H, Hammes HP, et al. Combined inhibition of VEGF and PDGF signaling enforces tumor vessel regression by interfering with pericyte-mediated endothelial cell survival mechanisms. FASEB J. 2004;18338-40.
500. Bergers G, Song S, Meyer-Morse N, Bergsland E, Hanahan D. Benefits of targeting both pericytes and endothelial cells in the tumor vasculature with kinase inhibitors. J Clin Invest. 2003;1111287-95.
501. Jo N, Mailhos C, Ju M, Cheung E, Bradley J, Nishijima K, et al. Inhibition of platelet-derived growth factor B signaling enhances the efficacy of anti-vascular endothelial growth factor therapy in multiple models of ocular neovascularization. Am J Pathol. 2006;1682036-53.
502. Harris PA, Boloor A, Cheung M, Kumar R, Crosby RM, Davis-Ward RG, et al. Discovery of 5-[[4-[(2,3-dimethyl-2H-indazol-6-yl)methylamino]-2-pyrimidinyl]amino]-2-methyl-benzenesulfonamide (Pazopanib), a novel and potent vascular endothelial growth factor receptor inhibitor. J Med Chem. 2008;514632-40.
503. Kumar R, Knick VB, Rudolph SK, Johnson JH, Crosby RM, Crouthamel MC, et al. Pharmacokinetic-pharmacodynamic correlation from mouse to human with pazopanib, a multikinase angiogenesis inhibitor with potent antitumor and antiangiogenic activity. Mol Cancer Ther. 2007;62012-21.
504. van der Graaf WT, Blay JY, Chawla SP, Kim DW, Bui-Nguyen B, Casali PG, et al. Pazopanib for metastatic soft-tissue sarcoma (PALETTE): a randomised, double-blind, placebo-controlled phase 3 trial. Lancet. 2012;3791879-86.
505. Takahashi K, Saishin Y, Saishin Y, King AG, Levin R, Campochiaro PA. Suppression and regression of choroidal neovascularization by the multitargeted kinase inhibitor pazopanib. Arch Ophthalmol. 2009;127494-9.
506. Yafai Y, Yang XM, Niemeyer M, Nishiwaki A, Lange J, Wiedemann P, et al. Anti-angiogenic effects of the receptor tyrosine kinase inhibitor, pazopanib, on choroidal neovascularization in rats. Eur J Pharmacol. 2011;66612-8.
507. Thakur A, Scheinman RI, Rao VR, Kompella UB. Pazopanib, a multitargeted tyrosine kinase inhibitor, reduces diabetic retinal vascular leukostasis and leakage. Microvasc Res. 2011;82346-50.
508. Mannermaa E, Vellonen KS, Urtti A. Drug transport in corneal epithelium and blood-retina barrier: emerging role of transporters in ocular pharmacokinetics. Adv Drug Deliv Rev. 2006;581136-63.
509. Katragadda S, Budda B, Anand BS, Mitra AK. Role of efflux pumps and metabolising enzymes in drug delivery. Expert Opin Drug Deliv. 2005;2683-705.

510. Gou M, Gong C, Zhang J, Wang X, Wang X, Gu Y, et al. Polymeric matrix for drug delivery: honokiol-loaded PCL-PEG-PCL nanoparticles in PEG-PCL-PEG thermosensitive hydrogel. J Biomed Mater Res A. 2010;93219-26.
511. Karla PK, Quinn TL, Herndon BL, Thomas P, Pal D, Mitra A. Expression of multidrug resistance associated protein 5 (MRP5) on cornea and its role in drug efflux. J Ocul Pharmacol Ther. 2009;25121-32.
512. Karla PK, Pal D, Quinn T, Mitra AK. Molecular evidence and functional expression of a novel drug efflux pump (ABCC2) in human corneal epithelium and rabbit cornea and its role in ocular drug efflux. Int J Pharm. 2007;33612-21.
513. Karla PK, Earla R, Boddu SH, Johnston TP, Pal D, Mitra A. Molecular expression and functional evidence of a drug efflux pump (BCRP) in human corneal epithelial cells. Curr Eye Res. 2009;341-9.
514. Davis AA, Bernstein PS, Bok D, Turner J, Nachtigal M, Hunt RC. A human retinal pigment epithelial cell line that retains epithelial characteristics after prolonged culture. Invest Ophthalmol Vis Sci. 1995;36955-64.
515. Constable PA, Lawrenson JG, Dolman DE, Arden GB, Abbott NJ. P-Glycoprotein expression in human retinal pigment epithelium cell lines. Exp Eye Res. 2006;8324-30.
516. Pissuwan D, Boyer C, Gunasekaran K, Davis TP, Bulmus V. In vitro cytotoxicity of RAFT polymers. Biomacromolecules. 2010;11412-20.
517. Prabhu A, Shelburne CE, Gibbons DF. Cellular proliferation and cytokine responses of murine macrophage cell line J774A.1 to polymethylmethacrylate and cobalt-chrome alloy particles. J Biomed Mater Res. 1998;42655-63.
518. Yoo HS, Choi HK, Park TG. Protein-fatty acid complex for enhanced loading and stability within biodegradable nanoparticles. J Pharm Sci. 2001;90194-201.
519. Tuzlakoglu K, Reis RL. Biodegradable polymeric fiber structures in tissue engineering. Tissue Eng Part B Rev. 2009;1517-27.
520. Tamboli V, Mishra GP, Mitra AK. Novel pentablock copolymer (PLA-PCL-PEG-PCL-PLA) based nanoparticles for controlled drug delivery: Effect of copolymer compositions on the crystallinity of copolymers and in vitro drug release profile from nanoparticles. Colloid Polym Sci. 2013;2911235-45.
521. Frank A, Rath SK, Venkatraman SS. Controlled release from bioerodible polymers: effect of drug type and polymer composition. J Control Release. 2005;102333-44.
522. Huang MH, Li S, Hutmacher DW, Schantz JT, Vacanti CA, Braud C, et al. Degradation and cell culture studies on block copolymers prepared by ring opening polymerization of epsilon-caprolactone in the presence of poly(ethylene glycol). J Biomed Mater Res A. 2004;69417-27.
523. Li S, Molina I, Martinez MB, Vert M. Hydrolytic and enzymatic degradations of physically crosslinked hydrogels prepared from PLA/PEO/PLA triblock copolymers. J Mater Sci Mater Med. 2002;1381-6.
524. Li S, Dobrzynski P, Kasperczyk J, Bero M, Braud C, Vert M. Structure-property relationships of copolymers obtained by ring-opening polymerization of glycolide and epsilon-caprolactone. Part 2. Influence of composition and chain microstructure on the hydrolytic degradation. Biomacromolecules. 2005;6489-97.
525. Gomez-Gaete C, Tsapis N, Besnard M, Bochot A, Fattal E. Encapsulation of dexamethasone into biodegradable polymeric nanoparticles. Int J Pharm. 2007;331153-9.
526. Wu DQ, Chu CC. Biodegradable hydrophobic-hydrophilic hybrid hydrogels: swelling behavior and controlled drug release. J Biomater Sci Polym Ed. 2008;19411-29.

527. Brubaker RF, Bourne WM, Bachman LA, McLaren JW. Ascorbic acid content of human corneal epithelium. Invest Ophthalmol Vis Sci. 2000;411681-3.
528. Delamere NA. Ascorbic acid and the eye. Subcell Biochem. 1996;25313-29.
529. Burzle M, Suzuki Y, Ackermann D, Miyazaki H, Maeda N, Clemencon B, et al. The sodium-dependent ascorbic acid transporter family SLC23. Mol Aspects Med. 2013;34436-54.
530. Luo S, Wang Z, Patel M, Khurana V, Zhu X, Pal D, et al. Targeting SVCT for enhanced drug absorption: synthesis and in vitro evaluation of a novel vitamin C conjugated prodrug of saquinavir. Int J Pharm. 2011;41477-85.
531. Manfredini S, Pavan B, Vertuani S, Scaglianti M, Compagnone D, Biondi C, et al. Design, synthesis and activity of ascorbic acid prodrugs of nipecotic, kynurenic and diclophenamic acids, liable to increase neurotropic activity. J Med Chem. 2002;45559-62.
532. Pfaffl MW. A new mathematical model for relative quantification in real-time RT-PCR. Nucleic Acids Res. 2001;29e45.
533. Savini I, Rossi A, Pierro C, Avigliano L, Catani MV. SVCT1 and SVCT2: key proteins for vitamin C uptake. Amino Acids. 2008;34347-55.
534. Koskela TK, Reiss GR, Brubaker RF, Ellefson RD. Is the high concentration of ascorbic acid in the eye an adaptation to intense solar irradiation? Invest Ophthalmol Vis Sci. 1989;302265-7.
535. Varma SD, Richards RD. Ascorbic acid and the eye lens. Ophthalmic Res. 1988;20164-73.
536. Devamanoharan PS, Henein M, Morris S, Ramachandran S, Richards RD, Varma SD. Prevention of selenite cataract by vitamin C. Exp Eye Res. 1991;52563-8.
537. Barar J, Asadi M, Mortazavi-Tabatabaei SA, Omidi Y. Ocular Drug Delivery; Impact of in vitro Cell Culture Models. J Ophthalmic Vis Res. 2009;4238-52.
538. Katragadda S, Talluri RS, Pal D, Mitra AK. Identification and characterization of a Na+-dependent neutral amino acid transporter, ASCT1, in rabbit corneal epithelial cell culture and rabbit cornea. Curr Eye Res. 2005;30989-1002.
539. Liang WJ, Johnson D, Ma LS, Jarvis SM, Wei-Jun L. Regulation of the human vitamin C transporters expressed in COS-1 cells by protein kinase C [corrected]. Am J Physiol Cell Physiol. 2002;283C1696-704.
540. Stebbing J, Ellis P. An overview of drug development for metastatic breast cancer. Br J Nurs. 2012;21S18-22.
541. Bareford LM, Phelps MA, Foraker AB, Swaan PW. Intracellular processing of riboflavin in human breast cancer cells. Mol Pharm. 2008;5839-48.
542. Shennan DB. Mammary gland membrane transport systems. J Mammary Gland Biol Neoplasia. 1998;3247-58.
543. Vadlapudi AD, Vadlapatla RK, Pal D, Mitra AK. Biotin uptake by T47D breast cancer cells: functional and molecular evidence of sodium-dependent multivitamin transporter (SMVT). Int J Pharm. 2013;441535-43.
544. Cole SP, Bhardwaj G, Gerlach JH, Mackie JE, Grant CE, Almquist KC, et al. Overexpression of a transporter gene in a multidrug-resistant human lung cancer cell line. Science. 1992;2581650-4.
545. Gros P, Ben Neriah YB, Croop JM, Housman DE. Isolation and expression of a complementary DNA that confers multidrug resistance. Nature. 1986;323728-31.
546. Kessel D, Botterill V, Wodinsky I. Uptake and retention of daunomycin by mouse leukemic cells as factors in drug response. Cancer Res. 1968;28938-41.

547. Ling V, Thompson LH. Reduced permeability in CHO cells as a mechanism of resistance to colchicine. J Cell Physiol. 1974;83103-16.
548. Riehm H, Biedler JL. Cellular resistance to daunomycin in Chinese hamster cells in vitro. Cancer Res. 1971;31409-12.
549. Marshman E, Taylor GA, Thomas HD, Newell DR, Curtin NJ. Hypoxanthine transport in human tumour cell lines: relationship to the inhibition of hypoxanthine rescue by dipyridamole. Biochem Pharmacol. 2001;61477-84.
550. Plagemann PG, Wohlhueter RM, Woffendin C. Nucleoside and nucleobase transport in animal cells. Biochim Biophys Acta. 1988;947405-43.
551. Rivenzon-Segal D, Rushkin E, Polak-Charcon S, Degani H. Glucose transporters and transport kinetics in retinoic acid-differentiated T47D human breast cancer cells. Am J Physiol Endocrinol Metab. 2000;279E508-19.
552. Gallagher SM, Castorino JJ, Wang D, Philp NJ. Monocarboxylate transporter 4 regulates maturation and trafficking of CD147 to the plasma membrane in the metastatic breast cancer cell line MDA-MB-231. Cancer Res. 2007;674182-9.
553. Harris T, Eliyahu G, Frydman L, Degani H. Kinetics of hyperpolarized 13C1-pyruvate transport and metabolism in living human breast cancer cells. Proc Natl Acad Sci U S A. 2009;10618131-6.
554. Jhaveri MS, Rait AS, Chung KN, Trepel JB, Chang EH. Antisense oligonucleotides targeted to the human alpha folate receptor inhibit breast cancer cell growth and sensitize the cells to doxorubicin treatment. Mol Cancer Ther. 2004;31505-12.
555. Pinard MF, Jolivet J, Ratnam M, Kathmann I, Molthoff C, Westerhof R, et al. Functional aspects of membrane folate receptors in human breast cancer cells with transport-related resistance to methotrexate. Cancer Chemother Pharmacol. 1996;38281-8.
556. Okabe M, Szakacs G, Reimers MA, Suzuki T, Hall MD, Abe T, et al. Profiling SLCO and SLC22 genes in the NCI-60 cancer cell lines to identify drug uptake transporters. Mol Cancer Ther. 2008;73081-91.
557. Tamai I. Oral drug delivery utilizing intestinal OATP transporters. Adv Drug Deliv Rev. 2012;64508-14.
558. Menniti FS, Knoth J, Diliberto EJ, Jr. Role of ascorbic acid in dopamine beta-hydroxylation. The endogenous enzyme cofactor and putative electron donor for cofactor regeneration. J Biol Chem. 1986;26116901-8.
559. Murad S, Grove D, Lindberg KA, Reynolds G, Sivarajah A, Pinnell SR. Regulation of collagen synthesis by ascorbic acid. Proc Natl Acad Sci U S A. 1981;782879-82.
560. Patak P, Willenberg HS, Bornstein SR. Vitamin C is an important cofactor for both adrenal cortex and adrenal medulla. Endocr Res. 2004;30871-5.
561. Hong SW, Lee SH, Moon JH, Hwang JJ, Kim DE, Ko E, et al. SVCT-2 in breast cancer acts as an indicator for L-ascorbate treatment. Oncogene. 2013;321508-17.
562. Padayatty SJ, Levine M. Reevaluation of ascorbate in cancer treatment: emerging evidence, open minds and serendipity. J Am Coll Nutr. 2000;19423-5.
563. Baader SL, Bill E, Trautwein AX, Bruchelt G, Matzanke BF. Mobilization of iron from cellular ferritin by ascorbic acid in neuroblastoma SK-N-SH cells: an EPR study. FEBS Lett. 1996;381131-4.
564. Head KA. Ascorbic acid in the prevention and treatment of cancer. Altern Med Rev. 1998;3174-86.

565. Kang JS, Cho D, Kim YI, Hahm E, Kim YS, Jin SN, et al. Sodium ascorbate (vitamin C) induces apoptosis in melanoma cells via the down-regulation of transferrin receptor dependent iron uptake. J Cell Physiol. 2005;204192-7.
566. Maramag C, Menon M, Balaji KC, Reddy PG, Laxmanan S. Effect of vitamin C on prostate cancer cells in vitro: effect on cell number, viability, and DNA synthesis. Prostate. 1997;32188-95.
567. Cameron E, Campbell A. The orthomolecular treatment of cancer. II. Clinical trial of high-dose ascorbic acid supplements in advanced human cancer. Chem Biol Interact. 1974;9285-315.
568. Cameron E, Pauling L. Supplemental ascorbate in the supportive treatment of cancer: Prolongation of survival times in terminal human cancer. Proc Natl Acad Sci U S A. 1976;733685-9.
569. Cameron E, Pauling L. Supplemental ascorbate in the supportive treatment of cancer: reevaluation of prolongation of survival times in terminal human cancer. Proc Natl Acad Sci U S A. 1978;754538-42.
570. Ohno S, Ohno Y, Suzuki N, Soma G, Inoue M. High-dose vitamin C (ascorbic acid) therapy in the treatment of patients with advanced cancer. Anticancer Res. 2009;29809-15.
571. Kurbacher CM, Wagner U, Kolster B, Andreotti PE, Krebs D, Bruckner HW. Ascorbic acid (vitamin C) improves the antineoplastic activity of doxorubicin, cisplatin, and paclitaxel in human breast carcinoma cells in vitro. Cancer Lett. 1996;103183-9.
572. Harris HR, Bergkvist L, Wolk A. Vitamin C intake and breast cancer mortality in a cohort of Swedish women. Br J Cancer. 2013;109257-64.
573. Chen Q, Espey MG, Sun AY, Pooput C, Kirk KL, Krishna MC, et al. Pharmacologic doses of ascorbate act as a prooxidant and decrease growth of aggressive tumor xenografts in mice. Proc Natl Acad Sci U S A. 2008;10511105-9.
574. Ullah MF, Khan HY, Zubair H, Shamim U, Hadi SM. The antioxidant ascorbic acid mobilizes nuclear copper leading to a prooxidant breakage of cellular DNA: implications for chemotherapeutic action against cancer. Cancer Chemother Pharmacol. 2011;67103-10.
575. Ait-Mohamed O, Battisti V, Joliot V, Fritsch L, Pontis J, Medjkane S, et al. Acetonic extract of Buxus sempervirens induces cell cycle arrest, apoptosis and autophagy in breast cancer cells. PLoS One. 2011;6e24537.
576. Holliday DL, Speirs V. Choosing the right cell line for breast cancer research. Breast Cancer Res. 2011;13215.
577. Mizuno N, Niwa T, Yotsumoto Y, Sugiyama Y. Impact of drug transporter studies on drug discovery and development. Pharmacol Rev. 2003;55425-61.

VITA

Varun Khurana was born on July 4th, 1986 in New Delhi, India. He completed his secondary education from Mira Model School, New Delhi, India. He later obtained his Bachelor of Pharmacy degree from Maharaja Surajmal Institute of Pharmacy (MSIP), Delhi, which is affiliated to Guru Gobind Singh Indraprastha University (GGSIPU), Delhi in June 2008.

Varun Khurana joined the Department of Pharmaceutical Sciences at University of Missouri-Kansas City (UMKC), School of Pharmacy in August 2008 in pursuit of a doctorate degree under the guidance of Dr. Ashim K. Mitra. He served as Vice Chair (2009-10), Chair Elect (2010-11) and Chair (2011-12) of AAPS-UMKC Student Chapter, School of Pharmacy. He has been awarded with Graduate Teaching Assistantship (GTA) for Advances in Drug Therapy, and Pharmacokinetics and Biopharmaceutics (2009-12). He has also received Best Seminar Speaker in Spring 2013 at Division of Pharmaceutical Sciences, UMKC.

Mr. Khurana is an active member of American Association of Pharmaceutical Scientists (AAPS), Association of Research in Vision and Ophthalmology (ARVO) and Pharmaceutical Sciences Graduate Student Association (PSGSA). He has authored/co-authored several peer reviewed research and review articles in reputed international journals and has also presented his research work in several national conferences.